The Regulation of Oncogenic MAP Kinase Signalling by Dual-Specificity MAP Kinase Phosphatases

Andrew M. Kidger

Supervisor: Professor Stephen M. Keyse

PhD Thesis

University of Dundee

Submitted: August 2016

Table of Contents

List of Tables

List of Figures

Acknowledgements

I would like to thank Steve for all his advice and guidance throughout my PhD. I would also like to thank all the members of the Keyse lab who have contributed to all the work I have performed in the lab and for making it an enjoyable place to work. In particular thanks go to Linda for all her assistance and training when I was starting in the lab, to Jane for all her help in the MRSU and for sparing me the pain of maintenance and genotyping for my final 2 years and to Julia for enthusiastically taking on a lot of the work within the pancreas and lung projects. I also need to thank anyone else in the JWCC, CRC or MRSU who has either helped with my work or given valuable advice during my PhD.

Furthermore, I need to thank all of the PhD students in the Division of Cancer Research who as well as ensuring I never had a dull day at work, have contributed to all the fantastic memories I have of Dundee and Scotland as a whole. In particular Alana, Lois and Lauren for allowing me use of their spare rooms when commuting got too intense, Alana (and Max) for being my most reliable and enthusiastic hillwalking companions, and to all of you who made the long journey down to our wedding (even the ones of you who nearly missed it – naming no names…). Finally, I must also thank my beautiful wife Simone for all her love and support during our time in Scotland and the course of my PhD. I love you and couldn't have done it without you.

Declarations

I declare that this thesis is based on results obtained from research which I have personally carried out in the Cancer Division of the Medical Research Institute at University of Dundee from October 2012 to September 2016 using funding provided by a Cancer Research UK PhD Studentship. I declare that the entire thesis is my own composition. Any work other than my own is clearly stated in the text and acknowledged with reference to any relevant investigators or contributors. This thesis has never been presented previously, in whole or in part, for the award of any higher degree. I have consulted all the references cited within the text of this thesis.

Signed ……. Date ……

I confirm that Andrew Kidger has carried out the research under my supervision and that he has fulfilled the conditions of the relevant Ordinance and Regulations of the University of Dundee, thereby qualifying him to submit this thesis in application for the degree of Doctor of Philosophy.

Signed ……. Date ……

Abbreviations

ADEX	Aberrantly differentiated exocrine
ADM	Acinar to ductal metaplasia
ALL	Acute lymphoblastic leukemia
AP-1	Activator protein 1
ARF	Alternative reading frame
ATF-2	Activating transcription factor 2
ATM	Ataxia telangiectasia mutated
ATP	Adenosine triphosphate
BCI	2-benzylidene-3-(cyclohexylamino)-1-Indanone hydrochloride
BCL-2	B-cell lymphoma 2
BRCA1/2	Breast Cancer 1/2
C/EBP	CCAAT-enhancer-binding protein
CDK4	Cyclin-dependent kinase 4
ChIP	Chromatin immunoprecipitation
ChIP-chip	Chromatin immunoprecipitation with promoter microarray
CK19	Cytokeratin-19
CRC	Colorectal cancer
CRE	c-AMP response element
CRM1	Chromosome region maintenance-1
DAB	3, 3 -diaminobenzidine
DEN	Diethylnitrosamine
DKO	Double knockout
DMBA	7,12-Dimethylbenz[a]anthracene
DMEM	Dulbecco’s modified Eagles medium
DNA	Deoxyribonucleic acid
DUSP	Dual-specificity phosphatase
ECM	Extra-cellular matrix
EDTA	Ethylenediaminetetraacetic acid
EGF	Epidermal growth factor
EGFR	Epidermal growth factor receptor
Egr	Early growth-response

EMT	Epithelial to mesenchymal transition
ERK	Extracellular signal-regulated kinase
ES cell	Embryonic stem cell
ESCC	Oesophageal squamous cell carcinoma
EVT5	Ets Varient Gene 5
EyA	Eyes-absent
FAK	Focal adhesion kinase
FBS	Foetal Bovine Serum
FCP	F-cell production
FGF	Fibroblast growth factor
FOXO1	Forkhead box protein O1
GEF	guanine nucleotide exchange factor
GEMM	Genetically engineered mutant mice
GPCRs	G-protein coupled receptors
GTP	Guanosine triphosphate
HRP	Horseradish peroxidase
IECs	Intestinal epithelial crypt cells
IHC	Immunohistochemistry
IPMN	Intraductal papillary mucinous neoplasia
JNK	c-Jun N-terminal kinase
KIM	Kinase interaction motif
KO	Knockout
KSR	Kinase suppressor of Ras
LKB1	Liver kinase B1
LMWPTP	Low molecular weight PTP
LOH	Loss of heterozygosity
LPS	Lipopolysaccharide
LSL	Lox-STOP-Lox
MAPK	Mitogen-activated protein kinase
MAPKAPK	MAPK-activated protein kinase
MAPKK	MAPK kinase
MAPKKK	MAPK kinase kinase
MCN	Mucinous cystic neoplasia

MEFs	Mouse embryonic fibroblasts
MEK	MAPK/ERK Kinase
MEKi	MEK inhibition
MK2	MAPK-activated protein kinase 2
MKP	MAP kinase phosphatase
MLCK	Myosin light chain kinase
MNK	MAPK-interacting kinase
MOI	Multiplicity of infection
MP1	MEK partner-1
MSK	Mitogen- and stress-activated kinase
mTOR	Mammalian target of rapamycin
NES	Nuclear export sequence
NGF	Nerve growth factor
NLK	NEMO-like kinase
NLS	Nuclear localisation sequence
NPC	Nasopharyngeal carcinoma
NSCLC	Non-small-cell lung cancer
OIS	Oncogene-induced senescence
PanIN	Pancreatic intraepithelial neoplasia
PBS	Phosphate-buffered saline
PDAC	Pancreatic ductal adenocarcinoma
PDGF	Platelet-derived growth factor
PDK1	3-phosphoinositide-dependent protein kinase 1
PDX1	Pancreatic and duodenal homeobox 1
PI3K	Phosphoinositide 3-kinase
PKA	Protein kinase-A
PPM	Mg+-dependent protein phosphatases
PPP	Protein phosphatase P
PRL	Phosphatase of regenerating liver
PTC	Papillary thyroid carcinoma
PTEN	Phosphatase and tensin homolog
Ptf1α	Pancreas-specific transcription factor 1α
PTP	Protein tyrosine phosphatase

qRT-PCR	Quantitative real-time polymerase chain reaction
Rb	Retinoblastoma
RET/PTC	Rearranged in transformation/papillary thyroid cancer
RNA	Ribonucleic acid
ROS	Reactive oxygen species
RSK	Ribosomal S6 kinase
RTKs	Receptor tyrosine kinases
SAGE	Serial analysis of gene expression
SAPK	Stress-activated protein kinase
SCC	Squamous cell carcinoma
SH2	Src homology 2
SHH	Sonic hedgehog
SOS	Son of Sevenless
Sox9	SRY-Box 9
SRF	Serum response factor
TBS	Tris-buffered saline
TF	Transcription factor
TGFβ	Transforming growth factor-β
TKI	Tyrosine kinases inhibitor
TPA	12-O-tetradecanoylphorbol-13-acetate
UBF	Upstream binding factor
WT	Wild-type
αSMA	αSmooth muscle actin

Abstract

Oncogenic activation of the Ras-ERK pathway is frequently observed in human cancers. Dual-specificity MAP kinase phosphatases (DUSPs or MKPs) are important negative regulators of this pathway and could therefore play an important role in modulating the oncogenic potential of signalling. DUSP5 and DUSP6/MKP-3 are ERK-specific MKPs, which are classical negative feedback regulators of pathway activity, but are differentially localised, with DUSP5 found in the nucleus and DUSP6/MKP-3 in the cytoplasm. However, to date their potential roles in modulating the oncogenic potential of the Ras-ERK pathway is unclear. This project aimed to use a range of biochemical and genetic techniques in order to determine whether these enzymes play functional roles in modulating the spatiotemporal regulation of ERK signalling and, in particular, to use murine cancer models to explore the effects of MKP deletion on the initiation and/or progression of mutant Ras-induced tumours.

Here we show that DUSP5 is an essential regulator of nuclear ERK activity and gene expression in response to acute Ras/ERK pathway activation and this work provides a mechanistic underpinning for our observation that DUSP5 has a tumour suppressor function in the murine model of DMBA/TPA-induced skin carcinogenesis. We also show that the endogenous expression of mutant $KRas^{G12D}$ in murine fibroblasts induces the expression of both DUSP5 and DUSP6/MKP-3, suggesting these proteins are involved in the negative feedback response, which constrains ERK activity following constitutive pathway activation. Finally, using mouse models of $KRas^{G12D}$-driven pancreatic cancer, we demonstrate that the deletion of either DUSP5 or DUSP6/MKP-3 accelerates the initiation of acinar-to-ductal metaplasia (ADM) and pancreatic intra-epithelial neoplasia (PanINs). However, with respect to the development of invasive pancreatic ductal adenocarcinoma (PDAC), loss of DUSP6/MKP-3 seems a more potent driver. Our data confirm that these MKPs do play an important role in modulating the initiation and development of Ras-induced tumours in this clinically relevant murine cancer model. The variable penetrance of the pancreatic phenotypes observed following the loss of either DUSP5 or DUSP6/MKP-3 could reflect either the differing ability of these MKPs to regulate the strength of ERK activity or differential effects on the nuclear and cytoplasmic fractions of ERK respectively.

Chapter 1 Introduction

1.1 Signal transduction and protein phosphorylation

To enable optimal survival and functional activity a cell needs to be able to adapt to changes in its external environment or intracellular conditions. A cells ability to adapt to changing conditions depends on its capacity to transduce signals from such stimuli to initiate an appropriate physiological response. As well as enabling individual cells to respond to their environment, such communication is essential to enable cells to act in unison to form functioning tissues as part of multicellular organisms.

Cell surface receptors enable cells to detect changes in their external environment. These include transmembrane proteins such as receptor tyrosine kinases (RTKs), G-protein coupled receptors (GPCRs) or integrin receptors, which are activated by the binding of extracellular ligands initiating an intracellular signalling cascade to alter cellular activity or cell fate. Changes in intracellular homeostasis, such as nutrient shortages, the accumulation of reactive oxygen species (ROS) or the presence of deoxyribonucleic acid (DNA) damage can be detected by specialised intracellular receptors leading to signal transduction to initiate a response in order to oppose these perturbations or stresses. The cellular response to these signals or stresses can be mediated by processes, which operate at both the gene and protein level, including: changes in gene expression, rates of protein degradation and alterations in the activity or subcellular localisation of proteins.

In most cases signal transduction involves the stepwise amplification of a small initial signal, to generate a response of a greater magnitude that is able to cause significant changes in cellular activity. This occurs by the signalling molecule at each step of the signalling cascade activating more than one molecule of its downstream target, thereby gradually building up the signal magnitude to ensure a robust response. Signal transduction is predominantly enabled through post-translational modifications of the amino acid side-chains of signalling proteins and effectors. Post-translational modifications can alter the structural conformation and thus enzymatic activity of a protein, block or enable the binding of proteins to their substrates or target proteins for degradation. These modifications include acetylation, nitrosylation, O-GlcNAcylation,

SUMOylation, ubiquitination, phosphorylation and others. This project is focused on the activity of signalling pathways, which are driven by sequential phosphorylation and dephosphorylation.

Protein phosphorylation is a rapid and reversible process, making it an ideal molecular switch to enable signal transduction (Fig. 1.1). Protein kinases are enzymes that catalyse the covalent addition of a phosphate group, from adenosine triphosphate (ATP), to a free hydroxyl group on the side chain of an amino acid residue within the target protein. This is an anabolic process requiring energy from the breakdown of ATP. Proteins can be phosphorylated on nine amino acids: tyrosine, serine, threonine, cysteine, arginine, lysine, aspartate, glutamate and histidine (Manning et al., 2002). However, serine, threonine and tyrosine phosphorylation are predominant in eukaryotic cells, giving rise to the two major classes of protein kinases named after the amino acid residues they target for phosphorylation, the serine/threonine or tyrosine protein kinases. Most protein kinases were first described as putative amino acid sequences deduced from the coding nucleotide sequences of cloned cDNA's rather than the traditional biochemical approach of enzyme assays using purified protein (Hanks et al., 1988). These two families were initially thought to be mutually exclusive, however a group of protein kinases have been discovered that would have been classified via their primary structure as serine/threonine kinases but are actually able to phosphorylate tyrosine residues (Lindberg et al., 1992). Furthermore, a number of kinases have been shown to be dual-specificity protein kinases, that are capable of phosphorylating both tyrosine and serine/threonine residues, thus constituting a further subfamily of protein kinases (Lindberg et al., 1992).

Phosphorylation can regulate protein function and cell signalling by two mechanisms. The addition of a negatively charged phosphate group is able to induce conformational changes in the phosphorylated protein, as this alters the surface charge and thus hydrophobicity of a region of the protein, which helps to determine the tertiary (globular) structure of a protein. Conformational changes can alter the enzymatic activity and binding ability of a protein therefore altering its function in a signalling system. Secondly, phosphorylation can alter the ability of a target protein to associate with its binding partners through the generation or disruption of charge-based interactions, without the requirement for any conformational change (Johnson and O'Reilly, 1996).

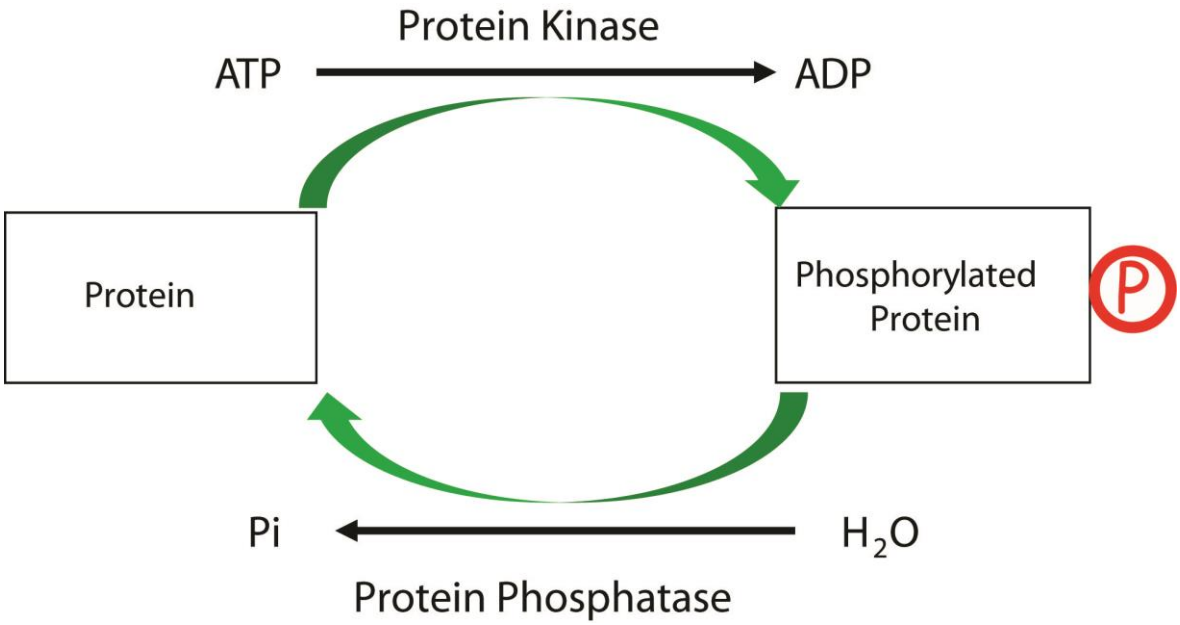

Figure 1.1 Protein Phosphorylation. The reversible modification of proteins by phosphorylation is mediated by two classes of enzyme, protein kinases and protein phosphatases. Protein kinases transfer the terminal phosphate of adenosine triphosphate (ATP) to a hydroxyl group on an amino acid side chain of the protein, typically on serine, threonine or tyrosine residues. In the reverse process protein phosphatases catalyse the removal of the phosphate by hydrolysis. Protein phosphorylation is able to regulate the activity or binding ability of a protein through the induction of conformational changes in the protein's globular structure.

The reverse reaction of protein dephosphorylation is carried out by a class of enzymes known as protein phosphatases, which catalyse the removal of the phosphate group by hydrolysis (Fig. 1.1). These can be broadly classified into two main families, the protein tyrosine phosphatases (PTPs) and the serine/threonine protein phosphatases (Barford, 1996; Mustelin, 2007). The latter group is comprised of three structurally distinct families i) The Mg+-dependent protein phosphatases (PPM) group of exemplified by PP2C ii) The Mg^{+}-dependent FCP (F-cell production) phosphatases, which act on the C-terminal domain of RNA polymerase 2. iii) PPP (protein phosphatase P) family phosphatases which comprise the largest group of ser/thr phosphatases and include PP1, PP2A, PP2B (calcineurin), PP5 and many others (Cohen, 2004; Mustelin, 2007).

Like the ser/thr phosphatases, PTPs, which are defined as phosphatases with some degree of structural homology to known enzymes with *bona fide* PTP activity, can also be broken down into four evolutionarily distinct groups (Table 1.1) (Tonks, 2006). The class 1 cysteine-dependent protein tyrosine phosphatases comprise the largest of these and includes the transmembrane (receptor type) PTPs such as PTPalpha and CD45, the non-receptor type PTPs exemplified by PTP1B, T-cell PTP and Shp1, but also a very large and diverse group of dual-specificity protein phosphatases or DUSPs (Alonso et al., 2004; Mustelin, 2007). The latter includes the thr/tyr dual-specificity MAP kinase phosphatases (MKPs), but also atypical DUSPs (VHR, PIR, Laforin), slingshot phosphatases (SSH1-3), phosphatases of regenerating liver (PRLs), CDC14 phosphatases, the PTENs (PTEN, TPIP, Tensin) and myotubularins. The latter two groups are not protein phosphatases, but instead act on inositol phospholipids (Patterson et al., 2009). The class 2 PTPs comprise a small family of CDC25 cell cycle regulatory phosphatases while class 3 PTPs, although widely distributed in nature, contain only one mammalian member in the low molecular weight PTP (LMWPTP). The final class of PTPs are the eyes-absent (EyA) PTPs, which use an aspartate residue as a nucleophile, require a divalent metal ion in the active site to catalyze phosphate hydrolysis and have some structural similarity to haloacid dehalogenases (HAD) (Mustelin, 2007; Tonks, 2006). The subjects of this thesis are the members of the MKP subfamily of DUSPs and as such the cellular consequences of their phosphatase activity are determined by the functions of their target kinase(s), in this case the MAPKs.

Protein Tyrosine Phosphatase (PTP) Group	Sub-group	Family	Number of classified phosphatases	Substrate Specificity
Class I Cys-based PTPs	Classical PTPs	Transmembrane PTPs	21	P-Tyr
		Non-receptor PTPs	17	P-Tyr
	"VH1-like" dual-specificity PTPs (DUSPs)	MAP Kinase Phosphatases (MKPs)	10	P-Tyr, P-Thr
		Atypical DUSPs	19	P-Tyr, P-Thr, mRNA
		PRLs	3	P-Tyr
		Slingshots	3	P-Ser
		CDC14s	4	P-Ser, P-Thr
		PTENs	5	D3-phosphoinositides
		Myotubularins	16	PI(3)P
Class II Cys-based PTPs	-	LMWPTP	1	P-Tyr
Class III Cys-based PTPs	-	CDC25	3	P-Tyr, P-Thr
Asp-based PTPs	-	EyA Proteins	4	P-Tyr, P-Ser

Table 1.1 Classification and substrate specificity of protein tyrosine phosphatases (PTPs). The PTPs are divided into four groups: the Class I, II and III Cys-based PTPs and the Asp-based PTPs. These groups are further divided into additional sub-groups and families, of which the number of phosphatases and their substrate specificities are outlined. The subject of this thesis is the Dual-specificity MAP kinase phosphatases (MKPs), which are highlighted in red. PRL (phosphatases of regenerating liver), PTEN (Phosphatase and tensin homolog), LMWPTP (low molecular weight PTP), EyA (eyes-absent). Compiled from: Alonso et al., 2004; Patterson et al., 2009; Tonks, 2006.

1.2 Mitogen-activated protein kinase (MAPK) signalling

1.2.1 MAPK pathways

The mitogen-activated protein kinase (MAPK) cascades constitute a group of highly conserved signal transduction pathways which regulate numerous cellular functions including proliferation, differentiation, survival, migration and inflammation, as well as stress responses such as growth arrest or apoptosis (Chang and Karin, 2001; Kyriakis and Avruch, 2012; Wada and Penninger, 2004). MAPK cascades can be activated by a diverse range of extracellular and intracellular stimuli including growth factors, cytokines, metabolic state, DNA damage and other cellular stresses (Raman et al., 2007). The core MAPK signalling module is comprised of three kinases, which sequentially activate each other. Active MAPK kinase kinase (MAPKKK) phosphorylates and activates MAPK kinase (MAPKK), a dual-specificity protein kinase, enabling the phosphorylation of both the threonine and tyrosine residues of a conserved T-X-Y motif within the kinase activation loop which is required to activate the MAPK itself (Marshall, 1994; Ray and Sturgill, 1988). Following activation the terminal MAPK is able to directly phosphorylate cytoplasmic targets in a wide range of cellular compartments or shuttle into the nucleus to phosphorylate nuclear targets including transcription factors to induce changes in gene expression (Pearson et al., 2001; Wortzel and Seger, 2011).

There are four major groups of MAPK signalling cascades in mammalian cells (Fig. 1.2). These are the prototypical Ras-activated extracellular signal-regulated kinases 1 and 2 (ERK1/2), the three stress activated c-Jun N-terminal kinases (JNK1, 2 & 3), the four p38 MAPKs (p38α, β, δ and γ) and ERK5 (Pearson et al., 2001). In addition to these conventional MAPKs there are less well-characterised atypical MAPKs including ERK3/4, NEMO-like kinase (NLK) and ERK7. Atypical MAPKs are unable to be phosphorylated by MAPKK proteins, and hence lack the classical three tiered-cascade organisation shared by conventional MAPKs (Coulombe and Meloche, 2007). The ERK1/2, JNK and p38 pathways are the best characterised MAPK pathways, with the most known about their negative feedback regulation and involvement in human cancer progression.

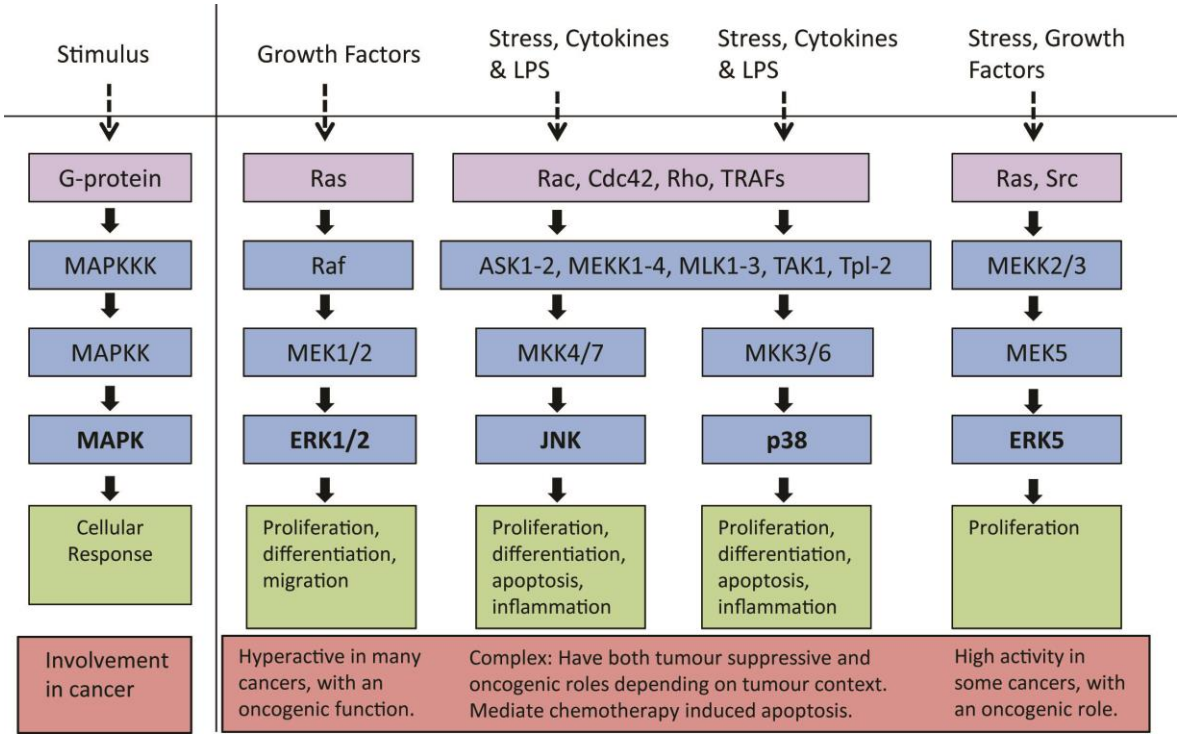

Figure 1.2 The major MAPK signalling pathways and their functions. Schematic outlining the components of the major MAPK modules in mammalian cells, some of the biological endpoints associated with pathway activity and a description of their characterised roles in cancer. For detail see text.

1.2.2 The classical ERK pathway

The classical ERK pathway is the prototypical MAPK cascade (Boulton et al., 1990). The MAPK components of this pathway, ERK1 and ERK2, are closely related isoforms which exhibit 83% amino acid identity and are coexpressed in most cell types (Boulton et al., 1991). Consequently it was proposed that these isoforms have overlapping, potentially redundant, functions (Cobb and Goldsmith, 2000). This interpretation is supported by RNAi silencing experiments, which demonstrated that the combined expression level of ERK1 and ERK2 determines the biological outcome of ERK signalling both *in vitro* and *in vivo*, although ERK2 is expressed at a much higher level in most cell types. Furthermore, the kinase activities of ERK1/2 against known targets appear indistinguishable *in vitro* (Lefloch et al., 2008). Overexpression and knockout studies had previously demonstrated differential effects of ERK1 and ERK2 in mice (Pagès et al., 1999; Vantaggiato et al., 2006; Yao et al., 2003). However, these studies usually observed a greater effect of the loss of ERK2 than of ERK1, which could be explained by the more significant effect of ERK2 ablation would have on total ERK1/2 levels due to its higher level of expression. A recent study has convincingly demonstrated functional redundancy between ERK1 and ERK2 by rescuing the embryonic lethality of ERK2 null mice using transgenic ERK1 expression (Frémin et al., 2015). The developmental consequences of ERK1 expression correlated with global ERK1/2 activity in a dose-dependent manner, supporting the conclusions of Lefloch and colleagues (2008) that ERK1 and ERK2 are totally redundant and that it is the combined expression level and activation state of ERK1 and ERK2, which determines the biological outcome of ERK1/2 (hereafter referred to as ERK) signalling.

The ERK pathway is classically activated via growth factor signalling through RTKs, stimulating sequential activation of the small G-protein Ras, and the Raf, MAPK/ERK Kinase (MEK), ERK kinase cascade (Fig. 1.3) (Shaul and Seger, 2007). Growth factor ligands, such as epidermal growth factor (EGF), bind to their respective RTKs inducing receptor dimerization, activation and autophosphorylation of intracellular tyrosine residues. These phosphorylated residues allow the binding of Src homology 2 (SH2) or phosphotyrosine-binding domain-containing proteins, to initiate intracellular signalling cascades including the MAPK and Phosphoinositide 3-kinase (PI3K) pathways amongst many others. The MAPK pathway is initiated by the binding of the SH2 protein Grb2 to a phosphorylated tyrosine residue, allowing the recruitment of the guanine nucleotide

exchange factor (GEF) Son of Sevenless (SOS). SOS sequesters GDP from Ras GTPases (KRas, NRas, and HRas) enabling GTP binding, causing a conformational change and activating Ras (Cargnello and Roux, 2011; English et al., 1999; Greene and Kaplan, 1995). Active Ras functions as an adaptor protein which is able to bind and activate multiple downstream effectors initiating signalling systems including the ERK, PI3K, Ral and phospholipase C pathways (Rajalingam et al., 2007). With regard to the ERK pathway active Ras is able to bind and activate multiple MAPKKKs, including A-Raf, B-Raf, and Raf-1 (cRaf) through the induction of dimer formation (Moodie et al., 1994; Morrison et al., 1988; Reuter et al., 1995). Activated Raf is then able to promote the activation of the MAPKK isoforms MEK1 and MEK2 by phosphorylation of dual serine residues (Zheng and Guan, 1994), this is followed by the sequential activation of ERK by phosphorylation of its T-E-Y motif (the dually phosphorylated and activated (*p*-T-E-*p*-Y) form of ERK will be subsequently referred to as *p*-ERK) (Ray and Sturgill, 1988).

Hundreds of proteins with diverse biological functions have been characterised as ERK substrates or binding partners, these include direct targets such as transcription factors, and also other protein kinases (Ramos, 2008; Yoon and Seger, 2006). Cytoplasmic targets of ERK include: members of the apoptotic regulatory B-cell lymphoma 2 (BCL-2) family that regulate cell survival (Balmanno and Cook, 2009), myosin light chain kinase (MLCK), which regulates migration (Klemke et al., 1997) and paxillin/focal adhesion kinase (FAK), that regulates microtubule formation (Ishibe et al., 2004). Nuclear targets are primarily transcription factors, including ELK-1, c-Fos, NF-AT, c-Myc and STAT3, which alter gene expression to induce diverse biological outcomes, including the promotion of proliferation (Pearson et al., 2001; Ramos, 2008). The kinase targets of ERK include the p90 ribosomal S6 kinases (RSKs), mitogen- and stress-activated kinases (MSKs), and MAPK-interacting kinases (MNKs) (Cargnello and Roux, 2011). These downstream kinases constitute an additional amplification step within the ERK cascade, enabling them to influence a wider range of biological processes. Furthermore, ERK has also been shown to have the ability to regulate some target proteins through non-catalytic mechanisms, for example it is able to activate topoisomerase-2a in a phosphorylation-independent process to cause DNA unwinding (Rauch et al., 2011; Shapiro et al., 1999).

Given such a diverse spectrum of functions it is not surprising that aberrations in ERK signalling have been revealed in a broad range of pathologies including multiple cancers, diabetes, inflammation, and cardiovascular disease (Ramos, 2008). This thesis is concerned with the influence of altered feedback regulation within the MAPK cascades on cancer development.

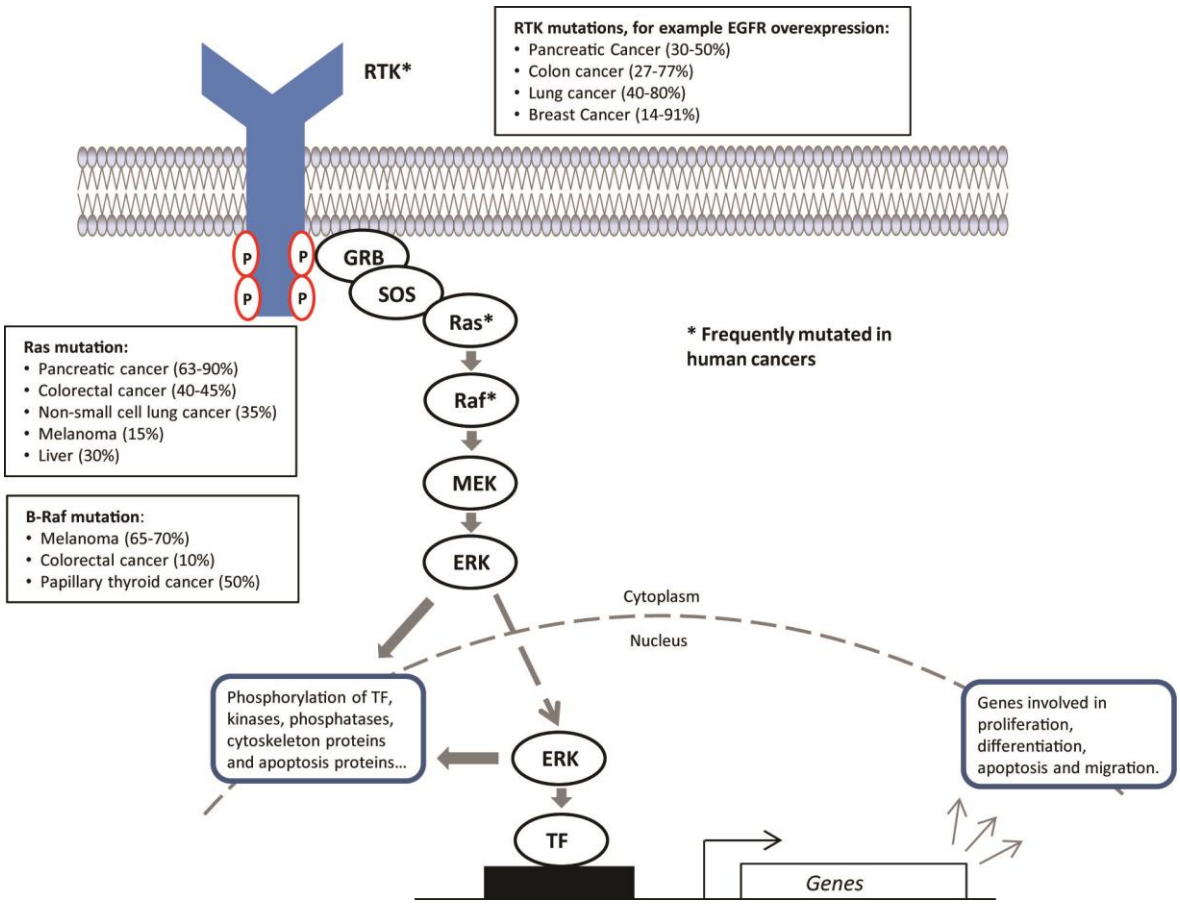

Figure 1.3 The Ras-ERK MAPK cascade and the major mechanisms of oncogenic activation of this signalling pathway. Schematic showing the architecture of the core components of the Ras- extracellular signal regulated kinase (ERK) pathway from the receptor tyrosine kinase (RTK) at the plasma membrane, through the adaptor protein GRB (growth receptor bound protein), the guanine nucleotide exchange factor SOS (son of sevenless) to the small GTPase Ras. Once GTP bound and activated, Ras activates the Raf MAPK kinase kinase (MAPKKK), the initial component of the MAPK module. Raf activity induces the sequential phosphorylation and activation of the remaining MAPK module consisting of, MEK (MAPKK) and ERK itself. Once activated in the cytoplasm, ERK can phosphorylate regulate a large number of cytoplasmic proteins. Additionally, activated ERK is also able to translocate to the cell nucleus where it can phosphorylate and activate transcription factors (TF) and induce the expression of ERK target genes. These encode many proteins involved in the regulation of cell proliferation and/or differentiation, as well as many other cellular processes. Oncogenic activation of the Ras-ERK pathway can occur by overexpression or mutation of a number of components. Commonly occurring mutations are indicated with asterisks, along with the identification of the major cancer types in which these mutations are found to occur at a high frequency.

1.2.3 The classical ERK pathway and cancer

Due to the ability of ERK to influence many of the hallmarks of cancer (Hanahan and Weinberg, 2000, 2011), it is no surprise that ERK deregulation has been implicated in the initiation, progression and maintenance of approximately a third of human cancers. Oncogenic activating mutations or overexpression are commonly found upstream of ERK in genes encoding RTKs, Ras, BRaf and CRaf (Fig. 1.3) (Dhillon et al., 2007; Downward, 2003). In contrast, mutations in MEK and ERK itself are rarely seen in human cancers. This is likely to be due to these proteins requiring dual phosphorylation for their activation, therefore multiple nucleotide base changes would be necessary for their oncogenic activation reducing this probability of this occurring in nature to drive human tumourigenesis (Cowley et al., 1994). RTK or Ras mutations can activate multiple downstream signalling cascades as well as the ERK pathway, making their relative contribution to tumourigenesis somewhat difficult to fully assess (as discussed for pancreatic cancer below). However, the importance of the ERK pathway in human malignancy can be clearly demonstrated by the finding that the MAPKKK BRaf is the driving oncogene in 40-60% of malignant melanomas as well as in a number of other cancer types to a lesser degree. $BRaf^{V600E}$ is the most common mutation, leading to increased kinase activity and hence activation of MEK and ERK (Wan et al., 2004). The development of the $BRaf^{V600E}$-specific inhibitor vemurafenib, and its efficacy in inhibiting ERK activation and tumour cell proliferation in preclinical models, as well as to elicit clinical responses in $BRaf^{V600E}$-positive melanoma patients, demonstrates the dependency of these tumours on Raf-ERK signalling (Bollag et al., 2010; Joseph et al., 2010; Lito et al., 2012).

Many Ras or BRaf mutant cancer cell lines are sensitive to MEK inhibition (MEKi) *in vitro* and *in vivo* (Roberts and Der, 2007), however these initial responses have failed to translate into sustained clinical success due to a variety of drug resistance mechanisms. Some tumour cells can display intrinsic resistance to MEKi through parallel oncogenic pathways active in the tumour. This explains why within a panel of human cancer cell lines BRaf mutant cells have been shown to be far more sensitive to MEKi (addicted to ERK signalling) than those driven by Ras mutations (Solit et al., 2006). Alternatively, the limited success of MEKi in Ras mutant cells could also be due to the loss of ERK-dependent negative feedback systems within the ERK signalling cascade, leading to

reactivation of MEK-ERK following MEKi treatment. ERK signalling is also required to inhibit many RTKs; therefore MEKi induces the rapid activation of an array of RTKs, which would usually be suppressed. This adaptive kinome reprogramming initiates additional oncogenic signalling to compensate for the inhibition of the ERK pathway and minimise the efficacy of MEKi. Finally, tumour cells can evolve acquired resistance to MEKi through a range of mechanisms including the amplification of upstream driving-oncogenes such as Ras or Raf or the accumulation of additional gain of function mutations for example in MEK (Caunt et al., 2015; Little et al., 2011; Poulikakos and Rosen, 2011).

Oncogenic mutations in the ERK pathway lead to sustained ERK activation, which is able to promote cell proliferation, survival, motility and other tumour phenotypes. However, the magnitude of ERK activation is also important in determining its tumourigenic effects. It has been known for a long time that excessive hyperactivation of the ERK pathway *in vitro* elicits cell cycle arrest and senescence by inducing the accumulation of cyclin-dependent kinase inhibitors including CDKN2A and p21 (Meloche and Pouysségur, 2007; Serrano et al., 1997). The can be demonstrated by the fact that although Ras and BRaf mutations are amongst the most frequently mutated oncogenes in human cancers (present in around 30% and 7% of cancers respectively), and both overlap as driver-mutations for colon and lung cancer they are almost never identified in the same tumour (Borràs et al., 2011; Goydos et al., 2005; Karnoub and Weinberg, 2008; Kinno et al., 2014; Pylayeva-Gupta et al., 2011; Sensi et al., 2006). This mutual exclusivity has been experimentally demonstrated by that fact that the co-activation of $BRraf^{V600E}$ and $KRas^{G12D}$ markedly reduced tumour initiation in a mouse model of lung cancer due to elevated oncogene-induced senescence (OIS) (Cisowski et al., 2015). Therefore, for optimal tumour promotion a sustained elevated level, but not excessive hyperactivation, of ERK signalling is required. This conclusion can be further validated by the observation that epidermal growth factor receptor (EGFR) and KRas mutations are mutually exclusive in human lung adenocarcinoma and that their forced co-activation human lung cancer cell lines results in synthetic lethality. Subsequent co-activation of EGFR and KRas mutations in a mouse model of lung cancer results in tumours with only a single mutation, reinforcing the conclusion that their co-expression is deleterious to tumour development (Unni et al., 2015).

1.2.4 The Stress-activated MAPK pathways

The stress-activated protein kinase (SAPK) group of MAPKs comprise the JNK and p38 MAPK families. They display more complex signalling cascade than the prototypical ERK pathway, due to the presence of a large number of MAPKKK proteins which are known to activate these pathways. Both the JNK and p38 pathways can be activated by a variety of environment and cellular stresses, including oxidative stress, DNA-damaging agents, ultraviolet (UV) irradiation, and inflammatory cytokines amongst other stimuli (Cargnello and Roux, 2011; Pearson et al., 2001). Such stimuli induce the activation of an array of MAPKKK proteins including MEKK1-4, MLK1-3, ASK1, TPL2, TAK1 and TAO1/2. It remains unresolved whether MAPKKKs simultaneously regulate the JNK and p38 pathways or whether one pathway is pre-selected through targeting of the activated MAPKKK to a particular substrate (Rincón and Davis, 2009). Signalling specificity becomes apparent at the MAPKK level, with MKK4/7 being responsible for JNK activation (Dérijard et al., 1995; Tournier et al., 1997) and MKK3/6 for p38 activation (Dérijard et al., 1995; Han et al., 1996), although MKK4 has also been shown to possess limited activity towards p38 (Meier et al., 1996).

The first JNK family member was identified as a cycloheximide-activated hepatic protein kinase that phosphorylates MAP-2 on serine and threonine residues, then subsequently as a UV-responsive protein kinase that binds and activates the transcription factor c-Jun (Hibi et al., 1993; Kyriakis and Avruch, 1990; Pulverer et al., 1991). There are three isoforms of JNK (JNK1, 2, 3), encoded by three distinct genes with greater than 85% homology. These genes give rise to 10 alternatively spliced isoforms of JNK, which display different activities towards their target proteins, including the transcription factors c-jun, activating transcription factor 2 (ATF-2) and Elk-1 (Gupta et al., 1996). JNK1 and JNK2 are expressed in a broad range of human tissues, whereas JNK3 expression is localised to neuronal and cardiac tissue as well as the testis (Mohit et al., 1995). The deletion of a combination of JNK1/2, in mice results in embryonic lethality due to defects in patterns of apoptosis during brain development, whereas single JNK knockout or combinations of JNK1/3 or JNK2/3 do not (Kuan et al., 1999). This experiment demonstrates that there is some functional redundancy between JNK1 and JNK2, although this is not always the case in other tissues or in response to different stimuli. Furthermore, it helps to demonstrate the important roles JNKs can play in the control of apoptosis in response to many cellular

stresses (Dhanasekaran and Reddy, 2008). Mouse embryonic fibroblasts (MEFs) isolated from JNK1/2 or MKK4/7 knockout mice are resistant to UV irradiation induced apoptosis. This loss of JNK signalling prevented cytochrome c release, indicating a requirement for JNK in promoting the intrinsic apoptotic pathway in response to genotoxic stress (Tournier et al., 2000). Furthermore, the targeted activation of JNK1/2 protects cells from apoptosis following serum starvation (Molton et al., 2005). JNK1 and JNK2 have also been shown to play important and differential roles in the control of cell proliferation. $JNK2^{-/-}$ MEFs proliferate faster than wild-type littermates, whereas $JNK1^{-/-}$ and $JNK1^{-/-}$/$JNK2^{-/-}$ MEFs proliferate slower (Tournier et al., 2000). JNK1 activity promotes c-Jun activation, AP-1 complex formation and induction of AP-1-target genes, including genes such as cyclin D1, which are responsible for cell cycle progression. Whereas, JNK2 was shown to primarily bind c-Jun in its inactive state and target c-Jun for degradation (Sabapathy et al., 2004). Finally, JNKs also have important roles in the development of and regulation of immune cell function (Rincón and Davis, 2009).

p38α was discovered simultaneously by three groups in 1994 as a MAP kinase activated in response to various stresses including heat shock, osmotic stress and lipopolysaccharide (LPS) (Han et al., 1994; Lee et al., 1994; Rouse et al., 1994). The p38 MAP kinase family consists of four isoforms: p38α, β, δ and γ, of which the archetypal member p38α is the most studied. p38α and p38β are expressed ubiquitously in all tissues, whereas p38δ and p38γ exhibit more localised expression (Kyriakis and Avruch, 2012). Genetic deletion of p38α results in embryonic lethality in mice due to incomplete placental development (Adams et al., 2000; Mudgett et al., 2000), and conditional deletion in the embryo, to bypass these placental defects, also results in death shortly after birth due to lung defects (Hui et al., 2007). p38 signalling plays an important role in immune and inflammatory responses (Cuadrado and Nebreda, 2010). In response to extracellular mediators of inflammation, such as cytokines, chemokines and LPS, p38 signalling can induce the production of pro-inflammatory cytokines to intensify the immune response. p38 signalling regulates pro-inflammatory cytokine expression is through the modulation of transcription factors including NF-κB (Rincón and Davis, 2009), and at the post-transcriptional level through the regulation of mRNA stability (Clark et al., 2009; Gaestel, 2013). MAPK-activated protein kinase 2 (MK2) deficient mice demonstrate a significant reduction in TNFα protein production, despite no change in the mRNA expression,

following an LPS challenge showing MK2 to be the major kinase downstream of p38 responsible for the post-transcriptional regulation of cytokine biosynthesis (Kotlyarov et al., 1999). Furthermore, p38α has been associated with the regulation of cell proliferation and apoptosis. p38α signalling activates the G1/S and G2/M checkpoints to inhibit proliferation and it has been implicated with the induction of apoptosis following cellular stress (Thornton and Rincon, 2008).

1.2.5 The JNK pathway and cancer

Sequencing of human tumour samples has revealed that components of the JNK pathway are frequently mutated in a diverse range of cancers including pancreatic, lung and colorectal (CRC). Genes mutated include MKK4, MKK, JNK1 and JNK2 and the mutations were typically truncating or mis-sense mutations indicating that loss of JNK signalling might contribute to tumorigenesis (Davies et al., 2005; Greenman et al., 2007; Jones et al., 2008). However, the role of the JNK isoforms in cancer appears complex, with JNK1 and JNK2 exhibiting both oncogenic and tumour suppressive functions across a range of *in vitro* and *in vivo* model systems (Wagner and Nebreda, 2009; Weston and Davis, 2007).

Initial *in vitro* experiments demonstrated JNK signalling promoted Ras, c-Abl or Met-induced cell transformation, suggesting an oncogenic role for JNK activity (Clark et al., 1997; Raitano et al., 1995; Rodrigues et al., 1997). However, strikingly this is not the case for transformation assays performed *in vivo*. Injection of Ras-transfected JNK1/2 null cells into athymic, immunocompromised mice caused a significant increase in the number and size of Ras-induced tumour nodules compared to wild-type Ras-transfected cells, even though these same JNK1/2 null cells were found to be resistant to Ras-induced transformation *in vitro* (Kennedy et al., 2003). This observation correlates with the occurrence of loss of function mutations in the JNK pathway in human tumours in suggesting that JNKs are tumour suppressive. This is further supported by evidence that mice lacking JNK signalling, through ablation of MKK4 and MKK7, show increased sensitivity to $KRas^{G12D}$-driven pancreatic carcinogenesis (Davies et al., 2014). However, experiments utilising mice lacking individual JNK isoforms demonstrate a more complex role of JNK signalling in cancer, possibly reflecting their divergent functions elucidated *in vitro*. Furthermore, the same JNK isoform has the ability to act as an oncogene in some cancer types, but a tumour suppressor in others, demonstrating potential tissue-specific

roles of the JNK isoforms. For instance, JNK1$^{-/-}$ mice show increased sensitivity to 7,12-Dimethylbenz[a]anthracene/12-O-tetradecanoylphorbol-13-acetate (DMBA/TPA)-induced skin carcinogenesis, whereas JNK2$^{-/-}$ mice were protected. The differential effects of JNK1 or JNK2 ablation were mediated by the opposing abilities of JNK1 and JNK2 to influence ERK and AKT activity, with JNK1 loss promoting their activity and JNK2 loss inhibiting it (Chen et al., 2001; She et al., 2002). Whereas, in the diethylnitrosamine (DEN)-induced liver cancer model JNK1$^{-/-}$, but not JNK2$^{-/-}$, mice show decreased sensitivity to tumourigenesis. JNK1 was shown to promote the growth and proliferation of liver tumours and cell lines through its ability to inhibit p53-dependent pro-apoptotic signalling (Hui et al., 2008; Sakurai et al., 2006).

1.2.6 The p38 MAPK pathway and cancer

Unlike the ERK and JNK pathways, there is very limited evidence for mutations within the p38 pathway in human cancers. As mentioned above, MKK4 inactivating mutations have been discovered in a range of human cancers (Greenman et al., 2007), and although it is able to activate p38 it is primarily thought to target JNK, therefore it is unclear whether alterations in p38 signalling would occur or have any functional role in these cancers. The only other link to p38 signalling of any significance is the amplification of the p53-inducible phosphatase WIP1/PPM1D in around 11% of breast cancers, and some ovarian cancers (Bulavin et al., 2002; Lu et al., 2008). WIP1/PPM1Ds oncogenic function has been linked to its ability to dephosphorylate p38α, inhibiting p38α's ability to negatively regulate tumour cell proliferation (Bulavin et al., 2004). However, WIP1/PPM1Ds is also capable of negatively regulating the activity the tumour suppressors p53, ATM and CDKN2A, therefore the relative importance of p38α signalling to the pro-oncogenic effects of WIP1/PPM1D is unclear (Lu et al., 2008).

In experimental systems the role of p38 isoforms appears complex. Both *in vitro* and *in vivo* studies demonstrate a tumour suppressive role for p38α. Immortalised p38α$^{-/-}$ MEFs show increased sensitivity to HRas^{V12}-driven transformation in culture and generate an elevated tumour burden following their injection into athymic mice (Dolado et al., 2007). Fetal haematopoietic cells and MEFs from p38α$^{-/-}$ mice demonstrate increased proliferation, which is dependent on the ability if p38α loss to induce the hyperactivation of the JNK pathway (Hui et al., 2007). In murine models the conditional deletion of p38α

has been shown to sensitise mice to $KRas^{G12V}$-induced lung tumours (Ventura et al., 2007) and DEN-induced liver cancer (Hui et al., 2007). Although the majority of evidence supports a tumour suppressive role for p38α, there is some evidence that in certain contexts it could be oncogenic. p38α may promote tumour development through the upregulation of autophagy (Comes et al., 2007), the promotion of tumour cell invasion (Rousseau et al., 2006) and the induction of pro-inflammatory cytokines and thus an elevated inflammatory response, which is known to be a causative factor in many cancer types (Kumar et al., 2003; Schieven, 2009).

More recently, the roles of other p38 isoforms in cancer development have begun to be elucidated. Evidence from MEFs lacking p38γ and p38δ suggests that loss of either isoform promotes increased migration, whereas only p38δ loss impaired cell contact inhibition and only p38γ loss promotes $KRas^{V12}$-driven proliferation, transformation and tumour formation in athymic mice (Cerezo-Guisado et al., 2011). In murine models the loss of p38δ has been shown to protect mice from DMBA/TPA-induced skin tumours and $KRas^{G12D}$-driven lung tumours (Schindler et al., 2009), whereas conditional p38γ ablation attenuates colitis-associated tumourigenesis (Yin et al., 2016). Furthermore the dual-deletion of p38γ and p38δ protects mice from DMBA/TPA-induced skin tumourigenesis and colitis-associated tumourigenesis (Reino et al., 2014; Zur et al., 2015). In summary, although both p38γ and p38δ appear to show a tumour suppressive phenotype *in vitro* and in immunocompromised mice, they demonstrate strong oncogenic phenotypes across multiple cancer models, including most strikingly in inflammation-associated cancer. This highlights the key role of p38γ and p38δ in the regulation of the inflammatory response as well as the importance of this process in cancer development.

Within both the JNK and p38 families' individual isoforms have shown diverse roles in cancer development and additionally specific isoforms have demonstrated opposing functions in different tumour contexts. This contrasts with the ERK pathway where both isoforms appear functionally redundant (Frémin et al., 2015) and are primarily known to act in an oncogenic manner. The roles of the JNK and p38 isoforms are likely to be both cell context and cell-type dependent due to many factors including: the wide range of stimuli which are able to activate these pathways, their range of tissue specific

expression, the fact that many stimuli will activate both pathways simultaneously and the crosstalk which occurs between them (Wagner and Nebreda, 2009).

1.2.7 Spatiotemporal regulation of MAPK signalling

The duration, magnitude and subcellular localisation of MAPK activation are all crucial parameters, which determine the biological outcome of signalling. These factors can be modulated in a variety of ways to determine the dynamics of MAPK signalling, including through alterations in the kinetics and magnitude of the stimuli that initiate signalling activity, post-translational modifications of the MAPK itself, the binding of MAPKs to scaffold proteins or the influence of negative feedback regulation within the MAPK pathway (Ebisuya et al., 2005; Kholodenko et al., 2010; Marshall, 1995). This section will outline evidence for how many of these factors can cooperate in regulating the spatiotemporal activity of the ERK pathway, as this pathway is the primary focus of this thesis.

The importance of temporal control of ERK activity was first revealed when it was demonstrated to be a critical factor in the regulation of cell fate decisions. EGF stimulation of rat pheochromocytoma (PC12) cells was shown to induce transient ERK activation and to induce cell proliferation, whereas nerve growth factor (NGF) stimulation generated sustained ERK activation, increased nuclear *p*-ERK accumulation and induced neural differentiation (Marshall, 1995; Traverse et al., 1992). The EGF receptor undergoes rapid internalisation and degradation following activation in comparison to other receptors, explaining its more transient signalling (Countaway et al., 1992). However, the overexpression of the EGFR is able to convert this transient response to a more sustained activation of ERK and mimic the effects of NGF in causing neuronal differentiation (Traverse et al., 1994). Therefore, differences in signalling dynamics are one factor that can determine the spatiotemporal effects of different growth factor stimuli on ERK activation and thus signalling outcome. Similar effects have also been demonstrated in the balance between continued cell proliferation or apoptosis in developing T cells (Werlen et al., 2003).

One of the principle mechanisms controlling ERK subcellular localisation is the regulation of ERK targeting to the nucleus. Nuclear translocation of ERK was initially thought to

require phosphorylation-dependent dimerization of ERK (Cobb and Goldsmith, 2000; Khokhlatchev et al., 1998). However, subsequent studies have shown that ERK nuclear translocation can occur by the passive diffusion of ERK monomers or the active transport of dimers (Adachi et al., 1999), and can in fact be dimerization independent (Casar et al., 2008; Lidke et al., 2010). Nuclear translocation of ERK requires phosphorylation of ERK by MEK, as MEK is able to anchor inactive ERK in the cytoplasm (Adachi et al., 2000; Rubinfeld et al., 1999), and the MEK-mediated phosphorylation of ERK is necessary for the dissociation of ERK from MEK (Adachi et al., 1999). Furthermore, a 3 amino acid sequence (SPS) has been identified that when phosphorylated induces nuclear translocation of ERK. This could be a mechanism which targets activated ERK to the nucleus (Chuderland et al., 2008; Zehorai et al., 2010). Finally, it has been shown that ERK homodimers are essential for binding to many cytoplasmic substrates and scaffolds, but nuclear substrates almost exclusively associate with ERK monomers (Casar et al., 2008). Together these findings establish dimerization and nuclear translocation signal activation as key determinants of the spatial specificity of ERK signalling.

Scaffold proteins can also regulate the spatial distribution of MAPKs, by targeting MAPKs to specific subcellular organelles and substrates, to modulate the signalling outcome. Cytoplasmic scaffold proteins such as PEA-15 can sequester ERK in the cytosol, to constrain ERK-dependent transcription (Formstecher et al., 2001). Other scaffold proteins can localise ERK to precise subcellular localisations to promote a specific biological response. For example, following hepatocyte growth factor stimulation of epithelial cells the multidomain scaffold protein paxillin facilitates the localisation of Raf-MEK-ERK complexes at focal adhesions. ERK-dependent phosphorylation of paxillin induces the recruitment of focal adhesion kinase (FAK) to stimulate microtubule formation and cell migration (Ishibe et al., 2004). Furthermore, scaffold proteins such as Kinase suppressor of Ras (KSR) and MEK partner-1 (MP1), have been shown to sequester ERK pathway components together to facilitate more efficient sequential activation, thereby increasing the magnitude of ERK signalling (Kolch, 2005). The magnitude of ERK signalling can regulate the ensuing biological outcome. In most cell types ERK activation is necessary for cell cycle progression. However, ERK hyperactivation, induced by cellular stress or oncogenic transformation, elicits cell cycle arrest through the induction of cell cycle

inhibitory proteins including the p53, p21, p16Ink4a and retinoblastoma (Rb) (Meloche and Pouysségur, 2007; Serrano et al., 1997).

The opposing action of upstream pathway activators and negative regulatory mechanisms can modulate the duration and magnitude of MAPK activation (Caunt and Keyse, 2013) (Fig. 1.4 outlines many of the key negative feedback systems within the ERK pathway). Negative regulatory mechanisms can be induced as classical negative feedback systems or as crosstalk from alterative signalling pathways and can act at multiple levels within the MAPK pathway (Fey et al., 2012; Shin et al., 2009). Negative feedback systems within the ERK pathway can be controlled through post-translational modifications of pathway components or regulators or through transcriptional activation of negative regulators. ERK-mediated feedback phosphorylation of the upstream pathway components MEK (Catalanotti et al., 2009; Eblen et al., 2004), Raf (Dougherty et al., 2005), the Ras-activating GEF SOS (Douville and Downward, 1997) or some RTKs (Ramos, 2008) can inhibit their activity generating rapid negative feedback loops to dampen and constrain ERK pathway activation. ERK signalling can also induce transcriptional negative feedback through the de novo expression of immediate early genes such as sprouty proteins and phosphatases which target ERK, primarily MKPs. Sprouty proteins are also regulated through phosphorylation in response to ERK activation and inhibit ERK signalling at the level of RTKs, SOS and Raf (Hanafusa et al., 2002; Mason et al., 2006; McKay and Morrison, 2007). The interplay of fast and delayed feedback loops allows complex signalling responses to be generated in response to a constant stimulus. Computational modelling has demonstrated the ability of tuneable combinations of these feedback systems to generate a variety of temporal responses in ERK signalling following a constant stimulus, including sustained, bistable switch-like or oscillating responses, allowing ERK to signal for distinct biological outcomes (Kholodenko et al., 2010; von Kriegsheim et al., 2009).

Dephosphorylation and inactivation of MAPKs themselves constitutes a major negative feedback system within MAPK cascades. This can be performed by 3 classes of protein phosphatases: serine/threonine-specific phosphatases, tyrosine-specific phosphatases or dual-specificity phosphatases (DUSPs) (Fig. 1.5) (Keyse, 2000). The focus of this thesis are

the MKPs, a sub-family of cysteine-dependent phosphatases within the DUSPs, which specifically target the MAPKs.

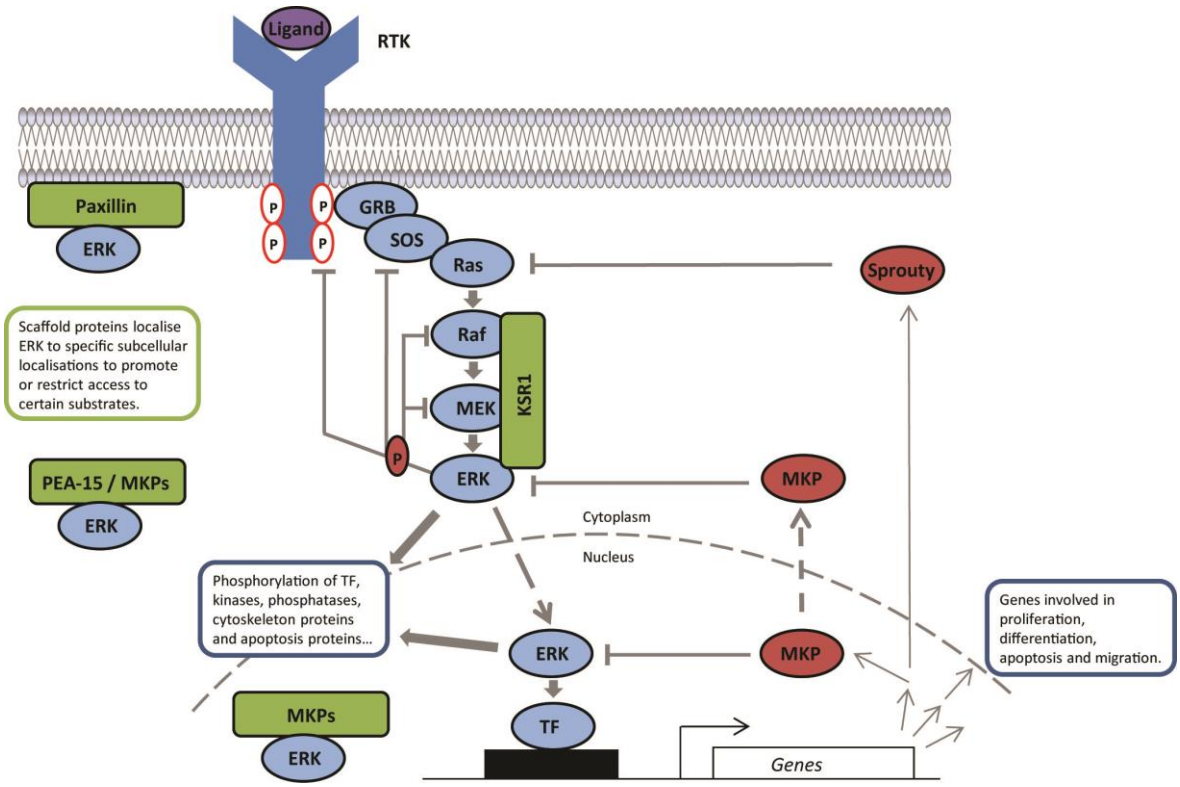

Figure 1.4 Spatiotemporal regulation of the Ras-ERK MAPK pathway. Schematic showing the architecture of the core components of the Ras- extracellular signal regulated kinase (ERK) pathway (Blue), as well as major negative feedback systems (Red) and scaffold proteins (green) which can regulate ERK pathway activity and localisation. The Ras-ERK pathway is classical activated through ligand-induced receptor tyrosine kinase (RTK) activation at the plasma membrane, inducing binding of the adaptor protein GRB (growth receptor bound protein) and the guanine nucleotide exchange factor SOS (son of sevenless). SOS promotes GTP binding to the small GTPase Ras. Active, GTP-bound Ras induces the sequential activation of the MAPK module consisting of, Raf, MEK and ERK itself. Once activated in the cytoplasm, ERK can phosphorylate and regulate a plethora of cytoplasmic proteins, including inhibitory phosphorylation of upstream Ras-ERK pathway components such as RTKs, SOS or Raf, thus exerting negative feedback control over pathway activation. Additionally, activated ERK is also able to translocate to the cell nucleus where it phosphorylates and activates transcription factors (TF) and induces the expression of ERK target genes. These encode many proteins involved in the regulation of cell proliferation and/or differentiation, as well as many other cellular processes. One major class of ERK target genes are negative feedback regulators of the ERK pathway itself, including the Sprouty proteins and MAPK phosphatases (MKPs). The scaffold protein KSR1 is able to localise all components of the ERK MAPK module together, facilitating efficient sequential activation, thereby increasing the magnitude of ERK signalling. Other scaffold proteins sequester active or inactive ERK to particular subcellular compartments to either promote ERK activation of specific targets, or to sequester ERK prior to subsequent activation.

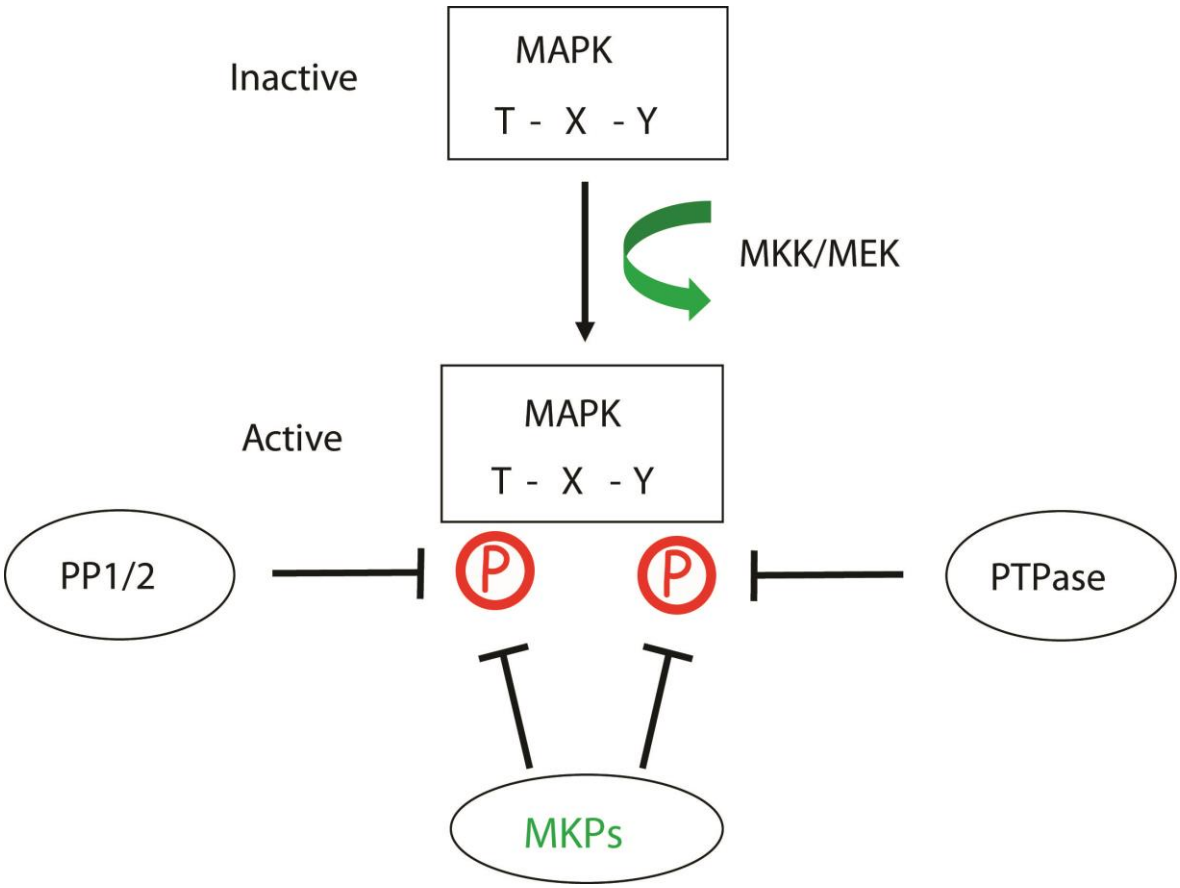

Figure 1.5 Regulation of MAPK phosphorylation and activity. Phosphorylation of the threonine and tyrosine residues in the T-X-Y motif of the MAPK activation loop are critical for kinase activation. Dual phosphorylation of these residues by upstream MAPKKs such as MEK or MKK facilitates MAPK activation. Three groups of phosphatase can mediate the dephosphorylation of the T-X-Y motif resulting in MAPK inactivation. Ser/Thr protein phosphatases such as PP2A can act upon the Thr residue, whilst tyrosine phosphatases such as PTPase family target the Tyr residue. DUSPs/MKPs have the ability to inactivate MAP kinases through dephosphorylation of both of these phosphorylated residues.

1.3 Dual-specificity MAP kinase phosphatases (MKPs/DUSPs)

1.3.1 MKP classification, structure & function

MKPs are DUSPs with the ability to specifically dephosphorylate both the threonine and tyrosine residues of the T-X-Y motif within the kinase activation loop of MAPKs and which are required for MAPK activation (Fig. 1.5) (Patterson et al., 2009). There are ten catalytically active MKPs in mammalian cells. The MKPs share a common structure consisting of an N-terminal non-catalytic domain and a conserved C-terminal catalytic domain, containing the conserved cysteine-dependent PTPase consensus active site sequence C(X)5R (Dickinson and Keyse, 2006). All classical PTPases employ a common catalytic mechanism in which the cysteine residue of the active site initiates nucleophilic attack on the substrate phosphorous atom (Tonks, 2006). At the same time as the ester bond is cleaved, a conserved aspartic acid residue acts as a general acid to protonate the oxygen of the tyrosine leaving group. The resulting phospho-cysteine intermediate is resolved by the activation of water by the same aspartic acid residue (now acting as a general base) and its hydrolysis to yield the restored enzyme and inorganic phosphate (Labbé et al., 2012; Tonks, 2006). Structural studies reveal that DUSPs such as the MKPs have a very shallow active site cleft when compared with classical PTPs and it is this feature, which is thought to underpin the ability of these enzymes to dephosphorylate both tyrosine and Ser/Thr residues (Stewart et al., 1999; Yuvaniyama et al., 1996). The N-terminal non-catalytic domain has been shown to be a regulatory region, containing a kinase interaction motif (KIM), which facilitates the specific binding of MKPs to their target MAPKs. Many MKPs also contain either nuclear localisation signals (NLS) or nuclear export signals (NES) that determine their subcellular localisation (Caunt and Keyse, 2013; Owens and Keyse, 2007).

The MKPs have been divided into three subfamilies based on their gene structure, amino acid sequence homology, substrate specificity and subcellular localisation (Table 1.2) (Camps et al., 1998; Keyse, 2000; Theodosiou and Ashworth, 2002). One group comprises of the mitogen or stress-inducible, nuclear MKPs, DUSP1/MKP-1, DUSP2, DUSP4/MKP-2 and DUSP5. These inducible MKPs exhibit nuclear localisation and the ability to bind and dephosphorylate all three major classes of MAPK (ERK, JNK and p38), with the exception

of DUSP5 which is highly ERK-selective. A second group consists of the cytoplasmic ERK-selective MKPs: DUSP6/MKP-3, DUSP7 and DUSP9/MKP-4. Finally, a third group contains the JNK/p38-specific MKPs DUSP8, DUSP10/MKP-5 and DUSP16/MKP-7, which are found in both the nucleus and the cytoplasm.

MKPs are predominantly expressed at relatively low levels in unstimulated cells and are transcriptionally induced as immediate early genes following mitogenic or stress stimulation and MAPK pathway activation. Following the removal of a transient stimulus MKP transcription is reduced, allowing ubiquitination and protein degradation to restore MKP expression to basal levels (Bermudez et al., 2010). Therefore, MKPs were first thought to solely act as classical negative feedback regulators of MAPK signalling. However, subsequently a range of other pathways which are able to induce MKP expression have been identified. For example, Wnt-β-catenin signalling has been demonstrated to induce DUSP6/MKP-3 expression during zebrafish development and in murine hepatoma cells (Tsang et al., 2004; Zeller et al., 2012). Furthermore, DUSP1/MKP-1 is transcriptionally regulated by p53 during responses to oxidative stress (Liu et al., 2008), and transforming growth factor-β (TGFβ) can induce DUSP4/MKP-2 expression in a SMAD3-dependent manner in lymphocytes (Ramesh et al., 2008). Thus as well as acting as negative feedback regulators of MAPK activity MKPs can mediate crosstalk between a variety of other signalling pathways and the MAPK cascades in a range of different contexts. It is likely that the full extent of MKP mediated crosstalk is yet to be discovered.

Post-translational modification of MKPs also plays a key role in the control of their expression levels and activity. Phosphorylation by MAPKs has been shown to mediate either MKP protein stability or to increase the rate of degradation. For example, ERK-mediated phosphorylation of Ser359/364 in DUSP1/MKP-1 increases protein stability and thus the strength of negative feedback (Brondello et al., 1999), whereas phosphorylation of Ser296/323 results in ubiquitin ligase recruitment and increased DUSP1/MKP-1 degradation (Lin and Yang, 2006; Lin et al., 2003). ERK-mediated phosphorylation of Ser159/197 on DUSP6/MKP-3 promotes its ubiquitin-mediated degradation (Marchetti et al., 2005), this occurs to such an extent that DUSP6/MKP-3 expression is lost immediately following platelet-derived growth factor (PDGF) stimulation, before being restored through ERK-mediated transcriptional activation (Jurek et al., 2009). This demonstrates

how reductions in MKP expression can also be essential for optimal MAPK activation following a stimulus and that MKPs have a more complex role in modulating MAPK activity than solely as negative feedback regulators. This can also be demonstrated by the observation that protein kinase-A (PKA) is able to phosphorylate the KIM motif of DUSP9/MKP-4, preventing the phosphatase from binding and inactivating ERK and p38 substrates (Dickinson et al., 2011). This post-translational regulation of an MKP by a non-MAPK pathway highlights another mechanism by which MKPs can facilitate crosstalk between distinct signalling pathways.

Finally, whilst some MKPs are intrinsically active, others including DUSP1/MKP-1, DUSP4/MKP-2 and DUSP6/MKP-3 undergo “catalytic activation”, a process in which binding of the MAPK substrate to the amino-terminal non-catalytic domain of the phosphatase induces an allosteric change within the catalytic domain of the MKP. This causes several residues within the active site of the enzyme, and particularly the conserved aspartic acid “general acid” residue, to adopt an optimal conformation for catalysis. (Camps et al., 1998; Slack et al., 2001). This catalytic activation is thought to further reinforce the substrate selectivity of MKPs, which is already determined by the ability of the KIM to recognise and specifically bind particular MAPKs, and thus to further prevent any promiscuous activity against non-MAPK substrates (Caunt and Keyse, 2013). Other MKPs such as DUSP5 and DUSP10/MKP-5 do not have the ability to undergo catalytic activation, as binding to their substrates does not increase their basal activity (Mandl et al., 2005; Tanoue et al., 1999). The crystal structures of the catalytic domains for DUSP5 and DUSP10/MKP-5 show the general acid-containing loop to already be in the optimal position for catalysis, unlike that of DUSP6/MKP-3 (Jeong et al., 2006, 2007; Stewart et al., 1999). This provides an explanation for the lack of catalytic activation of DUSP5 and DUSP10/MKP-5. However, at the present time it is unclear as to why some MKPs undergo catalytic activation while others do not.

Family	MKP	Subcellular Localisation	Substrate Specificity	Inducible by MAPKs:	Domain Structure
Nuclear inducible MKPs	DUSP1 / MKP-1	Nuclear	JNK = p38 > ERK	ERK, p38	
	DUSP2	Nuclear	ERK = p38 > JNK	ERK, JNK	
	DUSP4 / MKP-2	Nuclear	ERK = JNK > p38	ERK	
	DUSP5	Nuclear	ERK	ERK	
Cytoplasmic ERK-selective MKPs	DUSP6 / MKP-3	Cytoplasmic	ERK	ERK	
	DUSP7 / MKP-X	Cytoplasmic	ERK	N/D	
	DUSP9 / MKP-4	Cytoplasmic	ERK > p38	N/D	
JNK/p38-specific MKPs	DUSP8	Cytoplasmic/ nuclear	JNK = p38	N/D	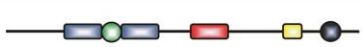
	DUSP10 / MKP-5	Cytoplasmic/ nuclear	JNK = p38	N/D	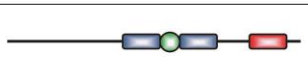
	DUSP16 / MKP-7	Cytoplasmic/ nuclear	JNK = p38	N/D	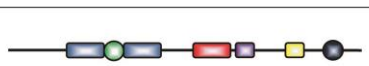

Table 1.2 MAP kinase phosphatase (MKP) structure, function and classification. The 10 mammalian dual-specificity MKPs divided into three groups based on their similarity, subcellular localisation and substrate specificity. The schematics in the final column demonstrate the domain structures of the MKPs, highlighting the localisation of the kinase interaction motif (KIM) within the N-terminal non-catalytic domain and the catalytic site within the C-terminal domain. N/D, not determined.

1.3.2 Spatiotemporal regulation of MAPK signalling by MKPs

Through their ability to specifically regulate the phosphorylation status, activity and subcellular localisation of MAPKs, MKPs are able to modulate the magnitude, duration and spatial limits of MAPK activity. In addition to this, MKPs bind MAPK substrates in a phosphorylation-independent manner, so are also able to anchor substrate MAPKs in distinct subcellular compartments following dephosphorylation (Caunt and Keyse, 2013; Karlsson et al., 2004; Mandl et al., 2005). Furthermore, due to the differing mechanisms and kinetics of induction, substrate specificity and subcellular localisation of each individual MKP, the family as a whole is able to precisely influence MAPK activity in in a context-dependent manner. Together these properties indicate that MKPs have a greater role than simply acting as negative feedback regulators of MAPK activity and are able to regulate MAPK kinetics, substrate targeting and crosstalk (Caunt and Keyse, 2013).

The temporal regulation of MAPK signalling by MKPs can mediate multiple functional responses including autoregulation, a signalling "memory" and crosstalk between signalling pathways (Caunt and Keyse, 2013). Following a mitogenic stimulation transcriptional activation of the ERK-specific MKPs DUSP5 and DUSP6/MKP-3 is induced in an ERK-dependent manner (Ekerot et al., 2008; Kucharska et al., 2009). This forms a delayed auto-regulatory negative-feedback loop; therefore such MKP expression would constrain sustained, but not transient, ERK activation. However, if cells are quickly exposed to a subsequent stimulus and the MKP protein is still present, it will modulate the initial response to this signal potentially constraining transient ERK activation. Consequently, the cell will have retained a temporal memory from the initial signal which will affect the biological response to subsequent stimuli (Caunt and Keyse, 2013). Furthermore, MKPs can facilitate crosstalk between discrete MAPK pathways. This can occur through the induction of MKPs with a broad MAPK-specificity, for example the MKPs DUSP1/MKP-1 and DUSP4/MKP-2 are transcriptionally induced by the ERK pathway yet can target the ERK, JNK and p38 or ERK and JNK pathways respectively (Brondello et al., 1997; Chu et al., 1996), thus enabling ERK activation to regulate JNK and p38 signalling output (Staples et al., 2010). Finally, any non-MAPK signalling pathways which are able to induce MKP expression, such as p53, β-catenin or TGFβ, are able to modulate MAPK signalling. This places MKPs as key regulators of MAPK crosstalk to consolidate multiple signalling inputs.

The ability of MKPs to anchor dephosphorylated MAPKs in a precise subcellular location could perform a capacitor-like function, whereby the accumulation of inactive MAPKs would facilitate rapid reactivation in this location in response to upstream signalling (Caunt and Keyse, 2013). By such a process you could conceive how the physiological levels of the ERK-specific MKPs such as DUSP5 and DUSP6/MKP-3 could mediate the kinetics of ERK activation. High levels of DUSP6/MKP-3 protein would induce the cytoplasmic accumulation of dephosphorylated ERK, facilitating rapid reactivation of this ERK store by active MEK. Conversely, the nuclear MKP DUSP5 would sequester inactive ERK in the nucleus, possibly restricting it's assess to MEK and preventing rapid reactivation. However, such a role for DUSP5 might not be the case as, although primarily a cytoplasmic protein, MEK has been shown to have the ability to translocate to the nucleus and ERK activation in the nucleus has been observed (Chuderland et al., 2008; Mandl et al., 2005; Zehorai et al., 2010). Alternatively, dephosphorylated, anchored MAPKs may have the ability to modulate specific sets of substrates in a non-catalytic manner to generate unique signalling outcomes, and thus specific localisation by MKPs could promote such outcomes (Caunt and Keyse, 2013; Rauch et al., 2011).

A more detailed understanding of MKP regulation could help elucidate how mechanisms of autoregulation within MAPK pathways and systems of crosstalk with other pathways modulate the signalling outcome. This thesis is focused on the ERK-specific MKPs DUSP5 and DUSP6/MKP-3, in particular any differences in their ability to modulate the ERK pathway activity resulting from their differential localisation and their roles in cancer development and progression. See Kidger and Keyse, (2016a) for a comprehensive review on the roles of all the MKPs in cancer.

1.3.3 DUSP5

DUSP5 (also known as B23, hVH3) was first identified through screening a mammary epithelial cell cDNA library for sequences encoding putative protein tyrosine phosphatases using low-stringency hybridisation probes for the catalytic domains of the human VHR and mouse 3CH134 phosphatases (Ishibashi et al., 1994). DUSP5 mRNA was shown to be induced in response to mitogenic signalling (including serum, EGF and TPA) and some cellular stresses such as heat shock (Ishibashi et al., 1994; Kwak and Dixon, 1995). The DUSP5 gene was subsequently shown to be located on human chromosome

10 (Martell et al., 1994). Through its amino acid sequence homology and subcellular localisation, DUSP5 can be classified as a member of the nuclear-inducible group of MKPs (Kwak and Dixon, 1995), although unlike other members of this subgroup of MKPs it shows a substrate specificity for ERK and does not interact with JNK and p38 MAPK isoforms (Mandl et al., 2005). DUSP5's N-terminal non-catalytic domain contains a KIM motif to allow specific binding to ERK and an NLS, which facilitates its nuclear localisation. These features combined with its catalytic activity allow DUSP5 to specifically dephosphorylate nuclear *p*-ERK, and then anchor this inactive ERK in the nucleus (Mandl et al., 2005).

The induction of DUSP5 mRNA and protein in response to growth factor stimulation is dependent on ERK activation (Kucharska et al., 2009), demonstrating that DUSP5 can act as a classical negative feedback regulator of the ERK pathway. Recently, the transcription factors serum response factor (SRF) and ELK1 have been shown to be essential for the EKR-mediated induction of DUSP5 (Buffet et al., 2015). DUSP5 protein has a short half-life and is rapidly downregulated by ubiquitination and proteasomal degradation (Kucharska et al., 2009). DUSP5 is also phosphorylated *in vitro* and *in vivo* on three sites (Thr321, Ser346 and Ser376) in its N-terminal regulatory domain by ERK in a manner that is dependent on the KIM-mediated binding of DUSP5 to ERK. However, mutation which abrogate this phosphorylation does not seem to affect the stability of DUSP5 protein (Kucharska et al., 2009), in a similar manner to the ERK-dependent phosphorylation of other MKPs such as DUSP1/MKP-1 and DUSP6/MKP-3 (Brondello et al., 1999; Lin and Yang, 2006; Marchetti et al., 2005). In fact further analysis could not reveal any function for the ERK-mediated phosphorylation of DUSP5 in terms of effects on substrate specificity, cellular localisation, or its ability to anchor ERK in the nucleus (Kucharska et al., 2009). However, DUSP5 was found to be stabilised by complex formation with ERK independently of any phosphorylation events, indicating that substrate binding by DUSP5 may prolong its ability to dephosphorylate and act as a nuclear anchor for ERK (Kucharska et al., 2009).

DUSP5 is one of the least studied of the MKPs. This is probably because for many years it was assumed to behave similarly to DUSP1/MKP-1 and DUSP4/MKP-2, and also due to a lack of reagents, in particular commercially available DUSP5-specific antibodies. However,

despite this a number of physiological roles have been proposed for DUSP5. These include, a role in p53-dependent suppression of cell proliferation, as DUSP5 was revealed to be a direct transcriptional target of p53 (Brynczka et al., 2007; Ueda et al., 2003). DUSP5 is also proposed to play a role in T-cell development due to the observation that it was highly induced following IL-2 stimulation of T-cells, where it was assumed to be involved in regulating ERK activity (Kovanen et al., 2003). The same group subsequently demonstrated that in transgenic mice overexpressing DUSP5 in the lymphoid compartment thymocyte development was arrested at the double positive stage and that these animals went on to develop autoimmune symptoms. Furthermore, DUSP5-overexpressing mature T cells exhibited decreased IL-2-dependent gene expression and proliferation (Kovanen et al., 2008). However, whilst striking these results are probably more reflective of the role of ERK in immune system development, IL-2 signalling, and immune tolerance as the overexpression of DUSP5 will act as a potent ERK inhibitor rather than recapitulating its true physiological role. Consequently, either knockdown or the genetic ablation of DUSP5 would be much more informative in revealing the *bona fide* role(s) of DUSP5. DUSP5 overexpression was also used to demonstrate that DUSP5 expression (or ERK inhibition) can help to attenuate collagen-induced arthritis in mice (Moon et al., 2014).

Genetic ablation or siRNA knockdown of DUSP5 have also linked this MKP to other physiological functions including: a negative regulator of corneal epithelial cell proliferation (Wang et al., 2010), as a negative regulator of IL-33-dependent eosinophil function and survival (Holmes et al., 2015), and as a regulator of cardiac fibroblast proliferation and cardiac hypertrophy (Fan et al., 2014; Ferguson et al., 2013; Tao et al., 2015; Wickramasekera et al., 2013).

1.3.4 DUSP6/MKP-3

DUSP6/MKP-3 (also known as MKP-3) was independently identified by three groups, and shown to selectively bind and dephosphorylate ERK, with only very weak catalytic activity against either the JNK or p38 MAPKs (Groom et al., 1996; Mourey et al., 1996; Muda et al., 1996). DUSP6/MKP-3 displayed cytoplasmic localisation (Groom et al., 1996; Mourey et al., 1996), making it the prototypical member of the cytoplasmic ERK-selective subgroup of MKPs. The cytoplasmic localisation of DUSP6/MKP-3 is facilitated by the

presence of a leucine-rich NES within the N-terminal non-catalytic domain, which mediates the nuclear export of DUSP6/MKP-3 via the canonical chromosome region maintenance-1 (CRM1)-dependent nuclear export pathway. Nuclear export is an active process, and its inhibition with leptomycin B results in nuclear accumulation of DUSP6/MKP-3, suggesting that it can shuttle between the nucleus and cytoplasm. Furthermore the NES, along with DUSP6/MKP-3s KIM motif, can facilitate the anchorage of dephosphorylated ERK within the cytoplasm (Karlsson et al., 2004). As mentioned previously, DUSP6/MKP-3 undergoes catalytic activation following its binding to ERK, undergoing a conformational change to bring critical residues within the active site of the enzyme site into the optimal position for catalysis (Camps et al., 1998; Nichols et al., 2000; Stewart et al., 1999).

The mechanisms of transcriptional control of DUSP6/MKP-3 expression were first revealed during studies investigating the role of fibroblast growth factor (FGF) signalling in embryogenesis. Initial studies identified DUSP6/MKP-3 expression to occur at sites of FGF signalling in mouse embryos (Dickinson et al., 2002). This DUSP6/MKP-3 expression was subsequently shown to be induced by FGF signalling, although there was initially debate over whether this occurred in a PI3K (Kawakami et al., 2003) or MEK-dependent manner (Eblaghie et al., 2003) during chick embryogenesis. Further studies revealed the transcriptional induction of DUSP6/MKP-3 to be dependent on ERK activity. This was demonstrated through the observation that DUSP6/MKP-3 expression co-localised with ERK activity, and was sensitive to ERK inhibition through the use of a MEK inhibitor or by ectopic expression of DUSP6/MKP-3 itself during chick embryogenesis (Smith et al., 2006). In contrast, mice lacking PDK1, an essential mediator of PI3K signalling still display DUSP6/MKP-3 expression (Smith et al., 2006). Additionally, DUSP6$^{-/-}$ mouse embryos displayed increased ERK activity, ERK-dependent gene expression and reporter gene output from the DUSP6/MKP-3 promoter (Li et al., 2007). Furthermore, the utilisation of chemical inhibitors of both the ERK and PI3K pathways supported these results, demonstrating a reduction in DUSP6/MKP-3 induction in NIH 3T3 cells or during chick embryogenesis following MEK, but not PI3K, inhibition (Ekerot et al., 2008). Finally, DUSP6/MKP-3 induction by ERK activity has been shown to be dependent on ERK mediated ETS transcription factor activity and direct binding to the DUSP6/MKP-3 promoter (Ekerot et al., 2008; Zhang et al., 2010).

DUSP6/MKP-3 protein levels can be modulated by post-translational modifications, which alter protein stability. Phosphorylation of Ser159/197 on DUSP6/MKP-3 promotes its ubiquitin-mediated degradation, this can be mediated by ERK (Marchetti et al., 2005), or by the phosphorylation of Ser159 alone by the PI3K/mammalian target of rapamycin (mTOR) pathway (Bermudez et al., 2008). This ability of the PI3K/mTOR pathway to promote DUSP6/MKP-3 degradation constitutes a mechanism of crosstalk by which PI3K/mTOR signalling could regulate ERK activity. This could be particularly important in Ras-driven cancers, which are able to activate both signalling pathways, or in allowing mutations in components of the PI3K/mTOR pathway to promote additional ERK-dependent tumourigenic functions.

A significant physiological role for DUSP6/MKP-3 was first suggested when morpholino-mediated DUSP6/MKP-3 knockdown was shown to disrupt axial polarity during zebrafish embryogenesis, due to deregulation of FGF signalling (Tsang et al., 2004). However, this phenotype was not recapitulated in DUSP6/MKP-3 knockout mice, where an analysis of murine embryogenesis revealed that DUSP6/MKP-3 loss elevated levels of *p*-ERK and promoted a severe variably penetrant phenotype comprising partial postnatal lethality, skeletal dwarfism and hearing loss. These phenotypic traits are characteristic of activating mutations of FGF receptors, again indicating an essential role for DUSP6/MKP-3 in the control of FGF signalling during embryogenesis (Li et al., 2007). However, a second line of DUSP6/MKP-3 knockout mice showed no such problems, were viable into adulthood, fertile, and otherwise overtly normal, apart from demonstrating an increase in basal ERK phosphorylation in the heart, spleen, kidney and brain. The increased ERK activation in the heart was associated with increased myocyte proliferation, enlarged organ size and protection against heart failure following long term pressure overload in adult mice (Maillet et al., 2008). At present it is unclear why these results are so divergent but variations in the mouse strain genetic background are a possible cause.

More recently, DUSP6/MKP-3 has been shown to be involved in glucose homeostasis, diabetes and obesity. DUSP6/MKP-3 expression has been shown to be significantly induced in mice following diet-induced obesity or in genetically obese mice (Wu et al., 2010; Xu et al., 2005a). DUSP6/MKP-3 promotes gluconeogenic gene transcription in hepatoma cells and *in vivo*, following its upregulation in a Forkhead box protein O1

(FOXO1)-dependent manner (Feng et al., 2014a; Jiao et al., 2012), and DUSP6/MKP-3 ablation protects mice from diet-induced obesity and improves insulin sensitivity (Feng et al., 2014b). Finally, alterations in DUSP6/MKP-3 expression has been observed in human tumours and there is increasing evidence that DUSP6/MKP-3 plays a role in the pathogenesis of several types of cancer, as detailed below.

1.3.5 MKPs and cancer

Given the roles of MKPs as negative feedback regulators of MAPKs, it is not surprising that alterations in the expression levels of MKPs have been detected in cancers, particularly those driven by mutations in upstream components of the MAPK pathways themselves. Based on such observations MKPs have been implied to have key roles in cancer induction, progression and in mediating the response of tumour cells to chemotherapy (Keyse, 2008; Kidger and Keyse, 2016b). Kidger and Keyse, (2016a) summarises the current evidence for the deregulation of MKPs in cancer. The overall picture is somewhat contradictory and confusing with many MKPs being implicated in both the promotion and suppression of tumourigenesis, depending on the cancer type and state of progression. However, much of this evidence is based on correlations between altered levels of MKP expression and prognosis or tumour progression in relatively small numbers of patients, and there is limited evidence defining functional roles for altered MKP expression in cancer. This provokes the question, are MKPs playing a significant role in the development and maintenance of tumours and if so are they tumour suppressors or oncogenes?

Elevated MKP expression has been associated with poor prognosis or chemoresistance in many cancer types (Keyse, 2008). With regard to JNK or p38-specific MKPs this could be mediated through their ability to antagonise pro-apoptotic signalling. For example, DUSP1/MKP-1 overexpression in prostate and breast cancer is inversely correlated with JNK activity, implying an oncogenic function for DUSP1/MKP-1 through the inhibition of JNK/p38-mediated apoptosis (Magi-Galluzzi et al., 1997; Wang et al., 2003). However, the ability of MKPs to antagonise MAPK-induced proliferation makes them logical tumour suppressors and many studies have associated loss of MKP expression with cancer progression (Bermudez et al., 2010; Keyse, 2008). Independent studies have revealed the downregulation of DUSP2, DUSP4/MKP-2 and DUSP6/MKP-3 expression in lung

adenocarcinoma and have linked these events to increased ERK activation and tumour progression (Chitale et al., 2009; Lin et al., 2011; Okudela et al., 2009). In multiple cases both elevated and decreased MKP expression has been observed in the same tumour, but at differing stages of tumour progression. Typically in these cases the MKP is initially overexpressed in low grade tumours, followed by loss of expression in higher grade cancers. This distinctive pattern of MKP expression has been demonstrated for DUSP1/MKP-1 in human epithelial tumours, including prostate, colon and bladder, (Loda et al., 1996), DUSP4/MKP-2 in ovarian tumours, (Sieben et al., 2005) and DUSP6/MKP-3 in pancreatic cancer (Furukawa et al., 2003). For both DUSP4/MKP-2 in ovarian tumours and DUSP6/MKP-3 in pancreatic cancer MKP down regulation coincides with tumour progression to invasive carcinoma (Furukawa et al., 2003; Sieben et al., 2005). A hypothesis to explain this dynamic alteration of MKP expression through tumour progression could be that the initial overexpression is a feedback response to increased MAPK signalling in the tumour. This MKP-mediated negative feedback could have an oncogenic function through the tempering of ERK activation to prevent oncogenic mutations inducing excessive ERK signalling which is able to induce cell cycle arrest, cell senescence or apoptosis (Caunt and Keyse, 2013; Deschênes-Simard et al., 2014; Meloche and Pouysségur, 2007; Shojaee et al., 2015) or alternatively through antagonising JNK/p38 activity to constrain pro-apoptotic signalling. Subsequently, if the tumour evolves and acquires additional mutations, which can override the blocks to cell cycle progression or pro-apoptotic signalling then a loss of MKP activity could confer a selective advantage, as reduced MAPK signalling would be now primarily constraining the proliferative capacity of the tumour.

The ability of MKPs to respond to multiple stimuli, including oncogenic activation of the MAPK pathway themselves, and regulate MAPK signalling to mediate diverse cellular processes, means it is no surprise that MKPs have demonstrated altered expression in cancer and have been implicated to have roles in tumourigenesis. What is perhaps more surprising it that these alterations in MKP expression levels have been implicated in modulating both the oncogenic and tumour suppressive properties of the MAPKs. However, when viewed in perspective of the diverse biological outcomes that MAPK signalling pathways can induce dependent on the cellular context, as well as the diverse and often opposing roles MAPKs have shown in human cancers, a tissue-specific and

cellular context-dependent role for MKP signalling in cancer appears logical. The ability of MKPs to display an oncogenic or tumour suppressive function could be influenced by the cancer type, mutational background of the tumour and nature of the driving oncogene(s), in particular whether it is likely to rewire MAPK pathways (Caunt and Keyse, 2013). Therefore, future studies investigating the role of MKPs in human cancers ideally need to perform analysis of MKP expression with regard to tumour grade and the mutational background of the tumour. Furthermore, mouse knockout models could be utilised to determine whether MKPs have significant functional roles in the initiation and progression of cancers, or whether alterations in their activity are simply a consequence of signalling pathway deregulation and rewiring in cancers. Together these approaches could elucidate under what scenarios MKP expression is being altered, and whether such alterations in MKP expression are having functional consequences on the outcome of MAPK signalling and tumour progression in particular cancers.

1.3.5.1 DUSP5 and cancer

Perhaps due to it being one of the least well studied MKPs, relatively little is known about the potential roles in cancer for DUSP5. However, given its function as a nuclear ERK-specific negative feedback regulator, DUSP5 mRNA and protein levels would be expected to be increased and to play some role in cancers driven by activating mutations upstream of ERK. This is indeed the case with both DUSP5, and the cytoplasmic ERK-specific phosphatase DUSP6/MKP-3, being identified amongst a subset of the most consistently, upregulated genes in mutant Ras and BRaf-driven colorectal and endometrial cancer cell lines (Kreeger et al., 2009; Vartanian et al., 2013; Yun et al., 2009). A functional role for DUSP5 in mutant Ras-driven cell lines was postulated due to high DUSP5 expression correlating with decreased ERK activity (Kreeger et al., 2009). Furthermore, oncogenic activation of $KRas^{G12V}$ and $BRaf^{V600E}$ in normal intestinal epithelial crypt cells (IECs) leads to elevated cytoplasmic, but not nuclear, *p*-ERK levels. This spatial restriction correlated with the potent upregulation of the nuclear MKPs DUSP4/MKP-2 and DUSP5 (Cagnol and Rivard, 2012). The potential importance of elevated DUSP5 expression can be demonstrated by the requirement for DUSP5, and DUSP6/MKP-3, expression to enable the proliferation of MCF7 breast cancer cells following phorbol-ester treatment. MCF7 cells display an ERBB2 gene amplification, therefore increasing ERK pathway activation downstream of this RTK. DUSP5 and DUSP6/MKP-3 were shown to be upregulated in an

ERK-dependent manner via the transcription factors ETS2 and c-JUN respectively following phorbol-ester treatment. The siRNA-mediated knockdown of DUSP5 or DUSP6/MKP-3 promoted cell-cycle arrest and senescence, indicated by p21 accumulation, whereas the stable-overexpression of DUSP5 or DUSP6/MKP-3 promoted increased proliferation (Nunes-Xavier et al., 2010).

Recently the first evidence for altered expression levels, and possible functional roles, of DUSP5 in human cancers has emerged. DUSP5 has been shown to be downregulated in human CRC cell lines and tissue samples through hypermethylation (Togel et al., 2012). Loss of DUSP5 expression due to aberrant hypermethylation has been detected in advanced gastric cancers, but not in the normal gastric mucosa, and DUSP5 promoter hypermethylation correlated with significantly shortened patient survival. Furthermore, restoring DUSP5 expression in DUSP5 hypermethylated gastric cancer cell lines decreased their proliferative capacity and colony-forming ability (Shin et al., 2013). Loss of DUSP5 expression has also been detected in prostate cancer, where it again correlated with poor patient outcome (Cai et al., 2015). However, this study solely detected DUSP5 expression through immunohistochemistry (IHC) and the DUSP5 antibody employed in this study was shown to detect DUSP5 solely in the cytoplasm and on the cell membrane in prostate epithelial and prostate cancer cells. This conflicts with the established subcellular localisation for DUSP5 (Mandl et al., 2005), bringing the specificity of their antibody and thus these results into question. Overall, DUSP5 has shown elevated expression in response to oncogenic stimulation of the ERK pathway, and has been demonstrated to be lost in some cancers, implying a tumour suppressive role for DUSP5. Although the fact that DUSP5 was required for proliferation of some cancer cells (Nunes-Xavier et al., 2010) indicates that in certain contexts DUSP5 could play an oncogenic role through the prevention of OIS.

1.3.5.2 DUSP6/MKP-3 and cancer

DUSP6/MKP-3, like DUSP5, has been shown to be consistently, highly upregulated in many mutant Ras or BRaf-driven cancer cell lines, where it is presumed to constrain oncogenic ERK signalling (Bloethner et al., 2005; Croonquist et al., 2003; Haigis et al., 2008; Packer et al., 2009; Pratilas et al., 2009; Vartanian et al., 2013; Yun et al., 2009). Indeed, siRNA-mediated DUSP6/MKP-3 knockdown promoted increased ERK activation

and proliferation in $Kras^{G13D/+}$-driven CRC cell lines, suggesting a tumour suppressive role for DUSP6/MKP-3 in CRC (Haigis et al., 2008). However as mentioned previously, DUSP6/MKP-3 knockdown promoted cell-cycle arrest and senescence in MCF7 breast cancer cells, implying that in alternative contexts DUSP6/MKP-3 is required for proliferation and therefore plays an oncogenic role (Nunes-Xavier et al., 2010).

The first evidence of a link between DUSP6/MKP-3 and human cancer was observed in pancreatic ductal adenocarcinoma (PDAC), where DUSP6/MKP-3 protein was shown to be overexpressed in the precursor lesions of PDAC, pancreatic intraepithelial neoplasia (PanINs), but then subsequently down regulated in approximately 80% of poorly differentiated, invasive PDAC (Furukawa et al., 2003). PDAC is initiated by activating mutations in KRas in approximately 90% of cases, indicating that ERK signalling may play a key role in disease pathogenesis (Kleeff et al., 2016). DUSP6/MKP-3 was initially investigated due to its location in chromosomal region 12q21-23.1, which is frequently hemizygously deleted in primary pancreatic cancer with poor prognosis (Kimura et al., 1996, 1998; Yatsuoka et al., 2000). Loss of heterozygosity (LOH) of chromosome 12q was detected in around 30% of pancreatic tumour samples tested (Kimura et al., 1996; Yatsuoka et al., 2000), which would not account for the total loss of DUSP6/MKP-3 expression in PDAC tissues. However, no mutations have been detected in the DUSP6/MKP-3 gene in PDAC cell lines (Furukawa et al., 1998), suggesting an epigenetic mechanism promoting the abrogation of DUSP6/MKP-3 in pancreatic cancer. Subsequently, aberrant hypermethylation of the DUSP6/MKP-3 promoter has been associated with DUSP6/MKP-3 suppression in pancreatic cancer cell lines and tissues. In PDAC cell lines hypermethylation was reversible after treatment with the DNA methyltransferase inhibitor 5-azacytidine or the histone deacetylase inhibitor trichostatin A, resulting in restored DUSP6/MKP-3 expression (Xu et al., 2005b). Furthermore, adenovirus-mediated ectopic expression of DUSP6/MKP-3 in such cells reduces *p*-ERK levels in a dose-dependent manner, inhibiting their proliferation and inducing apoptosis (Furukawa et al., 2003). However, conclusions drawn from the overexpression of DUSP6/MKP-3, driven by constitutively active promoters, should be treated with caution due to its ability to result in near complete ablation of ERK activity in a manner which endogenous or physiological levels of DUSP6/MKP-3 might not be able to achieve. Finally, whilst the expression of many tumour suppressors involved in pancreatic cancer

development, such as p53, CDKN2A or SMAD4, is lost during, and thought to contribute to, PanIN progression, the loss of DUSP6/MKP-3 is only observed in invasive carcinoma (Furukawa et al., 2005). This evidence has led to the proposal that DUSP6/MKP-3 expression is induced as a negative feedback regulator of ERK activity in PanINs, which is able to restrain the progression of PanINs to invasive carcinoma in a manner that is independent of other major tumour suppressors. Consequently, DUSP6/MKP-3 suppression could be an important factor in the development of malignancy of PDAC (Furukawa, 2009; Furukawa et al., 2006).

DUSP6/MKP-3 has also demonstrated a tumour suppressive function in non-small-cell lung cancer (NSCLC) (Okudela et al., 2009), another cancer type which exhibits KRas mutations in ~30% of cases (Karachaliou et al., 2013; Suda et al., 2010). In a similar manner to pancreatic cancer, low-grade and pre-neoplastic lung lesions expressed high levels of DUSP6/MKP-3 protein compared to the normal bronchial epithelial tissue, DUSP6/MKP-3 levels were then shown to decrease in an inverse correlation with increasing histological grade and the proliferative capacity of the tumours (Okudela et al., 2009). Furthermore, LOH of the DUSP6/MKP-3 locus was identified in 17.7% of 64 tumour samples analysed, where it was associated with reduced DUSP6/MKP-3 expression levels. In contrast, no mutations in the protein-coding exons of the DUSP6/MKP-3 gene were identified. This study also demonstrated that restoration of DUSP6/MKP-3 expression suppressed proliferation in lung cancer cells (Okudela et al., 2009), however such overexpression experiments retain the caveat described above. Despite this, further *in vitro* studies in NSCLC cell lines support this data with an inverse correlation between levels of DUSP6/MKP-3 and ERK activation detected in H441 cells. Again, DUSP6/MKP-3 overexpression inhibited proliferation and promoted apoptosis, while this was supported by siRNA knockdown experiments demonstrating the opposing phenotype by increasing ERK activation and proliferation rates (Zhang et al., 2010). More recently multiple quantitative real-time polymerase chain reaction (qRT-PCR)-based studies on large cohorts of patient samples have identified a downregulation of DUSP6/MKP-3 expression in NSCLC (Díaz-García et al., 2014; Skrzypski et al., 2013), and low DUSP6/MKP-3 expression correlated with shortened patient survival (Díaz-García et al., 2014). Finally, studies in oesophageal squamous cell carcinoma (ESCC) and nasopharyngeal carcinoma (NPC) also suggest a tumour suppressor role for DUSP6/MKP-3. DUSP6/MKP-3 protein

was shown to be significantly downregulated in ESCC and NPC tissue, compared to adjacent normal tissue, and decreased DUSP6/MKP-3 expression correlated with decreased patient survival. Restoration of DUSP6/MKP-3 expression ESCC and NPC cell lines impairs both cell invasion and epithelial to mesenchymal transition (EMT)-associated properties of these cell lines, implicating DUSP6/MKP-3 to have a functional role restraining malignant progression and metastasis in these cancers (Wong et al., 2012). Subsequent studies focusing on ESCC support this data, with reduced DUSP6/MKP-3 expression observed in ESCC tissue, at both the protein and mRNA level, and associated with increased pathological grade. Low DUSP6/MKP-3 expression in ESCC cell lines was shown to be due to promoter hypermethylation and the restoration of DUSP6/MKP-3 expression promoted increased apoptosis in these cell lines (Ma et al., 2013).

While the studies above present strong evidence suggesting a tumour suppressor role for DUSP6/MKP-3 in multiple cancer types, alternative studies in a range of other cancer types have indicated it might be oncogenic. In poorly differentiated and papillary thyroid carcinomas (PTC) DUSP6/MKP-3 is overexpressed at both the protein and mRNA level, compared to benign neoplasms, and increasing DUSP6/MKP-3 expression is associated with high-risk features of PTC, such as increased tumour size (Degl'Innocenti et al., 2013; Kim et al., 2014; Lee et al., 2012). Thyroid carcinomas frequently carry gene rearrangements that generate oncogenic forms of RTKs, such as RET/PTC (rearranged in transformation/papillary thyroid cancer) or $BRaf^{V600E}$ and RAS mutations, therefore the ERK pathway is thought to play a central role in thyroid carcinogenesis. DUSP6/MKP-3 siRNA-mediated knockdown in PTC cell lines reduced proliferation and invasion, implicating an oncogenic role for DUSP6/MKP-3 in thyroid cancers (Degl'Innocenti et al., 2013). This is supported by evidence from breast cancer, where DUSP6/MKP-3 has been shown to be overexpressed in HER2-positive breast cancers and triple-negative MDA-MB-231 cells (Boulding et al., 2016; Lucci et al., 2010), and DUSP6/MKP-3 knockdown suppressed proliferation, migration and invasion in MDA-MB-231 cells (Song et al., 2015). Furthermore, DUSP6/MKP-3 is overexpressed in glioblastoma tissue samples and many cancer cell lines, where it has been shown to promote increased colony formation in soft agar and proliferation in mouse xenograft models (Messina et al., 2011).

The strongest evidence for an oncogenic role of DUSP6/MKP-3 comes from a recent study of pre-B-cell transformation by BCR-ABL1 activation, as a model of acute lymphoblastic leukemia (ALL) (Shojaee et al., 2015). Malignant transformation of human pre-B cells by BCR-ABL1 or $NRas^{G12D}$ activation induced immediate cell death in virtually all cells, and the small fraction which survived acquired permissiveness through robust activation of ERK negative feedback systems. Three of the most strongly upregulated genes were DUSP6/MKP-3, sprouty-2, and the transcription factor ETV5 (Ets Varient Gene 5), which were induced in an ERK-dependent manner, and subsequently shown all to be essential for oncogenic transformation of pre-B cells in mouse models for ALL. High DUSP6/MKP-3 expression strongly correlated with shorter overall survival for adults with Philadelphia chromosome positive (Ph^+) pre-B ALL, but showed no correlation with survival in myeloid leukemias, indicating a lineage-specific role for DUSP6/MKP-3. This lineage-specific role for DUSP6/MKP-3 was supported by evidence that B-cell progenitors from $DUSP6^{-/-}$ mice were resistant to BCR-Abl1 induced transformation and colony formation, suggesting an oncogenic role for DUSP6/MKP-3. In contrast, myeloid progenitors from $DUSP6^{-/-}$ mice showed elevated BCR-Abl1 induced transformation and colony formation, suggesting a tumour suppressive function for DUSP6/MKP-3. To validate the hypothesis that DUSP6/MKP-3 might be a therapeutic target in human ALL a previously described pharmacological DUSP6/MKP-3 inhibitor, BCI (2-benzylidene-3-(cyclohexylamino)-1-Indanone hydrochloride), was utilised. BCI treatment caused a rapid increase in ERK activity in patient-derived Ph^+ ALL cells, coupled with the induction of a cell cycle arrest and p53-mediated cell death. Furthermore, BCI treatment is able to overcome resistance to tyrosine kinases inhibitors (TKIs) in Ph^+ ALL cells, by inducing ERK hyperactivation and the associated induction of senescence and apoptosis (Shojaee et al., 2015). However, although biochemical studies have demonstrated that BCI inhibits DUSP6/MKP-3 through the prevention of ERK-dependent allosteric changes which enable its catalytic activity, this drug is non-specific in terms of MKP binding and it also displays clear toxicity, therefore the development of more specific compounds is required before DUSP6/MKP-3 inhibition could be considered in the clinic (Korotchenko et al., 2014; Molina et al., 2009).

Interestingly, evidence from melanoma paints a heterogeneous role for DUSP6/MKP-3 in tumourigenesis. Melanoma is another cancer in which $BRaf^{V600E}$ is frequently a driving oncogene, and has been shown to upregulate DUSP6/MKP-3 possibly as a mechanism to

restrain ERK activity (Bloethner et al., 2005; Packer et al., 2009). DUSP6/MKP-3 is upregulated in, non-BRaf mutant, tumourigenic mouse melanocytes, where it promotes growth and invasion. These cells appear to have many features in common with a distinct subtype of thick primary human melanoma, which display high DUSP6/MKP-3 levels and poor prognosis. However, in $BRaf^{V600E}$ expressing human melanoma cell lines ectopic expression of DUSP6/MKP-3 suppresses colony formation and invasion (Li et al., 2012). Consequently, as well as displaying opposing roles in cancer development across distinct cancer types, it appears likely that DUSP6/MKP-3 can promote alternative outcomes in different subtypes of the same cancer.

In addition to oncogenic or tumour suppressive roles in cancer DUSP6/MKP-3 has been implicated to be involved in the resistance to chemotherapy in a number of cancers. The elevated expression of DUSP6/MKP-3 has been associated with tamoxifen resistance in breast cancer (Cui et al., 2006) and cisplatin resistance in glioblastoma (Messina et al., 2011). In this second study DUSP6/MKP-3 knockdown increased the sensitivity of glioblastoma cell lines and xenografts to cisplatin treatment (Messina et al., 2011). Furthermore, in two recent papers DUSP6/MKP-3 has been shown to play a key role in the response of tumour cells to targeted therapeutics, which aim to inhibit signalling from mutations upstream of ERK. Hrustanovic et al. (2015) demonstrated that EML4-ALK positive lung adenocarcinoma is able to acquire resistance to ALK-specific TKIs via either decreased expression of DUSP6/MKP-3 or a gain in copy number of the wild-type KRAS gene, resulting in ERK pathway reactivation, which the tumour is dependent on for survival. Stable re-expression of DUSP6/MKP-3 was able to re-sensitise TKI resistant cells, causing decreased ERK activity and increased cell death, whereas DUSP6/MKP-3 knockdown promoted increased TKI resistance in drug naïve cells. Furthermore, decreased DUSP6/MKP-3 protein expression was detected in TKI-resistant patient tumour samples relative to drug naïve samples (Hrustanovic et al., 2015). Activating mutations in EGFR are also a common driver mutation for lung cancer, occurring in approximately 14% of NSCLC, and consequently EGFR TKI development is a therapeutic option for this disease (Russo et al., 2015). However, resistance to EGFR TKIs is an emerging problem, which can either occur via intrinsic or acquired resistance. Phuchareon et al. (2015) utilised EGFR mutant lung cancer cell lines to demonstrate that EGFR TKI treatment caused high levels of cell death, yet surviving cells were capable of proliferating and forming colonies in

drug, suggesting they exhibit innate resistance. Such resistant cells only displayed a temporary blockade of ERK activity following EGFR TKI treatment, although EGFR inhibition was continually effective. Drug treatment was shown to cause a significant decrease in DUSP6/MKP-3 expression, due to the loss of activity of the transcription factor Ets1 caused by TKI-mediated inhibition of PI3K signalling, rather than any alteration in ERK activity. Loss of DUSP6/MKP-3 expression correlated with the rebound in ERK activity shortly after EGFR TKI treatment, and reconstitution of DUSP6/MKP-3 expression was able to prevent this rebound in ERK activity. Elevated ERK activity following EGFR TKI treatment promotes NSCLC cell survival via phosphorylation of the pro-apoptotic BH3-only protein Bim, which promotes its proteasomal degradation and therefore cell survival. This study demonstrates the importance of crosstalk in modulating the activity of MKPs, and how this can allow them to modulate ERK activity to promote significant cellular phenotypes, such as in this case tumour cell survival and resistance to drug treatment (Phuchareon et al., 2015).

Overall, there is some evidence for both oncogenic and tumour suppressive functions for DUSP6/MKP-3 depending on the cancer type and cellular context. Furthermore, DUSP6/MKP-3 is able to modulate the effects of many chemotherapeutic treatments. Together these traits make a strong case to further develop knowledge of the role of DUSP6/MKP-3 in the development and progression of many cancers. As much of the evidence linking DUSP6/MKP-3 to cancer is based on correlations between expression and patient outcome or cell based studies, one obvious area to focus such efforts would be through the development of mouse models to investigate the functional effects of DUSP6/MKP-3 ablation on the development of individual cancer types and to mechanistically investigate any observed phenotypes.

1.4 Pancreatic cancer

1.4.1 Pancreatic cancer overview and epidemiology

Pancreatic cancer is among the most lethal malignancies worldwide, being responsible for the 4th highest number of cancer-related deaths in the western world (Ferlay et al., 2015). It has a very poor prognosis with a 5 year survival rate of less than 7%, due to a lack of therapeutic options and a poor response to chemotherapy (Jemal et al., 2010).

Consequently, if outcomes are not improved pancreatic cancer is projected to surpass colon and breast cancers to become the second leading cause of cancer-related mortality by 2030 (Rahib et al., 2014). Pancreatic ductal adenocarcinoma (PDAC), is the most common form of pancreatic cancer occurring in 75-80% of cases, however there are a range of other rare malignant neoplasms of the pancreas including: neuroendocrine tumours (~15%), colloid carcinomas (~2%), solid pseudopapillary tumours (~2%), acinar carcinomas (~1%) and pancreatoblastomas (~0.5%) (Kleeff et al., 2016).

The poor prognosis of pancreatic cancer is attributed to several factors; perhaps the most important being that it is usually diagnosed at an advanced stage. Late diagnosis is due to pancreatic cancer often displaying non-specific or very few symptoms at early stages, a lack of reliable biomarkers and difficulties detecting early-stage tumours with current imaging techniques (Ryan et al., 2014). Pancreatic cancer is very aggressive and therefore often displays local perineural or vascular invasion or distant metastasis prior to detection. Consequently, pancreatic cancer is frequently diagnosed too late for therapeutic intervention to be successful, with only 10–15% of patients diagnosed eligible for surgery, the only option with curative potential (Gillen et al., 2010). Pancreatic cancers are also characterised by a range of genetic and epigenetic abnormalities, as well as dense stromal reaction, making them very heterogeneous. These traits make pancreatic cancers very resistant to chemotherapy, radiotherapy and many molecularly targeted therapies (Kleeff et al., 2016).

Although treatment strategies and patient care have gradually improved, increases in incidence and mortality are continuing to rise in Europe and North America, which is likely to be due to an aging population (Siegel et al., 2015). Age is the major risk factor determinant of pancreatic cancer, with the majority of patients diagnosed over 50 years old, with incidence increasing with age. Significant preventable risk factors include smoking, obesity and diet, particularly high alcohol intake which has been linked to chronic pancreatitis, a major risk factor in its own right (Kleeff et al., 2016). Furthermore, diabetes mellitus is both significant risk factor for, and a potential consequence of, pancreatic cancer (Bosetti et al., 2014). Finally, there is also a hereditary element to pancreatic cancer, with around 10% of patients displaying a family history and there are a range of genetic syndromes associated with pancreatic cancer including Peutz-Jeghers

syndrome, hereditary pancreatitis and Li-Fraumeni syndrome. Together such syndromes are associated with mutations in genes such as LKB1, PRSS1, CDKN2A, BRCA1/2, ATM and p53 all of which are associated with an increased risk of disease with variable penetrance (Rustgi, 2014).

1.4.2 The mutational spectrum of human pancreatic cancer

Global genomic analysis has confirmed the major genes involved in the initiation and progression of pancreatic cancer, as well as revealing the complex array of infrequently mutated genes, chromosomal rearrangements, copy number changes and epigenetic alterations found in this disease (Bailey et al., 2016; Biankin et al., 2012; Jones et al., 2008; Waddell et al., 2015; Witkiewicz et al., 2015). Activating mutations in KRas are the predominant driving mutation in pancreatic cancer, occurring in >90% of tumours. The other signature mutations of human pancreatic cancers include the frequent inactivation the tumour suppressors p53, SMAD4, and CDKN2A, with each occurring in around 50-80% of cancers. Furthermore, there is a small subset of genes which are mutated in around 10% of pancreatic cancers including, TGFBR2, ARID1A and MUC16 amongst others. However, above these common gene alterations few others stand out amongst the varied mutational spectrum of pancreatic cancer, with the majority of remaining genes having a mutational frequency of <2% (Bailey et al., 2016; Biankin et al., 2012; Jones et al., 2008; Waddell et al., 2015; Witkiewicz et al., 2015). Despite this, computational analysis has shown that many of these diverse mutations do converge on either distinct signalling pathways or cellular processes, including KRas, TGF-β, Wnt, Notch or Hedgehog signalling, and axon guidance, chromatin remodelling, G1/S transition or DNA repair processes. Consequently deregulation of these pathway and processes could be essential for pancreatic cancer development and could be key nodes to target with therapeutic strategies (Bailey et al., 2016; Ying et al., 2016).

Using such genomic data, four pancreatic cancer subtypes have been proposed based on their genomic structural variation. These subtypes are stable (<50 structural variants), scattered (50-200), unstable (>200) or locally rearranged (<50), which has few structural events but these a clustered around particular chromosomes indicated amplified oncogenes (Waddell et al., 2015). Pancreatic cancers have also been grouped through mRNA expression analysis. Micro-dissected pancreatic epithelium from tumours clusters

into three subgroups (Collisson et al., 2011), whereas if the surrounding stroma is included four subgroups are identified (Bailey et al., 2016): squamous, pancreatic progenitor, immunogenic and aberrantly differentiated exocrine (ADEX). These epithelial subtypes seem to be histopatholgically distinct and diverge based on their similarity to the developing or adult pancreas. Furthermore the subgroup which least resembles the normal pancreas, the squamous subtype, is associated with worse prognosis, indicating there is some functional difference between these subtypes (Bailey et al., 2016). Interestingly, these expression analysis-derived subtypes do not group with the structural variation-derived subtypes (Bailey et al., 2016; Waddell et al., 2015). However, defining molecular subtypes based on expression analysis results in differential classification depending on the input material and the assumptions made during analysis (Kleeff et al., 2016), as other groups have identified two epithelial and two stromal tumour subtypes when transcripts presumed to be from the normal pancreas are first excluded (Moffitt et al., 2015).

1.4.3 The histological progression of pancreatic cancer

Pancreatic cancer usually arises in the head of the pancreas, enabling invasion into surrounding tissues including the spleen, peritoneal cavity, intestine and lymph nodes, and with metastasis commonly occurring in the liver and lungs (Hezel et al., 2006). As mentioned previously pancreatic cancer has many subtypes including PDAC, neuroendocrine tumours and colloid carcinomas, however from herein PDAC will be the focus of this thesis. Within PDAC there are a range of subtypes including typical PDAC, and the less common types displaying colloid, adenosquamous, or sarcomatoid histology. Typical PDAC primarily exhibits a glandular morphology, with many duct-like structures forming within a dense stroma, however there can be significant differences in histology, tumour grade, cellular atypia or degree of differentiation between tumours, or within regions of the same tumour (Hezel et al., 2006; Kleeff et al., 2016). PDAC tumours are graded based on their degree of differentiation, ranging from well differentiated (low grade) tumours, baring greater morphological resemblance to normal pancreatic tissue, to poorly differentiated (high grade) tumours. Generally, the more poorly differentiated the tumour, the more aggressive and malignant it is, with high grade tumours correlating with worse prognosis (Wasif et al., 2010).

Histopathologic studies have identified three morphologically distinct PDAC precursor lesions: PanINs, intraductal papillary mucinous neoplasia (IPMNs) and mucinous cystic neoplasia (MCNs). PanINs are the most common precursor lesions in humans. They are the smallest of the three precursor lesions found forming small ducts, which display a progressive divergence in morphological appearance relative to normal pancreatic ducts. PanINs are graded from stages 1, 2 & 3 to represent the stepwise progression in morphological dysplasia, due to accumulating genetic alterations (Fig. 1.6) (Hezel et al., 2006; Ryan et al., 2014). PanIN1a are characterized by the formation of a columnar, mucinous epithelium with basally located nuclei within small regular shaped ducts. PanIN1b begin to acquire a papillary or basally pseudostratified architecture. Whereas PanIN2 and 3 gain increasing levels of architectural disorganization, nuclear atypia and loss of polarity, with PanIN3s also displaying the characteristic budding off of small groups of epithelial cells into the lumen (Hruban et al., 2001, 2006a). High grade PanINs eventually transform into PDAC following invasion beyond the basement membrane of the ductal structure.

Activating mutations in KRas and the aberrant expression of sonic hedgehog (SHH) are thought to be key processes in the development of PanINs (Morris et al., 2010a). However, the cell of origin for PanIN initiation and subsequent PDAC formation are still unclear. Current theories focus on the dedifferentiation of acinar tissue and the formation of PanINs through acinar to ductal metaplasia (ADM) or a possible adult stem cell role for centroacinar cells, making them susceptible to oncogenic transformation (Roy and Hebrok, 2015) – these theories will be discussed in further detail below. As mentioned previously activating mutations in KRas occur in ~90% of PDAC cases, however KRas mutations are also present at >90% frequency in all grades of human PanIN, including the lowest grade PanIN1a lesions (Kanda et al., 2012). This evidence places activating KRas mutations as the key molecular driver for PDAC formation. Interestingly, >99% of PanIN1As contain mutations in KRAS, CDKN2A, the small g-protein GNAS, or BRAF, prompting the hypothesis that as well as KRas these other genes can occasionally initiate PDAC development (Kanda et al., 2012).

KRas mutations are thought to initiate the senescence program to constrain the proliferation and expansion of PanIN1As until the subsequent loss of the tumour

suppressors CDKN2A, p53 and SMAD4 are able to bypass such inhibition to allow continued PanIN proliferation and malignant progression (Caldwell et al., 2012). CDKN2A is frequently the initial tumour suppressor lost, with low grade PanINs often displaying a lack of expression (Furukawa et al., 2005). Loss of function of CDKN2A usually occurs by mutation, deletion or promoter hypermethylation, and by the time lesions have progressed to invasive PDAC almost all (~95%) have lost CDKN2A expression (Hezel et al., 2006). CDKN2A encodes two overlapping tumour suppressors, INK4A and ARF. INK4A is an inhibitor of cyclin-dependent kinase 4 (CDK4), which prevents the interaction of cyclin D with CDK4, therefore promoting a G1 cell-cycle arrest (Serrano et al., 1993). Whereas, ARF stabilizes the transcription factor p53 by inhibiting its MDM2-dependent proteasomal degradation, allowing p53 to activate a plethora of genes to induce a cell cycle arrest (Nakamura, 2004). The p53 gene is frequently mutated (50-70%) in PDAC, usually by mutation of the DNA binding domain, which prevents its ability to induce target gene expression and cell-cycle arrest (Furukawa, 2009). Mutant p53 is resistant to degradation and accumulates in the nucleus, where it can be identified by IHC. This nuclear overexpression of mutant p53 is not found in low grade PanINs, only later-stage PanIN2 or PanIN3s (Furukawa et al., 2005; Maitra et al., 2003). This is consistent with a role for p53 in initially preventing the progression of PanINs. However, the accumulation of DNA damage and other cellular stress in higher grade PanINs, would generate selective pressure to eliminate p53 function to enable the renewed proliferation and survival of such highly aberrant cells (Hezel et al., 2006). Finally, SMAD4, the other major tumour suppressor lost during PDAC development, is also lost in high grade PanINs (Furukawa et al., 2005; Maitra et al., 2003). SMAD4 is a key component of the TGFβ signalling pathway, which can promote wide ranging cellular outcomes including differentiation, apoptosis, EMT and migration depending on the signalling context. In primary premalignant tumours TGFβ signalling has been frequently shown to have a tumour suppressive role through the induction of differentiation, cytostasis or apoptosis (Massagué, 2008, 2012), indicating why the loss of SMAD4 could promote PanIN progression. However, the exact functional consequences of SMAD4 loss in PDAC progression are not fully understood (Furukawa, 2009).

IPMNs are larger lesions than PanINs, usually forming grossly visible lesions (>1cm) which arise in the main pancreatic duct or on its branches. At the cellular level IPMNs resemble

PanINs, and are also associated with abundant mucin production. IPMN can develop into two major types of invasive cancer, typical PDAC and a colloid type characterized by excessive mucin production (Shi and Hruban, 2012). MCNs are large, grossly visible, mucin-producing epithelial cystic lesions. They are characterised by a distinctive ovarian-type stroma and an absence of a connection to the duct system. Both IPMNs and MCNs develop increasing dysplasia and morphological disorganization as they progress through increasing grades towards PDAC (Hezel et al., 2006). Furthermore, they display many molecular events in common with PanINs including high prevalence of KRas, CDKN2A, p53 and SMAD4 aberrations. However, there are subtle differences with lower frequencies of KRas mutations and CDKN2A or SMAD4 inactivation discovered in IPMN than PDAC. Furthermore, a range of distinct molecular events have been described in IPMN and MCN, together this indicates that the development of each type of precursor lesion might represent variations in a common theme promoting pancreatic tumourigenesis (Bailey et al., 2016; Hezel et al., 2006).

PDAC is characterised by a strong desmoplastic reaction, forming an abundant, dense collagenous stroma around the tumour or precursor lesions. The stroma is formed of extra-cellular matrix (ECM) proteins, including collagens, fibronectin and laminin, as well as glycoproteins and a cellular element of pancreatic stellate cells, immune cells and endothelial cells (Kleeff et al., 2016). Pancreatic stellate cells (also referred to as cancer associated fibroblasts), a subpopulation of cells in the normal pancreas, produce collagenous stroma following pancreatic injury, inflammation and cancer development (Jaster, 2004). Reciprocal interactions between PDAC tumour cells and adjacent stromal cells have been reported to regulate oncogenic signalling and promote proliferation, migration and survival functions of each other, indicating pancreatic stellate cells to play an important role in pancreatic cancer development, maintenance and resistance to therapy (Apte et al., 2013; Tape et al., 2016).

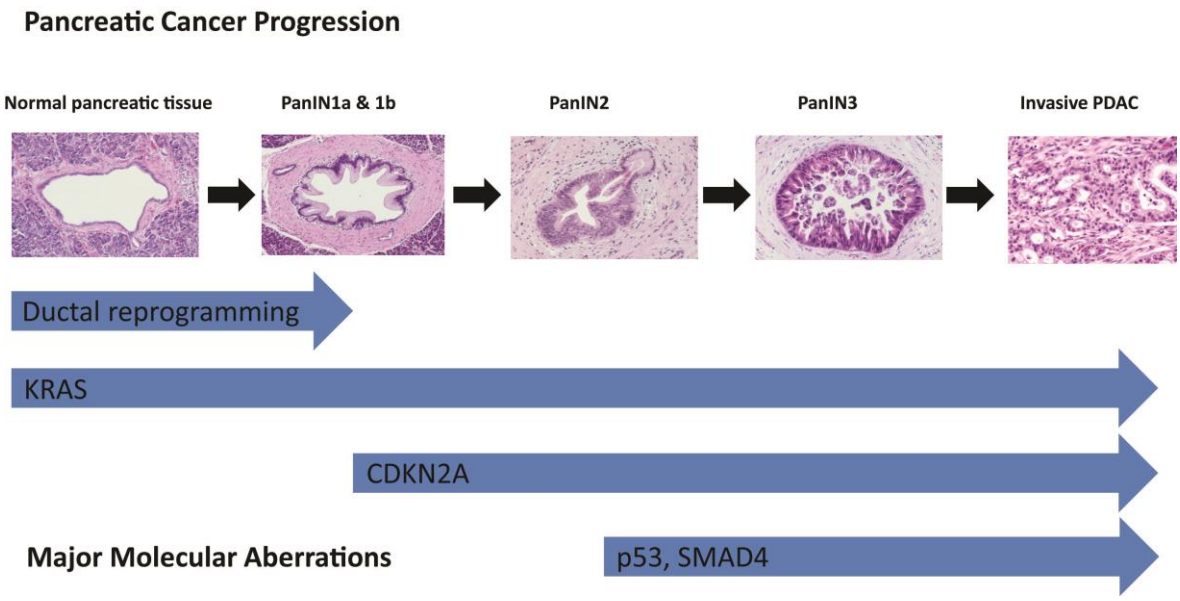

Figure 1.6 Histological progression and key molecular aberrations observed during the development of pancreatic cancer. Images demonstrating the histological progression of pancreatic cancer from normal pancreatic tissue, through pancreatic intraepithelial neoplasia (PanIN) precursor lesions, to invasive pancreatic ductal adenocarcinoma (PDAC). PanIN1a are characterised as epithelial lesions composed of tall columnar cells, with basally located nuclei which exhibit abundant mucin production. PanIN1b display the additional development of a papillary or pseudostratified architecture. PanIN2 are characterised by the further development of nuclear abnormalities, including some loss of polarity, nuclear crowding, enlarged nuclei and hyperchromatism. PanIN3 additionally display: true cribriforming (the budding off of small clusters of epithelial cells into the lumen of the lesion), a loss of nuclear polarity, abnormal mitoses, prominent macro-nuclei and dystrophic goblet cells (inverted goblet cells with mucinous cytoplasm oriented toward the basement membrane and nuclei oriented towards the ductal lumen). The schematic below displays the prominent genes which acquire molecular aberrations during pancreatic cancer progression. (Hezel et al., 2006; Hruban et al., 2001, 2006a, 2006b; Morris et al., 2010a) (Images from: http://pathology.jhu.edu/pc/professionals/DuctLesions.php, a web resource generated following the National Cancer Institute, Pancreas Cancer Think Tank - Hruban et al., 2006a).

1.4.4 Mouse models of pancreatic cancer

Genomic analysis has revealed the major genes which are mutated during PDAC development, however causative roles for these mutant genes cannot be confirmed without the use of model systems to demonstrate functional consequences of such mutations. Disease models utilised for pancreatic cancer include traditional cell line and xenograft models, as well as more physiologically relevant models such as genetically engineered mutant mice (GEMMs) and organoid cultures (Baker et al., 2016; Kleeff et al., 2016). A range of GEMMs have been generated to validate human PDAC genes, investigate the mechanisms by which these act to promote tumour progression and develop new therapeutic or diagnostic approaches (reviewed in Gopinathan et al., 2015; Guerra and Barbacid, 2013; Herreros-Villanueva, 2012; Pérez–Mancera et al., 2012; Westphalen and Olive, 2012). Together with genomic studies from human patients, such studies have allowed the generic molecular mechanism of pancreatic carcinogenesis to be inferred (Fig. 1.6) (Furukawa, 2009; Hruban et al., 2000).

PanIN initiation typically requires the acquisition of KRAS activating mutations, which occur in >90% of cases. The subsequent progression to invasive PDAC is promoted by the loss of tumours suppressors including p53 (50-70%), CDKN2A (>95%), SMAD4 (55%) and DUSP6/MKP-3 (40%) (Caldas et al., 1994; Furukawa, 2009; Hezel et al., 2006). The first GEMM used to validate such a model was the development of an endogenous, oncogenic Kras ($Kras^{LSL\text{-}G12D}$) allele, which could be specifically expressed in the pancreas using tissue-specific Cre recombinase expression driven by either the pancreatic and duodenal homeobox 1 (PDX1) or pancreas-specific transcription factor 1α (Ptf1α) promoters. This mutant KRas-driven model generated a full spectrum of PanINs which slowly progressed to invasive PDAC, demonstrating that Kras ability to be a major driver of PDAC initiation (Hingorani et al., 2003). Further GEMMs were rapidly developed that demonstrated the importance of the loss of tumour suppressors in the progression from PanINs to PDAC. Genetic ablation of CDKN2A or p53, or endogenous expression of $Trp53^{R172H}$, an ortholog of one of the most common human p53 mutations, cooperate with $Kras^{G12D}$ expression to drive the accelerated malignant progression of PanINs to invasive PDAC and in many cases increased metastatic potential (Aguirre et al., 2003; Bardeesy et al., 2006a; Hingorani et al., 2005). Interestingly, the loss of SMAD4 in a $Kras^{G12D}$ background induces PDAC development through progression via either IPMNs (Bardeesy et al., 2006b; Kojima

et al., 2007) or MCNs (Izeradjene et al., 2007) rather than PanINs. Progression via IPMN or MCN following SMAD4 ablation was slower than the accelerated PanIN progression following CDKN2A or p53 loss, supporting the evidence from human tumours that IPMN/MCN derived tumours are associated with improved prognosis and survival (Bardeesy et al., 2006b; Izeradjene et al., 2007). However, the final MCN-derived PDAC tumours often have acquired additional mutations in CDKN2A or p53, therefore generating a similar mutational spectra to PanIN-derived PDAC suggesting that the sequence and context in which these mutations are acquired has an impact on tumour development and histology (Izeradjene et al., 2007).

Combining genetic alterations in putative oncogenes or tumour suppressor genes with oncogenic KRas activation has become the standard strategy to determine their function in pancreatic cancer development (Kleeff et al., 2016). The use of such strategies has revealed the importance of many signalling pathways in tumour initiation and progression, including EGFR (Ardito et al., 2012; Navas et al., 2012), phosphatase and tensin homolog (PTEN) (Ying et al., 2011), JNK (Davies et al., 2014), STAT3 (Corcoran et al., 2011), NRF2 (DeNicola et al., 2011) and LKB1 (Morton et al., 2010). Such approaches have also been used to probe the relative importance of the signalling pathways downstream of KRas for pancreatic development (Collisson et al., 2012; Eser et al., 2013). The findings of such studies will be discussed in detail below. Recently, the development of transposon-mediated insertional mutagenesis approaches in KRas mutant, PDAC-sensitised mice has enabled screening strategies to reveal novel functional genes involved in PDAC development (Mann et al., 2012; Pérez-Mancera et al., 2012). Furthermore, GEMMs have helped to reveal the important oncogenic function of pancreatic inflammation (Guerra et al., 2007, 2011) and immune cells (Bayne et al., 2012; Pylayeva-Gupta et al., 2012) in PDAC development. The use of Cre-drivers localised to specific pancreatic cell types has been used to investigate the cell of origin for pancreatic cancer. Interestingly this has revealed that ductal cells are not the most susceptible to oncogenic transformation, despite the ductal appearance of PanINs, instead a range of cell types appear able to generate PDAC (Morris et al., 2010a; Roy and Hebrok, 2015). Current insights into the cellular origin of PDAC will be discussed below. Finally, pancreatic cancer GEMMs have been used as pre-clinical models to test therapeutic strategies for PDAC, for example the dual-targeting of the ERK and PI3K pathways or additional combinations,

although to date such approaches have had limit efficacy (Alagesan et al., 2014; Hayes et al., 2016; Ischenko et al., 2015).

Recently, the development of more complicated GEMMs enabling the inducible, pancreas-specific, and reversible expression of genes of interest has enabled studies to investigate the role of key PDAC genes in the maintenance of established tumours and to investigate the functional consequences of targeting such pathways. Two independent, inducible $KRas^{G12D}$-driven PDAC models have demonstrated that PDAC remains dependent on $KRas^{G12D}$ expression for tumour maintenance and that ablation of the $KRas^{G12D}$ expression causes rapid tumour regression (Collins et al., 2012; Ying et al., 2012). $KRas^{G12D}$ was shown to reprogram metabolic pathways to increase glucose uptake and drive anabolic glucose metabolism to give tumour cells a selective advantage in low glucose conditions, therefore highlighting the potential to target metabolic pathways in PDAC therapeutics (Son et al., 2013; Ying et al., 2012). However, although such studies point to a strong tumour regression upon targeting mutant KRas signalling subsequent studies revealed that PDAC tumours would evolve to acquire resistance to KRas targeting, enabling $KRas^{G12D}$–independent PDAC recurrence. One primary resistance mechanism was revealed to be the amplification and overexpression of the transcriptional coactivator Yap1, promoting renewed cell proliferation and tumour regrowth (Kapoor et al., 2014). The importance of Yap1 overexpression as a tumour resistance mechanism to mutant KRas loss can be illustrated by the fact it was independently revealed to be the top hit in a genome-wide screen to identify genes which rescue the survival of KRas-dependent cancer cells upon KRas suppression (Shao et al., 2014).

1.4.5 Key unresolved questions in pancreatic cancer

1.4.5.1 The cell of origin of pancreatic cancer

Although many of the mutational events involved in PDAC tumour progression are now well characterised the cellular origin/s of PDAC are still unclear. PDAC and PanINs possess ductal morphology and markers, therefore this led to the initial assumption that they developed from pancreatic ductal cells (Morris and Hebrok, 2009). However, GEMMs have allowed evaluation of the ability of specific pancreatic cell types to form PDAC. Intriguingly, expression of oncogenic KRas under the control of the ductal promoter

cytokeratin-19 (CK19) failed to generate PanINs or PDAC and did not form a clearly malignant phenotype (Brembeck et al., 2003). However, pancreatic acinar tissue was known to be susceptible to transdifferentiation into a ductal-like state following insults including injury, inflammation or oncogenic transformation. This process, known as acinar to ductal metaplasia (ADM) occurs in two stages, an initial dedifferentiation of the acinar tissue, where it loses its function and identity, followed by a second stage were transdifferentiation leads to the original acinar cell adopting true duct-like characteristics (Roy and Hebrok, 2015).

Consequently, a range of studies were performed which demonstrated the ability of acinar tissue to undergo ADM and PanIN initiation following embryonic acinar-specific $KRas^{G12D}$-expression (Grippo et al., 2003; Tuveson et al., 2006). This was supported by evidence from a $KRas^{G12V}$-mutant elastase-cre driven model, whereby embryonic $KRas^{G12V}$-expression induced PanIN and PDAC formation. Surprisingly, adult mice were resistant to $KRas^{G12V}$-induced PanINs and PDAC, even in combination with the loss of tumour suppressors CDKN2A or p53, unless this was coupled with a caerulein challenge to induce pancreatitis (Guerra et al., 2007, 2011). However, studies using the $KRas^{G12D}$-mutant driven by inducible Ptf1α, Elastase, Mist1 and proCPA1 promoters have revealed adult acinar tissue to be susceptible to oncogenic transformation without associated pancreatitis, although such transformation was typically at low levels and could be exacerbated with the induction of pancreatitis (De La O et al., 2008; Friedlander et al., 2009; Habbe et al., 2008; Kopp et al., 2012). Furthermore, Friedlander et al. (2009) revealed that $Kras^{G12D}$ expressing Pdx1-positive cells in the adult pancreas can form PanINs in the absence of inflammatory pancreatitis, whereas $Kras^{G12D}$ insulin-positive cells can only form PanINs in the presence of pancreatitis. PanIN formation has also been induced within the ductal cell lineage, however this required combined expression of $KRas^{G12D}$ and homozygous expression of mutant p53 ($Tp53^{R172H}$), making it much less likely to occur than PanIN formation from an acinar origin, which in contrast only required $KRas^{G12D}$ expression (Bailey et al., 2015).

Overall, it appears that any pancreatic cell type is able to give rise to PanINs and PDAC, although out of the major cell types of acinar, ductal and insulin-positive (endocrine) cells, acinar cells seem to be more readily transformed. This comprises the acinar-centric

theory of PanIN formation, whereby ADM is the primary source of PanINs. Another possibility is that there is a subset of cells which display “stem cell-like” properties which are more readily transformed (Roy and Hebrok, 2015). Centroacinar cells could be such a cell type, as they display a stem cell-like location in the transition zone and have been shown to have the ability to differentiate into any pancreatic cell type when cultured *in vitro* (Rovira et al., 2010). This is supported by evidence including the predisposition of PDX1-positive cells to form PanINs following $KRas^{G12D}$ expression without the necessity for associated inflammatory pancreatitis, indicating that such cells are more able to form PanINs than mature acinar tissue (Friedlander et al., 2009). This developmental plasticity of pancreatic cell types is believed to be due to the frequent reactivation of SHH, Wnt/β-Catenin and Notch embryonic signalling pathways following mutant KRas expression or inflammation, causing the dedifferentiation of mature cell populations, enabling oncogenic transformation (De La O et al., 2008; Morris et al., 2010a, 2010b; Thayer et al., 2003).

1.4.5.2 The relative contribution of Ras effector pathways in pancreatic cancer development

Activating mutations in KRas drive >90% of PDAC, however KRas mutations can induce the activation of a range of effector signalling pathways, including the Raf-ERK, PI3K-AKT and Ral pathways, to exert their cellular consequences (Pylayeva-Gupta et al., 2011). Since KRas itself is considered a very difficult therapeutic target, many therapeutic strategies for pancreatic cancer have been conceived to target the pathways downstream of KRas (Bournet et al., 2016; Junttila et al., 2014). Therefore, understanding the relative contributions of such signalling pathways to PDAC progression and maintenance would help to optimise such therapeutic targeting strategies.

The precise role of the Raf-ERK pathway in pancreatic carcinogenesis is still not fully understood. High *p*-ERK activation is associated with poor survival amongst patients following surgical resection of pancreatic tumours (Chadha et al., 2006). Strikingly, activating BRaf mutations are one of the few mutations apart from KRas to have been identified in PanIN1As, indicating that they have the ability to drive PanIN formation and PDAC development (Kanda et al., 2012). Furthermore, up to 5% of PDAC tumours contain activating BRaf mutations, resulting in continuous ERK activity. Interestingly, such

tumours express wild type KRas, indicating that BRaf and KRas mutations have some degree of redundancy; otherwise you would expect a selective pressure to acquire KRas mutations (Calhoun et al., 2003). In support of such evidence $BRaf^{V600E}$-driven GEMMs of PDAC have been shown induce PanIN formation and PDAC development, in a manner which phenocopies $KRas^{G12D}$ expression (Collisson et al., 2012). Furthermore, MEK inhibition impaired the proliferation of PDAC cell lines *in vitro* and *in vivo* orthotopic xenograft models, and could act synergistically with PI3K pathway inhibition to inhibit tumour growth (Collisson et al., 2012). Together this evidence demonstrates that hyperactivation of the Raf-ERK pathway alone is sufficient to drive PDAC formation, indicating this pathway could play a key role as an effector of mutant KRas.

In addition to its activation by $KRas^{G12D}$ in pancreatic cancer, the PI3K pathway has been shown to be activated by other mechanisms including aberrant activation of RTKs, downregulation of PTEN, by mutations in the catalytic subunit of PI3K (p110/PIK3CA) and the amplification of AKT2 (Pérez–Mancera et al., 2012). In a manner similar to *p*-ERK, high levels of *p*-AKT (representing AKT that is activated via phosphorylation at Thr308 and Ser473) are associated with poor survival (Chadha et al., 2006). The pancreas-specific knockout of PTEN, a negative regulator of PI3K signalling, induced AKT activity, ductal metaplasia and the formation of PDAC at a low frequency (Stanger et al., 2005). In $KRas^{G12D}$-driven PDAC GEMMs PTEN ablation can cooperate with $KRas^{G12D}$ expression and the loss of other tumour suppressors to accelerate PDAC formation (Hill et al., 2010; Kennedy et al., 2011; Ying et al., 2011). More recently, PI3K-p110a, 3-phosphoinositide-dependent protein kinase 1 (PDK1) and Rac1, but not CRaf, have been shown to be essential for $KRas^{G12D}$-driven PanIN and PDAC formation (Baer et al., 2014; Eser et al., 2013; Wu et al., 2014). Furthermore, the expression of the mutant PI3K subunit $p110a^{H1047R}$ in the pancreas is able to phenocopy $KRas^{G12D}$-induced PanIN formation and the progression to metastatic PDAC (Eser et al., 2013). Together such studies demonstrate that in the context of $KRas^{G12D}$-driven PDAC the PI3K-pathway might play more of an essential role than that of the Raf-ERK pathway. However, before this conclusion can be confirmed future studies should investigate the effects of total ablation of Raf-ERK signalling in $KRas^{G12D}$-driven PDAC, as was performed for $KRas^{G12D}$-driven NSCLC by Blasco and colleagues (2011).

Although some elements of the PI3K pathway have been shown to be essential for PDAC development and have shown efficacy in vitro and in GEMMs (Eser et al., 2013; Payne et al., 2015), their targeted inhibition has been largely unsuccessful in the clinic (Javle et al., 2010; Richards et al., 2011). Combinations of PI3K and MEK inhibitors have shown synergy and improved efficacy in PDAC GEMMs (Alagesan et al., 2014; Ischenko et al., 2015), demonstrating that both of these pathways act together to help promote PDAC growth and survival. Overall, this draws the conclusion that both of Raf-ERK and PI3K-AKT pathways have important independent roles in pancreatic tumourigenesis, and that improving our understanding of the function of both pathways and there interactions in PDAC will help to enable the generation of new therapeutic strategies.

1.4.5.3 Potential roles for MKPs in pancreatic cancer

Pancreatic cancer is predominantly driven by mutant KRas (Kleeff et al., 2016), and many MKPs have been shown to be strongly upregulated by such Ras-ERK pathway mutations in a variety of cancer types, where they often play a role in modulating tumour development (Díaz-García et al., 2014; Kim et al., 2014; Lee et al., 2012; Okudela et al., 2009; Shojaee et al., 2015). Taken together these traits indicate that MKPs might play functional roles in pancreatic cancer development, therefore investigating this hypothesis is a key focus of our group. Furthermore, investigating MKPs in pancreatic cancer could help demonstrate the relative important of the ERK pathway in this cancer and give significant insights into therapeutically modulating the ERK pathway in pancreatic cancer. As described previously, there is strong evidence demonstrating changes in DUSP6/MKP-3 expression throughout the progression of human PDAC (Furukawa et al., 2003, 2005). Loss of DUSP6/MKP-3 expression correlates with the progression from high grade PanINs to invasive PDAC, leading to the hypothesis that DUSP6/MKP-3 could constrain progression from high grade PanIN to PDAC and that DUSP6/MKP-3 loss could be a key event during pancreatic carcinogenesis (Furukawa et al., 2006). However, there is currently very limited evidence showing that these changes in DUSP6/MKP-3 expression which have been observed are playing a functional role in PDAC progression. Therefore, future studies could modulate DUSP6/MKP-3 expression in mouse models of PDAC to determine whether DUSP6/MKP-3 loss can promote PDAC progression.

There is only very limited evidence for changes in expression or possible functional roles for other MKPs in pancreatic cancer. DUSP1/MKP-1 has been shown to be overexpressed at both the mRNA and protein level in pancreatic cancer or chronic pancreatitis relative to normal pancreatic tissue. DUSP1/MKP-1 knockdown decreased the proliferation rate, colony formation ability and tumourigenic capacity following xenograft into nude mice of pancreatic cancer cell lines, suggesting DUSP1/MKP-1 has an oncogenic function in pancreatic cancer (Liao et al., 2003). DUSP4/MKP-2 is strongly upregulated in pancreatic cancer cell lines following the expression of mutant KRas or constitutively active MEK, and is able to prevent ERK hyperactivation (Yip-Schneider et al., 2001). More recently, DUSP4/MKP-2 has been shown to be downregulated during progression from high-grade IPMN to invasive pancreatic carcinoma by frequent genomic copy number aberrations occurring at 8p11.22-ter causing genomic loss of DUSP4/MKP-2 (Hijiya et al., 2016). Restoration of DUSP4/MKP-2 expression in pancreatic cancer cells with such genomic events suppressed invasiveness and increased anoikis via ERK inactivation. Utilising an orthotopic xenograft model of pancreatic cancer DUSP4/MKP-2 restoration was shown to promote increased survival, with mice displaying decreased tumour size and fewer metastases. Conversely, knockdown of DUSP4/MKP-2 promoted anoikis resistance, invasiveness and cell motility in pancreatic cancer cells expressing DUSP4/MKP-2. Together these results imply that DUSP4/MKP-2 downregulation may promote tumour growth and invasiveness in pancreatic cancer (Hijiya et al., 2016). Finally, DUSP10/MKP-5 has been shown to be a direct target of the microRNA miR-92a, which is overexpressed in pancreatic cancer cell lines. miR-92a-mediated downregulation of DUSP10/MKP-5 promotes elevated JNK signalling and cell proliferation (He et al., 2014).

1.5 Aims

The primary aim of this thesis was to determine whether the MKPs DUSP5 and DUSP6/MKP-3 are able to modulate the oncogenic potential of Ras-ERK pathway mutations, and thus play a functional role in the initiation and progression of cancer. Our approach involved the utilisation of murine cancer models to determine whether the loss of DUSP5 or DUSP6/MKP-3 could alter tumour development in these models, coupled with the use of *in vitro* cell culture based models and immunohistochemical analysis of tissue samples to investigate the mechanism by which DUSP loss could be modulating cancer development.

Our initial project aimed to determine whether DUSP5 loss influences the development of skin papillomas in the DMBA/TPA-induced model of skin carcinogenesis. In conjunction we investigated the biochemical consequences of DUSP5 loss in MEFs in response to TPA or oncogenic stimuli, to determine the mechanism by which DUSP5 loss modulated skin carcinogenesis. Our second project aimed to investigate the regulation of DUSP expression by mutant KRas in MEFs, and whether the loss of DUSP5 or DUSP6/MKP-3 has any functional biochemical consequences on ERK activity and its target substrate or the cellular phenotype of $KRas^{G12D}$ expressing MEFs. The final project aimed to use mouse models to determine any potential roles for DUSP5 and DUSP6/MKP-3 in the initiation and progression of $KRas^{G12D}$-driven pancreatic ductal adenocarcinoma.

Chapter 2 Materials & Methods

2.1 Mouse strains and *in vivo* procedures

2.1.1 Mouse strains and tumour models

DUSP5^{fl} and *DUSP6*^{fl} strains were generated by Taconics Artemis, and the *DUSP5*^{fl} strain has been described previously (Rushworth et al., 2014). *DUSP6* conditional mice were generated by homologous recombination. Briefly, a targeting construct was generated which introduced a neomycin selectable marker flanked by LoxP sites into intron 1, along with an additional LoxP site following exon 3 of the murine DUSP6 gene. Mouse C57BL/6N embryonic stem (ES) cells were electroporated with the linearized targeting construct and neomycin-resistant clones were identified by Southern blot. Chimeric mice were generated through the microinjection of positive clones into C57BL/6N blastocysts. Chimeras were crossed to generate mice expressing the conditional DUSP6 allele and germline transmission of the allele was confirmed by Southern blot. Targeted mice were crossed with *EIIaCre* transgenic mice, to enable the mosaic excision of the neomycin resistance cassette due to the pre-disposition of Cre to more efficiently recombine LoxP sites located closer together (Holzenberger et al., 2000). The resulting chimeric mice were crossed and their offspring screened for the neomycin cassette-free conditional DUSP6 allele by PCR.

Kras$^{LSL\text{-}G12D/+}$ and *Pdx1-cre* (Hingorani et al., 2003) strains were obtained for Owen Sansom (Beatson Institute, Glasgow). *Ptf1α-cre (P48*$^{+/Cre}$*)* mice (Kawaguchi et al., 2002) were obtained from Miguel Constância (University of Cambridge). *SerpinB2*$^{-/-}$ mice (Dougherty et al., 1999) were obtained from Jackson labs (strain B6.129S1-*Serpinb2*^{tm1Dgi}/J).

Kras$^{LSL\text{-}G12D/+}$; *DUSP5*^{fl} and *Pdx1-cre; DUSP5*^{fl} strains were intercrossed to generate *Kras*$^{LSL\text{-}G12D}$*; Pdx1-cre; DUSP5*^{fl} experimental mice as well as control cohorts for the initial pancreatic cancer study. For the second study pancreatic cancer study *Kras*$^{LSL\text{-}G12D}$, *Ptf1α-cre*, *DUSP5*^{f,}, *DUSP6*^{fl} and *SerpinB2*$^{-/-}$ strains were intercrossed to generate mice with the required genotype.

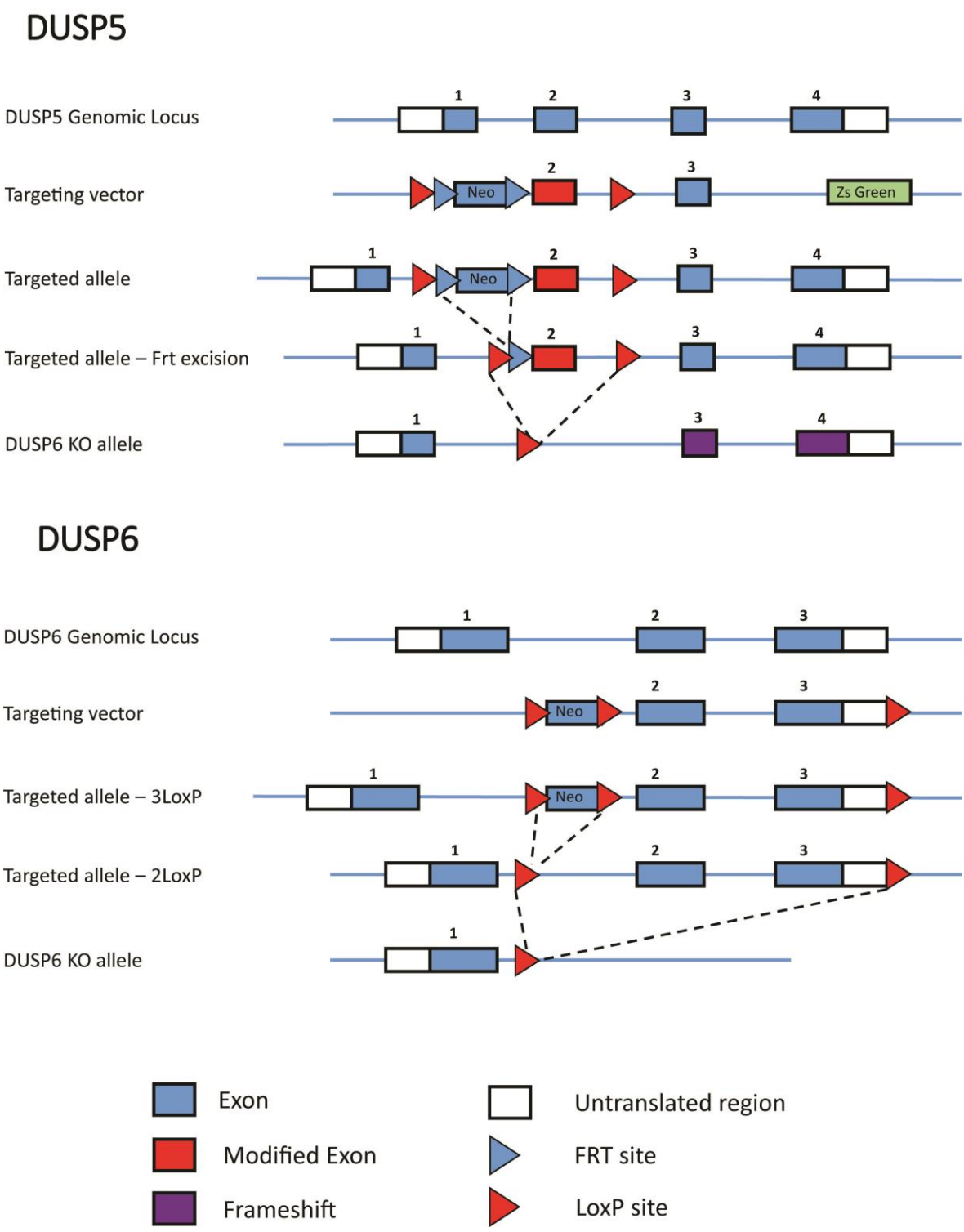

Figure 2.1 Targeting strategies utilised for the generation of the *DUSP5*^{fl} and *DUSP6*^{fl} strains.

For the pancreatic cancer studies both survival and age-matched cohorts were generated. These cohorts contained an equal balance of both male and female mice. All study mice were monitored closely through weighing and health assessment three times per week. Mice were removed from the study once they lost over 20% of their maximal body-weight, generated visible ascites or were moribund and visibly unwell.

All lines were maintained on a C57/B6 background. All animal procedures were performed under license (UK project license number 7008570) in accordance with the UK Home Office Animals (Scientific Procedures) Act (1986) and after local ethical review following institutional guidelines.

2.1.2 Skin carcinogenesis model

DMBA/TPA chemical carcinogenesis was performed as described by Abel and colleagues (2009). Briefly, the dorsal fur of 7.5 week-old mice was shaved and, at 8 weeks, animals were treated with DMBA (50µg in 100µL acetone). The following week, bi-weekly treatment with TPA (12.5ug in 100µL acetone) was commenced to promote papilloma formation. Treatment was continued for 25 weeks to enable the assessment of papilloma formation. During this time the initiation, number and size of papillomas was recorded weekly.

2.1.3 Genotyping

Genomic DNA for genotyping was obtained from ear notches. Ear notches were lysed overnight in 500µl lysis buffer (75mM NaCl, 25mM EDTA, 1% w/v SDS) containing 0.4mg/ml proteinase K (Life Technologies). 730µl chloroform (Sigma) and 157µl 5M NaCl (Sigma) was added to each sample and this incubated on a rotator for 45 min. Samples were then centrifuged at 13,000rpm for 10 min, the upper aqueous phase removed and added to an eppendorf containing 500µl isopropanol (VWR). The resulting samples were mixed by inversion, centrifuged at 13,000rpm for 10 min and the supernatant removed. The resulting DNA was washed in 500µl 70% ethanol, and resuspended in 80µl TE (Tris-EDTA – Life Technologies) buffer. All genotyping was performed by multiplex PCRs carried out using puReTaq Ready-to-go-PCR beads (GE Biosciences). The primers used and expected diagnostic products are outlined below.

PCR	Primers	PCR products
Cre	oMIR 15 (5'-CAAATGTTGCTT GTCTGGTG -3')	206bp (control) & 370bp (Cre)
	oMIR 16 (5'-GTCAGTCGAGTGCACAGTTT -3')	
	Cre 685 (5'-ACCTGAAGATGTTCGCGA TTATCT -3')	
	Cre 1054 (5'-ACCGTCAGTACGTGAGATATCTT -3')	
DUSP5	WT 5'-GCCTTCGATCTTCTCTTG TG-3'	667bp (WT), 418bp (KO) & 701bp (floxed)
	KO 5'-AGGGAGCTGCTGTTTTCAGC-3'	
	Common 5'-ACCATGAATGCACAGGAACC-3'	
DUSP6	WT 5'-TTCAGACCTCATCTGAAAGACATGAGTAGT-3'	250bp (WT), 400bp (KO) & 284bp (floxed)
	KO 5'-CGGCGCCTGCGCCGGGGTAACCTGCCGGTGCG-3'	
	Common 5'-TGCGAGTATGAGCGCCCATTTGGTGGATGC-3'	
$KRas^{LSL-G12D}$	WT 5'-CCCCAGCACAGTGCAGTTTTGACACCAGCTTCGGC-3'	450bp (WT) & 327bp (LSL-G12D)
	LSL 5'-AGCTAGCCACCATGGCTTGAGTAAGTCTGCA-3'	
	Common 5'-CCGAATTCAGTGACTACAGATGATCAGAG-3'	
SerpinB2	WT 5'-TTTGATAGGCGGGTTGTTTC TCTGT-3'	500bp (WT) & 650bp (KO)
	KO 5'-CAGCCGAACTGTTCGCCAGG-3'	
	Common 5'-GTTTGTCCACCATGCTCCCTCTA-3'	

Table 2.1 Genotyping PCR Primers

2.2 Tissue processing, histochemistry and immunohistochemistry

2.2.1 Tissue processing

Tissue samples were fixed in 4% formaldehyde saline solution (VWR) overnight, and then transferred to 70% ethanol, before processing using a Citadel Shandon 2000 (ThermoScientific) to allow paraffin wax infiltration. Processed tissue was placed at the required orientation and embedded in paraffin wax blocks. Paraffin blocks were sectioned at 5µm and sections adhered to glass microscopy slides (VWR). Slides were baked overnight at 60°C before use in histochemical or immunohistochemical staining.

2.2.2 Histochemistry

2.2.2.1 Haematoxylin & Eosin (H&E) staining

Slides were cleared by incubation in xylenes (2 x 10 min), followed by rehydration through decreasing concentrations of ethanol (100% x 2, 95%, 90% & 70% - 2 min each). This was followed by a brief rinse in distilled water. Slides were then incubated in Mayer's Haematoxylin (Sigma) for 15 min, before rinsing and "blueing" of the Haematoxylin in running tap water for 5 min. The process was repeated for the Eosin stain (Sigma) using an incubation time of 40s followed by rinsing in running tap water for 5 min. All slides were then dehydrated through increasing concentrations of ethanol (70%, 90%, 95% & 100% x 2 - 2 min each), cleared in xylenes (2 x 10 min) before mounting under coverslips using Omnimount mounting medium (National Diagnostics).

2.2.2.2 Alcian Blue staining

Slides were cleared by incubation in xylenes (2 x 10 min), followed by rehydration through decreasing concentrations of ethanol (100% x 2, 95%, 90% & 70% - 2 min each). This was followed by a brief rinse in distilled water before incubation in Alcian Blue solution (Sigma) for 30 min. Slides were then rinsed in running tap water for 5 min to remove any excess Alcian Blue. The slides were then counterstained with Nuclear Fast Red (Sigma) for 5 min, followed by rinsing in running tap water for 5 min. All slides were then dehydrated through increasing concentrations of ethanol (70%, 90%, 95% & 100% x 2 - 2 min each), cleared in xylenes (2 x 10 min) before mounting under coverslips using Omnimount.

2.2.3 Immunohistochemistry

Immunohistochemistry was performed using VectorStain ABC Kits (Vector Laboratories). Slides were cleared by incubation in xylenes (2 x 10 min), followed by rehydration through decreasing concentrations of ethanol (100% x 2, 95%, 90% & 70% - 2 min each). This was followed by a brief rinse in distilled water, before incubation with 3% hydrogen peroxide (VWR) for 5 min to quench endogenous peroxidase enzymes within the tissue. Slides were then washed in distilled water (3 x 2min), followed by antigen retrieval in sodium citrate (10mM, pH 6.0 – Sigma) for 20 min in a water bath at 99^{o}C. The sodium citrate solution containing the slides was then removed from the water bath and allowed to cool

for a further 20 min, before slides were rinsed in distilled water, then washed in Tris-buffered saline (TBS)-Tween (3 x 5 min). IHC pen was then used to create a hydrophobic barrier around the tissue to be stained. Slides were blocked for 45 min with goat serum solution (from the VectorStain ABC Kit). Primary antibody was diluted in the goat serum solution and incubated on the slides overnight at 4°C or at room temperature for 1-2 h. Slides were then washed in TBS-Tween (3 x 5 min), before incubation with biotinylated secondary antibody for 45 min and ABC-HRP (Horseradish peroxidase) complex for 30 min, with TBS-Tween washes (3 x 5 min) after each stage. Staining was visualised through the application of DAB reagent for the required time. DAB application time was initially optimised to produce clear staining whilst minimising background signal. Slides were then counterstained with Mayer's Haematoxylin for 5 min, before rinsing and "blueing" of the Haematoxylin in running tap water for 5 min. All slides were then dehydrated through increasing concentrations of ethanol (70%, 90%, 95% & 100% x 2 - 2 min each), cleared in xylenes (2 x 10 min) before mounting under coverslips using Omnimount mounting medium (National Diagnostics).

The primary antibodies used for immunohistochemistry and their relevant concentrations and DAB incubation times are outlined below.

Primary Antibody	**Supplier**	**Cat #**	**Dilution**	**Incubation**	**DAB**
aSMA	Abcam	Ab124964	1 : 2,500	O/N @ 4^{o}C	1 min
c-Cas3	Cell Signalling	9664	1 : 1,000	O/N @ 4^{o}C	5 min
CK19	DSHB	TROMA-III	1 : 10	O/N @ 4^{o}C	3-5 min
DUSP5	Abcam	Ab200708	Not optimised, also stained relevant KO tissue at all conditions attempted.		
DUSP6/MKP-3	Abcam	Ab76310			
Ki67	Cell Signalling	12202	1 : 400	O/N @ 4^{o}C	5 min
p21	Abcam	Ab109199	1 : 500	O/N @ 4^{o}C	3-5 min
p53	Vector	VP-P956	1 : 200	1-2h @ RT	1-3 min
pAKT (s473)	Cell Signalling	4060	1 : 50	O/N @ 4^{o}C	5-10 min
PDX1	Abcam	Ab47267	1 : 10,000	O/N @ 4^{o}C	1 min
pERK	Cell Signalling	4370	1 : 400	O/N @ 4^{o}C	5 min
Sox9	Millipore	Ab5535	1 : 40,000	O/N @ 4^{o}C	1 min

Table 2.2 Immunohistochemistry (IHC) antibodies and optimised conditions.

2.2.4 Imaging and analysis of staining

All slides required for imaging or analyses were scanned on a Leica Biosystems Aperio XT slide scanner and images taken and quantitative analysis performed on Aperio ImageScope software (Leica Biosystems).

2.3 RNA isolation from mouse tissue

For RNA (ribonucleic acid) isolation small tissue samples (~3mm^3) were removed from the organ of interest and placed in RNA Later RNase inhibitor solution (Life Technologies), on ice for no longer than 30 min. Tissue was then transferred to 300µl RLT lysis buffer (Qiagen) and scissor-minced in a 2ml eppendorf, before being lysed with a Tissue Ruptor homogeniser (Qiagen) until no visible tissue remained. Total RNA was isolated from the sample using an RNeasy fibrous tissue kit (Qiagen) according to the manufacturer's instructions. Reverse transcription and quantitative real-time PCR were then carried out as explained in section 2.7.

2.4 Generation of primary cell lines & cell culture

2.4.1 Generation of primary mouse embryonic fibroblast cell lines

Primary MEFs were isolated from E13.5 day old embryos generated by crossing parents heterozygous for the transgenes of interest to allow embryos of all genotypes to be derived from a single litter. To generate KRas$^{LSL\text{-}G12D/G12D}$ MEFs cells had to be isolated from E11.5 day embryos to overcome KRas knockout induced embryonic lethality, which occurs between E12-14 in mice (Johnson et al., 1997).

The uterus was dissected from a pregnant female and the embryos removed. From each embryo the yolk sac was removed to be used for genotyping. The embryo's head and internal organs were removed on a 10cm plate in phosphate-buffered saline (PBS) and the trunk was minced into fine pieces with scissors. 3ml/plate of 0.05% trypsin-EDTA (Life Technologies) was added, the solution was then pipetted to disaggregate the tissue. 3ml/plate Dulbecco's modified Eagles medium (DMEM), supplemented with 10% Foetal Bovine Serum (FBS) (Life Technologies) was added to terminate trypsinisation. Cells were then centrifuged at 1,200rpm for 5 min, resuspended in 2ml 0.05% trypsin-EDTA to

complete the disaggregation, then plated in DMEM, supplemented with 10% FBS, 100mM sodium pyruvate, 2.5 mM L-Glutamine and 100units/ml each of Penicillin and Streptomycin (Life Technologies).

Primary MEFs were subsequently cultured in DMEM, supplemented with 10% FBS, 100mM sodium pyruvate, 2.5 mM L-Glutamine and 100units/ml each of Penicillin and Streptomycin (Life Technologies).

2.4.2 Generation of primary murine pancreatic ductal adenocarcinoma cancer cell lines

Immediately following dissection and identification of pancreatic ductal adenocarcinoma (PDAC) a small piece of tumour (~0.3 x 0.3 x 0.3 cm) was removed and placed into ice-cold PBS for no longer than 30 min. The tumour sample was then placed in 0.5ml PBS in a 6cm plate and diced into small pieces. 5ml of 1mg/ml collagenase V (Sigma) diluted in DMEM (Life Technologies) was then added and the solution incubated at 37°C for 45min. The collagenase was subsequently quenched with 5ml PDAC media (DMEM supplemented with 20% FBS, 4.5 g l^{-1} glucose, 1mM L-glutamine, 0.11 g l^{-1} pyruvate, 50 $mgml^{-1}$ gentamycin, 100Uml^{-1} penicillin and 100$mgml^{-1}$ streptomycin – Life Technologies) and centrifuged at 350g for 5 min. The partly digested tumour was then resuspended in 2ml 0.05% trypsin/EDTA for 5min at 37°C. The trypsin was quenched with 2ml PDAC media, the solution centrifuged at 350g for 5 min and the cell pellet washed in PBS before being resuspended in 6ml PDAC media and seeded in a 25cm^2 cell culture flask (ThermoScientific). Cells were maintained in PDAC media and bulked up for a week following isolation, subsequently they were transferred into standard cell culture media (DMEM, supplemented with 10% FBS, 100mM sodium pyruvate, 2.5 mM L-Glutamine and 100units/ml each of Penicillin and Streptomycin - Life Technologies) for use in future experiments.

2.5 Immortalisation of mouse embryonic fibroblast cell lines

Primary MEF cell lines were immortalised for use in transfection experiments through the transfection and stable integration of ARF (p14arf) shRNA using a retroviral pSUPER-retro-shARF vector. Phoenix helper cells were plated 24h before transfection with the pSUPER-

retro-shARF vector using lipofectamine LTX (Life Technologies), allowing the production and packaging of the retrovirus. Virus-containing media was harvested 48h post-transfection, filter sterilised, and used to transfect primary MEFs in the presence of 8μg ml^{-1} polybrene. Transfected cells were subsequently selected in 2μg ml^{-1} puromycin (Sigma) for 7 days before use in further experiments.

shARF immortalised MEFs were subsequently cultured in DMEM, supplemented with 10% FBS and 100units/ml each of Penicillin and Streptomycin (Life Technologies).

The pSUPER-retro-shARF vector and phoenix helper cells were kindly provided by Prof Martin Eilers (Theodor-Boveri-Institute, Wurzburg, Germany).

2.6 Transfections of mouse embryonic fibroblasts

2.6.1 Adenoviral transfections

Primary or shARF immortalised MEF cell lines were plated 18h before transfection. For DUSP5 rescue experiments, Ad5-Empty, Ad5-egr1-DUSP5 and Ad5-egr1-DUSP5-KIM adenoviral vectors (C. Caunt, University of Bath) were transfected at titres in the range 0.1-3 pfu/nl, in DMEM, supplemented with 10% FBS (Life Technologies). Pfu/nl, rather than multiplicity of infection (MOI), was used as it more accurately reflected the amount of transgene delivery between experiments. For Cre-recombinase transfections Ad5-CMVempty and Ad5-CMVCre vectors (Gene Transfer Vector Core) were transfected at 250 MOI in DMEM, supplemented with 10% FBS (Life Technologies). In both protocols transfection media was replaced with culture media after 6 h and the cells were incubated at 37°C for 18 h before being treated as the experiment demanded.

2.6.2 siRNA transfections

shARF immortalised MEFs were transfected with a final concentration of 20nM of siRNA oligonucleotides (Life Technologies /Dharmacon). Solutions of siRNA oligonucleotides (balanced with negative control siRNA to ensure equal final concentrations if required) and Lipofectamine RNAimax (Life Technologies) were prepared separately in OptiMEM media. After 5 min, the solutions were mixed and incubated at room temperature for 20 min. The combined solution was added directly to the cells in culture media and

incubated at 37°C for 16 h. Subsequently, the media was changed and the cells treated as the experiment required. Throughout this project a combination of reverse and forward transfections were used depending on the requirements of the experiment in question. The siRNA oligonucleotides used in this project are listed in below.

siRNA Target Gene	Supplier	Catalogue Number
Non-targeting control	Life Technologies	4390843
Egr1	Life Technologies	S65378
	Life Technologies	S65380
	Dharmacon	J-040286-05-0005
	Dharmacon	J-040286-06-0005
Egr3	Life Technologies	S65385
Egr4	Life Technologies	S65387

Table 2.3 siRNA

2.6.3 Plasmid DNA transfections

Immortalised MEFs were transfected with plasmid DNA as follows. A mixture of plasmid DNA and Lipofectamine LTX plus reagent at 1 µl Plus Reagent per µg plasmid DNA (Life Technologies) was prepared in OptiMEM media (Life Technologies). After 5 min Lipofectamine LTX was added at 1:50, and the mixture incubated at room temperature for 20 min. This mixture was added directly to the culture media and the cells incubated at 37°C for 16 h. After this time, the cells were treated as the experiment demanded.

2.7 Quantitative real-time PCR

Total RNA was isolated from cells using Qiashredder and RNeasy kits (Qiagen) according to the manufacturer's instructions. 200ng of RNA was reverse-transcribed in a final volume of 50µl using Taqman reverse transcription reagents (Applied Biosystems). The thermal cycle used was: 25^{o}C for 5 min, 48^{o}C for 30 min, 95^{o}C for 5 min. The cDNA sample was diluted 1:3 in RNase-free water. A 4ng sample of cDNA was analysed by quantitative real-time PCR using Taqman pre- validated assay probes and Taqman 2x Universal Mastermix (Applied Biosystems). An Applied Biosystems 7500 machine was used with the

following cycling conditions: 50°C for 2 min, 95°C for 10 min, 95°C for 15s and 60°C for 1 min, with the final 2 steps repeated 40 times. Fluorescence output was considered to be directly proportional to the input cDNA concentration and was normalised against β-actin expression. Taqman qPCR probes used in this project are detailed in the table below.

Gene (murine)	**Taqman qPCR Probe ID**
ALDH1A3	Mm00474049_m1
Beta-actin	Mm00607939_s1
Car2	Mm00501576_m1
DUSP1/MKP-1	Mm00457274_g1
DUSP2	Mm00839675_g1
DUSP4/MKP-2	Mm00723761_m1
DUSP5	Mm01266104_m1
DUSP6/MKP-3	Mm00518185_m1
DUSP7	Mm01232570_m1
DUSP9/MKP-4	Mm00512648_g1
EGR1	Mm00656724_m1
EGR3	Mm00516979_m1
EGR4	Mm00842279_g1
Fos	Mm00487425_m1
SerpinB2	Mm00440905_m1
Sox9	Mm00448840_m1
Gene (Human)	**Taqman qPCR Probe ID**
Beta-actin	Hs99999903_m1
EGR1	Hs00152928_m1

Table 2.4 Taqman qRT-PCR Primers.

2.8 Subcellular fractionation

For subcellular fractionation experiments MEFs were seeded in 10cm tissue culture treated plates. Following the required stimulations cells were harvested by adding 5ml/plate of trypsin/EDTA mix and incubated at 37°C for 5 min. 10ml of DMEM containing

10% FBS was added to quench the trypsin, and the suspension centrifuged at 500g for 5 min. The cell pellet was washed in 1ml PBS, transferred to a 1.5ml micro-centrifuge tube and re-pelleted by centrifugation at 500g for 3 min. Cells were lysed in 100µl ice-cold CER I buffer (containing Halt protease and phosphatase inhibitors) from the NE-PER nuclear and cytoplasmic extraction reagent kit (Life Technologies). The NE-PER nuclear and cytoplasmic extraction reagent kit was then used according to the manufacturer's instructions to isolate the cytoplasmic and nuclear fractions. Briefly, cell lysates in CER I buffer were vortexed for 15 s, and incubated on ice for 10 min before the addition of 5.5µl CER II buffer. The lysate was then vortexed again and incubated for a further minute before centrifugation at maximum speed in a microcentrifuge for 5 min. The supernatant (cytoplasmic extract) was removed and retained. 50µl NER buffer was added to the remaining pellet to be incubated on ice for 40 min and vortexed every 10 min. Finally, the lysate was centrifuged at maximum speed in a microcentrifuge for 10 min, and the supernatant (nuclear extract) removed. Lysate concentration was then determined via Bradford assay and immunoblots performed as outlined below.

2.9 Immunoblot analysis

Cells were washed twice in cold PBS and lysed with MKK lysis buffer (20mM Tris Acetate, 270mM Sucrose, 1mM EDTA, 1mM EGTA, 1% v/v Triton X-100, 1% v/v B-mercaptoethanol) containing phosphatase and protease inhibitor tablets (Roche). The lysates were centrifuged for 10 min at 13000rpm to eliminate debris, the cleared lysate removed, and a Bradford assay performed to determine the protein concentration within each lysate. Lysate concentrations were normalised with further MKK buffer, followed by the addition of reducing agent (4x NuPAGE LDS sample buffer - ThermoScientific) before being boiled for 5 min at 95^{o}C. Equivalent quantities of protein were resolved in 4-12% gradient Bis-Tris Protein Gels (ThermoScientific), transferred onto Immobilon-FL PVDF membranes (Millipore), blocked in 5% milk or 5% BSA, then incubated with the required primary antibody at 4^{o}C overnight. Membranes were washed 3 times for 5 min with PBS-Tween before incubation with corresponding fluorescent-tagged secondary antibodies (Cell Signalling/ Life Technologies), diluted in 5% milk, for 1 hour at room temperature, avoiding exposure to light. Finally, membranes were washed a further 3 times for 5 min with PBS-Tween before reactive bands were visualised and quantified on a Li-Cor Odyssey imaging system (LI-COR Biosciences).

All immunoblots included in this thesis were performed a minimum of three times for quantification. Infrared fluorescent signals are directly proportional to the amount of antigen present on Li-Cor Odyssey scanned immunoblots, this linear relationship enables accurate and reproducible quantification of changes in protein levels and the detection of small consistent effects which might not be immediately obvious by eye. Figure 2.2 shows an immunoblot greyscale image from a Li-Cor scan and the multicolour image with the raw quantification values below.

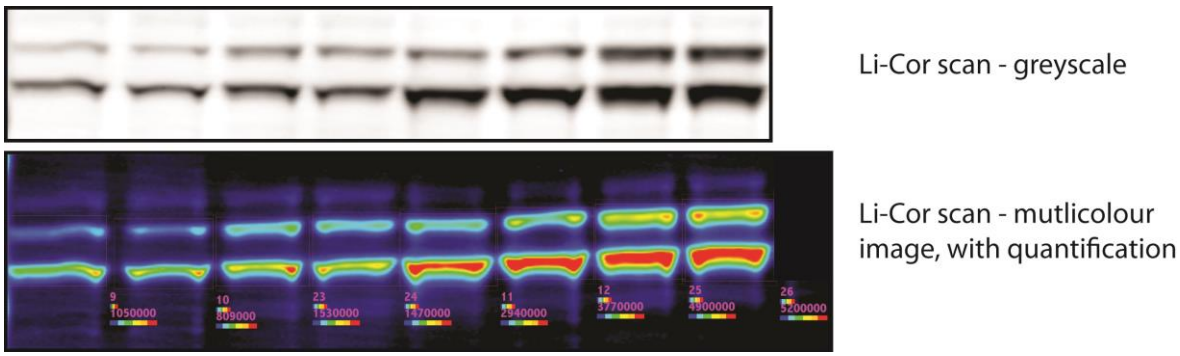

Figure 2.2 Fluorescent immunoblotting and quantification using a Li-Cor Odyssey. A representative image of the multicolour display and quantification values obtained for the same blot shown in greyscale above. The multicolour image and quantification demonstrate the ability of this technique to reliably detect consistent small changes in protein levels.

Quantification of the protein of interest was normalised to an appropriate loading control. Furthermore, to account for differences in raw Li-Cor fluorescence values between repeats quantification values were expressed relative to the control sample for each individual experiment. Figures are displayed containing the mean quantification from all of the experiments performed with a representative image of the immunoblots from one experiment alongside.

Primary and secondary antibodies used and their relevant concentrations and dilution buffers are outlined below.

Primary Antibody	Supplier	Cat #	Dilution	Buffer
AKT (11E7)	Cell Signalling	4685	1 : 1,000	5% BSA
Beta Tubulin (Clone AA2)	Sigma	T8328	1 : 10,000	5% Milk/BSA
DUSP1/MKP-1	Santa Cruz	sc-1102	1 : 100	5% Milk
DUSP4/MKP-2 (S18)	Santa Cruz	sc-1200	1 : 100	5% Milk
DUSP5	In house	N/A	1 : 2,000	5% BSA
DUSP6/MKP-3	Abcam	AB76310	1 : 1,000	5% Milk
DUSP9/MKP-4	In house	N/A	1 : 2,000	5% Milk
EGR1 (15F7)	Cell Signalling	4153	1 : 500	5% BSA
ERK	Cell Signalling	4695	1 : 1,000	5% BSA
GAPDH	Cell Signalling	2118	1 : 1,000	5% Milk/BSA
HA-tag - C29F4	Cell Signalling	3724	1 : 1,000	5% BSA
MEK	Cell Signalling	9122	1 : 1,000	5% BSA
p-AKT (ser473) D9E	Cell Signalling	4060	1 : 2,000	5% BSA
p-ERK (Thr202/Tyr204)	Cell Signalling	4370	1 : 1,000	5% BSA
p-MEK (ser217/221)	Cell Signalling	9154	1 : 1,000	5% BSA
Ras (27H5) - Pan	Cell Signalling	3339	1 : 1,000	5% BSA
Ras G12D	New East Bio	26036	1 : 200	5% BSA
SerpinB2 (M70)	Santa Cruz	Sc-25746	1 : 100	5% BSA
UBF	Brian McStay	N/A	1 : 1,000	5% BSA

Table 2.5 Primary antibodies – immunoblotting.

Secondary Antibody	Supplier	Cat #	Dilution	Buffer
Alexa Fluor® 680 conjugate, Donkey anti-Sheep IgG	ThermoScientific	A-21102	1 : 10,000	5% Milk
DyLight™ 680 Conjugate, Goat anti-rabbit IgG	Cell Signalling	5366	1 : 10,000	5% Milk
DyLight™ 800 Conjugate, Goat anti-rabbit IgG	Cell Signalling	5151	1 : 10,000	5% Milk
DyLight™ 800 Conjugate, Goat anti-mouse IgG	Cell Signalling	5257	1 : 10,000	5% Milk

Table 2.6 Secondary antibodies – immunoblotting.

2.10 Ras-GTP pulldown with Raf1-RBD-GST beads

For Ras-GTP pulldown experiments $1.5x10^6$ MEFs were seeded onto 15cm tissue culture treated plates. Following the required stimulations cells were washed twice in PBS and lysed in Mg2+ lysis buffer (MLB) (containing Halt protease and phosphatase inhibitors – Life Technologies) from a Ras Activation Assay Kit (Millipore). A Bradford assay was performed to allow 600µg of protein to be loaded per pulldown, and then the Ras Activation Assay (Ras-GTP pulldown with Raf1-RBD-GST) was performed according to the manufacturer's instructions. Briefly, 600µg of lysate was incubated with 10µg of Raf1-RBD-GST beads for 45 min at 4^oC with gentle agitation. Beads were then pelleted by centrifugation (10 s, 14,000xg, 4^oC) and washed three times in MLB. Ras was then disassociated from the Raf1-RBD-GST beads with the addition of 2X Laemmli reducing sample buffer and boiling at 95^oC for 5 min. Immunoblots were then performed as described previously.

2.11 Luciferase reporter assays

Murine Serpin B2 promoter-reporter constructs were kindly provided by Prof Toni Antalis (University of Maryland School of Medicine, Baltimore, Maryland) (Udofa et al., 2013). These luciferase reporter constructs consisted of wild type, truncated or mutant fragments of the murine Serpin B2 proximal promoter cloned into the pGL3 vector. Empty pGL3 vector was used as a negative control, and pRL-TK (*Renilla* luciferase driven by the herpes simplex virus thymidine kinase promoter) was co-transfected with the reporter constructs to normalize for transfection efficiency.

MEFs were seeded in 24-well tissue culture treated plates and transfected as described previously (2.6.3). MEFs were incubated for 16h post-transfection before treatment with 100ng/ml final concentration of TPA (12-O-Tetradecanoylphorbol-13-acetate) or a DMSO (Dimethyl sulfoxide) control for 8h. For detection of reporter expression the dual luciferase reporter assay (Promega) was used according to the manufacturer's instructions, and luminescence measured by an Orion II microplate luminometer (Berthold Systems).

2.12 Proliferation assays

Proliferation assays in MEFs were performed using an adaptation of the protocol described in Tuveson et al., (2004). Briefly, $6x10^4$ cells were plated in 6 well tissue culture treated plates before infection with 250 MOI of adenoviral Cre or empty adenoviral vector as described previously (2.6.1). Cell counts were then taken every 2-3 days until the cells reached confluence. Cells of each genotype of interest were taken from a minimum of three independent litters of MEFs to ensure other genetic differences between MEF lines could not influence the result. Data was presented as the fold increase in cell number or the relative difference between the empty and Cre-treated cells to demonstrate the effect of the knock-in or knockout of the gene of interest by adenoviral Cre.

2.13 Colony formation assays

Colony formation assays in MEFs were performed using an adaptation of the protocol described in Sage et al., (2000). Cells of each genotype of interest were taken from a minimum of three independent litters of MEFs and transfected with 250 MOI of adenoviral Cre or empty adenoviral vector as described previously (2.6.1). These cells were bulked up before being re-plated onto 10cm plates, in technical triplates, for colony formation assays.

To assess whether the cells have lost contact inhibition so form multi-layered colonies (foci), cells were seeded at high density (10^6 cells per 10cm plate). To determine whether cells have been transformed and are able to proliferate from single cells to form colonies (clonogenic growth) cells were seeded at low density (10^3 cells per 10cm plate). Cells were then grown for 2-3 weeks, with the media replaced every 2-3 days. After 2-3 weeks the media was removed and the cells washed with PBS, before fixation in ice-cold methanol. Cells were stained with 0.5% crystal violet (0.5% w/v in 25% methanol, 75% H_20 – Sigma) and the number of visible colonies approximately ≥2mm counted.

Chapter 3 DUSP5 loss promotes $HRas^{Q61L}$-driven skin tumourigenesis through the upregulation of SerpinB2

3.1 Introduction

DUSP5 is a nuclear-inducible, ERK-specific MKP, with the ability to selectively dephosphorylate and subsequently anchor ERK within the nucleus (Mandl et al., 2005). DUSP5 expression is specifically induced by ERK activity, making it a classical negative feedback regulator of the ERK pathway (Kucharska et al., 2009). Taken together this evidence indicates that DUSP5 has the ability to modulate the magnitude, duration and spatial localisation of ERK activity (Caunt and Keyse, 2013). Deregulation of the ERK pathway, leading to constitutively active ERK signalling, is often observed in human cancers due to the high frequency of activating mutations in upstream pathway components including RTKs, Ras isoforms and BRaf (Dhillon et al., 2007; Prior et al., 2012). The mechanism of action and functional consequences of such mutations in cancer has been the subject of intensive study and are relatively well understood. However, the importance of also understanding the roles of negative regulators of such pathways and their potential influence on tumourigenesis is only just coming to the fore (Lemmon et al., 2016).

Thus far, relatively little is known about the specific role(s) of MKPs in cancer development, and this is particularly the case for DUSP5 (Keyse, 2008). Many studies have revealed increased DUSP5 expression in mutant Ras and BRaf-driven cancer cell lines (Kreeger et al., 2009; Pratilas et al., 2009; Vartanian et al., 2013; Yun et al., 2009), where it is presumed that this phosphatase plays some role in modulating the increased ERK activity which results from oncogene activation. As one of the primary functions of the ERK pathway is to promote proliferation, DUSP5-mediated suppression of ERK activity, might be assumed to have a tumour suppressive effect. This is consistent with the observation that ectopic expression of DUSP5 decreased both ERK activity and proliferation in lung and colon cancer cells (Ueda et al., 2003). Furthermore, in both gastric and prostate cancer low levels of DUSP5 expression correlate with shortened patient survival (Cai et al., 2015; Shin et al., 2013), and the restoration of DUSP5 expression in gastric cancer cells decreased their proliferative capacity and colony-

forming ability (Shin et al., 2013). Together such evidence links DUSP5 with a tumour suppressive role. However, hyperactive ERK signalling can also promote cellular senescence (Deschênes-Simard et al., 2013; Meloche and Pouysségur, 2007), giving rise to the hypothesis that in certain contexts DUSP5 could have an oncogenic role by preventing the induction of oncogene induced senescence (OIS) by unrestrained ERK activity. This is supported by the observation that the expression of DUSP5 can promote the proliferation of certain cancer cells (Nunes-Xavier et al., 2010) and that another ERK-specific MKP, DUSP6/MKP-3 has been shown to be essential for the oncogenic transformation of pre-B-cells in murine models of ALL (Shojaee et al., 2015).

The majority of studies investigating the role of MKPs in human cancer development are limited by the fact they typically rely on correlations between MKP expression and clinical outcome (Keyse, 2008; Kidger and Keyse, 2016). Furthermore, the majority of experimental studies have used cancer cell lines, coupled with ectopic MKP overexpression to investigate their role *in vitro*. Therefore, there is a requirement for genetic loss of function experiments in animal models to reveal any potential roles for MKPs in tumourigenesis *in vivo*. Consequently, in work leading up to the studies described here we generated DUSP5$^{-/-}$ mice, which were then subjected to the two-stage DMBA/TPA-initiation/promotion skin carcinogenesis model (Abel et al., 2009) to investigate the functional consequences of DUSP5 loss on skin cancer development. In addition, we isolated DUSP5 wild type and knockout MEFs in order to investigate the biochemical and cellular consequences of DUSP5 ablation in an attempt to dissect out the mechanism(s) by which any effects on tumourigenesis could be occurring.

3.2 Work preceding this thesis

3.2.1 Loss of DUSP5 sensitises mice to DMBA/TPA-induced skin carcinogenesis

To investigate whether DUSP5 ablation had any effect on the formation of mutant Ras-induced skin papillomas we utilised the DMBA/TPA-induced, two-stage skin carcinogenesis model (Abel et al., 2009). Cohorts of $DUSP5^{+/+}$, $DUSP5^{+/-}$ and $DUSP5^{-/-}$ mice were initially treated with DMBA (50µg) at 8 weeks of age, to induce characteristic $HRas^{Q61L}$ mutations, followed by twice weekly promotion with TPA (12.5µg) for 25 wk. Mice from all three cohorts began to develop skin papillomas after 5-6 weeks and $DUSP5^{+/-}$ and $DUSP5^{-/-}$ mice reached 100% tumour incidence somewhat faster than $DUSP5^{+/+}$ mice (Fig. 3.1A). However, the major difference between the cohorts was that $DUSP5^{-/-}$ mice developed a significantly higher papilloma burden than $DUSP5^{+/+}$ mice, reaching an average of 20 papillomas per mouse by 25 weeks, compared to only 10 for $DUSP5^{+/+}$ mice, while $DUSP5^{+/-}$ animals showed an intermediate phenotype (Fig. 3.1B). None of the animals of any genotype went on to display invasive, squamous cell carcinomas or other malignant skin lesions, probably due to the very low rate of malignant conversion in DMBA/TPA-treated C57BL/6 mice (Abel et al., 2009). The papillomas from all three genotypes appeared very similar morphologically, being defined as squamous cell papillomas, and the size distribution of papillomas across the genotypes appeared unchanged (Fig. 3.1C & D). Finally, DNA sequencing revealed the presence of $HRas^{Q61L}$ mutations in ~90% of the papillomas of each genotype (Fig. 3.1E). This is the signature driving mutation in DMBA/TPA-induced skin cancers (Chakravarti et al., 1995), indicating that the mechanism of DMBA-induced mutagenesis promoting tumour initiation is unaltered following DUSP5 loss. Together this data indicates that DUSP5 acts as a tumour suppressor in the DMBA/TPA model of HRas-induced skin cancer.

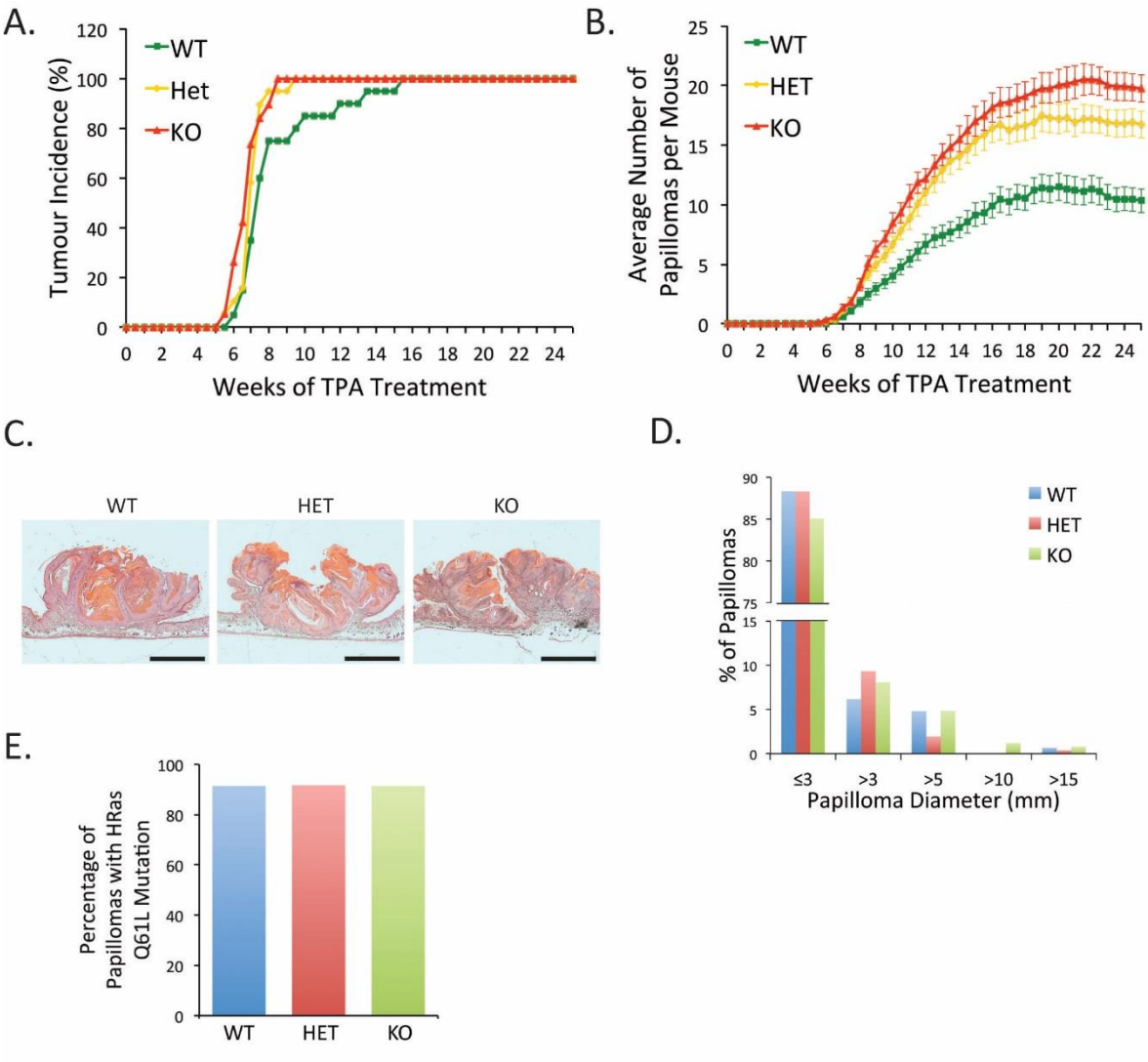

Figure 3.1 Loss of DUSP5 sensitises mice to DMBA/TPA-induced skin carcinogenesis. DUSP5$^{+/+}$ (WT), DUSP5$^{+/-}$ (HET), and DUSP5$^{-/-}$ (KO) animals (n = 19 per cohort) were exposed to DMBA followed by TPA treatment for 25 weeks. **A)** Tumour incidence. DUSP5 loss decreased latency (P values: WT/HET = 0.0304; WT/KO = 0.0029, repeated measures multivariate ANOVA with Tukey's post hoc analysis). **B)** Average number of tumours per mouse (P values: WT/HET = 0.000761; WT/KO = 0.000002, repeated measures multivariate ANOVA with Tukey's post hoc analysis). **C)** H&E stained sections of representative skin papillomas at 25 weeks. (Scale bar, 1mm). **D)** Tumour size distribution after 25 weeks. **E)** Percentage of papillomas from each genotype with HRas^{Q61L} mutations. Data courtesy of Dr Linda Rushworth.

3.2.3 Loss of DUSP5 does not alter whole cell *p*-ERK levels or the proliferation rate of MEFs

To investigate the molecular mechanism by which DUSP5 loss promotes sensitisation to DMBA/TPA-induced skin carcinogenesis, $DUSP5^{+/+}$, $DUSP5^{+/-}$ and $DUSP5^{-/-}$ MEFs were isolated from littermate embryos. DUSP5 is known to specifically target ERK (Mandl et al., 2005), therefore initially DUSP5 wild-type and knockout MEFs were subjected to TPA stimulation and *p*-ERK levels were determined by immunoblotting. Surprisingly, no clear changes in the magnitude or duration of ERK phosphorylation could be detected in $DUSP5^{-/-}$ MEFs compared to wild-type (Fig. 3.2A). Furthermore, expression levels of other MKPs capable of targeting ERK including DUSP1/MKP-1, DUSP4/MKP-2, DUSP6/MKP-3 and DUSP9/MKP-4 were also unchanged, indicating that compensatory upregulation of other MKPs does not occur in the absence of DUSP5 (Fig. 3.2A). Next we went on to investigate basic cellular phenotypes of DUSP5 MEFs. However, we found that DUSP5 loss had no effect on the proliferation rate of MEFs or their colony forming potential when transfected with Ras mutants (Fig. 3.2B & C).

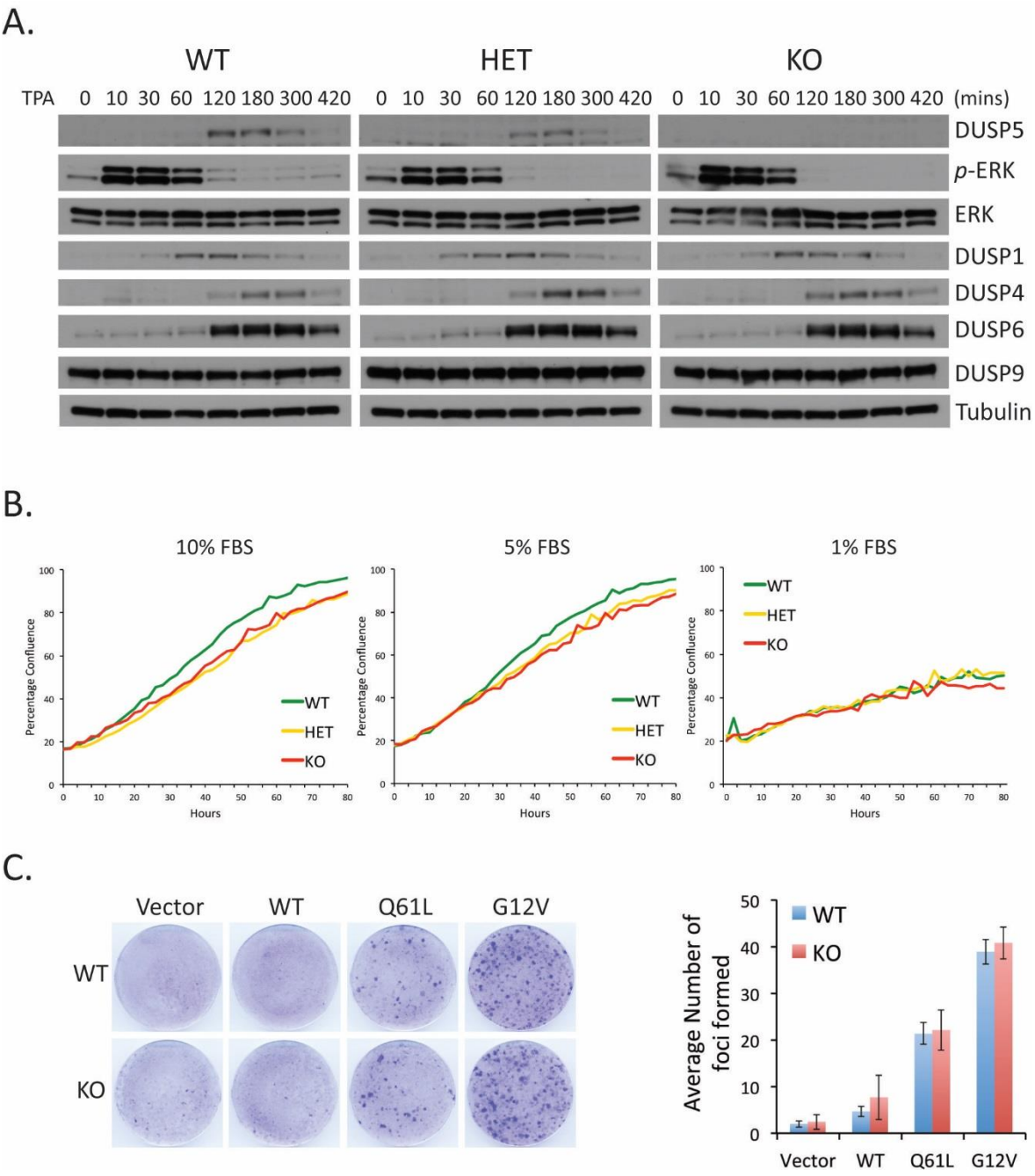

Figure 3.2 DUSP5 loss has no effect on the kinetics of ERK activation, and no clear cellular phenotype in MEFs. A) DUSP5$^{+/+}$ (WT), DUSP5$^{+/-}$ (HET), and DUSP5$^{-/-}$ (KO) primary MEFs were treated with 100ng/mL TPA for the indicated times. Cells were lysed and proteins analysed by immunoblotting using the indicated antibodies. **B)** Primary MEFs of each genotype were grown in the indicated serum conditions cell proliferation was monitored over 80 hours using an IncuCyte Zoom live cell imaging system. **C)** Transforming potential of immortalized WT and KO MEFs following expression of wild-type HRas (WT), HRas^{Q61L} (Q61L), or HRas^{G12V} (G12V). Representative images (Left) and quantification are shown (Mean ± SEM, n = 3). Data courtesy of Dr Linda Rushworth.

3.3 Results

3.3.1 DUSP5 loss specifically increases nuclear *p*-ERK activation following TPA stimulation

As DUSP5 is a solely nuclear phosphatase, and the nucleus contains only a fraction of the total protein of a cell, we hypothesised that spatial alterations in ERK activity might be occurring upon DUSP5 loss which would not be detected in whole cell lysates. To address this theory we performed subcellular fractionation of lysates from DUSP5$^{+/+}$ and DUSP5$^{-/-}$ MEFs following TPA stimulation. DUSP5 loss was shown to promote a significant increase in the levels of nuclear, but not cytoplasmic, *p*-ERK one hour after TPA stimulation (Fig. 3.3A).

To investigate this phenotype in a more detailed and quantitative manner we used confocal microscopy and high-content imaging to visualise and quantify the levels of *p*-ERK and total ERK at the single cell level in TPA-treated MEFs (Fig. 3.3B & C). This analysis revealed that DUSP5 ablation has two key effects on the spatiotemporal regulation of ERK signalling at short time points following TPA stimulation. In agreement with our biochemical analysis using subcellular fractionation, DUSP5 loss promoted a significant increase in the levels of nuclear *p*-ERK. This occurred rapidly following stimulation, peaking between 30-60 minutes after exposure to TPA, then as nuclear *p*-ERK levels decreased towards 360 minutes the difference in *p*-ERK levels between DUSP5$^{+/+}$ and DUSP5$^{-/-}$ MEFs was lost. This indicates that basal DUSP5 levels as well as its rapid induction by ERK activity (Kucharska et al., 2009) have a key role in restraining nuclear ERK activity following stimulation. The reduction in the difference in nuclear *p*-ERK levels over time could imply that other negative feedback mechanisms are now compensating for the lack of DUSP5, or that by later time points DUSP5 degradation will have commenced (Kucharska et al., 2009), meaning its ablation could have less influence on nuclear *p*-ERK levels. Secondly, DUSP5 loss reduces the levels of total ERK retained in the nucleus post-stimulation, reflecting DUSP5's role as a nuclear anchor for dephosphorylated ERK (Mandl et al., 2005). Finally, in contrast DUSP5 loss has no effect on cytoplasmic levels of either *p*-ERK or total ERK (Fig. 3.3B & C).

Wild type levels of DUSP5 can be restored in DUSP5$^{-/-}$ MEFs through their infection with adenovirus expressing Myc-tagged, wild-type DUSP5 under the control of an ERK-responsive early growth response 1 (Egr1) promoter. Utilising a viral titre, which gives rise to protein levels that closely mirror endogenous DUSP5 expression, both confocal and high content microscopy (Fig. 3.3B & C) and biochemical fractionation experiments (Fig. 3.3D) demonstrate that wild-type levels of nuclear *p*-ERK and total ERK can be rescued in DUSP5$^{-/-}$ MEFs (Fig. 3.3B, C & D). Crucially, an adenovirus expressing the DUSP5 KIM mutant, which is catalytically active, but unable to bind and inactivate ERK (Mandl et al., 2005), is unable to reverse the phenotypes observed in DUSP5$^{-/-}$ MEFs (Fig. 3.3B & C). This demonstrates that the increased nuclear *p*-ERK observed in DUSP5$^{-/-}$ MEFs is truly dependent on DUSP5 loss, and more precisely dependent on the ability of DUSP5 to bind and dephosphorylate ERK. Therefore, this non-redundant function of DUSP5 in the regulation of nuclear *p*-ERK levels implies that DUSP5 loss and the associated increase in nuclear ERK activity could contribute to the increased sensitivity of DUSP5$^{-/-}$ mice to Ras-driven carcinogenesis.

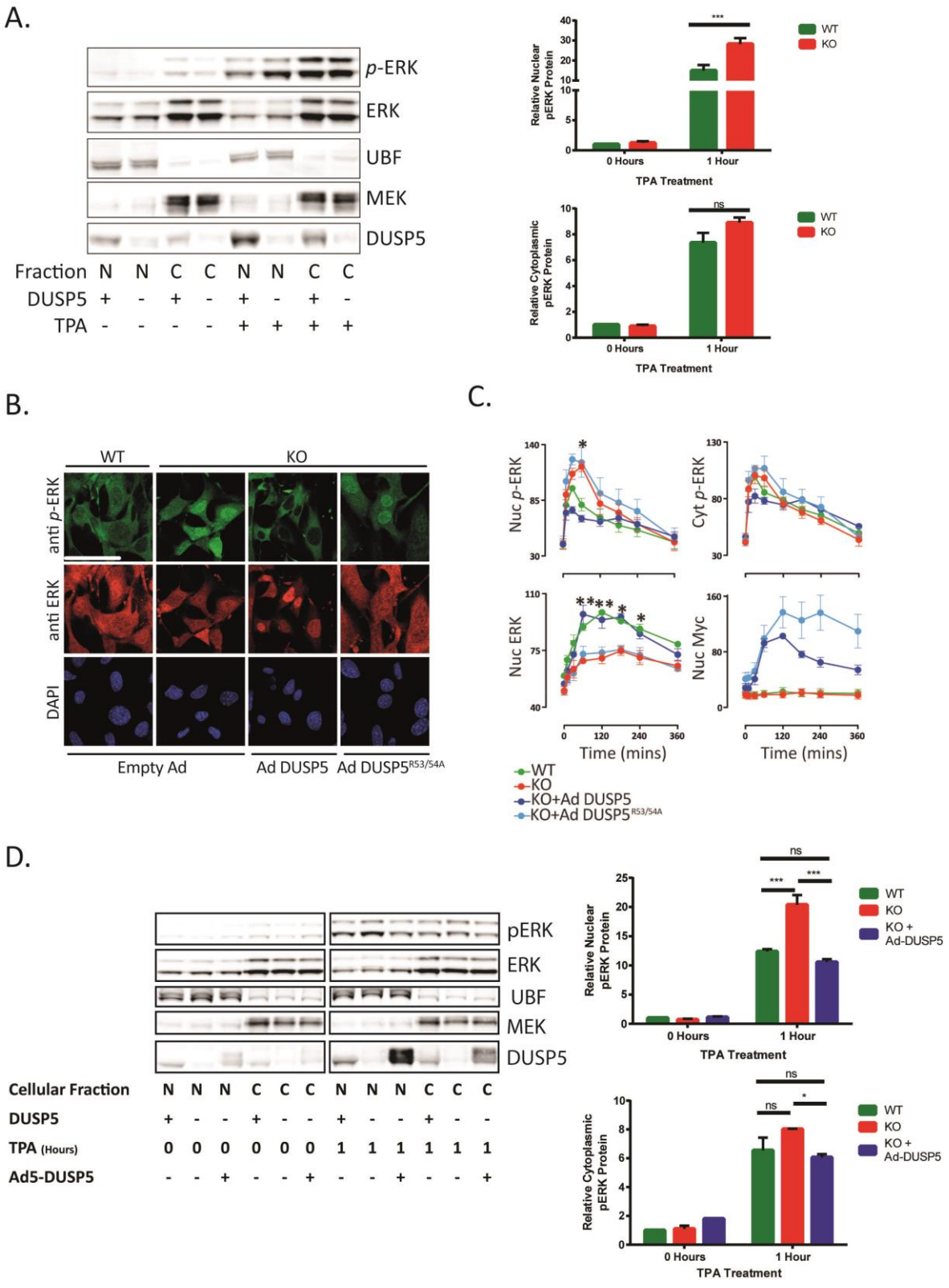

Figure 3.3 DUSP5 ablation increases nuclear *p*-ERK levels following TPA stimulation. A) DUSP5$^{+/+}$ (WT) and DUSP5$^{-/-}$ (KO) primary MEFs were stimulated with TPA for 0 or 1 hour, before lysis, subcellular fractionation and immunoblotting using the indicated antibodies. Upstream binding factor (UBF) and MEK were used to validate separation of nuclear (N) and cytoplasmic (C) proteins, respectively. A representative Western blot is shown (Left), alongside *p*-ERK quantification, relative to the WT unstimulated sample, utilising a Li-Cor Odyssey infrared scanner (Right). **B)** Representative confocal images of WT and KO MEFs, after 1 hour TPA stimulation, following infection with empty adenovirus (empty Ad), Ad-Egr1 promoter-driven DUSP5-Myc (Ad

DUSP5), or Ad-Egr1 promoter-driven KIM mutant of DUSP5-Myc (Ad DUSP5$^{R53/54A}$). (Scale = 60 µm). **C)** MEFs were infected with virus prior to the indicated TPA stimulation, and then stained for *p*-ERK, total ERK, Myc or DAPI, before image analysis using high content fluorescence microscopy. Graphs represent population average values for nuclear (Nuc) and cytoplasmic (Cyt) *p*-ERK, ERK, or Myc intensity, derived from four separate experiments, with 5,000–10,000 individual cells per condition. **D)** WT and KO MEFs were infected with either Ad5-Empty or Ad5-DUSP5 prior to TPA stimulation for 0 or 1 hour, followed by lysis, subcellular fractionation and immunoblotting using the indicated antibodies. A representative Western blot is shown (Left), alongside *p*-ERK quantification (Right). Mean values ± SEM are shown, n = 5 **(A)**, n = 4 **(B-C)**, n = 3 **(D)**. ns = not significant, *P < 0.05, **P < 0.01, ***P<0.001 using two-way ANOVA and Bonferroni post hoc test. Panels B-C courtesy of Dr Christopher Caunt.

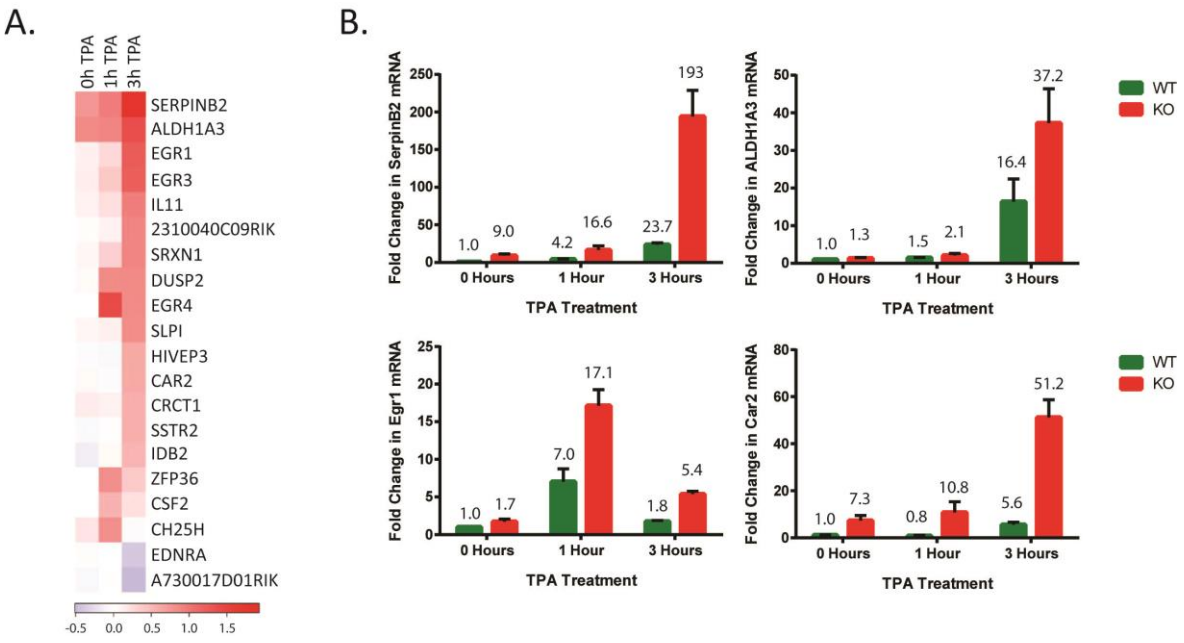

Figure 3.4 Loss of DUSP5 increases the expression of a subset of TPA-inducible genes. A) Heatmap showing significant gene expression changes detected by microarray following the indicated TPA treatment of DUSP5$^{+/+}$ (WT) and DUSP5$^{-/-}$ (KO) primary MEFs. Values are log2 ratios of KO/WT. **B)** Taqman RT-qPCR assay showing the fold change in mRNA levels (relative to WT unstimulated) of the indicated genes in WT and KO MEFs following TPA stimulation. Mean values ± SEM are shown (and displayed above the bar on the graph), n = 3. Panel A courtesy of Dr Philip East (CR-UK Bioinformatics & Biostatistics group).

3.3.2 DUSP5 loss increases the expression of a subset of TPA-inducible genes

As nuclear *p*-ERK is known to regulate the activity of many transcription factors (Cargnello and Roux, 2011; Yoon and Seger, 2006), a logical consequence of increased nuclear ERK activity following DUSP5 loss would be the alteration of ERK-dependent gene expression. Therefore, to investigate the effects of DUSP5 loss on gene expression we performed a microarray experiment to compare the gene expression profiles of $DUSP5^{+/+}$ and $DUSP5^{-/-}$ primary MEFs following 0, 1 or 3 hours of TPA stimulation (Fig. 3.4A). Surprisingly this revealed that although hundreds of genes are induced in response to TPA stimulation, only 20 genes showed significant differences in expression upon DUSP5 ablation (Rushworth et al., 2014 - www.ncbi.nim.nih.gov/geo accession No. GSE62433). Of these 20 genes, 18 were upregulated and 2 were downregulated on DUSP5 loss. RT-qPCR analysis could validate the upregulation of many of these genes following TPA stimulation of $DUSP5^{-/-}$ MEFs, relative to wild-type (Fig. 3.4B & data not shown). The most strongly upregulated gene following DUSP5 ablation was SerpinB2 (also known as plasminogen activator inhibitor 2, PAI-2). Interestingly, three members of the early growth-response (Egr) family of transcription factors were also significantly upregulated in cells lacking DUSP5.

We chose to focus on SerpinB2 because as well as being our top hit, it had previously been demonstrated to play a pro-oncogenic role in DMBA/TPA-mediated skin carcinogenesis, and it was suggested that this was due to the promotion of cell survival via the inhibition of apoptosis (Tonnetti et al., 2008; Zhou et al., 2001). SerpinB2 upregulation following DUSP5 loss and TPA stimulation could be validated at both the mRNA and protein level in three-independent pairs of $DUSP5^{+/+}$ and $DUSP5^{-/-}$ primary MEFs (Fig. 3.5A & B). SerpinB2 induction can clearly be shown to be ERK-dependent, as it is abrogated by pre-treatment of cells with PD184352, a specific MEK inhibitor (Fig. 3.5A & B). Furthermore, SerpinB2 upregulation in $DUSP5^{-/-}$ MEFs can be shown to be dependent on the loss of DUSP5-mediated inhibition of nuclear *p*-ERK activity, as SerpinB2 mRNA levels are very strongly suppressed by the re-expression of wild-type DUSP5, but not the DUSP5 KIM mutant, in $DUSP5^{-/-}$ MEFs (Fig. 3.6). Normalised expression levels of adenoviral DUSP5 wild-type and KIM mutant proteins were optimised via immunoblotting.

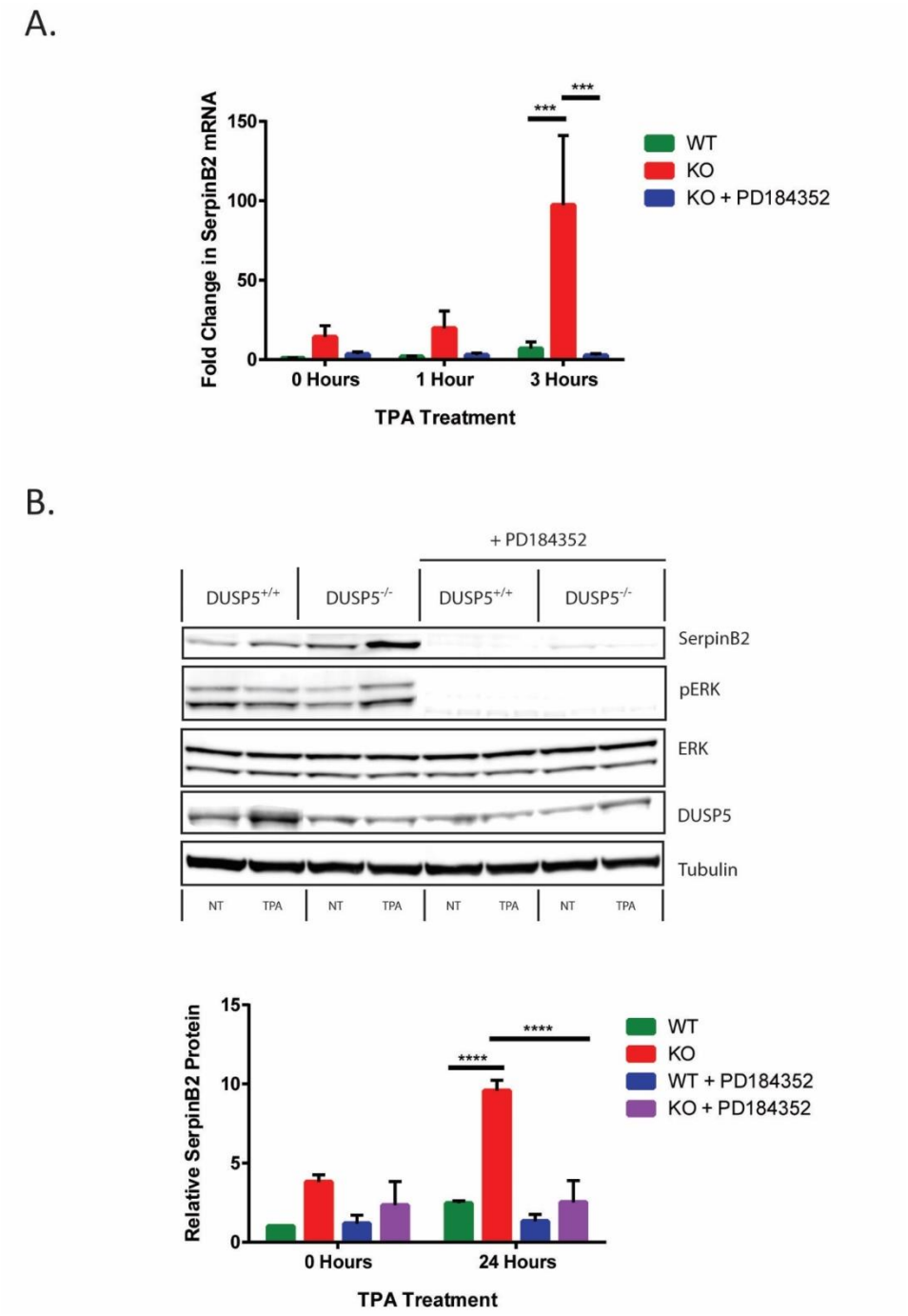

Figure 3.5 DUSP5 loss upregulates SerpinB2 in a MEK-dependent manner. SerpinB2 induction in DUSP5$^{+/+}$ (WT) and DUSP5$^{-/-}$ (KO) primary MEFs at either the mRNA **(A)** or protein **(B)** level following TPA stimulation for the indicated time, in the presence of the MEK inhibitor PD184352 or DMSO control. MEFs were pre-treated with MEK inhibitor 30 min prior to TPA stimulation, and maintained in MEK inhibitor for the duration of the experiment. **A)** Taqman RT-qPCR assay showing the fold change in SerpinB2 mRNA levels, relative to WT unstimulated. **B)** Immunoblot analysis using the indicated antibodies, following no treatment (NT) or 24 hour TPA stimulation (TPA). A representative Western blot is shown (Upper), alongside SerpinB2 quantification (Lower). DUSP5 is a 42kDa protein and the anti-DUSP5 sheep polyclonal antibody used detects a DUSP5 band at this molecular weight, which is inducible following TPA stimulation in DUSP5$^{+/+}$, but not DUSP5$^{-/-}$ MEFs. However, this antibody also detects a non-specific band also at approximately 42kDa, explaining why the DUSP5$^{-/-}$ MEFs still appear to show DUSP5 expression. Mean values ± SEM are shown, n = 4 (A), n = 3 (B). ***P < 0.001, ****P<0.0001 using two-way ANOVA and Bonferroni post hoc test.

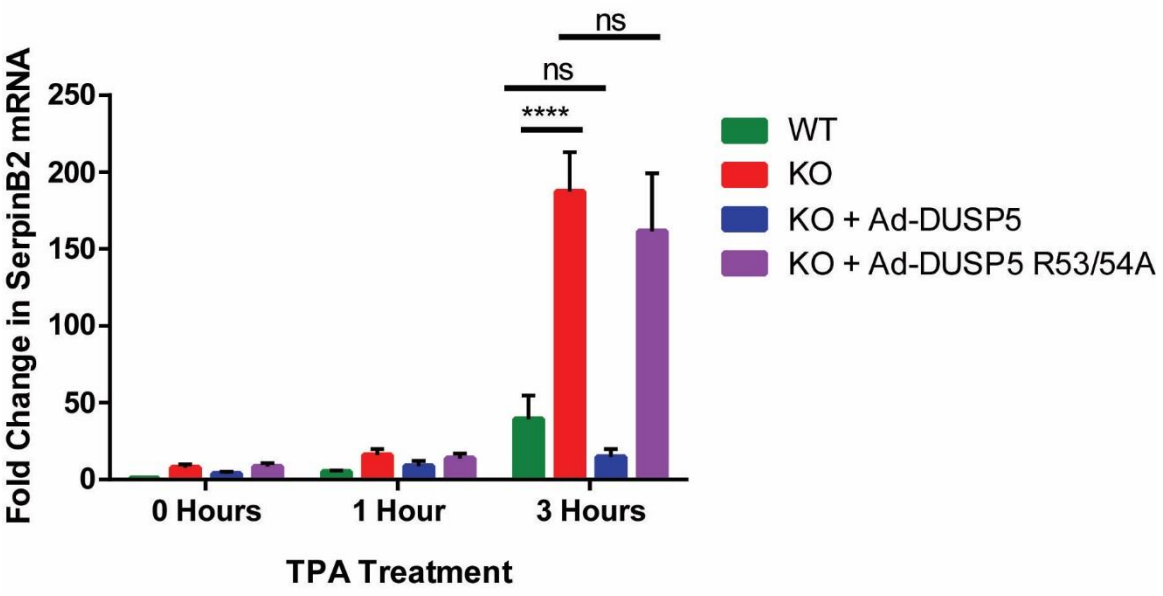

Figure 3.6 DUSP5 reintroduction rescues wild-type SerpinB2 expression. Taqman RT-qPCR assay showing the fold change in SerpinB2 mRNA levels (relative to WT unstimulated) in DUSP5$^{+/+}$ (WT) and DUSP5$^{-/-}$ (KO) primary MEFs following infection with empty adenovirus (control), Egr1 promoter-driven Ad-DUSP5-Myc (Ad-DUSP5), or Ad KIM mutant of DUSP5-Myc (Ad-DUSP5$^{R53/54A}$) as indicated and subsequent TPA stimulation. Mean ± SEM, n = 4. ns = not significant, ****P<0.0001 using two-way ANOVA and Bonferroni post hoc test.

3.3.3 SerpinB2 upregulation following DUSP5 loss is dependent on Egr1 expression and AP-1 transcription factors

The induction of SerpinB2 expression is somewhat delayed following TPA stimulation, with peak mRNA expression occurring after 3 hours (Fig. 3.5A). In contrast, Egr family transcription factors are canonical immediate early genes, with transcription occurring rapidly following TPA stimulation and mRNA expression levels peaking after only 1 hour (Fig. 3.4A & B). Therefore, we hypothesised that Egr family transcription factors could play some role in mediating the induction of SerpinB2 following TPA stimulation. To address this question we used siRNA to knockdown either Egr1 alone or a combination of Egr1, Egr3 and Egr4 in DUSP5$^{-/-}$ MEFs, and assayed SerpinB2 mRNA induction following TPA stimulation. This revealed that Egr1 knockdown significantly reduced TPA-inducible SerpinB2 mRNA levels, while combining knockdown of Egr1 with loss of Egr3 and Egr4 caused no further inhibition of SerpinB2 expression (Fig. 3.7A). Treatment with either Egr1, Egr3 or Egr4 siRNA induced a 60-80% decrease in the expression of their respective mRNAs following TPA stimulation (Fig. 3.7A). This indicates that the lack of an additional response following combined Egr1, 3 and 4 knockdown, in comparison to Egr1 knockdown alone, is not due to a lack of efficacy of the Egr3 and Egr4 siRNA. However, it could be due to the very low expression levels of Egr3 and Egr4 in MEFs relative to Egr1 expression (Fig. 3.7A). To ensure that the ability of the Egr1 siRNA used to inhibit TPA-induced SerpinB2 expression was not due to off-target effects of this particular siRNA we repeated the Egr1 siRNA knockdown experiment with a panel of three distinct Egr1 siRNAs. Each Egr1 siRNA inhibited SerpinB2 induction in a manner proportional to its ability to knockdown Egr1 mRNA (Fig. 3.7B), providing strong evidence that the inhibition of SerpinB2 induction is an on-target effect of Egr1 siRNA-mediated knockdown.

We went on to further validate this Egr1-dependent mechanism for SerpinB2 induction by performing siRNA rescue experiments. siRNA-mediated knockdown of murine Egr1 reduced TPA-inducible SerpinB2 expression at both the mRNA and protein level in MEFs, whereas ectopic overexpression of human EGR1 increased SerpinB2 expression (Fig. 3.7C & D). The mRNA produced by the human EGR1 gene is predicted to be resistant to knockdown by the murine Egr1 siRNA utilised, based on a lack of homology between the siRNA binding sequence in murine Egr1 mRNA and the human EGR1 mRNA. This resistance can be confirmed by the expression of human EGR1 mRNA and protein

following transfection of DUSP5$^{-/-}$ MEFs with both a human EGR1 containing plasmid and murine Egr1 siRNA (Fig. 3.7C & D). Combining siRNA-mediated knockdown of murine Egr1, with the expression of the siRNA resistant human EGR1 construct completely rescued any effects of Egr1 knockdown on SerpinB2 mRNA expression after 3 hours of TPA treatment or SerpinB2 protein levels after 24h of TPA treatment, indicating that the modulation of SerpinB2 expression is occurring in an Egr1 –dependent manner (Fig. 3.7C & D).

Finally, we obtained immortalised wild-type and Egr1 knockout MEFs (Krones-Herzig et al., 2005; Lee et al., 1995) and demonstrated that cells lacking Egr1 had reduced SerpinB2 mRNA levels following TPA stimulation and that this could be rescued by ectopic expression of human EGR1 in Egr1$^{-/-}$ MEFs (Fig. 3.7E). Taken together, our results strongly suggest that the increased induction of the transcription factor Egr1 plays a positive role in the subsequent up-regulation of SerpinB2 expression seen on loss of DUSP5.

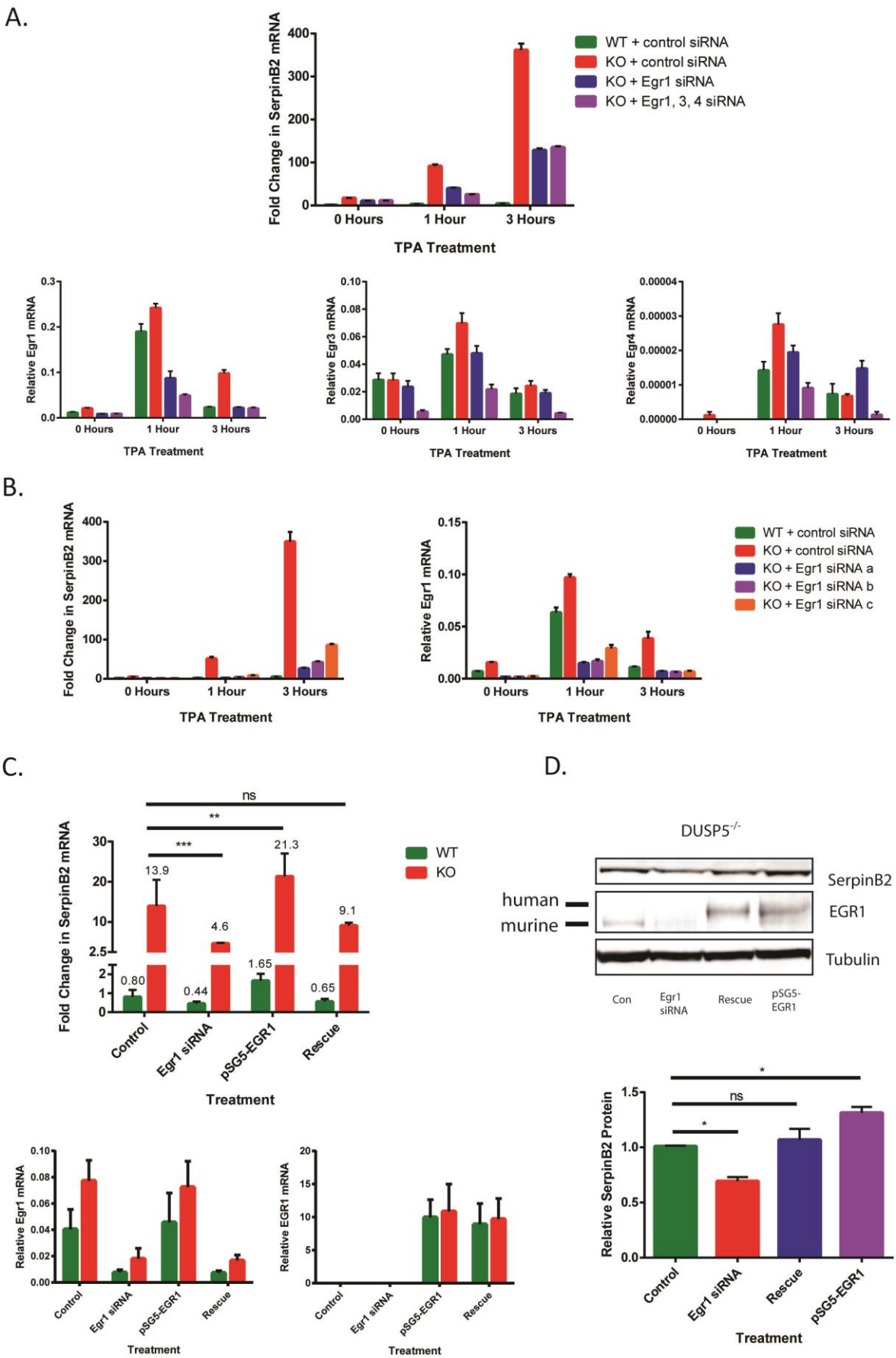
A.
Fold Change in SerpinB2 mRNA
WT + control siRNA
KO + control siRNA
KO + Egr1 siRNA
KO + Egr1, 3, 4 siRNA
0 Hours
1 Hour
3 Hours
TPA Treatment
Relative Egr1 mRNA
Relative Egr3 mRNA
Relative Egr4 mRNA
B.
Fold Change in SerpinB2 mRNA
Relative Egr1 mRNA
WT + control siRNA
KO + control siRNA
KO + Egr1 siRNA a
KO + Egr1 siRNA b
KO + Egr1 siRNA c
C.
ns
**
***
13.9
4.6
21.3
9.1
0.80
0.44
1.65
0.65
WT
KO
Control
Egr1 siRNA
pSG5-EGR1
Rescue
Treatment
Relative Egr1 mRNA
Relative EGR1 mRNA
D.
DUSP5-/-
human
murine
SerpinB2
EGR1
Tubulin
Con
Egr1 siRNA
Rescue
pSG5-EGR1
Relative SerpinB2 Protein

E.

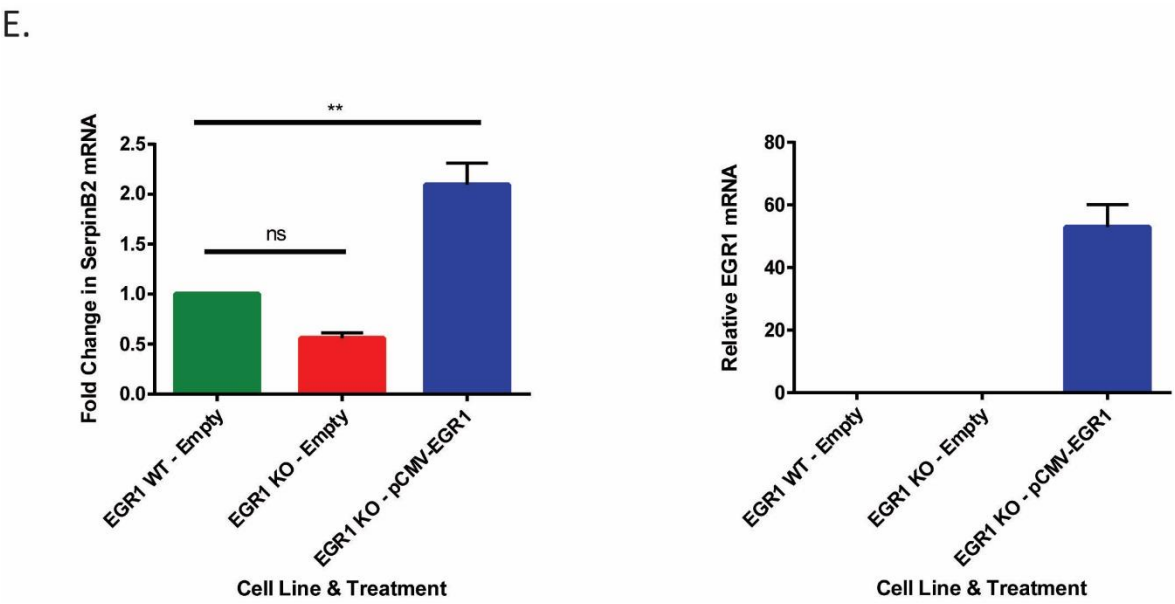

Figure 3.7 SerpinB2 upregulation following DUSP5 loss is dependent on Egr1 expression. A) Taqman RT-qPCR assay showing the fold change in SerpinB2 mRNA levels (relative to WT unstimulated) in DUSP5$^{+/+}$ (WT) and DUSP5$^{-/-}$ (KO) shARF immortalised MEFs following transfection with scrambled control siRNA, Egr1 siRNA or a combination of Egr1, 3 & 4 siRNA as indicated and subsequent TPA stimulation (Upper Panel). mRNA levels of Egr1, Egr3 & Egr4, relative to β-actin, from the same experiment demonstrate the efficacy of siRNA knockdown (Lower Panel) Representative figures of an experiment performed in duplicate. **B)** Taqman RT-qPCR assay showing the fold change in SerpinB2 mRNA levels (relative to WT unstimulated) in DUSP5$^{+/+}$ (WT) and DUSP5$^{-/-}$ (KO) shARF immortalised MEFs following transfection with scrambled control siRNA or multiple distinct Egr1 siRNAs and subsequent TPA stimulation (Left Panel). mRNA levels of Egr1, relative to β-actin, from the same experiment (Right Panel) Representative figures of an experiment performed in duplicate. **C-D)** SerpinB2 expression in DUSP5 WT and KO MEFs at either the mRNA **(C)** or protein **(D)** level following Egr1 knockdown (Egr1 siRNA + pSG5-Empty transfection), human EGR1 overexpression (scrambled siRNA + pSG5-EGR1), Egr1 siRNA rescue (Egr1 siRNA + pSG5-EGR1), or control (scrambled siRNA + pSG5-Empty) treatment. **C)** The fold change in SerpinB2 mRNA levels (mean value shown above bar), relative to WT control, following 3 hour TPA stimulation (Upper Panel). mRNA levels of murine (Egr1) or human EGR1, relative to β-actin, from the same experiment (Lower Panel). **D)** Immunoblot analysis using the indicated antibodies, following 24 hour TPA stimulation of only DUSP5 KO MEFs. A representative Western blot is shown (Upper Panel), alongside SerpinB2 quantification (Lower Panel). **E)** The fold change in SerpinB2 mRNA levels in Egr1$^{+/+}$ (WT) and Egr1$^{-/-}$ (KO) 3T3 immortalised MEFs following 3 hour TPA stimulation. Cells were transfected with a pCMV expression vector encoding wild-type human EGR1 (pCMV-EGR1) or an empty vector as indicated (Left Panel). mRNA levels of human EGR1, relative to β-actin, from the same experiment (Right Panel). Mean values ± SEM are shown, n = 3. ns = not significant, *P < 0.05, **P < 0.01, ***P<0.001 using two-way ANOVA and Bonferroni post hoc test **(C)** or one-way ANOVA and Bonferroni post hoc test **(D-E).**

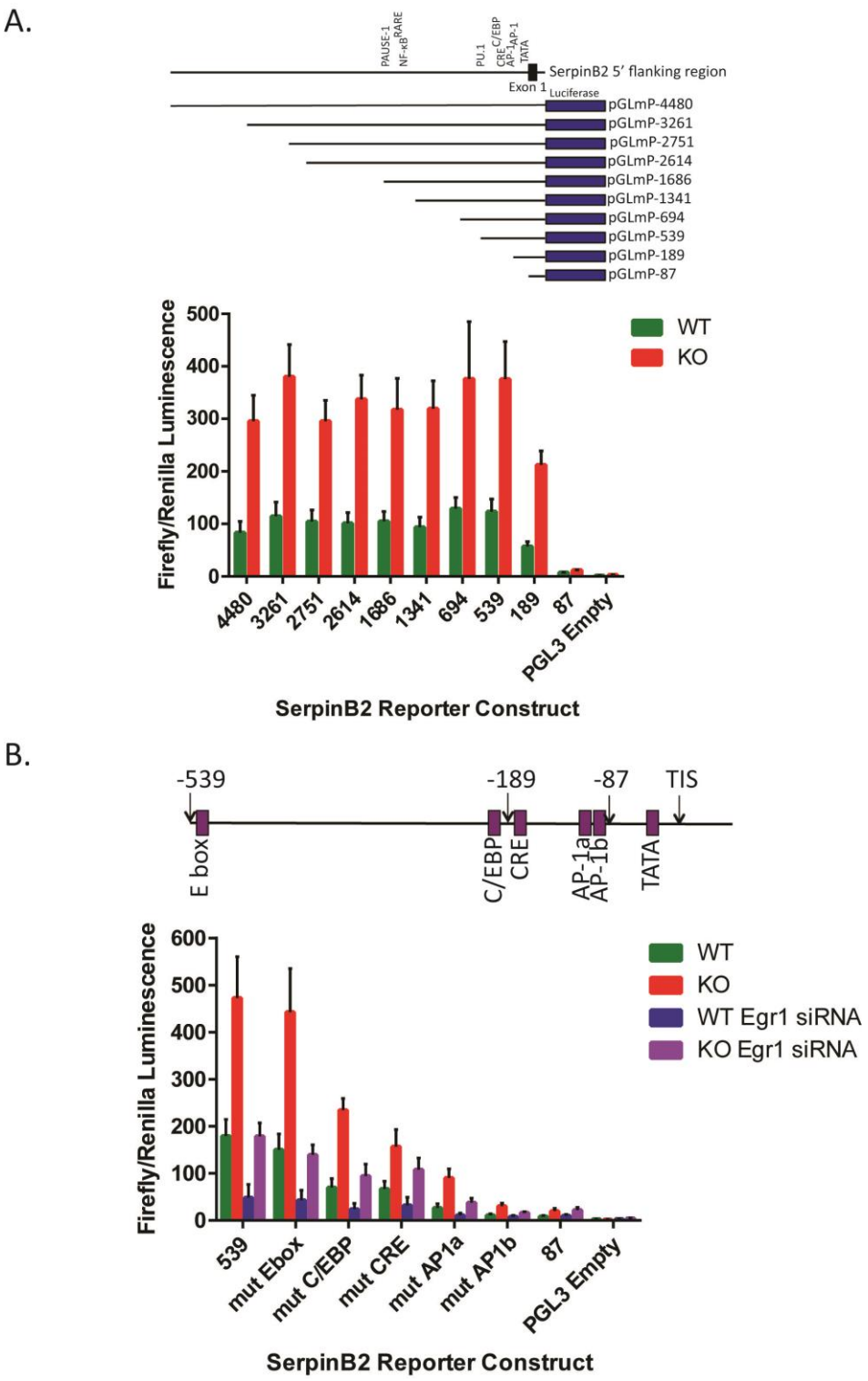

Figure 3.8 SerpinB2 upregulation required AP-1 transcription factor complexes. A) Relative activity in DUSP5$^{+/+}$ (WT) and DUSP5$^{-/-}$ (KO) shARF-immortalised MEFs of a series of truncated SerpinB2 promoter–reporter constructs following 8 h of TPA treatment (Lower). The truncated SerpinB2 promoter–reporter constructs used and the relative position of known transcription factor binding sites are outlined in the schematic above. **B)** Relative activity in WT and KO MEFs of SerpinB2 promoter–reporter constructs containing wild-type or mutant transcription factor binding sites as indicated. Assays were performed in the presence of scrambled control siRNA or Egr1 targeting siRNA as indicated, following 8 h of TPA treatment (Lower). The SerpinB2 promoter-reporter constructs used, and locations of the transcription factor binding sites which were mutated are outlined in the schematic above. All the mutant reporter constructs were made in the -539 truncated construct. Mean values ± SEM are shown, n = 5 **(A)**, n = 4 **(B)**.

To further investigate the mechanism of SerpinB2 induction we obtained SerpinB2 promoter–reporter constructs (Udofa et al., 2013) to analyse the mechanism of TPA-induced transcription in DUSP5$^{+/+}$ and DUSP5$^{-/-}$ MEFs. Utilising a range of differentially truncated SerpinB2 promoter–reporter constructs we can show that the region within 539 base pairs of the start of SerpinB2 exon one is crucial for inducible reporter activity following TPA stimulation of MEFs (Fig. 3.8A). Consistent with our previous experiments, SerpinB2 reporter activity was significantly increased following DUSP5 ablation. Furthermore, by utilising a panel of mutant 539 base pair reporter constructs in which individual canonical transcription factor binding sites had been ablated, TPA-inducible SerpinB2 reporter activity was shown to be dependent on two Activator protein 1 (AP-1) binding sites within the proximal promoter (Fig. 3.8B). Loss of c-AMP response element (CRE) and CCAAT-enhancer-binding protein (C/EBP) binding sites also reduced reporter activity, although not to the same degree as loss of the AP-1 sites. The decrease in reporter activity following the mutation of each particular binding site occurred to a similar degree in both DUSP5$^{+/+}$ and DUSP5$^{-/-}$ MEFs, indicating that DUSP5 loss does not alter the repertoire of transcription factors required to initiate SerpinB2 transcription.

Interestingly, and consistent with our previous experiments, siRNA-mediated knockdown of Egr1 significantly decreases the TPA-induced activity of all of the SerpinB2 reporters used here irrespective of whether they are wild type or lack individual transcription factor binding sites (Fig. 3.8B). This indicates that Egr1 might act in an indirect manner, possibly through the regulation of, or interaction with, either AP-1 complexes or transcription factors binding at the CRE or C/EBP sites to induce SerpinB2 expression. Alternatively, Egr1 could be acting via a binding site, which has not been mutated here. However, the latter appears very unlikely as there is no canonical Egr1 consensus sequence (5'-GCG TGG GCG-3') (Cao et al., 1990, 1990; Christy and Nathans, 1989) within the 539 base pair SerpinB2 reporter used here and interrogation of Encode Chip-seq data (http://genome.ucsc.edu/ENCODE/ - Landt et al., 2012) shows no evidence for Egr1 binding within the SerpinB2 promoter.

Whilst investigating the role of Egr1 in the regulation of TPA-induced SerpinB2 expression we noticed that DUSP5 levels were also decreased following Egr1, but not Egr3 or Egr4, knockdown (Fig. 3.9A). The effect of Egr1 knockdown on DUSP5 mRNA expression was

proportionally the greatest in unstimulated cells (Fig. 3.9A). This potentially reflects the increased ability of other transcription factors to induce DUSP5 expression and compensate for the loss of Egr1 following TPA stimulation, therefore subsequent investigations into the regulation of DUSP5 expression by Egr1 were performed in unstimulated cells. Analysis of DUSP5 mRNA and protein expression in the Egr1 siRNA rescue experiment (described in Fig. 3.7C-D) revealed that Egr1 expression is able to promote DUSP5 induction in MEFs (Fig. 3.9B & C). This was supported by evidence that DUSP5 expression is decreased in $Egr1^{-/-}$ mEFs and can be partially restored through ectopic EGR1 expression (Fig. 3.9D). DUSP5 has also been identified as a Egr1 target through genome-wide chromatin immunoprecipitation with promoter microarray (ChIP-Chip) (Kubosaki et al., 2009) and the DUSP5 gene also contains a Egr1 consensus binding site within its proximal promoter. Taken together, this evidence places Egr1 as a positive regulator of DUSP5 expression, suggesting that DUSP5 also acts to limit its own expression at the transcriptional level by down regulating ERK activation and thus Egr1 expression.

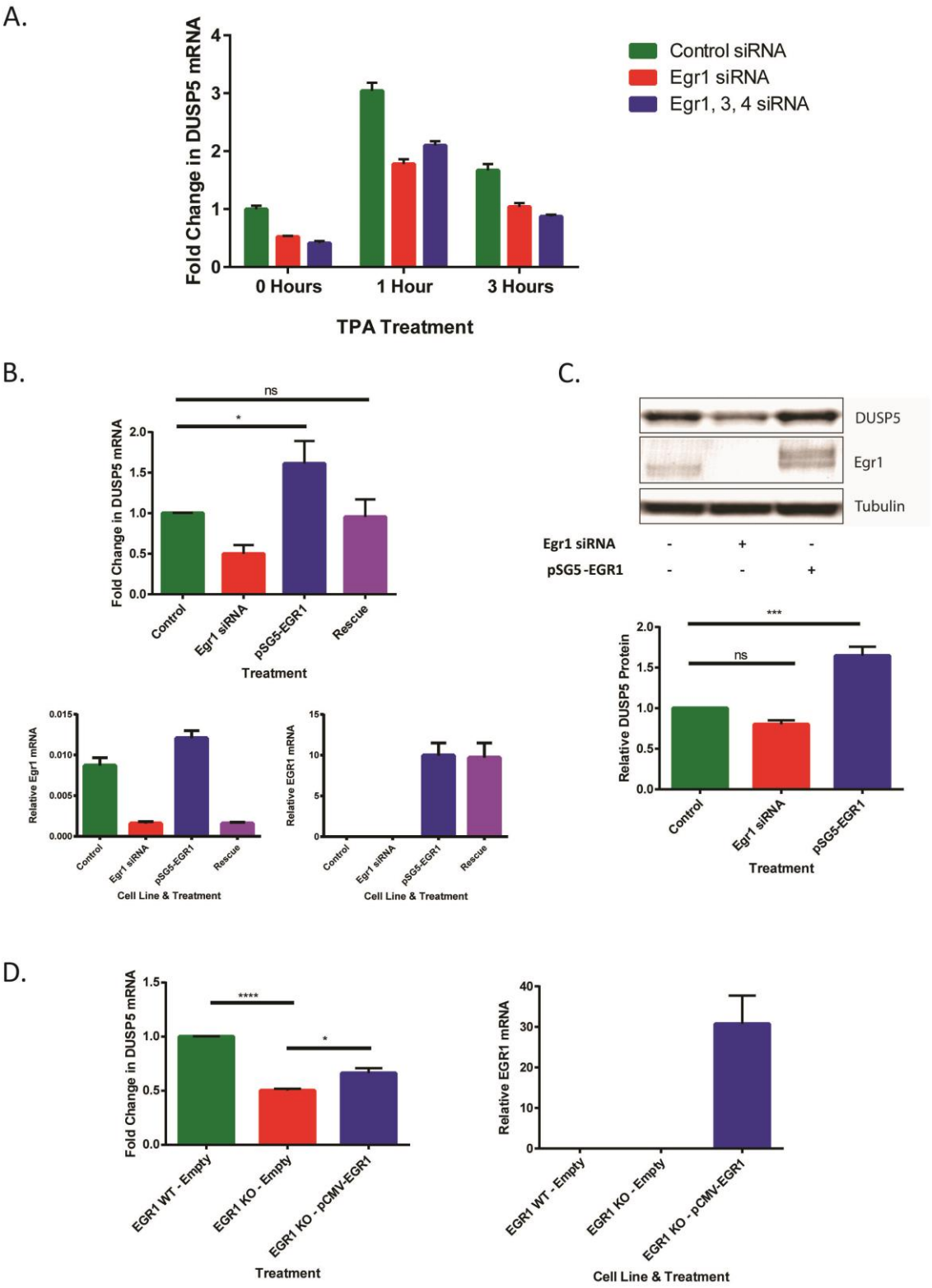

Figure 3.9 Egr1 regulates DUSP5 expression to complete a negative feedback loop controlling *p*-ERK levels. A) Taqman RT-qPCR assay showing the fold change in DUSP5 mRNA levels (relative to control unstimulated) in DUSP5$^{+/+}$ (WT) shARF immortalised MEFs following transfection with scrambled control siRNA, Egr1 siRNA or a combination of Egr1, 3 & 4 siRNA as indicated and subsequent TPA stimulation. mRNA levels of Egr1, Egr3 & Egr4, relative to β-actin, from the same experiment demonstrate are shown in Fig. 3.7A. Representative figure of an experiment performed in duplicate. **B-C)** DUSP5 expression in WT MEFs at either the mRNA **(B)** or protein **(C)** level following Egr1 knockdown (Egr1 siRNA + pSG5-Empty transfection), human EGR1 overexpression (scrambled siRNA + pSG5-EGR1), Egr1 siRNA rescue (Egr1 siRNA +

pSG5-EGR1), or control (scrambled siRNA + pSG5-Empty) treatment. **B)** The fold change in DUSP5 mRNA levels, relative to control following Egr1 manipulation (Upper Panel). mRNA levels of murine (Egr1) or human EGR1, relative to β-actin, from the same experiment (Lower Panel).**C)** Immunoblot analysis using the indicated antibodies, following Egr1 manipulation. The rescue condition was not performed for the immunoblot. A representative Western blot is shown (Upper), alongside DUSP5 quantification (Lower). **D)** The fold change in DUSP5 mRNA levels in $Egr1^{+/+}$ (WT) and $Egr1^{-/-}$ (KO) 3T3 immortalised MEFs following transfection with a pCMV expression vector encoding wild-type human EGR1 (pCMV-EGR1) or an empty vector as indicated (Left Panel). mRNA levels of human EGR1, relative to β-actin, from the same experiment (Right Panel). Mean values ± SEM are shown, n = 3. ns = not significant, *P < 0.05, ****P<0.0001 using one-way ANOVA and Bonferroni post hoc test.

3.3.4 $HRas^{Q61L}$ synergises with DUSP5 loss and TPA stimulation to further increase nuclear *p*-ERK and SerpinB2 expression

DMBA/TPA-mediated tumorigenesis is primarily driven by DMBA-induced $HRas^{Q61L}$ mutations, which when combined with periodic exposure to the tumour promoter TPA give rise to skin papillomas (Abel et al., 2009). Consequently, we investigated the effects of $HRas^{Q61L}$ expression either alone or in combination with TPA stimulation on both nuclear *p*-ERK levels and SerpinB2 mRNA and protein induction in $DUSP5^{+/+}$ and $DUSP5^{-/-}$ MEFs. The expression of mutant $HRas^{Q61L}$ in combination with TPA stimulation of $DUSP5^{-/-}$ MEFs caused a significant increase in levels of nuclear, but not cytoplasmic, *p*-ERK in comparison to wild-type MEFs (Fig. 3.10A & B). This synergistic increase in levels of nuclear *p*-ERK also correlates with increased SerpinB2 mRNA and protein expression in response to the same conditions. $HRas^{Q61L}$ expression, TPA stimulation or DUSP5 ablation all individually induce an increase in SerpinB2 expression at both the mRNA and protein level in MEFs. However, in combination they can synergise to drive a dramatic increase in SerpinB2 expression (Fig. 3.11A & B). $HRas^{Q61L}$ induced SerpinB2 expression is dependent on ERK activity as it can be abolished at the protein level by pre-treatment with the MEK inhibitor PD184352 (Fig. 3.11B). SerpinB2 promoter–reporter assays demonstrate that $HRas^{Q61L}$, TPA stimulation and DUSP5 loss combine to increase luciferase activity, in a manner which can be abrogated by MEK inhibitor treatment or AP-1 binding site mutations (Fig. 3.12). Therefore, the synergistic increase in SerpinB2 expression resulting from a combination of these conditions is due to elevated ERK-dependent transcription, mediated by AP-1 transcription factors. Together, these results demonstrate that as the upstream ERK pathway stimulus is increased, through mutant HRas expression, DUSP5 mediated negative feedback becomes more important in preventing elevated nuclear ERK activity and the resulting increase in SerpinB2 expression.

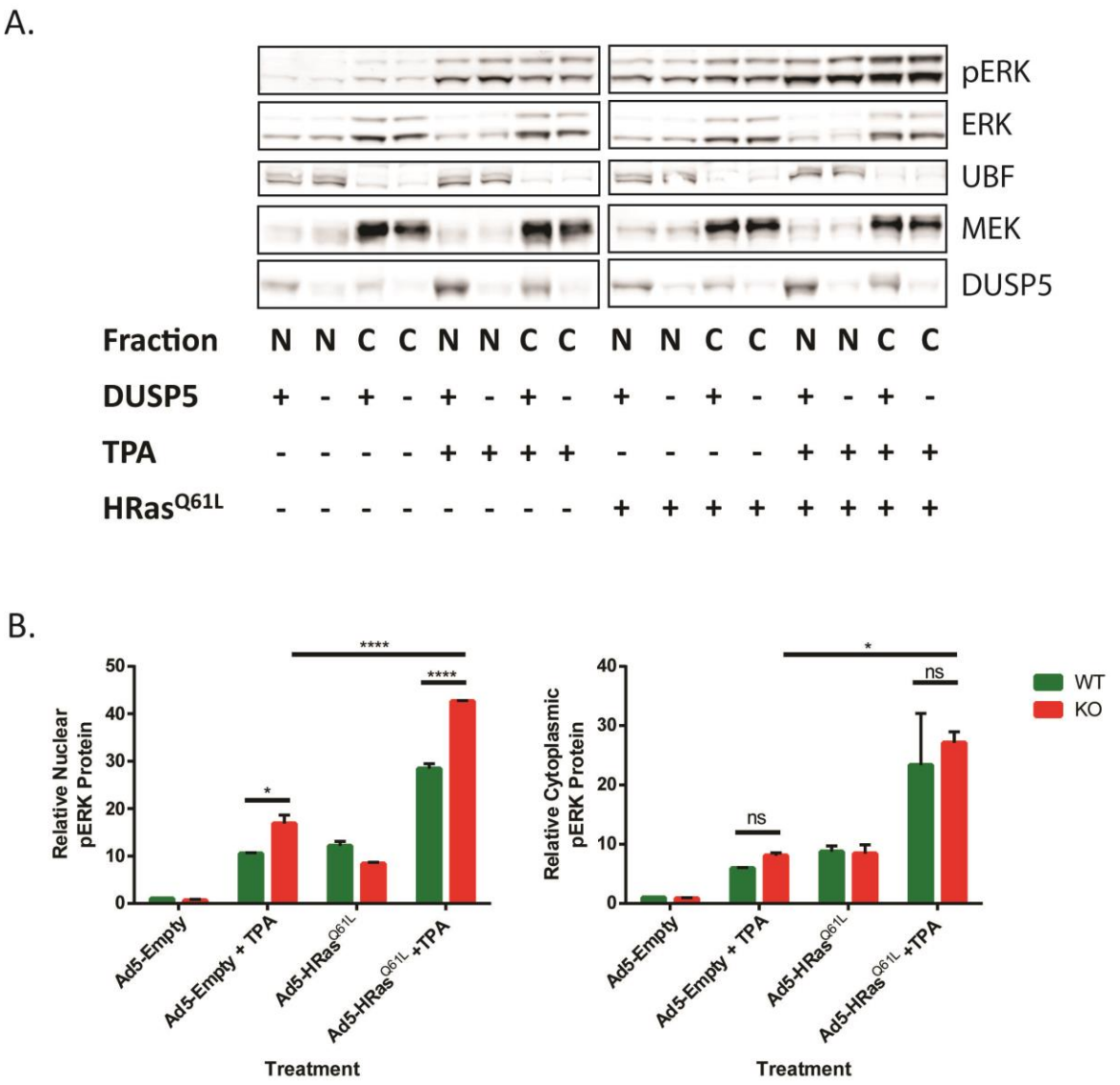

Figure 3.10 HRas^{Q61L} expression synergises with DUSP5 loss and TPA stimulation to further elevate nuclear *p*-ERK levels. DUSP5$^{+/+}$ (WT) and DUSP5$^{-/-}$ (KO) primary MEFs were infected with Ad5-HA-tagged HRas^{Q61L} (Ad5-HRas^{Q61L}) or empty adenovirus (Ad5-Empty), then stimulated with TPA for 0 or 1 hour, before lysis, subcellular fractionation and immunoblotting using the indicated antibodies. UBF and MEK were used to validate separation of nuclear (N) and cytoplasmic (C) proteins, respectively. A representative Western blot is shown **(A),** alongside *p*-ERK quantification **(B).** Mean ± SEM, n = 3. ns = not significant, *P < 0.05, ****P<0.0001 using two-way ANOVA and Bonferroni post hoc test.

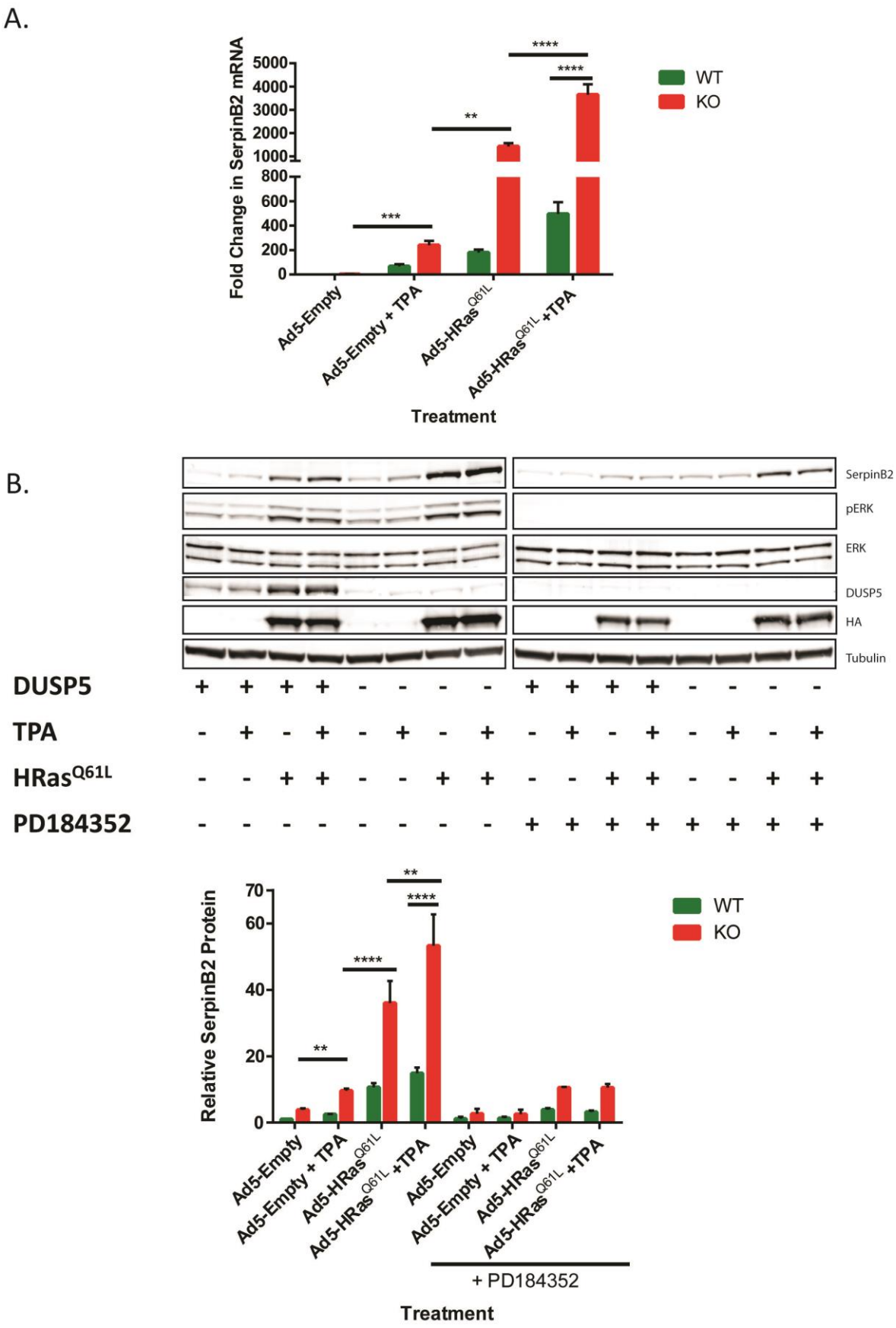

Figure 3.11 HRas^{Q61L} expression synergises with DUSP5 loss and TPA stimulation to further elevate SerpinB2 expression. DUSP5$^{+/+}$ (WT) and DUSP5$^{-/-}$ (KO) primary MEFs were infected with Ad5-HA-tagged HRas^{Q61L} (Ad5-HRas^{Q61L}) or empty adenovirus (Ad5-Empty), then stimulated with or without TPA as indicated, prior to analysis of SerpinB2 expression at the mRNA **(A)** or

protein **(B**) level. **A)** Taqman RT-qPCR assay showing the fold change in SerpinB2 mRNA levels, relative to WT unstimulated. TPA stimulations, where indicated, were for 3 hours. **B)** Immunoblot analysis using the indicated antibodies, following the conditions outlined above, with the additional variable of the pre-treatment using the MEK inhibitor PD184352 or a DMSO control. TPA stimulations, where indicated, were for 24 hours. A representative Western blot is shown (Upper), alongside SerpinB2 quantification (Lower). Mean values ± SEM are shown, n = 3. *P < 0.05, **P < 0.01, ***P < 0.001, ****P<0.0001 using two-way ANOVA and Bonferroni post hoc test.

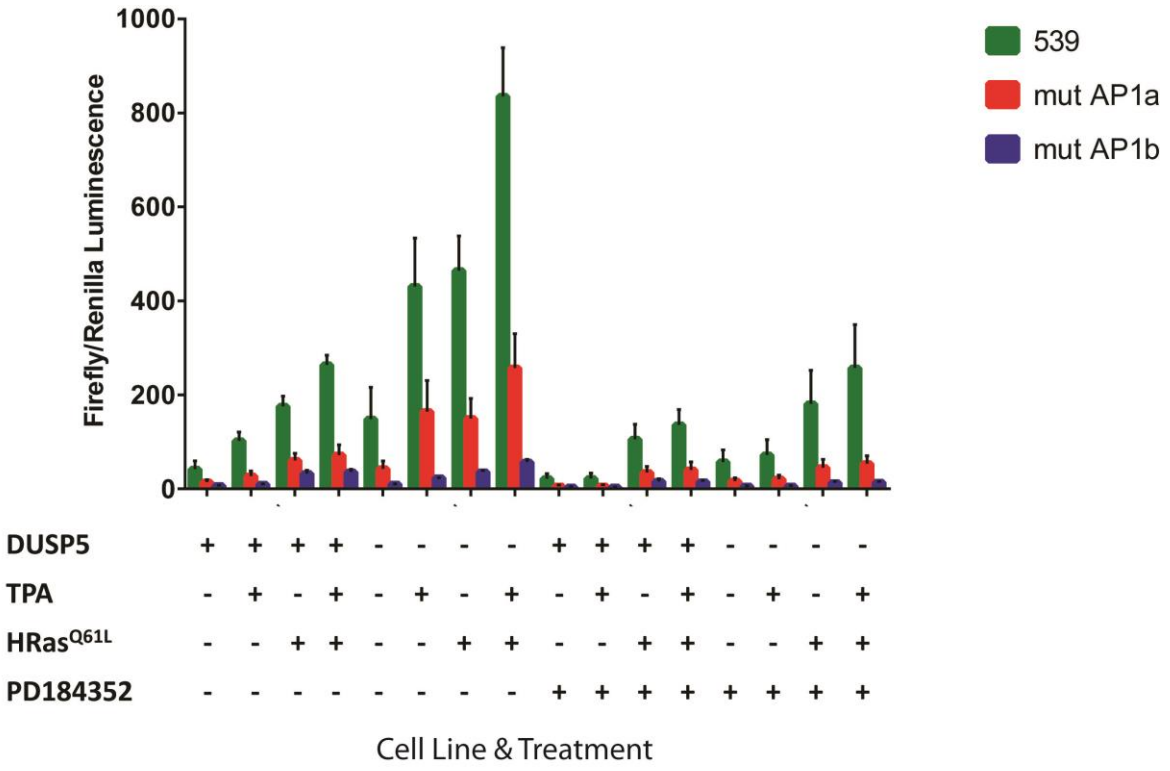

Figure 3.12 HRas^{Q61L}-mediated induction of SerpinB2 is also AP1 and MEK-dependent. Relative activity in DUSP5$^{+/+}$ (WT) and DUSP5$^{-/-}$ (KO) shARF-immortalised MEFs of SerpinB2 promoter–reporter constructs containing wild-type or AP1 mutant transcription factor binding sites as indicated. Cells were infected with Ad5-HA-tagged HRas^{Q61L} (Ad5-HRas^{Q61L}) or empty adenovirus (Ad5-Empty), then assays carried out in the presence or absence of TPA and the MEK inhibitor PD184352. Mean values ± SEM are shown, n = 3.

To determine whether SerpinB2 induction in response to TPA stimulation or $HRas^{Q61L}$ expression occurs *in vivo* and is elevated by DUSP5 loss, we analysed SerpinB2 mRNA (Fig. 3.13A) and protein (Fig. 3.13B) levels in DMBA/TPA-induced papillomas or in TPA-treated skin of $DUSP5^{+/+}$ and $DUSP5^{-/-}$ mice. SerpinB2 expression was higher in papillomas than in TPA-stimulated skin (Fig. 3.13B). This is in agreement with our previous *in vitro* data, showing together $HRas^{Q61L}$ expression (present in papillomas – Fig. 3.1E) and TPA stimulation synergise to induce greater SerpinB2 expression that solely TPA stimulation alone. Furthermore, at both the mRNA and protein level $DUSP5^{-/-}$ papillomas expressed higher SerpinB2 levels than their wild-type counterparts, demonstrating that *in vivo* $HRas^{Q61L}$ expression, TPA stimulation and DUSP5 loss synergise to promote elevated SerpinB2 expression.

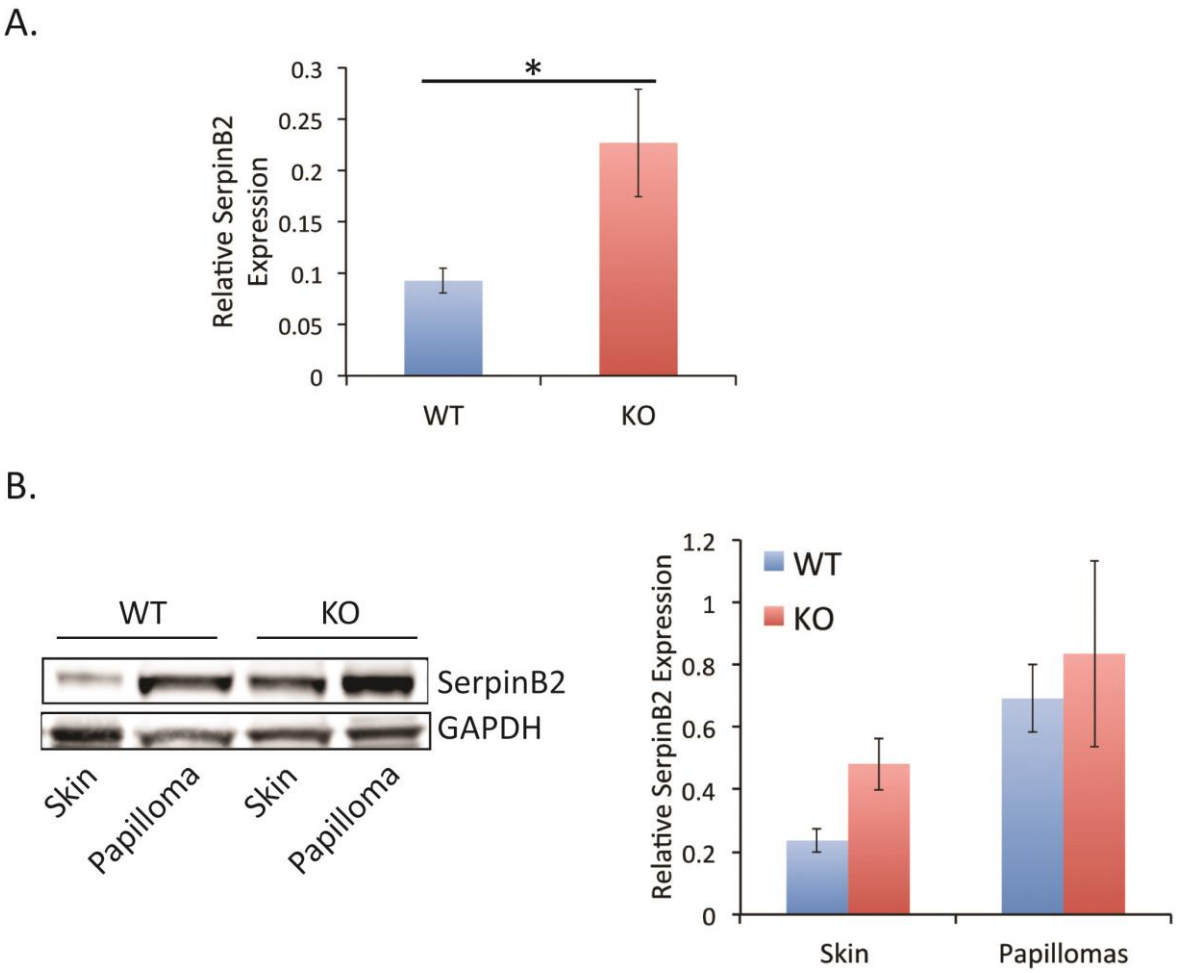

Figure 3.13 SerpinB2 expression is elevated following DUSP5 loss in murine skin and DMBA/TPA-induced papillomas. A) RT-qPCR assay showing relative SerpinB2 mRNA levels in DUSP5$^{+/+}$ (WT) and DUSP5$^{-/-}$ (KO) papillomas. Mean ± SEM, n = 12. *P < 0.05, using Mann–Whitney test. **B)** Immunoblot analysis of SerpinB2 protein expression in DUSP5 WT and KO mouse skin and papillomas. A representative Western blot is shown (Left), alongside SerpinB2 quantification (Right). Mean values ± SEM are shown, n = 4. Panel B courtesy of Dr Linda Rushworth.

3.3.5 SerpinB2 knockout abrogates the sensitisation of DUSP5$^{-/-}$ mice to DMBA/TPA-induced skin carcinogenesis

DUSP5 ablation promotes a significant increase in SerpinB2 expression in MEFs in response to HRas^{Q61L} or TPA stimulation (Fig. 3.11A & B) and the papillomas which arise in DUSP5$^{-/-}$ mice display elevated SerpinB2 relative to their DUSP5$^{+/+}$ littermates (Fig. 3.13A & B). Previously published work has shown that transgenic mice overexpressing SerpinB2 in basal skin keratinocytes are sensitised to DMBA/TPA-induced skin carcinogenesis (Zhou et al., 2001), while SerpinB2$^{-/-}$ mice have displayed resistance (Tonnetti et al., 2008). Therefore, we hypothesised increased SerpinB2 expression as a consequence of DUSP5 loss could be promoting the increased tumourigenesis that we observed in DUSP5$^{-/-}$ mice (Fig. 3.1A & B). To address this question we obtained SerpinB2$^{-/-}$ mice (Dougherty et al., 1999) and crossed them with DUSP5$^{-/-}$ mice to generate a double knockout (DKO) cohort. The 25 week DMBA/TPA-induced skin carcinogenesis protocol was then repeated on four cohorts of mice: DUSP5$^{+/+}$, DUSP5$^{-/-}$, SerpinB2$^{-/-}$ and DKO (Fig. 3.14A & B). As observed previously DUSP5$^{-/-}$ mice developed approximately double the papilloma burden of wild-type mice. However, this sensitisation could be completely abrogated by concomitant deletion of SerpinB2, with DKO mice displaying a similar tumour burden to wild-type animals (Fig. 3.14B). Interestingly, in our hands SerpinB2$^{-/-}$ mice did not display a reduced tumour burden relative to wild-type mice, in contrast to a previous study reporting such a phenotype (Fig. 3.14B) (Tonnetti et al., 2008). SerpinB2$^{-/-}$ mice did display a slightly delayed tumour onset relative to wild-type mice (Fig. 3.14A). Again as observed in our initial study, all tumours were squamous cell papillomas, displaying a similar morphology and size distribution across all genotypes (Fig. 3.14C). Finally, SerpinB2 expression can be detected by IHC in wild-type and DUSP$^{-/-}$ papillomas, with DUSP$^{-/-}$ papillomas displaying a greater staining intensity. DKO papillomas do not display SerpinB2 expression confirming the genetic knockout and validating our experimental system (Fig. 3.14D). Together these results allow us to conclude that the increased sensitivity of DUSP5$^{-/-}$ mice to DMBA/TPA-induced skin carcinogenesis is dependent on increased SerpinB2 expression, induced by the elevated nuclear ERK activity and ERK-dependent gene expression promoted by DUSP5 loss.

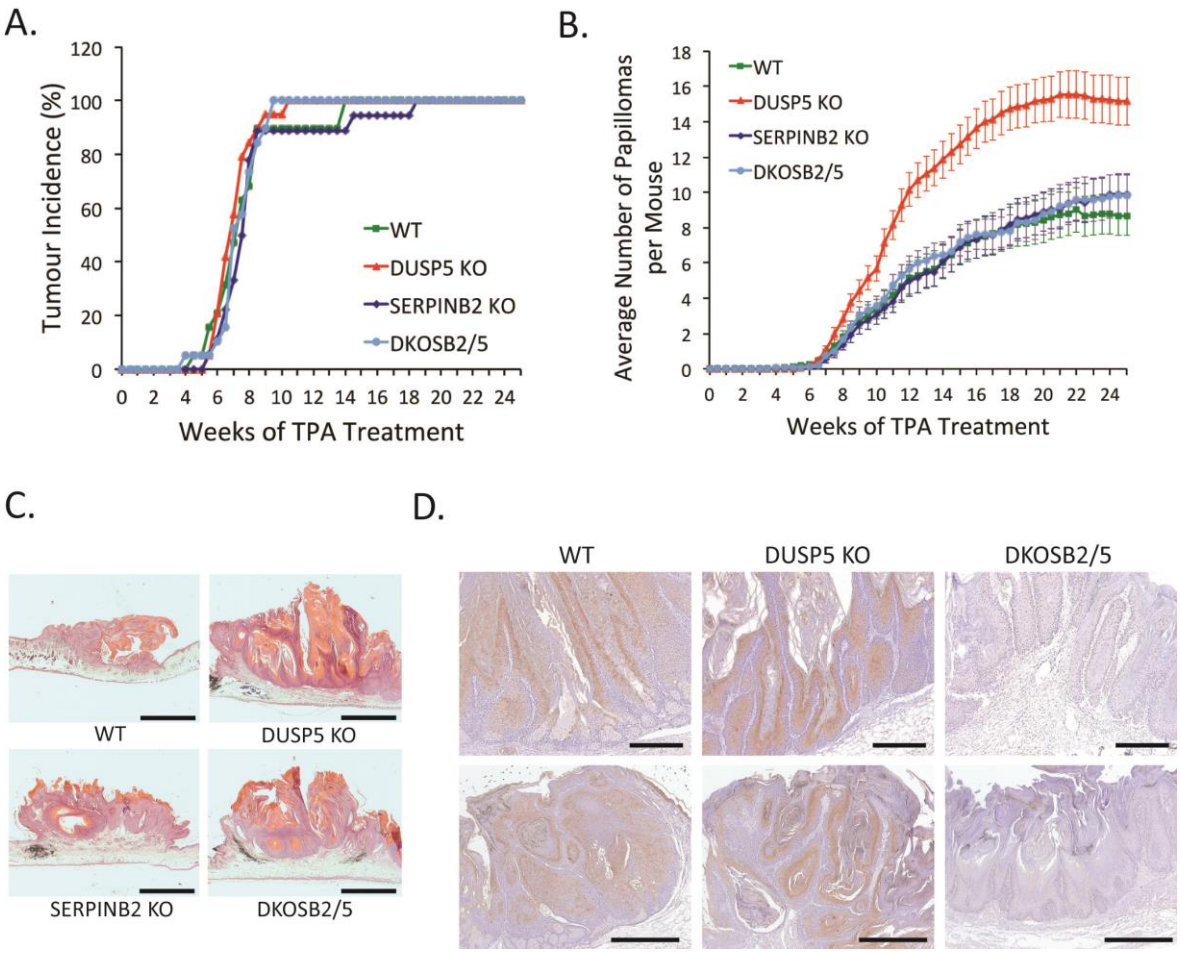

Figure 3.14 SerpinB2 ablation abrogates the sensitisation of DUSP5-/- mice to DMBA/TPA-induced skin carcinogenesis. DUSP5$^{+/+}$ (WT), DUSP5$^{-/-}$ (DUSP5 KO), SerpinB2$^{-/-}$ (SerpinB2 KO) and DUSP5$^{-/-}$; SerpinB2$^{-/-}$ (DKOSB2/5) animals (n = 19 per cohort) were exposed to DMBA followed by TPA treatment for 25 weeks. **A)** Tumour incidence. **B)** Average number of tumours per mouse. DUSP5 loss significantly increased tumour multiplicity over WT animals, whereas SerpinB2$^{-/-}$ or DKOSB2/5 mice were indistinguishable from WT animals (P values for WT/KO = 0.001, WT/SerpinB2−/− = 0.499 and WT/DKOSB2/5 = 0.851 by repeated measures multivariate ANOVA with Tukey's post hoc analysis). **C)** H&E stained sections of representative skin papillomas at 25 weeks. (Scale bar, 1mm). **D)** SerpinB2 IHC staining in WT, DUSP5 KO and DKOSB2/5 papillomas. (Scale bars: upper panels, 200μm and lower panels, 500μm). Data courtesy of Dr Linda Rushworth.

3.4 Discussion

DUSP5 is a nuclear, ERK-specific MKP which is induced as a negative feedback regulator following ERK activation (Kucharska et al., 2009; Mandl et al., 2005), therefore it has the potential to modulate ERK activity in response to oncogenic activation of the Ras-ERK pathway in cancer. However, prior to this study there has been no definitive experimental evidence that changes in DUSP5 expression can have a causative role in cancer development (Kidger and Keyse, 2016). This study demonstrates that DUSP5 acts as a tumour suppressor in the DMBA/TPA-induced model of HRas-driven skin carcinogenesis (Rushworth et al., 2014). DUSP5 loss promotes increased tumour burden *in vivo* (Fig. 3.1B), in a manner, which is dependent on the upregulation of the SerpinB2 (Fig 3.14B). At the molecular level DUSP5 exhibits a non-redundant function in suppressing nuclear ERK activity, such that DUSP5 loss promotes elevated nuclear *p*-ERK in response to TPA stimulation (Fig. 3.3). This then drives the upregulation of a cohort of ERK-dependent genes including SerpinB2 (Fig. 3.4A). Furthermore, $HRas^{Q61L}$ expression synergises with DUSP5 loss to promote additional increases in SerpinB2 expression (Fig. 3.11), implying that DUSP5-mediated negative feedback becomes even more essential to constrain the activity of oncogenic mutations within the Ras-ERK pathway. This supports the proposal that ERK-induced negative feedback regulators, such as DUSP5, are an essential response to activated upstream oncogenes and can help to constrain the tumourigenic effects of such mutations (Pratilas et al., 2009).

We demonstrate a tumour suppressive function for DUSP5 in HRas-driven skin papilloma formation, however this does not rule out an oncogenic role in other tumour contexts such as different organs or oncogenic driver mutations. For example, DUSP6/MKP-3 is essential for the oncogenic transformation of pre-B-cells in models of ALL (Shojaee et al., 2015), whereas it acts as a tumour suppressor in mutant KRas-driven pancreatic cancer (Chapter 5). This is likely to reflect the ability of hyperactive ERK signalling to promote cellular senescence or apoptosis (Deschênes-Simard et al., 2014), therefore alterations in the magnitude of ERK activity have the ability to promote or suppress proliferation and tumour growth depending on the cellular context. If MKP loss promotes increased ERK activity that does not exceed the threshold inducing senescence it will promote increased tumourigenesis, making the MKP a tumour suppressor in this context. Whereas, in the context of stronger Ras-ERK pathway stimulation MKP activity maybe essential to

constrain ERK activity to maintain it below the threshold inducing senescence, to enable proliferation, giving the MKP an oncogenic function.

Here we demonstrate that the nuclear MKP, DUSP5, is able to mediate spatially restricted changes in ERK activity specifically in the cellular compartment in which it is localised (Fig. 3.3). This proves that despite the ability of ERK to shuttle rapidly between the nucleus and cytoplasm (Lidke et al., 2010; Zehorai et al., 2010), the precise control of ERK activity in specific subcellular compartments can be mediated by MKPs. One interesting puzzle is why DUSP5 loss only promotes the upregulation of a small cohort of TPA-inducible genes (Fig. 3.4A), as you would expect the increase in nuclear *p*-ERK resulting from DUSP5 loss to increase the expression of most of the hundreds of ERK-responsive genes (Yoon and Seger, 2006). One hypothesis would be that as DUSP5 loss is only causing a small alteration in nuclear *p*-ERK levels, only genes which are strongly transcriptionally upregulated in response to ERK show a large enough change in their mRNA levels to be statistically significant hits in our microarray experiments. The raw microarray data supports this, as many well established ERK target genes such as cFos, cJun and DUSP6/MKP-3 are all marginally upregulated following DUSP5 loss (Rushworth et al., 2014 - microarray deposition). Although the changes in expression of such genes do not achieve statistical significance, the wide range of ERK target genes affected does imply that they are being affected by DUSP5 loss. This theory is also supported by evidence that SerpinB2 is known to be a gene which is strongly transcriptionally upregulated in response to cellular stresses or TPA stimulation (Stringer et al., 2012), therefore it is more likely to be sensitive to DUSP5 loss than other genes which might be transcribed in an ERK-dependent manner but are not typically induced in such a dynamic manner to particular stimuli. Alternatively, when present DUSP5 could be preferentially binding and inactivating ERK bound to specific gene promoters or enhancers within the nucleus, therefore it could be selectively minimising the transcription of certain genes. Signalling kinases such as the MAPKs do have the ability to localise to sites of active transcription via binding to transcription factor complexes within chromatin (Chow and Davis, 2006; Nadal et al., 2011). This was first demonstrated in yeast, where the p38 homolog Hog1 was shown to associate at stress-responsive promoters through transcription factor binding. Once localised to such promoters Hog1 acts to recruit and activate transcription factors, chromatin modulators and RNA Pol II (Nadal and Posas, 2010; Pokholok et al., 2006).

Subsequent studies in mammalian systems have also revealed that ERK signalling pathway complexes are able to bind chromatin and localise at ERK-inducible promoters to modulate transcriptional activity *in situ* (Lawrence et al., 2008; Nelson et al., 2011; Zhang et al., 2008). This evidence suggests it would be possible for DUSP5 to co-localise with, and regulate the activity of, ERK at such promoters and if any factors were able to modulate the binding of DUSP5 to ERK at specific promoters this would constitute a mechanism by which DUSP5 loss could differentially regulate specific ERK target genes.

In addition to SerpinB2, we demonstrated Egr1 to be upregulated upon DUSP5 loss (Fig. 3.4A). Egr1 is able to promote the expression of both SerpinB2 and DUSP5 (Fig. 3.7 & 3.9). This is supported by evidence from recent studies where SerpinB2 has been shown to be induced by Egr1 signalling during mammary cell migration (Tarcic et al., 2012), and DUSP5 was also identified as a TPA-induced Egr1 target gene in THP-1 leukemia cell lines (Kubosaki et al., 2009). Therefore, through the regulation of nuclear *p*-ERK levels, and thus Egr1 induction, DUSP5 acts as part of a negative feedback loop to regulate its own expression, and the expression of a cohort of ERK-dependent genes including SerpinB2. Interestingly, there is no Egr1 transcription factor binding site in the SerpinB2 promoter and using transcription factor binding site mutant SerpinB2 promoter-reporter constructs we could demonstrate that SerpinB2 induction requires AP1 family transcription factors in the presence or absence of DUSP5 (Fig. 3.8B). This is in agreement with previous studies which have shown that SerpinB2 induction following phorbol ester stimulation requires AP-1 activity in both immune cells and human cancer cell lines (Stringer et al., 2012). Together this indicates Egr1 is acting in an indirect manner, most likely through the regulation of, or interaction with, AP-1 transcription factors to induce SerpinB2 expression. This hypothesis is supported by previous studies which have demonstrated changes in expression of AP-1 transcription factor components, via microarray analysis, following the manipulation of Egr1 activity (Čermák et al., 2010; Zhang et al., 2014). Conversely, the DUSP5 promoter contains an Egr1 binding site and Egr1 binding to the DUSP5 promoter has been identified via chromatin immunoprecipitation with promoter microarray (ChIP-chip) analysis (Kubosaki et al., 2009). ChIP-chip enables the identification of the entire spectrum of *in vivo* DNA binding sites for any given protein. To do this the DNA binding regions of a specific protein of interest can be isolated using chromatin immunoprecipitation (ChIP), subsequent hybridisation of the isolated DNA

fragments with a DNA microarray enable the identification of the specific genomic regions isolated (Buck and Lieb, 2004). Therefore, in contrast to SerpinB2, it appears that the regulation of DUSP5 expression by Egr1 occurs in a direct manner.

Papillomas from DUSP5$^{-/-}$ mice displayed elevated SerpinB2 expression relative to DUSP5$^{+/+}$ papillomas (Fig. 3.13A & 3.14D) demonstrating that DUSP5 loss also promotes SerpinB2 *in vivo*. Experiments using DKO mice establish SerpinB2 upregulation as the mechanism promoting the increased tumour incidence in DUSP5$^{-/-}$ mice following DMBA/TPA treatment (Fig. 3.14B). This result is in line with previous studies which have demonstrated an oncogenic role for SerpinB2 in DMBA/TPA-induced skin cancer models. Bovine keratin 5 promoter-driven overexpression of SerpinB2 in basal keratinocytes sensitized transgenic mice to DMBA/TPA-induced papilloma formation (Zhou et al., 2001), whereas SerpinB2$^{-/-}$ mice have been shown to be resistant (Tonnetti et al., 2008). In contrast to this second study (Tonnetti et al., 2008), we did not observe resistance to DMBA/TPA-induced carcinogenesis in SerpinB2$^{-/-}$ mice. It is unclear why this is the case, as both studies used inbred C57BL/6 mice, ruling out genetic background. However, the DMBA/TPA treatment protocol of the two studies was slightly different with Tonnetti et al. (2008) using a lower initial dose of DMBA to initiate tumourigenesis and then monitoring the mice for a shorter (18 week) period. Furthermore, the resistance observed by Tonnetti et al. (2008) appears transient as by 17 weeks into their study the SerpinB2$^{-/-}$ mice had generated the same papilloma incidence and burden as wild-type mice.

However, this potential oncogenic role for SerpinB2 in cancer development is still subject to debate. In human cancers elevated SerpinB2 expression correlates with improved prognosis in multiple cancer types including breast and pancreas, but poor prognosis in others such as colorectal and ovarian cancer (Croucher et al., 2008). Furthermore, the relative contributions of the extracellular versus intracellular functions for SerpinB2 in cancer development are unresolved, and the molecular mechanism by which intracellular SerpinB2 could drive carcinogenesis is unclear (Croucher et al., 2008). The previous DMBA/TPA-induced carcinogenesis models indicated that intracellular SerpinB2 inhibited the induction of apoptosis to promote tumourigenesis (Tonnetti et al., 2008; Zhou et al., 2001). In contrast, further studies failed to detect any effects of SerpinB2 on apoptosis or cell proliferation (Fish and Kruithof, 2006; Major et al., 2011; Schroder et al., 2014),

although roles in autophagy (Chuang et al., 2013) and migration (Schroder et al., 2014) have been proposed. Therefore the mechanism by which intracellular SerpinB2 could regulate tumourigenesis appears unclear. Our initial experiments have not identified any changes in apoptosis or autophagy markers in wild-type, DUSP5$^{-/-}$ or SerpinB2$^{-/-}$ MEFs following a range of stimuli (Data not shown). Consequently, a more detailed analysis of cellular phenotypes following SerpinB2 loss or overexpression is required to determine the mechanism by which it is able to promote tumour progression in our model of HRas-driven skin carcinogenesis.

The extracellular protease function of SerpinB2, and other Serpin family members, has been shown to a mechanism by which brain metastatic cells from lung cancers, overcome the metastasis-suppressing effects of plasmin generation in the brain. In this system Serpins protect cancer cells from apoptosis and promote vascular co-option (Valiente et al., 2014). However, as the papillomas formed during the initiation phase of the DMBA/TPA-induced skin cancer model are still benign, non-invasive lesions (Abel et al., 2009), such action to remodel the stroma to enable migration or metastasis is unlike to be the mechanism driving increased sensitivity to tumourigenesis in our system. The mice used in our study were inbred C57BL/6 mice, a genetic background which is known to be highly resistant to the malignant conversion of papillomas into invasive squamous cell carcinomas (SCC) (Abel et al., 2009). Therefore, it would be interesting to generate DUSP5$^{-/-}$ on a more susceptible genetic background, such as FVB mice, to investigate whether DUSP5 loss and SerpinB2 overexpression have any further effects on the malignant progression and metastatic potential of DMBA/TPA-induced skin tumours.

In conclusion, this chapter demonstrates that DUSP5 acts as a tumour suppressor in HRas-driven skin carcinogenesis, through its non-redundant function in regulating nuclear ERK activity and resulting gene expression. DUSP5 loss promotes elevated nuclear *p*-ERK levels, driving the induction of SerpinB2 which is able to sensitise DUSP5$^{-/-}$ mice to DMBA/TPA-induced skin carcinogenesis.

Chapter 4 DUSP5 and DUSP6 are induced following endogenous KRas^{G12D} expression in MEFs, where they play distinct roles in modulating ERK signalling

4.1 Introduction

In the previous chapter we demonstrated that DUSP5 loss in combination with TPA stimulation or mutant HRas^{Q61L} expression resulted in increased nuclear *p*-ERK levels and the upregulation of a cohort of ERK-responsive genes, including SerpinB2. This was sufficient to drive a sensitisation to DMBA/TPA-induced skin carcinogenesis in DUSP5$^{-/-}$ mice, in a manner dependent on SerpinB2. This demonstrates that DUSP5 performs a non-redundant function in the control of nuclear ERK activity, ERK localisation and ERK-dependent gene expression (Rushworth et al., 2014). However, our *in vitro* experiments were performed following either ectopic expression of HRas^{Q61L} or acute stimulation with TPA, which do not accurately mimic the true physiological conditions within a cancer cell driven by Ras-ERK pathway mutations.

In previous studies it has been possible to study the effects of mutant Ras expressed at physiological levels, either through the knock-in of KRas^{G12D} at the endogenous gene locus in MEFs (Guerra et al., 2003; Tuveson et al., 2004) or through the generation of isogenic cell lines using homologous recombination, which differ only in the presence or absence of the mutant Ras allele (Haigis et al., 2008; Vartanian et al., 2013). Surprisingly, these studies have revealed that the presence of a constitutively active KRas mutant allele is not sufficient to cause increased levels of either *p*-ERK or *p*-AKT indicating that the activity of the PI3K and MEK-ERK pathways is relatively unaffected (Guerra et al., 2003; Haigis et al., 2008; Tuveson et al., 2004; Vartanian et al., 2013). In contrast, ectopic overexpression of mutant Ras does promote increased ERK activation in both MEFs and Hela cells (Rushworth et al., 2014; White et al., 1995). Despite this apparent lack of effector pathway activation, endogenous mutant Ras expression is still able to induce significant changes in gene expression (Vartanian et al., 2013) and result in the partial transformation of host cells (Guerra et al., 2003; Tuveson et al., 2004; Vartanian et al., 2013). However, full cellular transformation requires the acquisition of additional genetic events (Guerra et al., 2003; Tuveson et al., 2004). Furthermore, *in vivo* expression of

endogenous mutant Ras initially has mild phenotypic consequences, with progression to invasive tumours occurring rather slowly until facilitated by the gain of further mutations or loss of tumour suppressors (Guerra et al., 2003; Hingorani et al., 2003, 2005, Jackson et al., 2001, 2005; Johnson et al., 2001; Tuveson et al., 2006).

The lack of activation of Ras effector pathways following mutant Ras activation at endogenous levels suggests that negative feedback systems are induced and are able to restrain the activation of such pathways. Indeed Vartanian et al., (2013) revealed that strong negative feedback signalling to the EGF receptor plays a role in restraining Ras effector pathway activation following mutant KRas expression. Furthermore, they identified the upregulation of multiple MKPs, including DUSP5 and DUSP6/MKP-3, by mutant KRas, which could be a mechanism for restraining ERK activation. MKPs comprise a key negative feedback system of the MAPK pathways (Caunt and Keyse, 2013). Upregulation of DUSP5 and DUSP6/MKP-3 in the presence mutant Ras or BRaf signalling has also been identified in many other human cancer cell lines (Cagnol and Rivard, 2012; Haigis et al., 2008; Kreeger et al., 2009; Montero-Conde et al., 2013; Packer et al., 2009; Pratilas et al., 2009; Yun et al., 2009). This is supported by *in vivo* evidence from many human cancers, as the upregulation of MKPs has been demonstrated in many Ras and BRaf mutant human tumours (Caunt and Keyse, 2013; Kidger and Keyse, 2016a, 2016b).

Taken together there is a broad range of evidence pointing to roles for MKPs in constraining ERK activity following upstream oncogenic mutations such as those in Ras. However, the relative contribution of MKPs to the negative feedback mechanisms responsible for restraining *p*-ERK levels following constitutive pathway activation and the consequences of MKP loss have not been investigated. Therefore, this study aimed to utilise $KRas^{LSL\text{-}G12D/+}$ MEFs (Tuveson et al., 2004), as a model system to characterise the upregulation of MKPs by endogenous mutant Ras activation, and to investigate the biochemical and cellular consequences of DUSP5 and DUSP6/MKP-3 loss in the context of mutant Ras.

We focussed on changes in the expression of DUSP5 and DUSP6/MKP-3 in our experiments as they are both ERK-specific MKPs and are induced in response to ERK activity as classical negative feedback regulators of this pathway (Groom et al., 1996; Kucharska et al., 2009; Mandl et al., 2005; Mourey et al., 1996; Smith et al., 2006).

Therefore, any potential consequences of their ablation should be mediated through the ERK pathway downstream of mutant KRas without invoking changes in the activities of either JNK or p38 MAPK's, which could be the case with other MKPs. Furthermore, DUSP5 and DUSP6/MKP-3 display differential subcellular localisation, with DUSP5 localised to the nucleus (Mandl et al., 2005) while DUSP6/MKP-3 is found predominantly in the cytoplasm (Groom et al., 1996; Mourey et al., 1996). Thus, this study will also aim to investigate whether the loss of ERK negative feedback components in specific subcellular compartments can alter the spatiotemporal control of ERK activity and differentially regulate ERK signalling outcomes.

4.2 Results

4.2.1 KRas^{G12D} induces DUSP5 and DUSP6/MKP-3 expression in a MEK-dependent manner

To investigate potential changes in MKP expression following the expression of mutant KRas at endogenous levels, we used the well-established KRas$^{LSL\text{-}G12D}$ knock in allele. Prior to Cre-mediated recombination, this allele is effectively null (Jackson et al., 2001; Tuveson et al., 2004) and as homozygous deletion of KRas causes early embryonic lethality (Johnson et al., 1997) we first isolated littermate MEF cell lines from either wild-type or heterozygous KRas$^{LSL\text{-}G12D/+}$ mice. Before commencing any experiments we isolated MEFs from multiple litters of mice to ensure that for each experiment biological replicates could be performed in distinct MEF lines isolated from different parents, and that within each replicate the individual MEF lines used were derived from littermates. This should ensure that any effects observed result from the genetic changes we have introduced and not stochastic genetic variation within our cell lines.

To knock-in the KRas^{G12D} allele we infected MEFs with adenovirus expressing Cre-recombinase. We initially performed titration experiments to optimise the titre of adenoviral-Cre used to infect cells (Fig. 4.1A), followed by time course experiments to determine the minimum time period following infection by which the majority of KRas$^{LSL\text{-}G12D/+}$ MEFs in a given culture had undergone Cre-mediated recombination (Fig. 4.1B). Recombination of the KRas$^{LSL\text{-}G12D}$ allele was determined by performing PCR analysis of genomic DNA isolated from KRas$^{LSL\text{-}G12D/+}$ MEFs following infection with either empty adenovirus or adenoviral-Cre using oligonucleotide primers capable of distinguishing the WT, LSL-Kras^{G12D}, and recombined Kras^{G12D} alleles. Together these experiments demonstrate that infection using a viral titre of 250 MOI is sufficient to induce complete recombination of the KRas$^{LSL\text{-}G12D}$ allele in a culture of KRas$^{LSL\text{-}G12D/+}$ MEFs when assayed 24 hours post-infection (Fig. 4.1A-B). This same viral titre was used in all future experiments and the biological effects of KRas^{G12D} knock-in were not investigated until at least 24 hours post-infection. To confirm that our KRas^{G12D} knock-in MEFs were producing functional, constitutively active mutant KRas^{G12D} protein, we infected wild-type and KRas$^{LSL\text{-}G12D/+}$ MEFs with adenoviral-Cre or empty adenovirus and immunoprecipitated GTP-bound Ras using the Ras-binding domain of Raf1. Only Cre-treated KRas$^{LSL\text{-}G12D/+}$ MEFs

showed a significant increase in the level of active GTP-bound Ras and the presence of Ras^{G12D} protein (Fig. 4.1B), validating our experimental system.

Before assaying the expression of MKPs in response to $KRas^{G12D}$ expression in detail we wanted to determine the optimal experimental conditions to observe any potential responses. In previous studies investigating the biochemical activation of ERK and AKT following $KRas^{G12D}$ expression in MEFs, cells were lysed and samples taken at 48 hours post-infection (Tuveson et al., 2004). Consequently, we utilised this time point, but also wanted to assess whether additional serum stimulation would improve our ability to detect altered MKP regulation following $KRas^{G12D}$ expression. We considered this important because under basal, unstimulated conditions MKPs are typically expressed at very low levels and can be difficult to detect (Kucharska et al., 2009). However, our experiments revealed that DUSP5 and DUSP6/MKP-3 were expressed at higher levels in Cre-treated $KRas^{LSL\text{-}G12D/+}$ MEFs when compared to wild type MEFs under normal growth conditions (10% serum) and that overnight serum starvation and re-stimulation with 20% serum for 2 hours was not necessary to induce increased expression of DUSP5 and DUSP6/MKP-3 (Fig. 4.2). Consequently, we decided to use steady state growth conditions for all further experiments.

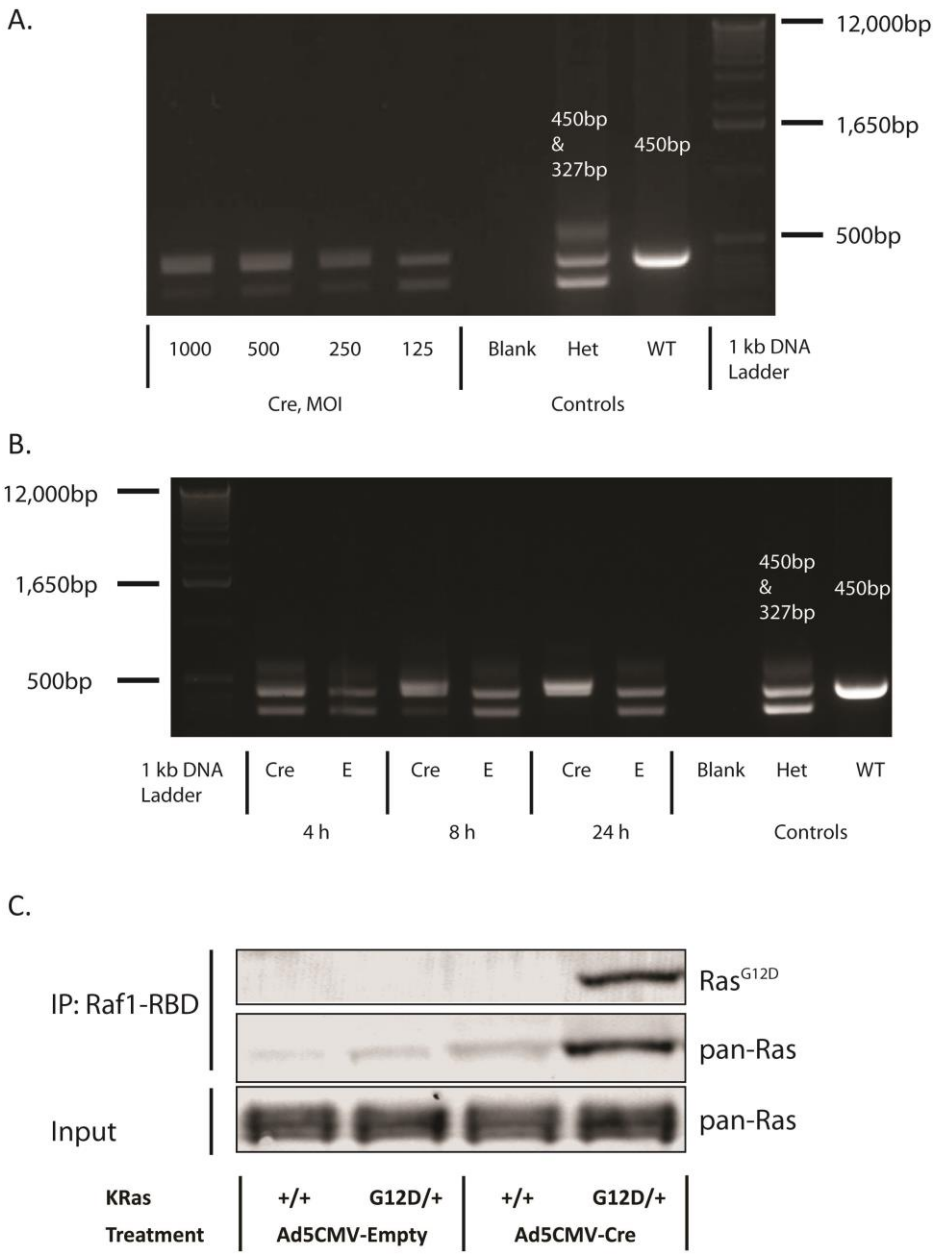

Figure 4.1 Validation of adenoviral-Cre mediated KRas^{G12D} knock-in in MEFs. A-B) PCRs of genomic DNA from KRas$^{LSL\text{-}G12D/+}$ MEFs demonstrating the excision of the Lox-STOP-Lox (LSL)-cassette from the KRas$^{LSL\text{-}G12D}$ allele upon adenoviral-Cre (Cre) treatment, but not empty adenovirus (E). Control lysates from untreated KRas$^{LSL\text{-}G12D/+}$ (Het) and KRas$^{+/+}$ (WT) MEFs validate the size of 450bp WT and 327bp LSL-cassette bands. Cre-mediated recombination of the KRas$^{LSL\text{-}G12D}$ allele results in the loss of the 327bp band and the formation of a 484bp fragment (450bp WT fragment, plus an additional 34bp from the single LoxP site remaining). **A)** Cells were treated with 500, 250 or 125 MOI of adenovirus and DNA isolated at 8 hours post infection. **B)** Cells were treated with 250 MOI of adenovirus and DNA isolated at 4, 8 or 24 hours post adenoviral infection. **C)** MEFs of the indicated genotype were infected with adenoviral-Cre (Ad5CMV-Cre) or empty adenovirus (Ad5CMV-Empty) 24h prior to lysis and pull down of GTP-bound Ras using the RAS-binding domain (RBD) of CRAF. GTP-bound Ras or Ras^{G12D} and input levels of total Ras in whole cell lysates were measured by immunoblotting.

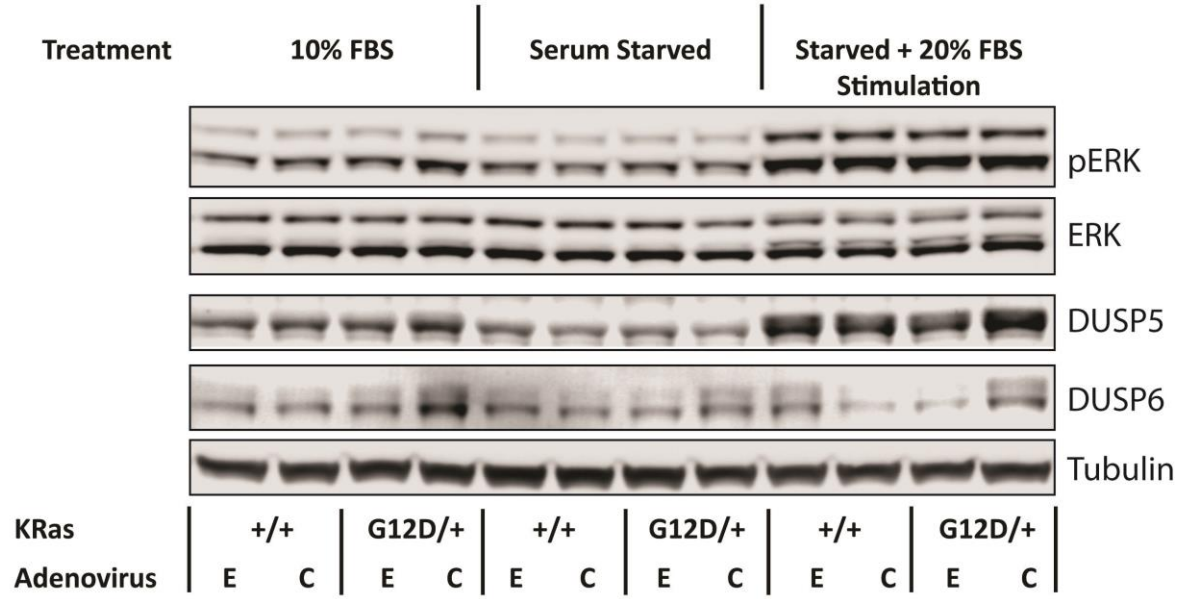

Figure 4.2 MKP induction following KRas^{G12D} knock-in under different serum conditions. MEFs of the indicated genotype were infected with adenoviral-Cre (C) or empty adenovirus (E) prior to modulation of their serum conditions. MEFs were either left to grow in 10% FBS, serum starved in 0.5% FBS for 18 hours, or serum starved in 0.5% FBS for 18 hours followed by a 20% FBS stimulation for 2 hours. Cells were lysed and proteins analysed by immunoblotting using the indicated antibodies. Representative image of experiment performed in duplicate.

To investigate the induction of MKPs following $KRas^{G12D}$ expression we infected $KRas^{LSL-G12D/+}$ MEFs with adenoviral-Cre or empty adenovirus and assessed protein and mRNA levels at 24, 48 and 72 hours post-infection (Fig. 4.3-4). Following $KRas^{G12D}$ knock-in a consistent upregulation of *p*-MEK (representing MEK that is activated via phosphorylation at Ser217/221) levels could be observed. In contrast, *p*-ERK levels only displayed a minor upregulation at 24 and 48 hours post $KRas^{G12D}$ expression, before returning to wild-type levels by 72 hours post-infection (Fig. 4.3A-B). Taken together this suggests that $KRas^{G12D}$ expression is promoting an increase in upstream ERK pathway activity, demonstrated by the consistently elevated *p*-MEK levels, however negative feedback regulation must be acting upon ERK itself to return ERK activity to wild-type levels by 72 hours post-$KRas^{G12D}$ expression. Several MKPs capable of dephosphorylating and regulating ERK, including DUSP2, DUSP4/MKP-2, DUSP5 and DUSP6/MKP-3 are consistently upregulated at both the mRNA and protein level following $KRas^{G12D}$ expression (Fig. 4.3-4), indicating that these enzymes are likely to play a key role in modulating ERK activity in response to $KRas^{G12D}$ expression. Interestingly, despite the observation that ERK activation is effectively constrained following $KRas^{G12D}$ expression, the levels of SerpinB2 mRNA and protein are increased at all time points (Fig. 4.3-4). We have previously shown that SerpinB2 expression is induced in an ERK-dependent manner in MEFs (Fig. 3.5), making it a robust readout of ERK-dependent gene expression. This implies that despite the lack of any observable changes in steady-state *p*-ERK levels, flux through the pathway could be increased to promote the activation of certain ERK targets. One explanation for the latter result is that ERK activity is altered in distinct subcellular compartments or fractions and that these changes are not readily detected by Western blotting of whole cell lysates.

The ERK-specific MKPs DUSP5 and DUSP6/MKP-3 have been shown to be induced in response to ERK activity and thus act as negative feedback regulators of pathway activity (Kucharska et al., 2009; Smith et al., 2006), however other studies have implied that DUSP6/MKP-3 can be regulated by the PI3-kinase pathway which is also activated as a downstream effector pathway by expression of mutant Ras (Park et al., 2014; Phuchareon et al., 2015). To explore this possibility under conditions where mutant Ras is expressed at endogenous levels, we treated $KRas^{LSL-G12D/+}$ MEFs with specific inhibitors of either MEK (PD184352) or PI3K (PI-103) following adenoviral-Cre treatment to determine which of these pathways was mediating $KRas^{G12D}$-induced MKP expression (Fig. 4.5-6). Following

treatment with PD184352 levels of *p*-MEK are increased, although ERK phosphorylation is inhibited (Fig. 4.5). This is because PD184352 is an allosteric, non-ATP competitive MEK inhibitor(Sebolt-Leopold et al., 1999; Solit et al., 2006), therefore the compound does not block MEK phosphorylation but prevents the structural changes in MEK which enable its activity. Consequently, *p*-MEK levels dramatically increase following PD184352 treatment due to the relief of negative feedback between ERK and Raf, stimulating enhanced MEK phosphorylation.

Our results clearly show that $KRas^{G12D}$–driven expression of both DUSP5 and DUSP6/MKP-3 is dependent on ERK activity, but not PI3K activity, at both the protein (Fig. 4.5) and mRNA levels (Fig. 4.6). Interestingly, DUSP6/MKP-3 protein expression was somewhat increased following PI3K inhibition in these cells, a result in agreement with previous experiments in which immortalised mouse fibroblasts (NIH3T3) exposed to fibroblast growth factor (FGF) were treated with these inhibitors (Ekerot et al., 2008). Furthermore, increased expression of DUSP2, DUSP4/MKP-2 and DUSP7 mRNA's was also shown to be induced by $KRas^{G12D}$ and abrogated by the inhibition of ERK, but not PI3K, activity (Fig. 4.6). Finally, DUSP9/MKP-4 mRNA was induced by $KRas^{G12D}$ but not significantly downregulated by either MEK or PI3K inhibition, whereas DUSP1/MKP-1 mRNA was not induced by $KRas^{G12D}$ (Fig. 4.6). Overall, this demonstrates that the majority of MKPs capable of targeting the Ras-ERK pathway are induced by ERK activity and can probably act as negative feedback regulators in response to mutant $KRas^{G12D}$ expression.

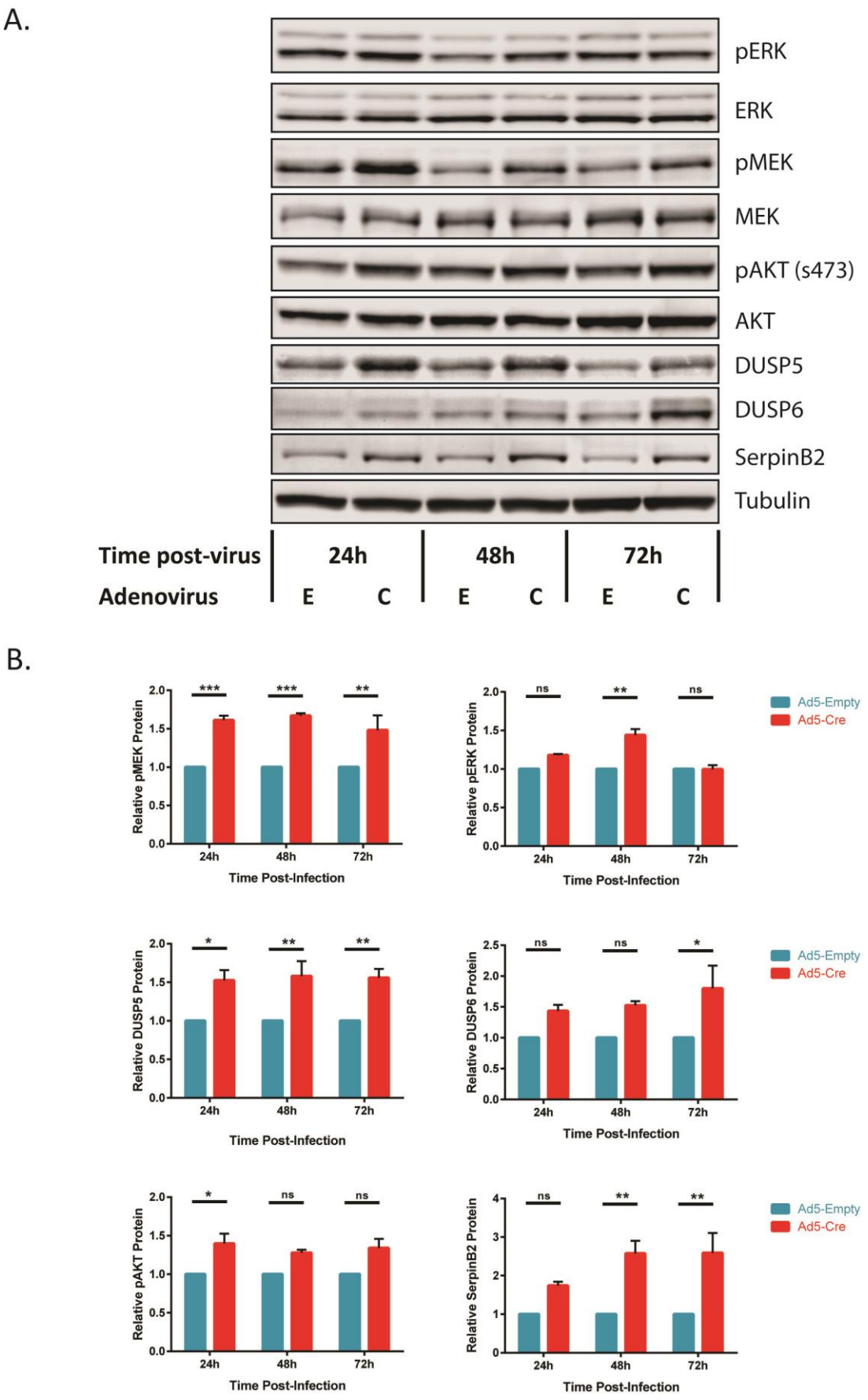

Figure 4.3 Ras effector pathway activation and MKP induction following KRas^{G12D} knock-in. KRas$^{LSL-G12D/+}$ MEFs were infected with adenoviral-Cre (C) or empty adenovirus (E) for 24, 48 or 72 hours prior to cell lysis, and immunoblotting using the indicated antibodies. A representative

Western blot is shown **(A)**, alongside protein quantification utilising a Li-Cor Odyssey infrared scanner **(B)**. Mean values ± SEM are shown, n = 3. ns = not significant, *P < 0.05, **P < 0.01, ***P<0.001 using two-way ANOVA and Bonferroni post hoc test, comparing Empty v Cre treatments.

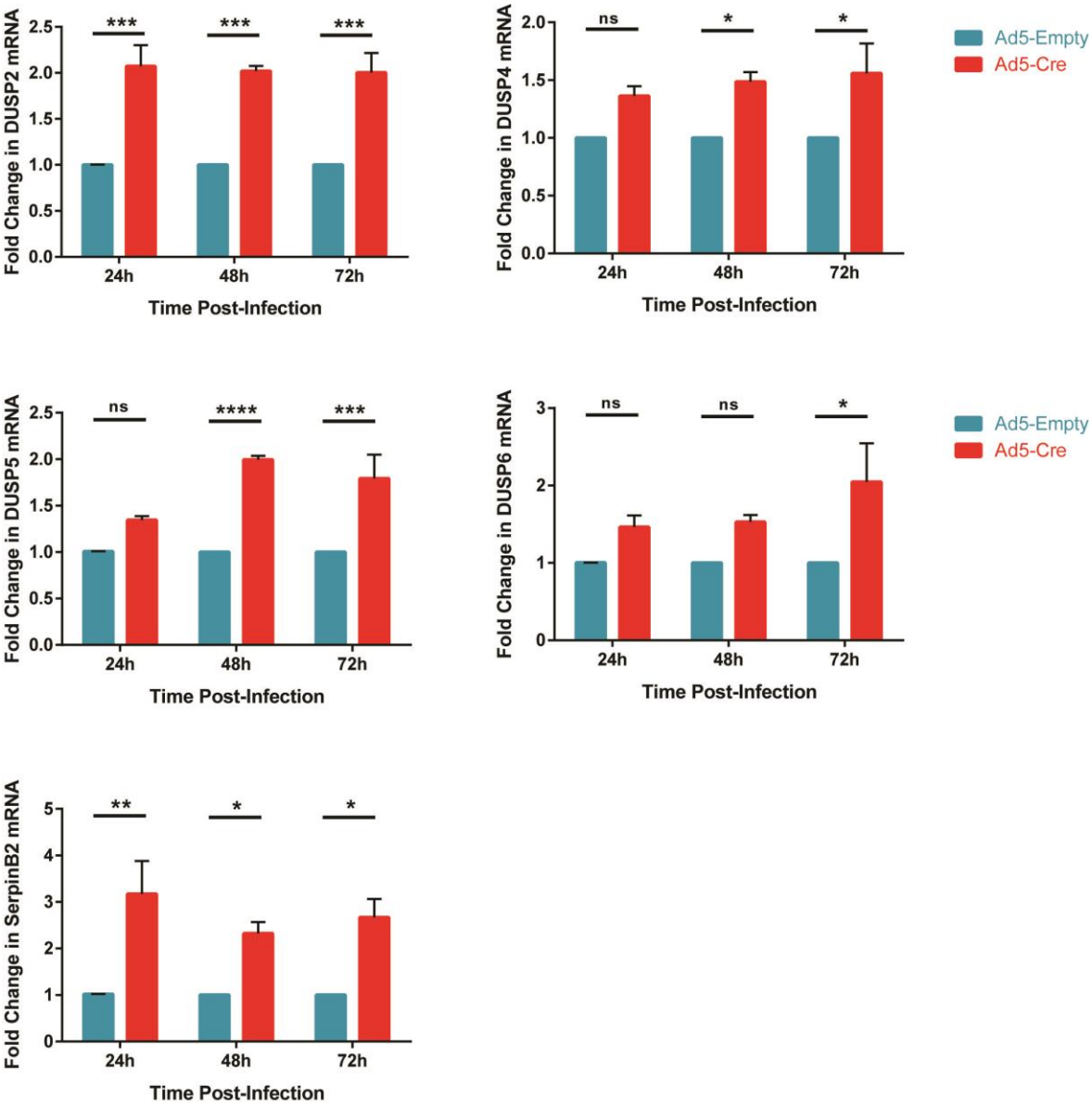

Figure 4.4 MKP induction following KRas^{G12D} knock-in. Taqman RT-qPCR assays showing the fold change in mRNA levels of the indicated genes following Cre-mediated KRas^{G12D}-knock-in, relative to empty adenovirus treatment. KRas$^{LSL\text{-}G12D/+}$ MEFs were infected with adenoviral-Cre (Ad5-Cre) or empty adenovirus (Ad5-Empty) for 24, 48 or 72 hours prior to cell lysis and RNA isolation. Mean values ± SEM are shown, n = 3. ns = not significant, *P < 0.05, **P < 0.01, ***P<0.001 using two-way ANOVA and Bonferroni post hoc test, comparing Empty v Cre treatments.

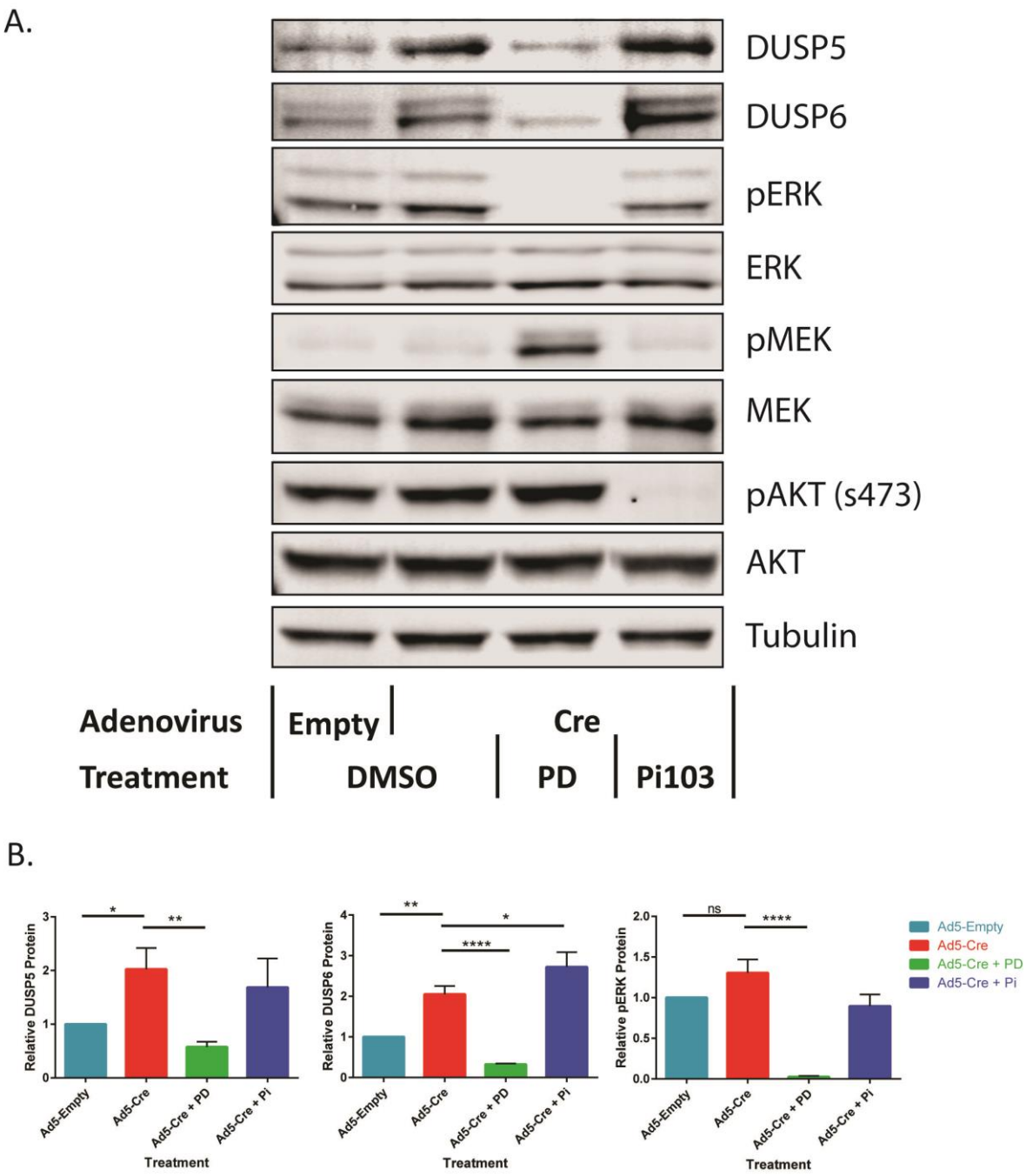

Figure 4.5 MKP induction following KRas^{G12D} knock-in is dependent on ERK, but not PI3K, pathway activation. KRas$^{LSL-G12D/+}$ MEFs were infected with adenoviral-Cre (Cre) or empty adenovirus (Empty) for 48 hours prior to cell lysis, and immunoblotting using the indicated antibodies. MEFs were also treated with DMSO control, the MEK inhibitor PD184352 (PD) or the PI3K inhibitor Pi103 4 hours prior to lysis. Western blot is shown **(A)**, alongside protein quantification **(B)**. Mean values ± SEM are shown, n = 3. ns = not significant, *P < 0.05, **P < 0.01, ****P<0.0001 using one-way ANOVA and Bonferroni post hoc test.

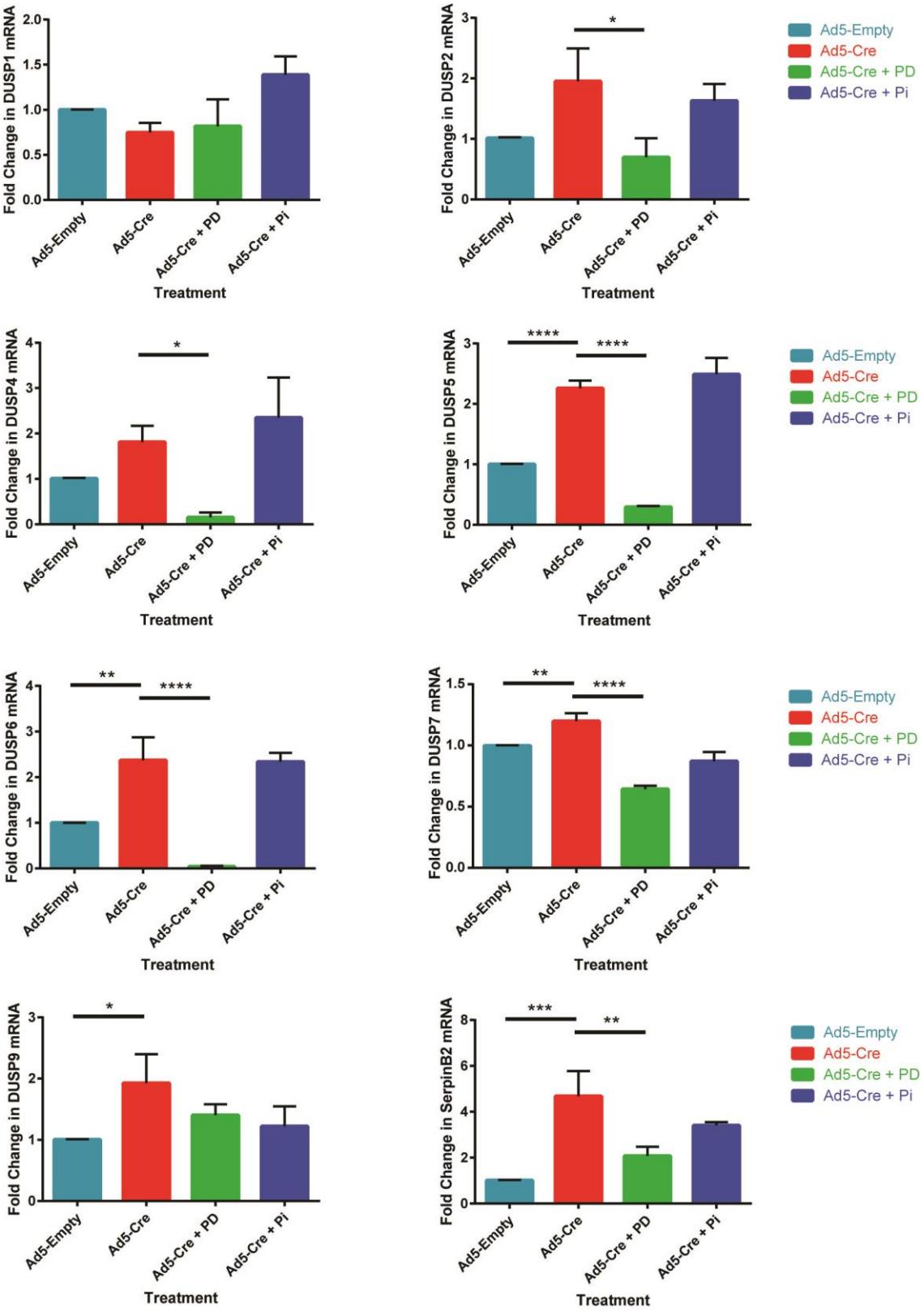

Figure 4.6 MKP induction following KRas^{G12D} knock-in is dependent on ERK, but not PI3K, pathway activation. Taqman RT-qPCR assays showing the fold change in mRNA levels of the indicated genes following Cre-mediated KRas^{G12D}-knock-in and inhibitor treatment, relative to empty adenovirus treatment. KRas$^{LSL-G12D/+}$ MEFs were infected with adenoviral-Cre (Ad5-Cre) or empty adenovirus (Ad5-Empty) for 48 hours, combined with treatment with DMSO control, the MEK inhibitor PD184352 (PD) or the PI3K inhibitor Pi103 4 hours prior to lysis. Mean values ± SEM are shown, n = 3. *P < 0.05, **P < 0.01, **P < 0.001, ****P<0.0001 using one-way ANOVA and Bonferroni post hoc test.

4.2.2 KRas^{G12D} expression induces DUSP5 and DUSP6/MKP-3 in a dose-dependent manner to constrain ERK activity

Thus far we have shown that multiple MKPs, including DUSP5 and DUSP6/MKP-3, are upregulated in response to mutant KRas^{G12D} expression (Fig. 4.3-4), and that this upregulation is dependent on ERK activity (Fig. 4.5-6). Together this indicates that MKPs act as negative feedback regulators to constrain constitutive activation of the ERK pathway. To extend these results and to determine whether MKPs are induced in a dose-dependent manner in response to oncogenic stimuli, we set out to generate MEFs, which were homozygous for the KRas$^{LSL-G12D}$ allele. Although KRas homozygous knockout is embryonic lethal in mice, death occurs between embryonic days 12-14 (E12-14) (Johnson et al., 1997), therefore we attempted to derive MEFs from mouse embryos at E11.5 in the hope that cells would still be viable at this early embryonic stage. This strategy, though resulting in lower yields of MEFs (in terms of cell numbers), was successful and enabled the isolation of homozygous mutant KRas (KRas$^{LSL-G12D/LSL-G12D}$) MEFs. These cells were viable, although E11.5 MEFs of all genotypes proliferated more slowly than cells derived from later (E13.5) embryos when grown prior to adenoviral infection. Initially we validated the genotype of our KRas$^{LSL-G12D/LSL-G12D}$ MEFs via PCR analysis of genomic DNA in the presence or absence of adenoviral-Cre treatment. KRas$^{LSL-G12D/LSL-G12D}$ MEFs amplified only the characteristic LSL-cassette PCR product prior to Cre-treatment and this was converted into the single KRas^{G12D} knock-in PCR product following Cre-mediated recombination (Fig. 4.7A). Furthermore, homozygous KRas^{G12D} knock-in promoted increased Ras^{G12D} protein levels and Ras activity, determined by the level of GTP-bound Ras, relative to the heterozygous KRas^{G12D} knock-in (Fig. 4.7B), demonstrating the expected functional consequences of the presence of two copies of the mutant allele.

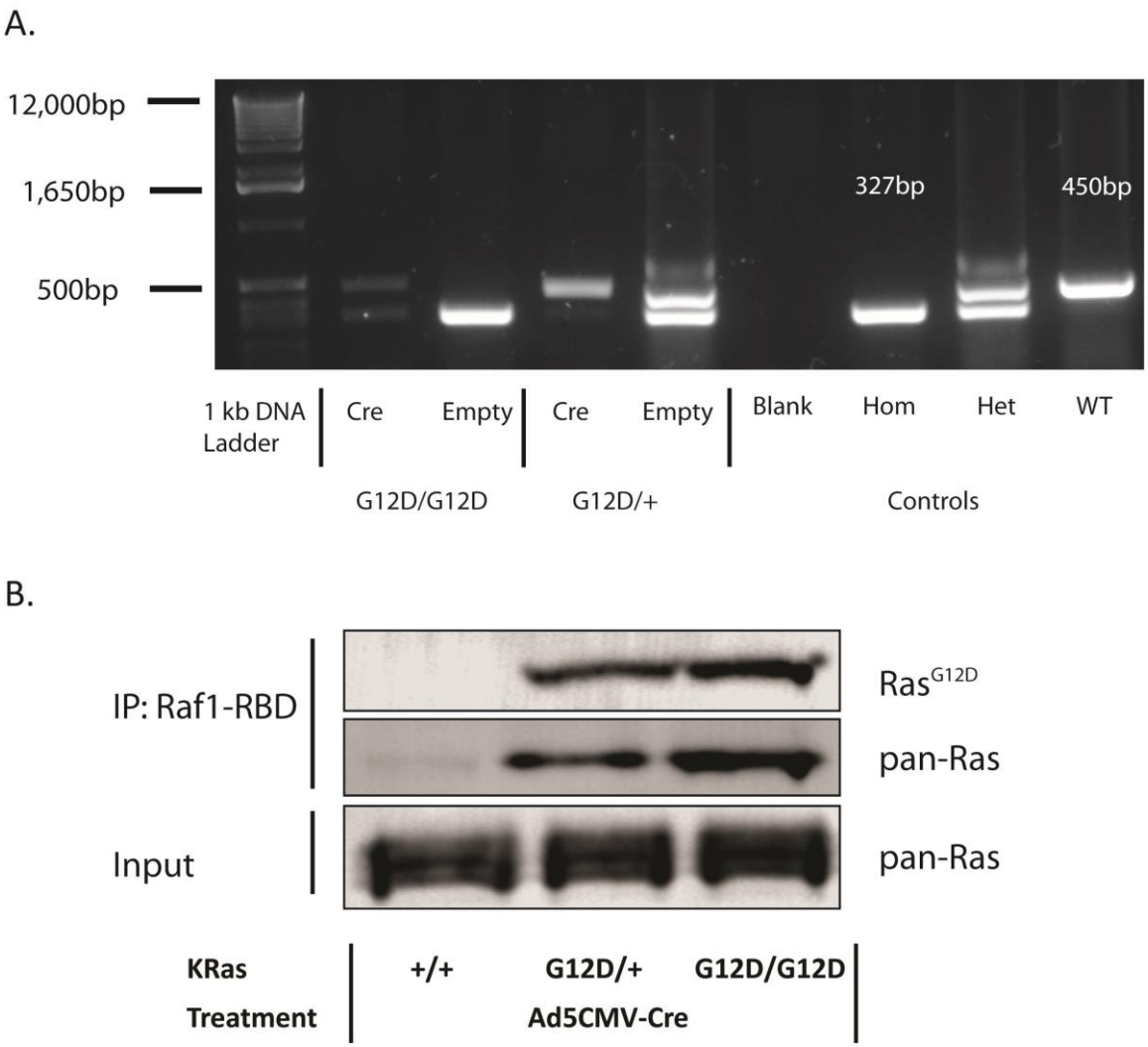

Figure 4.7 Validation of KRas^{G12D} homozygous MEFs. A) PCR of genomic DNA from KRas$^{LSL-G12D/LSL-G12D}$ (G12D/G12D) and KRas$^{LSL-G12D/+}$ (G12D/+) MEFs demonstrating the excision of the LSL-cassette upon adenoviral-Cre (Cre) treatment, but not empty adenovirus (Empty). Cells were lysed and DNA isolated 24 hours post adenoviral infection. Control lysates from untreated KRas$^{LSL-G12D/LSL-G12D}$ (Hom), KRas$^{LSL-G12D/+}$ (Het) and KRas$^{+/+}$ (WT) MEFs validate the size of 450bp WT and 327bp LSL-cassette bands. Cre-mediated recombination of the KRas$^{LSL-G12D}$ allele results in the formation of a 484bp fragment. **B)** MEFs of the indicated genotype were infected with adenoviral-Cre (Ad5CMV-Cre) 24h prior to lysis and pull down of GTP-bound Ras using the RAS-binding domain (RBD) of CRAF. GTP-bound Ras or Ras^{G12D} and input levels of total Ras in whole cell lysates were measured by immunoblotting.

To investigate the effects of increasing mutant KRas-driven oncogenic stimulus on ERK activity and MKP induction, wild-type, $KRas^{LSL\text{-}G12D/+}$ and $KRas^{LSL\text{-}G12D/LSL\text{-}G12D}$ MEFs were infected with adenoviral-Cre and Ras effector pathway activation and MKP induction compared between genotypes (Fig. 4.8-9). Expression of one or two alleles of mutant $KRas^{G12D}$ induced increased *p*-MEK levels relative to wild-type MEFs, and $KRas^{G12D/G12D}$ MEFs displayed marginally higher levels than heterozygous $KRas^{G12D/+}$ MEFs (Fig. 4.8). This indicates that mutant $KRas^{G12D}$ expression is driving increased activation of the ERK pathway in a dose-dependent manner, consistent with the increased Ras activity observed in these cells (Fig. 4.7B). However, *p*-ERK levels are not significantly increased following knock-in of either one or two copies of the $KRas^{G12D}$ allele, relative to wild-type MEFs (Fig. 4.8). Expression of the ERK-targeting MKPs DUSP2, DUSP4/MKP-2, DUSP5 and DUSP6/MKP-3 is reduced in empty adenovirus treated $KRas^{LSL\text{-}G12D/LSL\text{-}G12D}$ MEFs where KRas expression is absent, reflecting the importance of ERK pathway activity in inducing the expression of these MKPs (Fig. 4.6 & 4.8-9) (Brondello et al., 1997; Kucharska et al., 2009; Smith et al., 2006). However, when taking into account this reduced initial expression of these MKPs in $KRas^{LSL\text{-}G12D/LSL\text{-}G12D}$ MEFs, $KRas^{G12D}$ expression can be shown to promote a dose-dependent increase in DUSP5 and DUSP6/MKP-3 mRNA and protein levels and the mRNA expression of DUSP2 and DUSP4/MKP-2 (Fig. 4.8-9). Furthermore, the expression of DUSP7 and DUSP9/MKP-4 mRNA is significantly upregulated upon homozygous, but not heterozygous, $KRas^{G12D}$ expression (Fig. 4.9), perhaps reflecting the necessity for increased negative feedback activity in the presence of a stronger stimuli. Together these results indicate that MKPs are likely to play a role in maintaining the constant level of *p*-ERK observed following the expression of either one or two copies of mutant $KRas^{G12D}$.

Previous experiments demonstrated the upregulation of SerpinB2 mRNA and protein levels in response to the expression of one allele of mutant $KRas^{G12D}$ (Fig. 4.3-4). Again utilising SerpinB2 expression as a measure of ERK-dependent gene we can demonstrate that mutant $KRas^{G12D}$ expression induces ERK-target genes in a dose-dependent manner (Fig. 4.8-9), again indicating that although the apparent *p*-ERK levels assayed by Western blotting of whole cell lysates are not increased, signalling flux through the pathway is likely to be increased following $KRas^{G12D}$ expression. Interestingly, levels of *p*-AKT are not elevated following knock-in of one or two copies of the $KRas^{G12D}$ allele, implying that

negative feedback systems are also preventing increased PI3K signalling following constitutive KRas activation (Fig. 4.8).

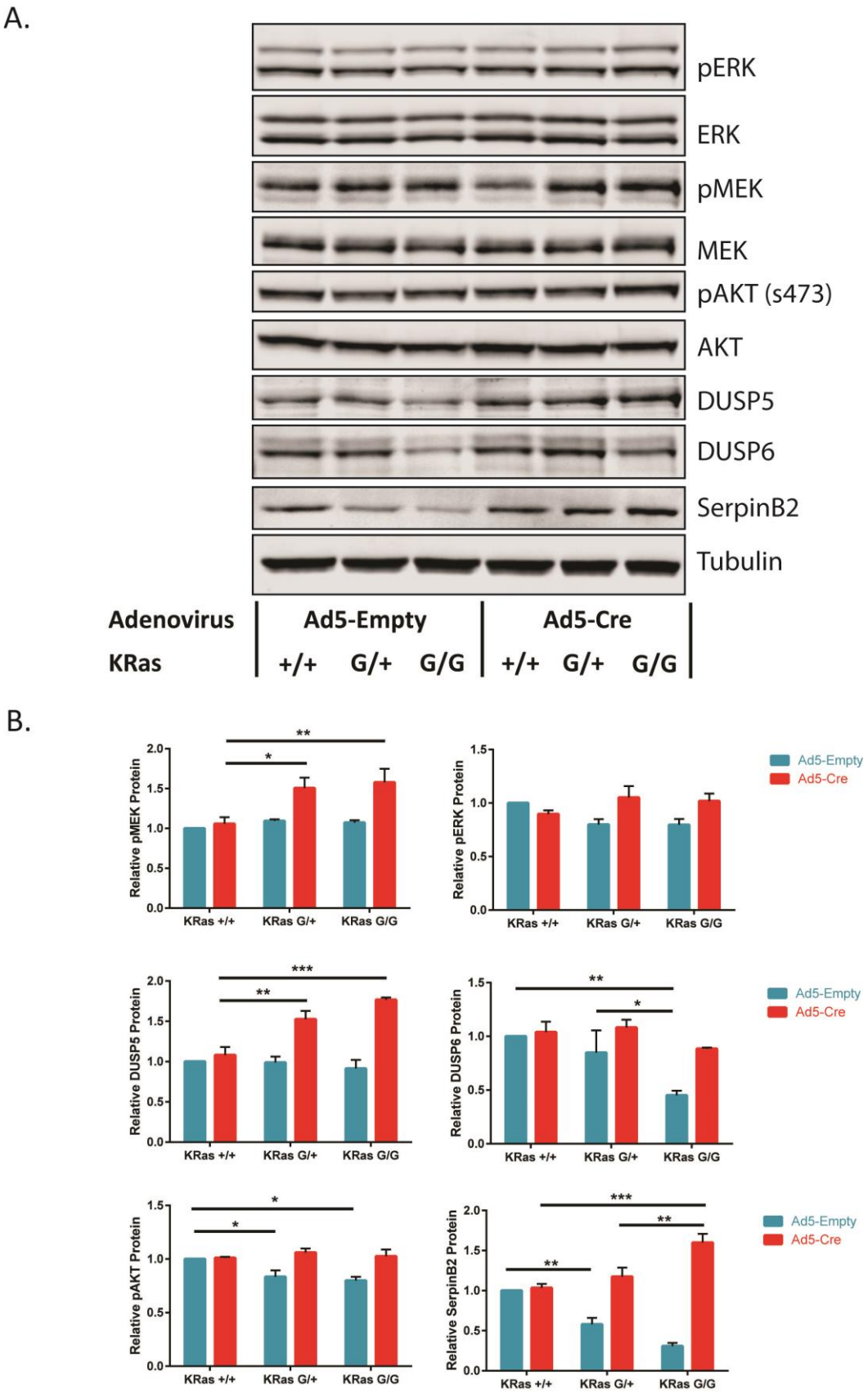

Figure 4.8 Dose-dependent MKP induction following KRas^{G12D} knock-in maintains constant levels of p-ERK. Wild-type (+/+), KRas$^{LSL\text{-}G12D/+}$ (G/+) and KRas$^{LSL\text{-}G12D/LSL\text{-}G12D}$ (G/G) MEFs were infected with adenoviral-Cre (Ad5-Cre) or empty adenovirus (Ad5-Empty) for 48 hours prior to cell lysis, and immunoblotting using the indicated antibodies. A representative Western blot is shown **(A)**, alongside protein quantification **(B)**. Mean values ± SEM are shown, n = 3 *P < 0.05, **P < 0.01, ***P<0.001 using two-way ANOVA and Bonferroni post hoc test, comparing KRas genotypes.

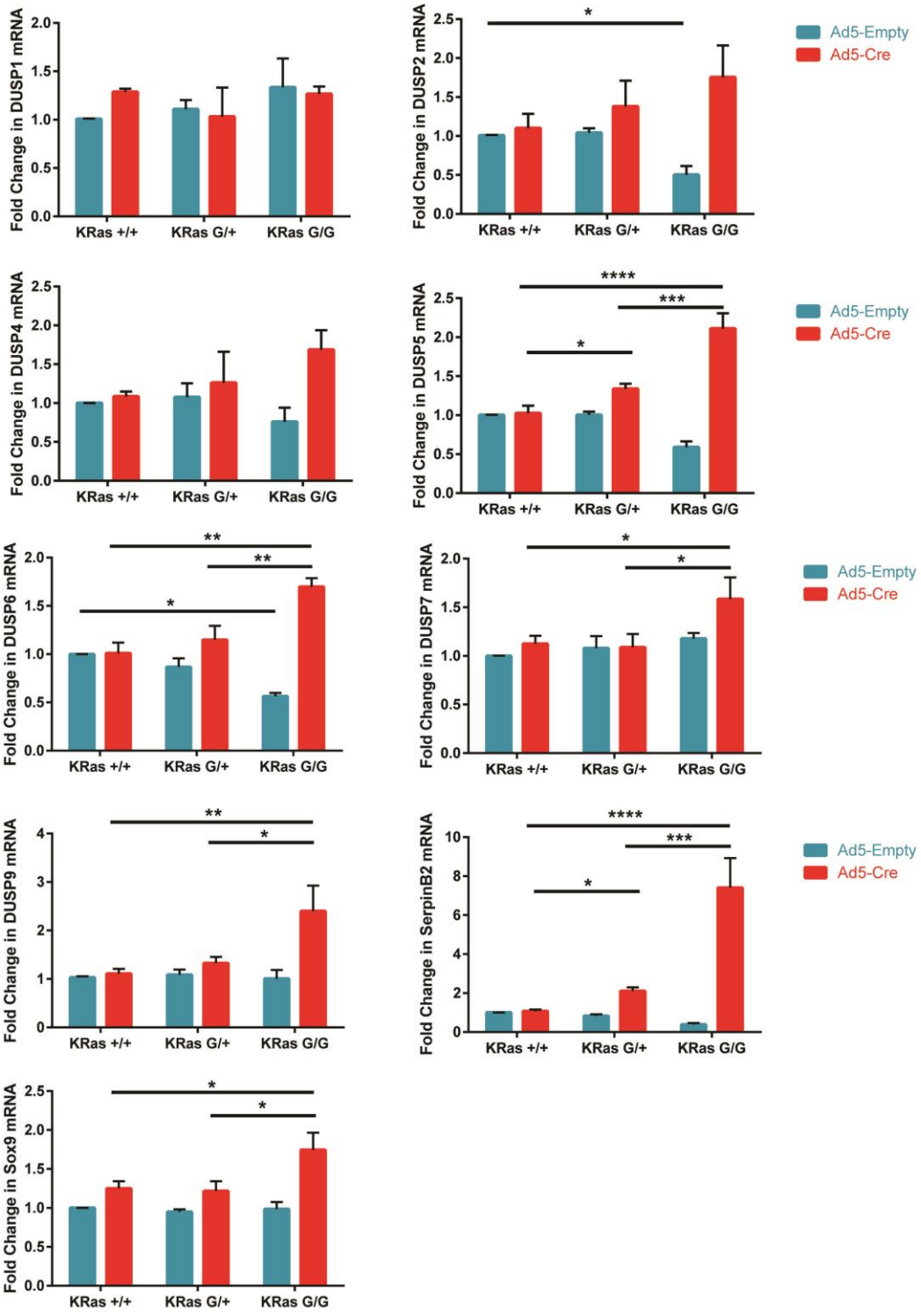

Figure 4.9 Dose-dependent MKP induction following KRas^{G12D} knock-in. Taqman RT-qPCR assays showing the fold change in mRNA levels of the indicated genes following Cre-treatment of MEFs of the indicated genotype, relative to wild-type cells infected with empty adenovirus. Wild-type (+/+), KRas$^{LSL-G12D/+}$ (G/+) and KRas$^{LSL-G12D/LSL-G12D}$ (G/G) MEFs were infected with adenoviral-Cre (Ad5-Cre) or empty adenovirus (Ad5-Empty) for 48 hours prior to cell lysis and RNA isolation. Mean values ± SEM are shown, n = 3. *P < 0.05, **P < 0.01, ***P<0.001, ***P<0.001 using two-way ANOVA and Bonferroni post hoc test, comparing KRas genotypes.

The knock-in of one allele of mutant $KRas^{G12D}$ has been shown to increase the proliferation rate of MEFs and also to enable colony formation through the loss of contact inhibition (Tuveson et al., 2004). Consequently, if there is an increase in ERK-dependent gene expression following homozygous $KRas^{G12D}$ expression, despite negative feedback systems including MKPs constraining total *p*-ERK levels, it could be hypothesised that homozygous $KRas^{G12D}$ expression would have an additional effects on cellular phenotypes relative to the activation of one $KRas^{G12D}$ allele. Therefore, we investigated whether modulation of cellular phenotypes, such as proliferation rate, occurs in a dose-dependent manner following the knock-in of one or two alleles of $KRas^{G12D}$.

To address this question we performed proliferation assays on wild-type, $KRas^{LSL\text{-}G12D/+}$ and $KRas^{LSL\text{-}G12D/LSL\text{-}G12D}$ MEFs in the presence or absence of adenoviral-Cre treatment. Empty adenoviral infected MEFs of all genotypes proliferated at a similar rate, which did not significantly differ from that of wild-type cells infected with adenoviral-Cre. Whereas, the knock-in of one or two alleles of $KRas^{G12D}$ significantly increased the proliferation rate of MEFs compared to wild-type cells (Fig. 4.10A). This increased proliferation upon $KRas^{G12D}$ expression can be clearly demonstrated by calculating the fold change in cell number (Fig. 4.10B) or the percentage increase in the gradient of the linear component of the growth curves (Fig. 4.10C) comparing the empty to Cre-treated MEFs of each genotype. This should normalise for any initial differences in proliferation rate of individual MEF cell lines due to genetic differences independent of KRas genotype. These graphs show that Cre-treatment of wild-type MEFs has no significant effect on proliferation rate, whereas the knock-in of one or two alleles of $KRas^{G12D}$ induces an approximate doubling or tripling or the proliferation rate respectively (Fig. 4.10B-C).

Colony formation assays were also performed on $KRas^{LSL\text{-}G12D/+}$ and $KRas^{LSL\text{-}G12D/LSL\text{-}G12D}$ MEFs. In agreement with previously published data, these assays demonstrated that when MEFs are seeded at high density $KRas^{G12D}$ expression can induce colony formation through the loss of contact inhibition (Fig. 4.11A) (Tuveson et al., 2004). However, in colony formation assays $KRas^{G12D}$ dose does not seem to affect the phenotype observed, with the knock-in of either one or two alleles of $KRas^{G12D}$ sufficient to permit colony formation. Furthermore, neither one nor two alleles of $KRas^{G12D}$ are sufficient to enable clonogenic growth, as neither genotype is able to form colonies when seeded at very low

density (Fig. 4.11B). Taken together these results demonstrate that despite negative feedback systems, such as MKPs, constraining *p*-ERK induction, $KRas^{G12D}$ expression is able to promote altered cellular phenotypes in MEFs.

A.

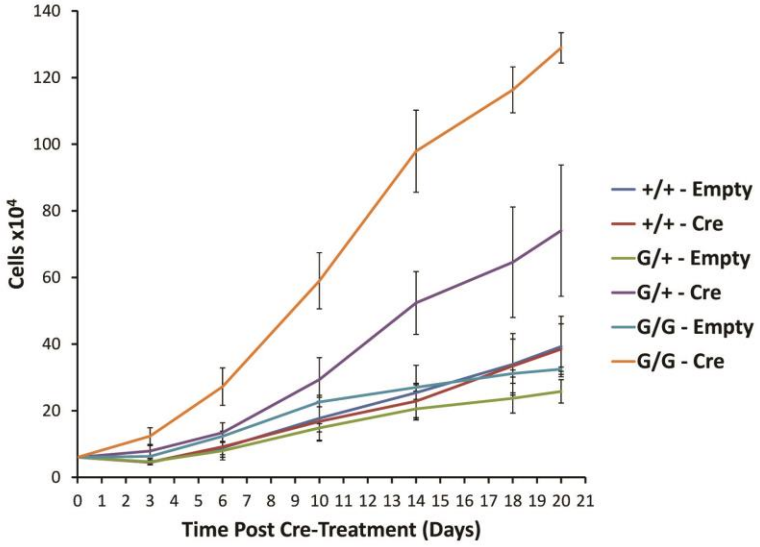

B.

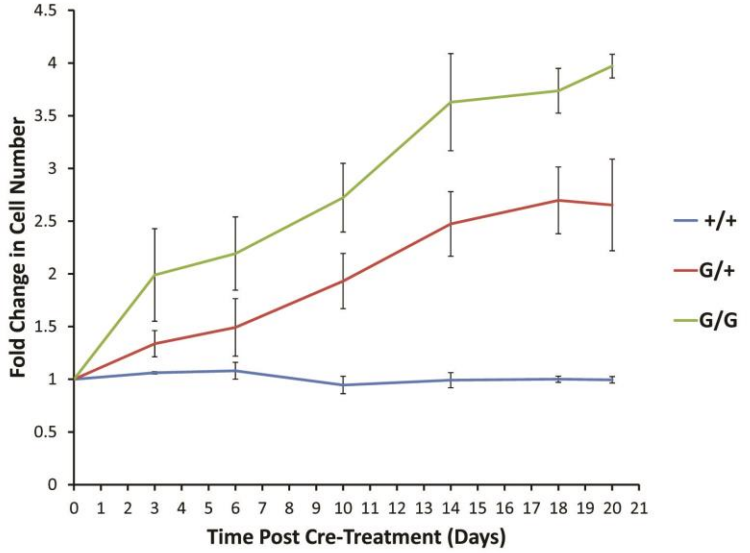

C.

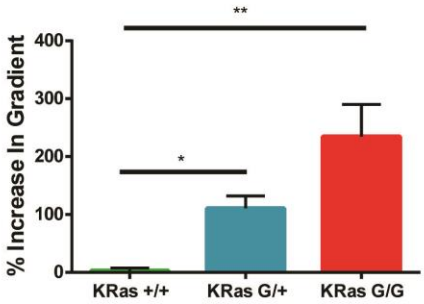

Figure 4.10 KRas^{G12D} knock-in promotes increased proliferation in MEFs. Wild-type (+/+), KRas$^{LSL-G12D/+}$ (G/+) and KRas$^{LSL-G12D/LSL-G12D}$ (G/G) MEFs were seeded at low density, infected with adenoviral-Cre (Cre) or empty adenovirus (Empty) and left to proliferate until confluent. **A)** Cell counts of each cell line and treatment. **B)** Fold change in cell number for each genotype post-cre treatment (Cre/empty cell count for each measurement). **C)** Percentage increase in gradient for each genotype post-cre treatment (Linear regression performed for every MEF line in each condition, to calculate the gradient. Then % increase in gradient of the cre-treated lines over the empty-treated lines calculated for each genotype). Mean values ± SEM are shown, n = 3. *P < 0.05, **P < 0.01, using one-way ANOVA and Bonferroni post hoc test.

A.

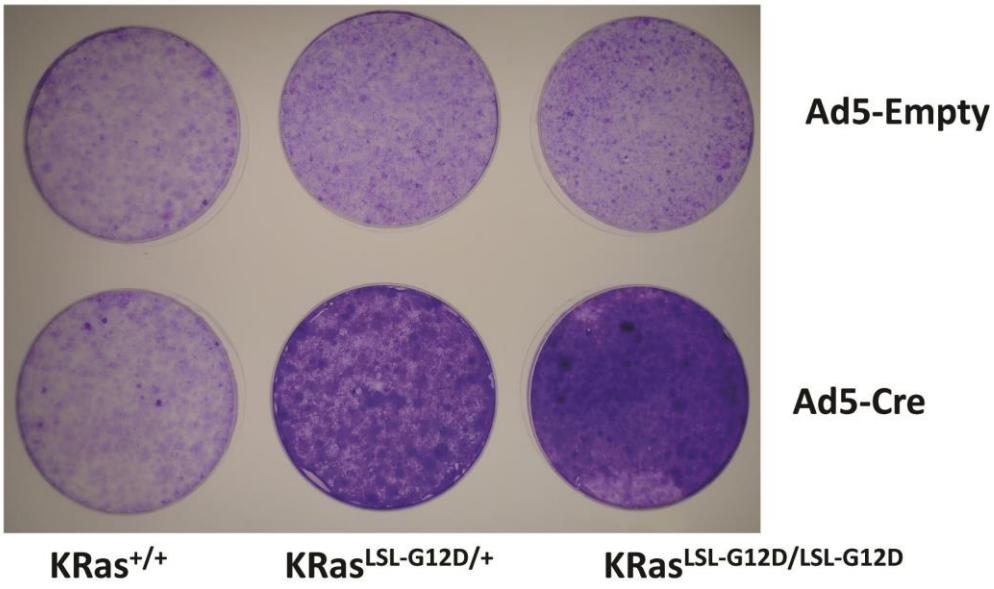

B.

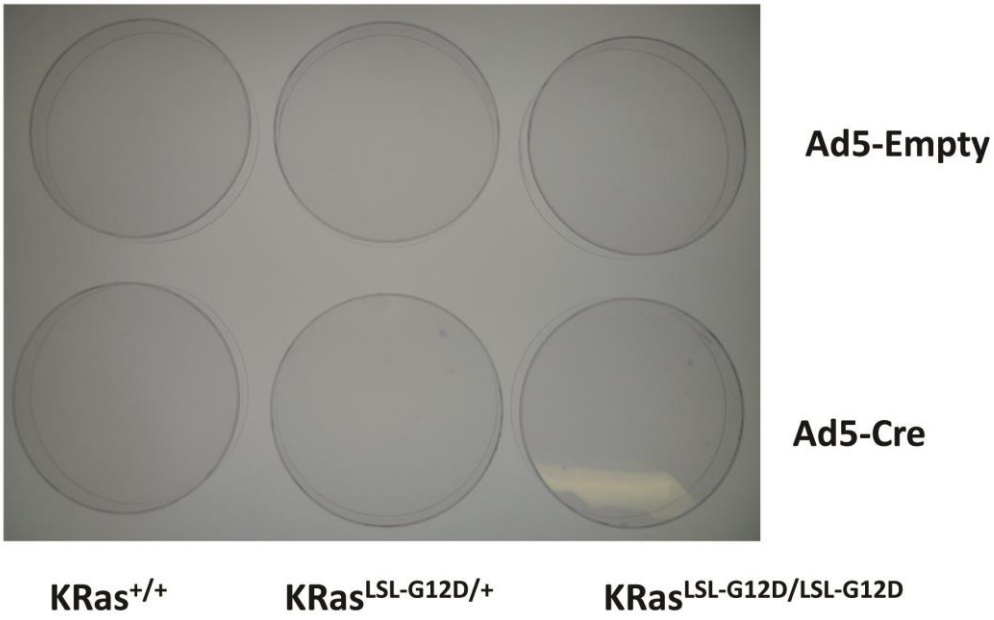

Figure 4.11 KRas^{G12D} knock-in enables loss of contact-inhibition and colony formation. MEFs of the indicated genotypes were infected with adenoviral-Cre (Ad5-Cre) or empty adenovirus (Ad5-Empty) prior to seeding at high **(A)** or low **(B)** density. MEFs were grown for 2-3 weeks until foci were visible, before fixation and visualisation with crystal violet. Representative images shown of experiments performed in triplicate. **B)** No colonies formed from cells seeded at very low density.

4.2.3 DUSP5 loss alters gene expression in KRas^{G12D} expressing MEFs

MKPs are a component of the negative feedback mechanism responsible for constraining ERK activity following KRas^{G12D} expression (Fig. 4.8-9). However, it is unknown whether individual MKPs perform non-redundant functions in the regulation of ERK activity is response to KRas^{G12D} expression. To address this question we first crossed DUSP5 knockout mice with KRas$^{LSL\text{-}G12D/+}$ mice and utilised this transgenic line to generate littermate MEFs which all contained the KRas$^{LSL\text{-}G12D/+}$ allele and were either DUSP5$^{+/+}$, DUSP5$^{+/-}$ or DUSP5$^{-/-}$. Subsequently, KRas^{G12D} expression was induced in these MEFs through adenoviral-Cre treatment and changes in Ras effector signalling and MKP induction investigated after 48 hours. Following the loss of one or two alleles of DUSP5 KRas^{G12D} MEFs demonstrated no changes in either *p*-MEK or *p*-AKT levels, however surprisingly whole cell *p*-ERK levels appeared slightly reduced (Fig. 4.12). There also appeared to be marginal compensatory upregulation of other MKPs including DUSP2 and DUSP6/MKP-3 following the homozygous loss of DUSP5 in KRas^{G12D} expressing MEFs (Fig. 4.12 & 4.13A). However, the most striking phenotype was the consistent upregulation of multiple ERK target genes including both SerpinB2 and Egr1 upon homozygous DUSP5 loss in KRas^{G12D} expressing MEFs (Fig. 4.12 & 4.13B). SerpinB2 and Egr1 expression was investigated following DUSP5 loss in KRas^{G12D} expressing MEFs because as well as being well established ERK transcriptional targets (Shaul and Seger, 2007; Stringer et al., 2012), both of these genes were top microarray hits upregulated in DUSP5$^{-/-}$ MEFs upon TPA stimulation (Fig. 3.4A) (Rushworth et al., 2014).

This indicates that DUSP5 loss might be inducing similar mechanistic changes in ERK activity following ERK pathway stimulation by mutant KRas^{G12D} expression as we observed following TPA stimulation, whereby DUSP5 loss is able to promote increased nuclear ERK activation and therefore elevated ERK-dependent gene expression (Fig. 3.3 & 3.4) (Rushworth et al., 2014). To address we performed preliminary experiments using subcellular fractionation (Fig. 4.14A-B) and high-content microscopy (Fig. 4.14C) to assess levels of nuclear and cytoplasmic *p*-ERK in KRas^{G12D} expressing MEFs in the presence or absence of DUSP5. Surprisingly, we were unable to identify any changes in *p*-ERK localisation following DUSP5 loss in the presence of KRas^{G12D}. At the present time it is unclear why we are unable to detect these changes in ERK activity or localisation, despite

clear evidence that signalling flux through the ERK pathway is increased as evidenced by the changes in ERK-dependent gene expression seen following DUSP5 loss in these cells (Fig. 4.12-13). This may reflect the sensitivity of our detection methods under conditions where pathway flux is changed, but less dramatically than after TPA-stimulation or ectopic oncogene expression or the fact that recombination is relatively slow in achieving full expression of mutant KRas compared with the acute effects of TPA or ectopic oncogene expression.

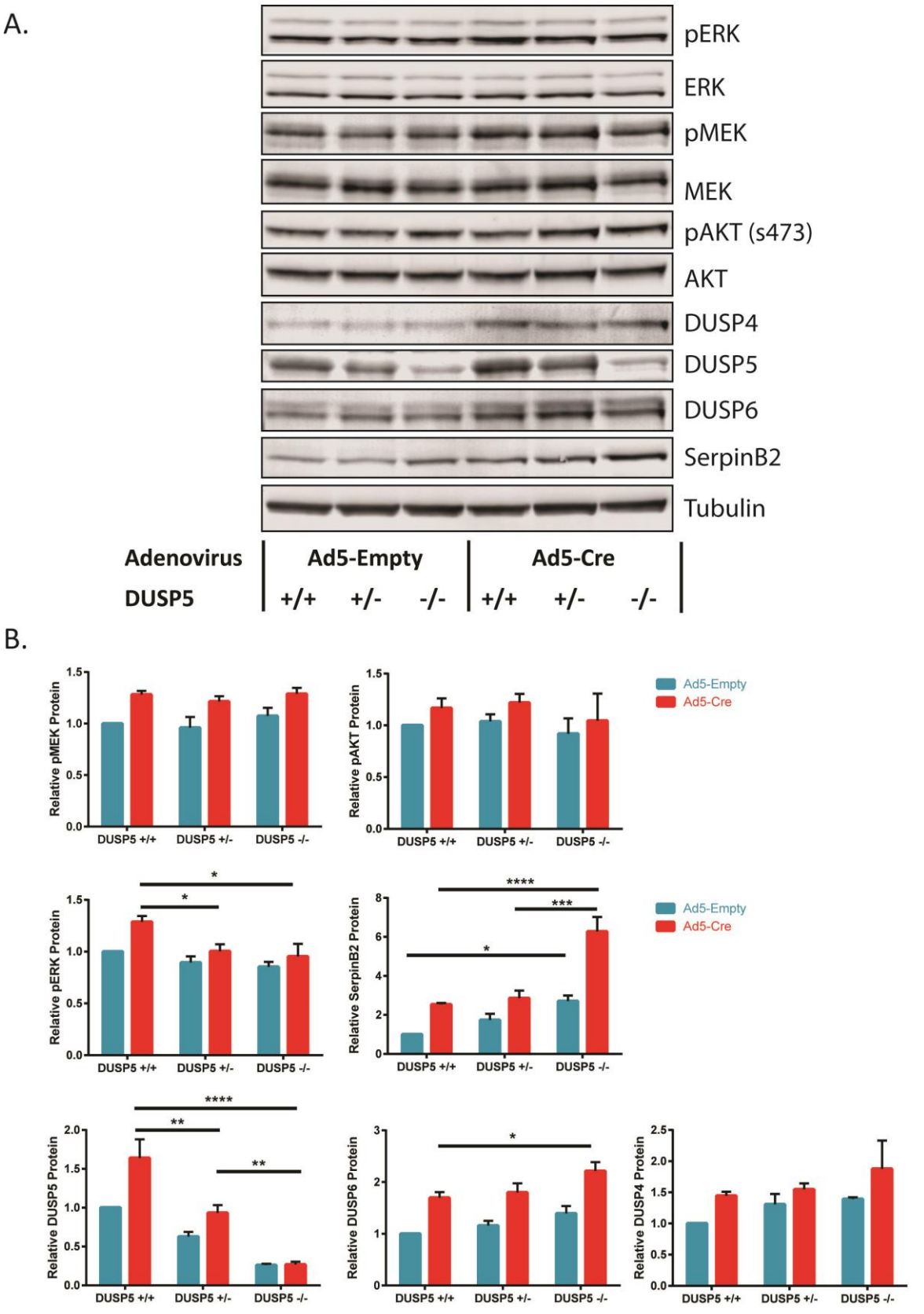

Figure 4.12 Ras effector pathway activation and MKP induction following KRas^{G12D} knock-in and DUSP5 knockout. KRas$^{LSL-G12D/+}$ MEFs which were either DUSP5$^{+/+}$, DUSP5$^{+/-}$ or DUSP5$^{-/-}$ were infected with adenoviral-Cre (Ad5-Cre) or empty adenovirus (Ad5-Empty) for 48 hours prior to cell lysis, and immunoblotting using the indicated antibodies. A representative Western blot is shown **(A)**, alongside protein quantification **(B).** Mean values ± SEM are shown, n = 3. *P < 0.05, **P < 0.01, ***P<0.001, ****P<0.0001 using two-way ANOVA and Bonferroni post hoc test, comparing DUSP5 genotypes.

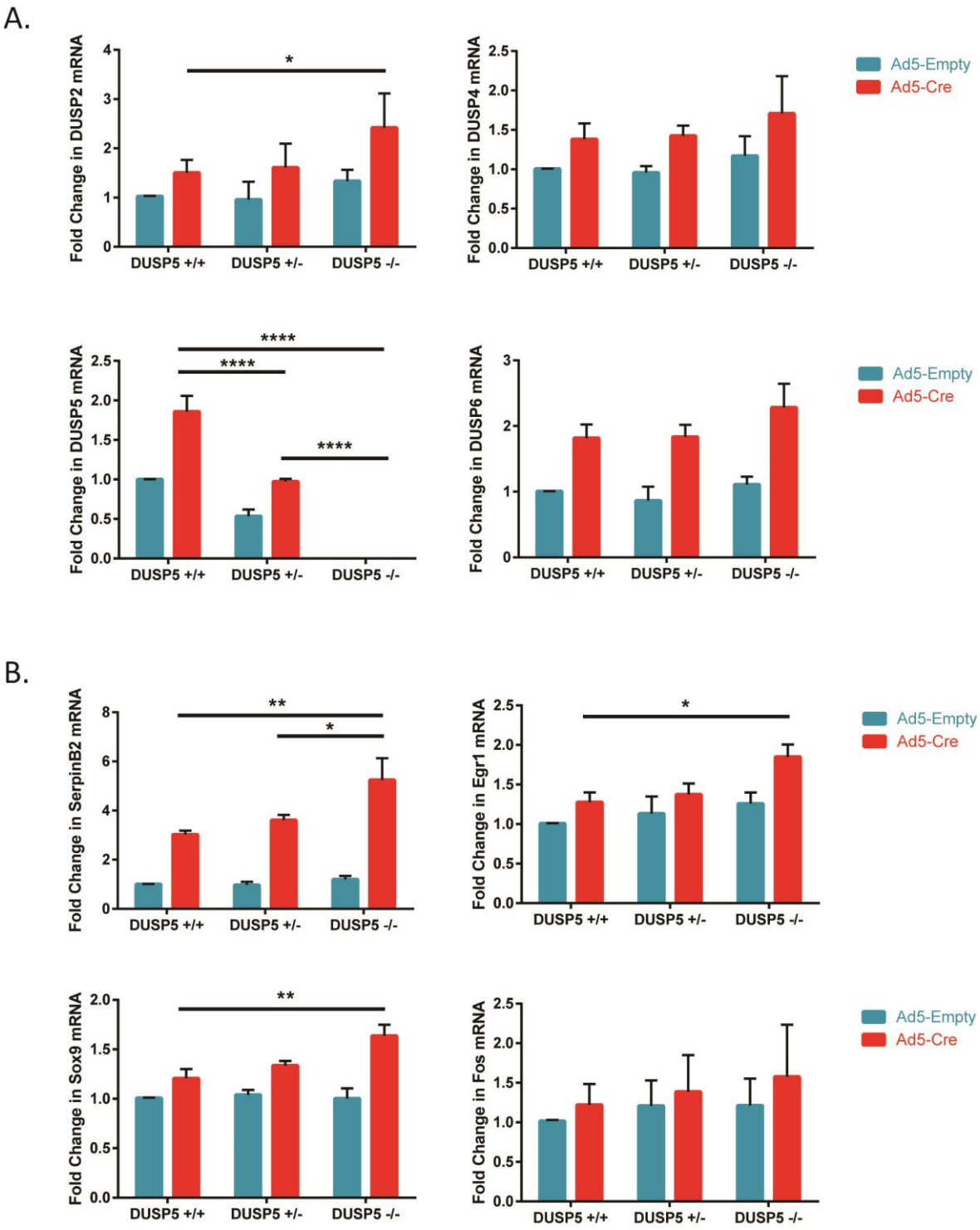

Figure 4.13 DUSP5 loss alters ERK-dependent gene expression following KRas^{G12D} knock-in. Taqman RT-qPCR assays showing the fold change in mRNA levels of the indicated genes following Cre-treatment of KRas$^{LSL-G12D/+}$ MEFs of the indicated DUSP5 genotype, relative to wild-type cells infected with empty adenovirus. MEFs were infected with adenoviral-Cre (Ad5-Cre) or empty adenovirus (Ad5-Empty) for 48 hours prior to cell lysis and RNA isolation. **A)** ERK-targeting MKPs. **B)** ERK-target genes. Mean values ± SEM are shown, n = 3. *P < 0.05, **P < 0.01, ****P<0.0001 using two-way ANOVA and Bonferroni post hoc test, comparing DUSP5 genotypes.

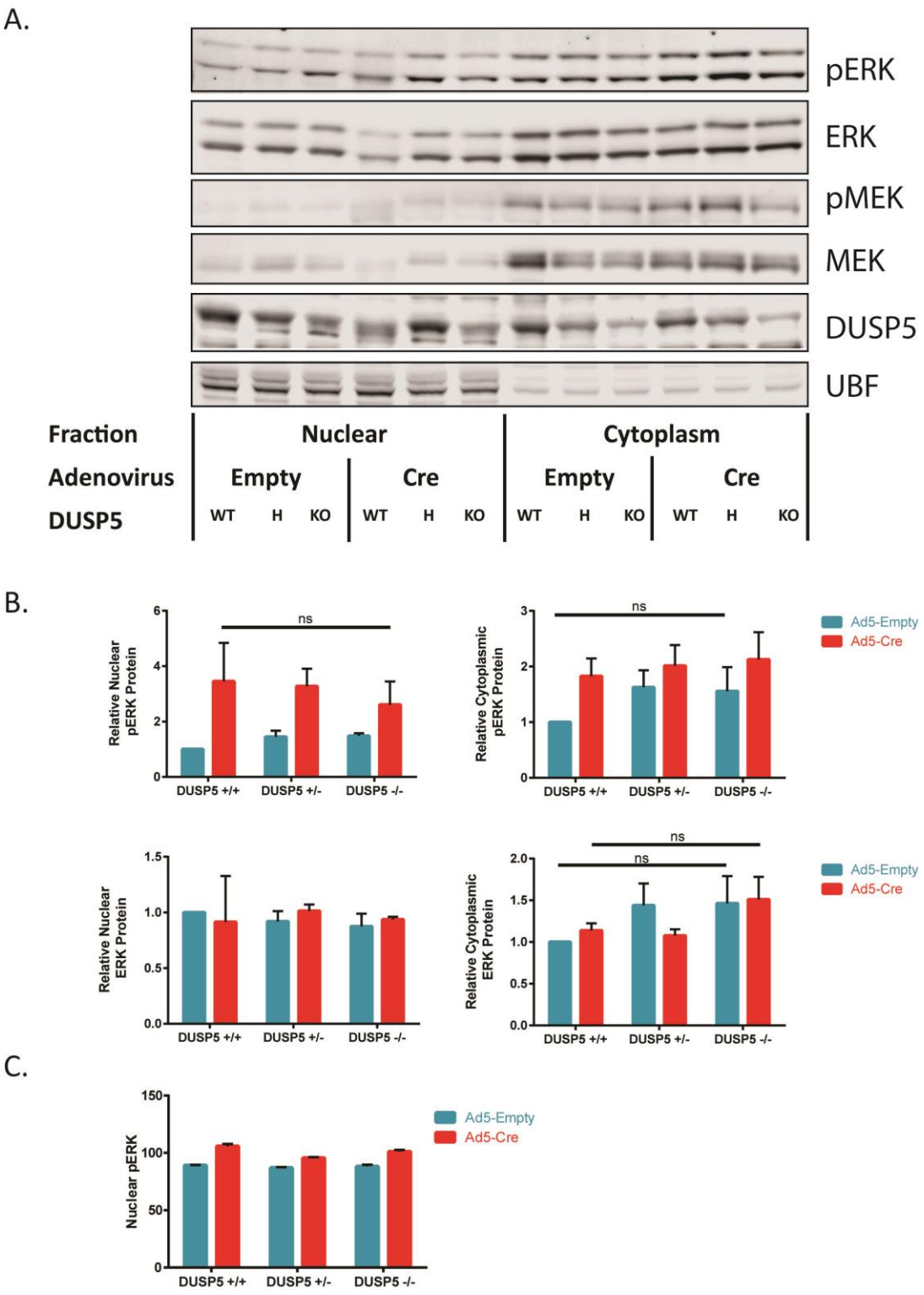

Figure 4.14 DUSP5 loss has no clear effect on ERK localisation or activation following KRas^{G12D} knock-in. A-B) KRas$^{LSL\text{-}G12D/+}$ MEFs which were either DUSP5$^{+/+}$, DUSP5$^{+/-}$ or DUSP5$^{-/-}$ were infected with adenoviral-Cre (Ad5-Cre) or empty adenovirus (Ad5-Empty) for 48 hours prior to cell lysis, subcellular fractionation and immunoblotting using the indicated antibodies. Upstream binding factor (UBF) and MEK were used to validate separation of nuclear (N) and cytoplasmic (C) proteins, respectively. A representative Western blot is shown **(A),** alongside protein quantification **(B).** Mean values ± SEM are shown, n = 3. ns = not significant. **C)** KRas$^{LSL\text{-}G12D/+}$ MEFs of the indicated DUSP5 genotype were infected with virus for 48 hours then stained for p-ERK or DAPI, before image analysis using high content fluorescence microscopy. Mean (± SEM) nuclear p-ERK intensity is shown derived from 5,000–10,000 individual cells per condition. Representative figure of an experiment performed in duplicate. Panel C courtesy of Dr Christopher Caunt.

4.2.4 DUSP6/MKP-3 loss causes no significant effects on $KRas^{G12D}$ signalling in MEFs

To continue our investigation into whether individual MKPs perform non-redundant functions in the regulation of ERK activity in response to $KRas^{G12D}$ expression, we generated MEFs containing the $KRas^{LSL\text{-}G12D/+}$ allele and a conditional DUSP6/MKP-3 allele. These cells enabled us to investigate whether DUSP6/MKP-3 plays any role in the regulation of $KRas^{G12D}$ induced ERK activity and to compare and contrast the effects of the loss of this cytoplasmic ERK-specific MKP, with that of the nuclear, ERK-specific MKP DUSP5. DUSP6/MKP-3 conditional mice were crossed with $KRas^{LSL\text{-}G12D/+}$ mice, and these mice were utilised to generate littermate MEFs which all contained the $KRas^{LSL\text{-}G12D/+}$ allele and were either $DUSP6^{+/+}$, $DUSP6^{+/fl}$ or $DUSP6^{fl/fl}$. $KRas^{G12D}$ expression and DUSP6/MKP-3 loss was induced in these cell lines through adenoviral-Cre treatment and changes in Ras effector signalling and MKP activation investigated. Following homozygous loss of DUSP6/MKP-3 $KRas^{G12D}$ expressing MEFs demonstrated no changes in either *p*-MEK or *p*-AKT levels, however whole cell *p*-ERK levels appeared slightly increased (Fig. 4.15). This indicates that DUSP6/MKP-3 might play a significant and non-redundant role in the negative feedback response constraining ERK activity induced by $KRas^{G12D}$ expression. The observed effect of DUSP6/MKP-3 loss on $KRas^{G12D}$-driven ERK activity could be enabled due to the lack of significant compensatory upregulation of other MKPs (Fig. 4.15 & 4.16A). However, despite the increase in whole cell *p*-ERK levels observed, the loss of DUSP6/MKP-3 in the presence of $KRas^{G12D}$ expression does not promote the upregulation of ERK target genes such as SerpinB2 and Egr1 (Fig. 4.16B).

Overall, these results demonstrate that although DUSP5 loss does not cause a detectable change in ERK activity or localisation in the presence of $KRas^{G12D}$ expression (Fig. 4.12 & 4.14), the loss of DUSP6/MKP-3 does cause an increase in levels of whole cell *p*-ERK (Fig. 4.15). In contrast, DUSP5 loss is sufficient to drive increased ERK-dependent expression of multiple target genes (Fig. 4.13B), including SerpinB2 and Egr1, whereas DUSP6/MKP-3 loss in not (Fig. 4.16B). Therefore, DUSP5 loss must be promoting some changes in nuclear ERK activity to be able to induce the observed changes in ERK-dependent gene expression. However, such changes in ERK activity are likely to be below the sensitivity threshold of our detection methods due to the relatively modest pathway stimulation resulting from $KRas^{G12D}$ expression, in contrast to the potent, acute stimulation following

TPA stimulation where changes in nuclear *p*-ERK levels could be detected (Fig. 3.3). The effects of DUSP6/MKP-3 loss are potentially restricted to solely cytoplasmic ERK activity, which could explain the lack of transcriptional effects. Furthermore, as the majority of ERK is localised to the cytoplasm the loss of a cytoplasmic MKP such as DUSP6/MKP-3 has the potential to cause greater alterations in whole-cell ERK activity, possibly explaining why a phenotype could be detected following the loss of DUSP6/MKP-3, but not DUSP5. Another potential cause for the lack of an observable change in *p*-ERK levels following $KRas^{G12D}$ expression and DUSP5 loss could be the induction of compensatory upregulation of other MKPs (Fig. 4.13A), whereas DUSP6/MKP-3 loss does not stimulate any such response (Fig. 4.16A). The compensatory upregulation of other MKPs did not occur following the TPA stimulation of $DUSP5^{-/-}$ MEFs (Fig. 3.2), these differing responses could reflect the difference between the prolonged pathway stimulation following $KRas^{G12D}$ expression and the acute stimulation in response to TPA.

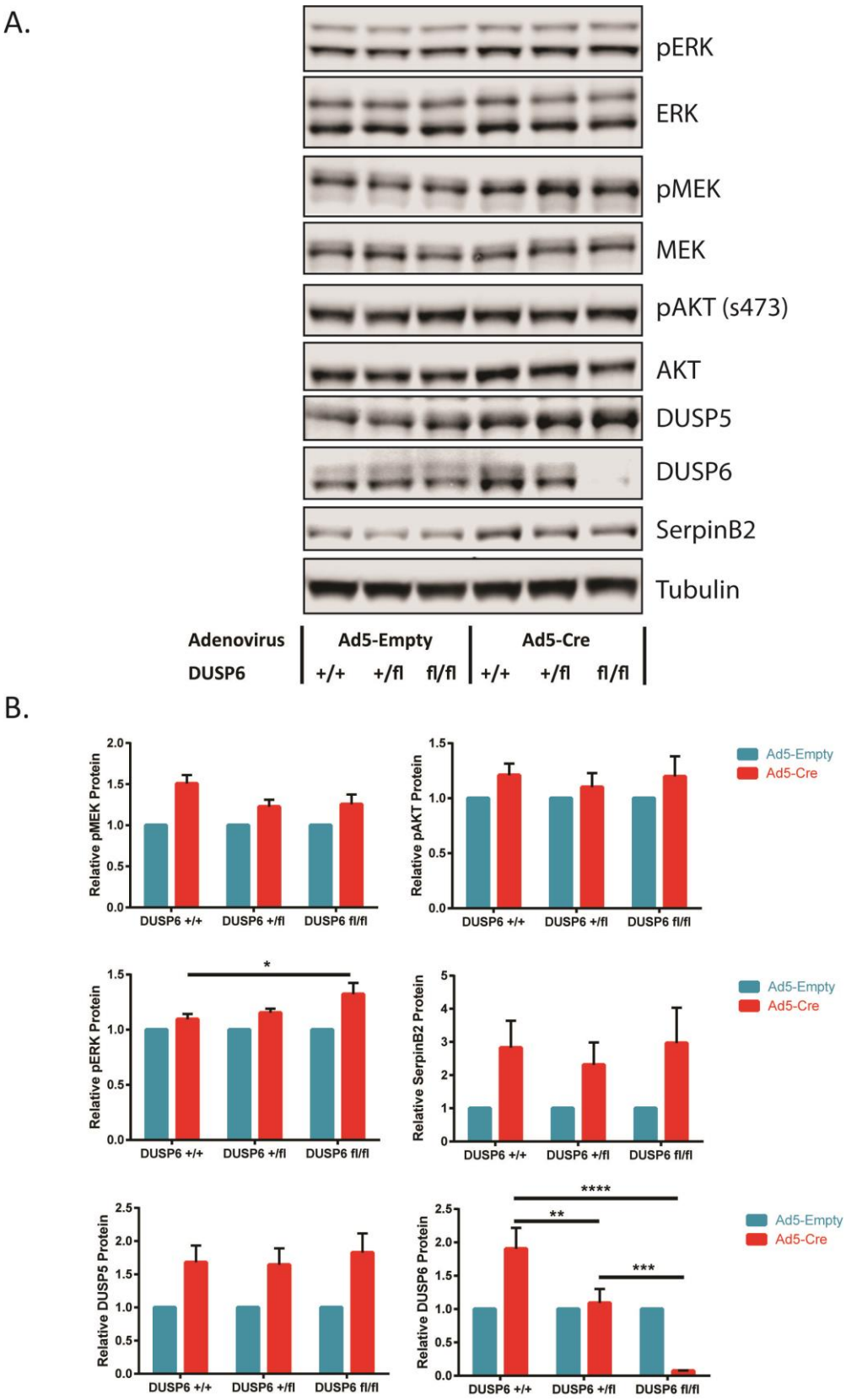

Figure 4.15 Ras effector pathway activation and MKP induction following KRas^{G12D} knock-in and DUSP6/MKP-3 knockout. KRas$^{LSL\text{-}G12D/+}$ MEFs which were either DUSP6$^{+/+}$, DUSP6$^{+/fl}$ or DUSP6$^{fl/fl}$ were infected with adenoviral-Cre (Ad5-Cre) or empty adenovirus (Ad5-Empty) for 48 hours prior to cell lysis, and immunoblotting using the indicated antibodies. A representative Western blot is shown **(A)**, alongside protein quantification **(B)**. Mean values ± SEM are shown, n = 3. *P < 0.05, **P < 0.01, ***P<0.001, ****P<0.0001 using two-way ANOVA and Bonferroni post hoc test, comparing DUSP6/MKP-3 genotypes.

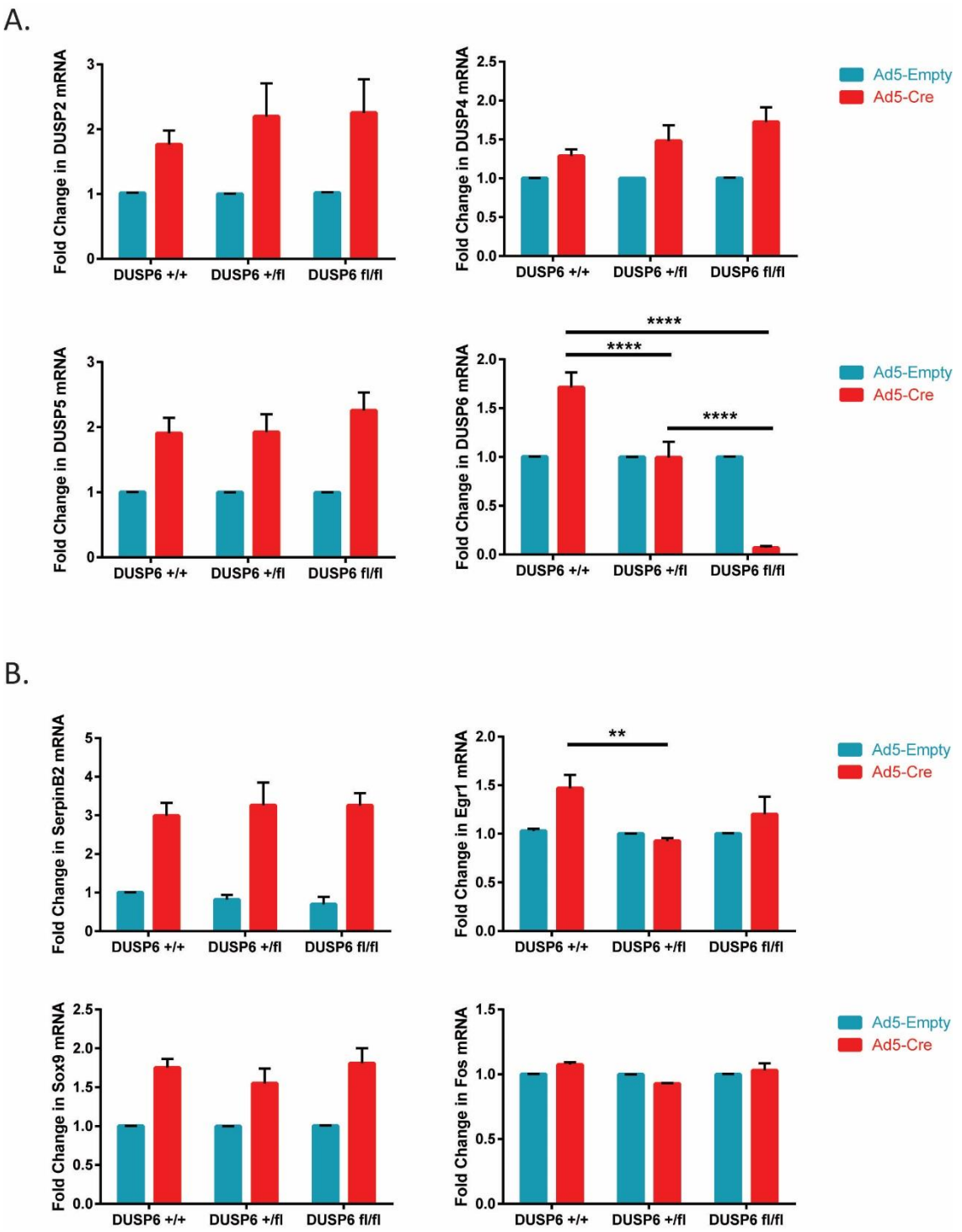

Figure 4.16 DUSP6/MKP-3 loss does not alter ERK-dependent gene expression following KRas^{G12D} knock-in. Taqman RT-qPCR assays showing the fold change in mRNA levels of the indicated genes following Cre-treatment of KRas$^{LSL-G12D/+}$ MEFs of the indicated DUSP6/MKP-3 genotype, relative to wild-type cells infected with empty adenovirus. MEFs were infected with adenoviral-Cre (Ad5-Cre) or empty adenovirus (Ad5-Empty) for 48 hours prior to cell lysis and RNA isolation. **A)** ERK-targeting MKPs. **B)** ERK-target genes. Mean values ± SEM are shown, n = 3. **P < 0.01, ****P<0.0001 using two-way ANOVA and Bonferroni post hoc test, comparing DUSP5 genotypes.

4.2.5 DUSP5 or DUSP6/MKP-3 ablation have no effect on KRas^{G12D} mediated proliferation and colony formation in MEFs

Despite the observation that loss of either DUSP5 or DUSP6/MKP-3 in KRas^{G12D} expressing MEFs appear to have limited biochemical consequences, we wanted to explore the possibility that the loss of either MKP is able to induce any changes in the cellular phenotypes of these MEFs. We hypothesised changes might be observed upon MKP loss because the expression of mutant KRas in MEFs or human cancer cells does not stimulate increased activation of Ras effector pathways, yet is able to drive increased proliferation, gene expression and partial transformation (Fig. 4.9-11) (Tuveson et al., 2004; Vartanian et al., 2013). This situation is analogous to the loss of DUSP5 or DUSP6/MKP-3 in the presence of KRas^{G12D} expression, as the loss of DUSP5 promotes no changes in ERK activity, but increases in ERK-dependent gene expression, whereas DUSP6/MKP-3 loss promotes a marginal increase in ERK activity, but no changes in ERK-dependent gene expression.

Initially, we investigated the proliferation rate of KRas^{G12D} expressing MEFs in the presence or absence of either DUSP5 or DUSP6/MKP-3. KRas$^{LSL\text{-}G12D/+}$ MEFs, which were either DUSP5$^{+/+}$, DUSP5$^{+/-}$ or DUSP5$^{-/-}$ were infected with adenoviral-Cre or empty adenovirus and allowed to proliferate until confluent. Adenoviral-Cre treated KRas$^{LSL\text{-}G12D/+}$; DUSP5$^{-/-}$ MEFs displayed the greatest increase in cell number throughout the assay, indicating that DUSP5 loss could promote an increased proliferation rate in KRas^{G12D} expressing MEFs, (Fig. 4.17A). However, on more careful examination this appears to be a potential consequence of the parental, non-KRas^{G12D} expressing cells, as the empty adenoviral treated KRas$^{LSL\text{-}G12D/+}$; DUSP5$^{-/-}$ MEFs also display increased proliferation over their DUSP5$^{+/+}$ and DUSP5$^{+/-}$ counterparts (Fig. 4.17A). In support of this theory, normalising the Cre-treated MEFs of each genotype to their empty-treated controls did not reveal a significant increase in proliferation of KRas^{G12D} expressing MEFs following DUSP5 loss, although there was a slight trend towards increased proliferation following the loss of one or two alleles of DUSP5 (Fig. 4.17B-C). To further validate this conclusion DUSP5$^{+/+}$, DUSP5$^{+/-}$ or DUSP5$^{-/-}$ with or without the KRas$^{LSL\text{-}G12D}$ allele were infected with empty or Cre-containing adenovirus and pulse-labelled with Edu after 48 hours, to determine the percentage of cells which have entered S-phase. Again, no increase in proliferation was observed in KRas^{G12D} expressing MEFs following DUSP5 loss (Fig. 4.17D).

Furthermore, in this assay DUSP5$^{-/-}$ MEFs in the absence of KRas^{G12D} did not display increased proliferation over their wild-type counterparts.

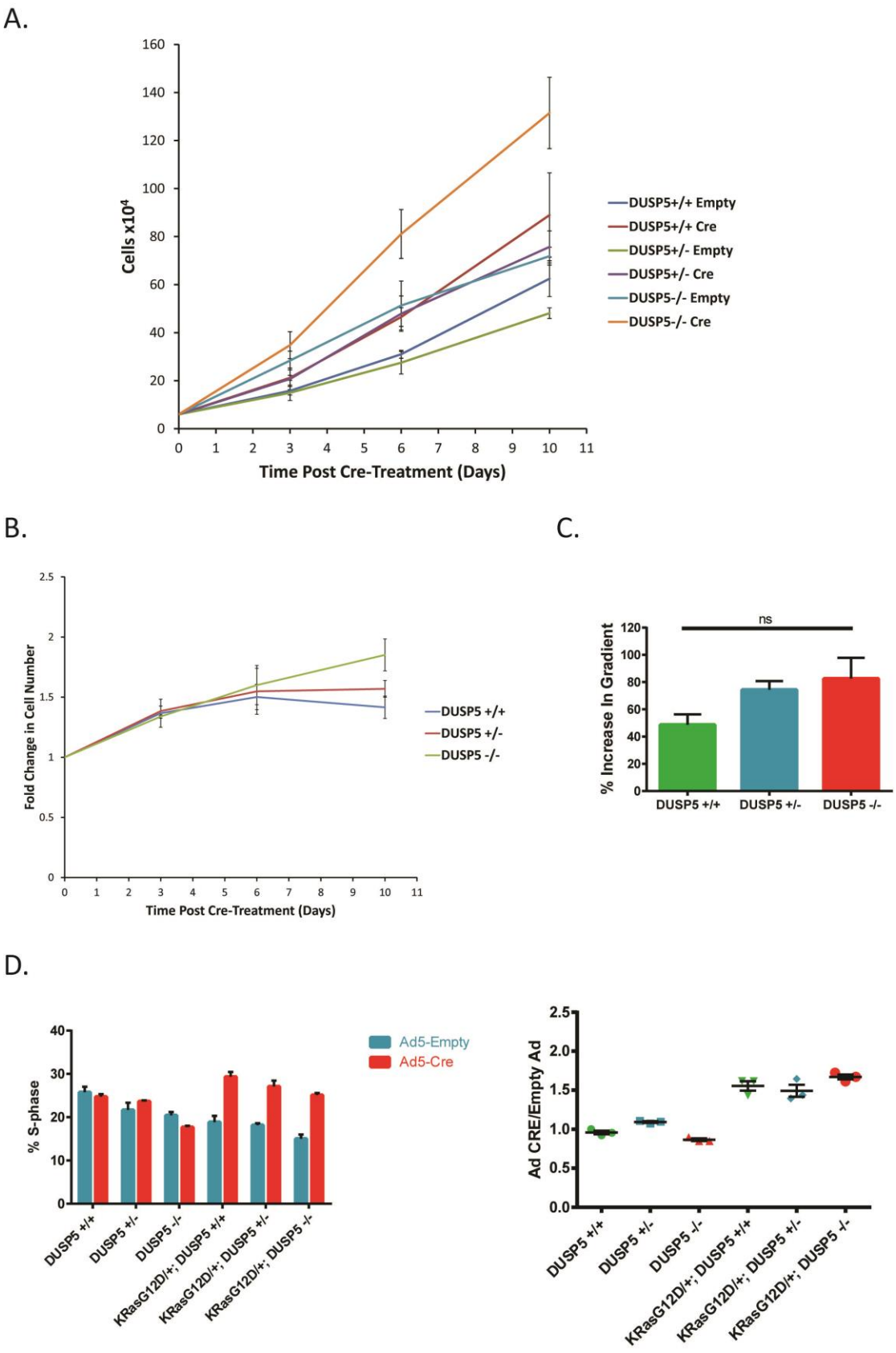

Figure 4.17 DUSP5 loss has no significant effect on proliferation in KRas^{G12D} knock-in MEFs. KRas$^{LSL\text{-}G12D/+}$ MEFs of each DUSP5 genotype (DUSP5$^{+/+}$, DUSP5$^{+/-}$ or DUSP5$^{-/-}$) were seeded at low density, infected with adenoviral-Cre (Cre) or empty adenovirus (Empty) and left to proliferate until confluent. **A)** Cell counts of each cell line and treatment. **B)** Fold change in cell number for each genotype post-cre treatment (Cre/empty cell count for each measurement). **C)** Percentage increase in gradient for each genotype post-cre treatment (Linear regression performed for every

MEF line in each condition, to calculate the gradient. Then % increase in gradient of the cre-treated lines over the empty-treated lines calculated for each genotype). **A-C)** Mean values ± SEM are shown, n = 3. ns = not significant, using one-way ANOVA and Bonferroni post hoc test. **D)** KRas wild-type and KRas $^{LSL-G12D/+}$ MEFs of the indicated DUSP5 genotype were infected with adenoviral-Cre (Cre) or empty adenovirus (Empty) and left to proliferate for 48 hours, prior to a 2 hour fluorescent EdU pulse label, immunostaining and high content microscopy. Plots show the mean (± SEM) percentage of EdU positive cells (% S-phase) derived from 5,000–10,000 individual cells per condition in technical triplicate (Left panel) and the relative increase in proliferation (Right panel). Representative figure of an experiment performed in duplicate. Panel D courtesy of Dr Christopher Caunt.

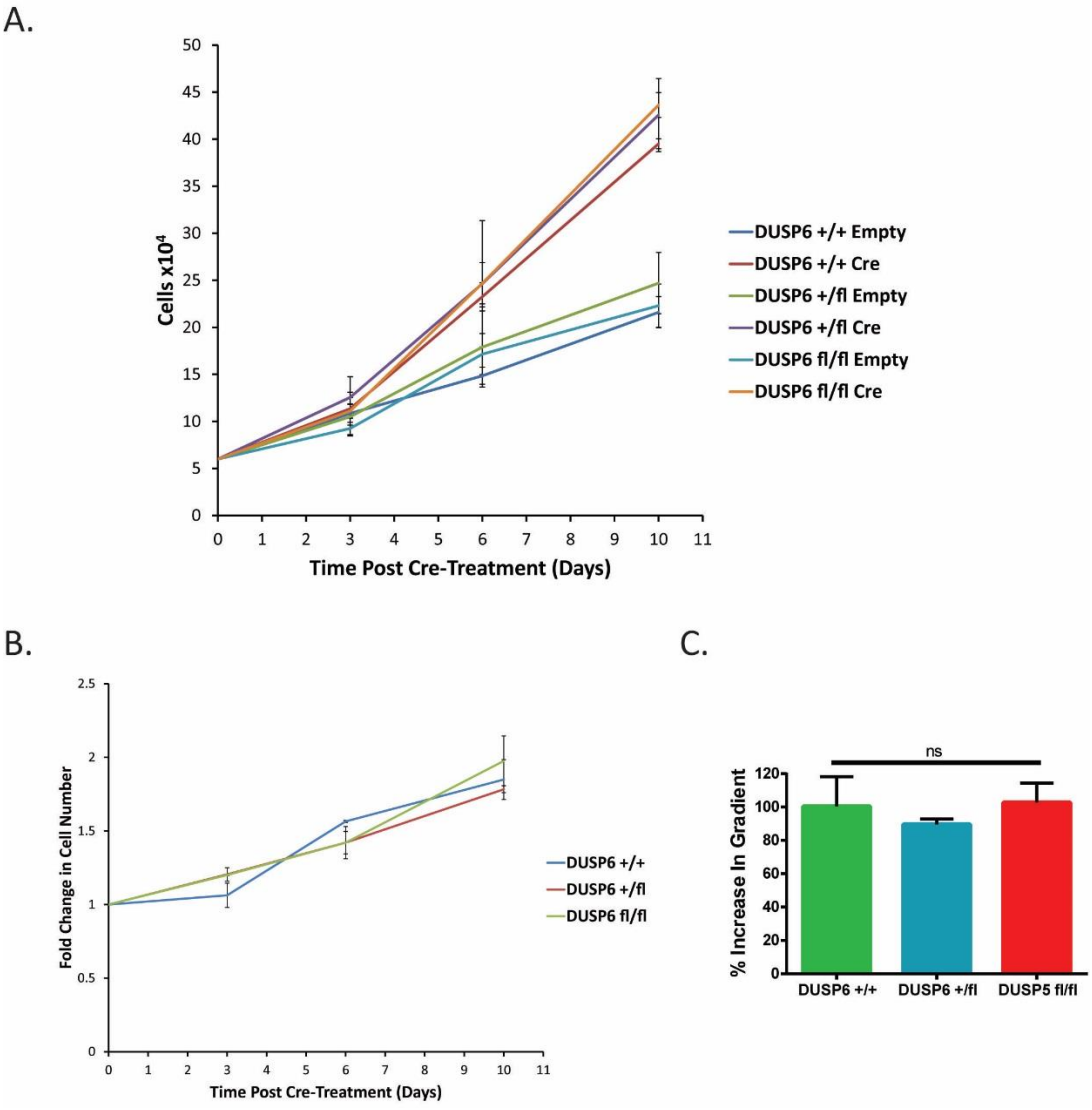

Figure 4.18 DUSP6/MKP-3 loss has no effect on proliferation in KRas^{G12D} knock-in MEFs. KRas$^{LSL-G12D/+}$ MEFs of each DUSP6/MKP-3 genotype (DUSP6$^{+/+}$, DUSP6$^{+/fl}$ or DUSP6$^{fl/fl}$) were seeded at low density, infected with adenoviral-Cre (Cre) or empty adenovirus (Empty) and left to proliferate until confluent. **A)** Cell counts of each cell line and treatment. **B)** Fold change in cell number for each genotype post-cre treatment (Cre/empty cell count for each measurement). **C)** Percentage increase in gradient for each genotype post-cre treatment (Linear regression performed for every MEF line in each condition, to calculate the gradient. Then % increase in gradient of the cre-treated lines over the empty-treated lines calculated for each genotype). Mean values ± SEM are shown, n = 3. ns = not significant, using one-way ANOVA and Bonferroni post hoc test.

Similarly to DUSP5, DUSP6/MKP-3 loss does not significantly alter the proliferation rate of $KRas^{G12D}$ expressing MEFs (Fig. 4.19A-C). $KRas^{G12D}$ expressing MEFs regardless of their DUSP6/MKP-3 genotype display almost an identical increase in their proliferation rate when compared to their empty adenovirus treated parental cell lines (Fig. 4.19B-C). However in contrast to DUSP5 (Fig. 4.17A), the DUSP6/MKP-3 parental cell lines display much more consistent proliferation rates (Fig. 4.18A). This could be due to the DUSP6/MKP-3 cell lines containing a conditional DUSP6/MKP-3 allele, so prior to Cre-treatment DUSP6/MKP-3 is present in all cell lines, making them genetically identical for our genes of interest. Whereas, the DUSP5 cell lines do not contain conditional alleles so even the cells not exposed to Cre-treatment are genetically different with regard to DUSP5. Despite this, we would not expect to see altered proliferation rates of the DUSP5 knockout cells relative to wild-type, as our previous experiments have detected a difference in their proliferation rates in short-term assays (Fig. 3.2B) (Rushworth et al., 2014).

To confirm this is the case in longer-term proliferation assays, we obtained mice expressing a conditional DUSP5 allele and isolated $DUSP5^{fl/fl}$ MEFs. $DUSP5^{fl/fl}$ MEFs expressed full length DUSP5 protein, which could be abrogated by Cre-treatment (Fig. 4.19A). Proliferation assays were subsequently performed comparing the effects of Cre-mediated DUSP5 ablation with DUSP6/MKP-3 ablation. Neither loss of DUSP5 nor DUSP6/MKP-3 promoted increased proliferation in MEFs (Fig. 4.19B-C). In contrast, there was a slight initial decrease in cell number in the Cre-treated, DUSP5 or DUSP6/MKP-3 knockout cells (Fig. 4.19B-C). This is likely to be due to the genotoxic effect of Cre-treatment (Loonstra et al., 2001), as the cell lines did not continue to proliferate more slowly over time as would be expected if the loss of either MKP was having a detrimental effect on proliferation. Instead following the initial drop in cell number the proliferation rate of the Cre-treated lines approximately mirrored the proliferation rate of their empty adenovirus treated counterparts (Fig. 4.19B). Furthermore, the DUSP5 knockout cells actually proliferated marginally faster towards the end of the assay and “made-up” the initial loss in cell number which was probably caused by Cre-mediated genotoxic stress (Fig. 4.19C). Together this indicates that potentially DUSP5 ablation might promote a very minor increase in proliferation, though this is within the experimental error of this approach.

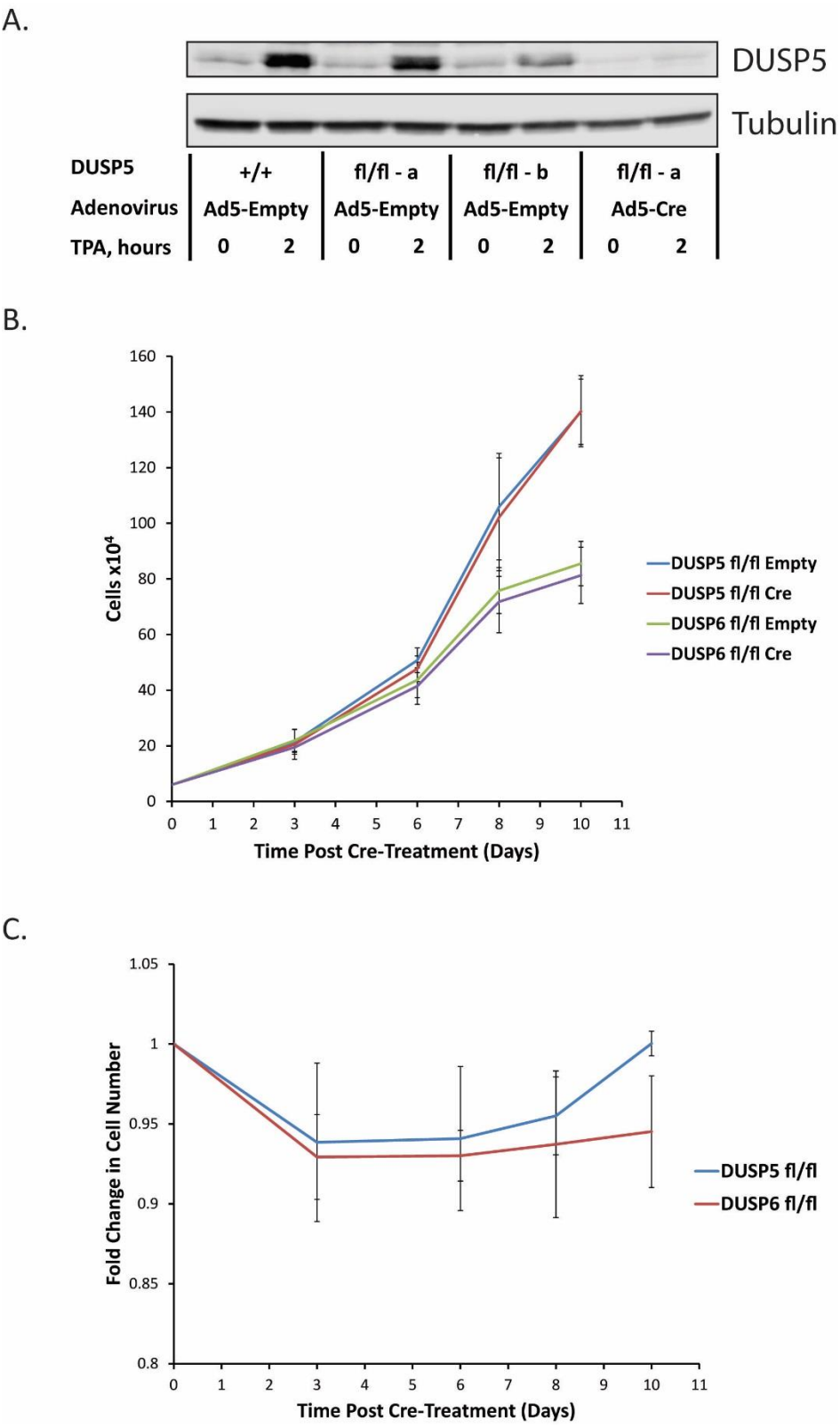

Figure 4.19 Conditional knockout of DUSP5 or DUSP6/MKP-3 has no effect on proliferation in MEFs. A) DUSP5$^{+/+}$ or DUSP5$^{fl/fl}$ MEFs (from two distinct embryos) infected with adenoviral-Cre (Ad5-Cre) or empty adenovirus (Ad5-Empty) for 48 hours prior to TPA stimulation, cell lysis, and immunoblotting using the indicated antibodies. **B-C)** DUSP5$^{fl/fl}$ and DUSP6$^{fl/fl}$ MEFs were seeded at low density, infected with adenoviral-Cre (Cre) or empty adenovirus (Empty) and left to proliferate until confluent. **B)** Cell counts of each cell line and treatment. **C)** Fold change in cell number for each genotype post-cre treatment (Cre/empty cell count for each measurement). Mean values ± SEM are shown, n = 3.

$KRas^{G12D}$ expression in MEFs is also sufficient to induce partial transformation, enabling colony formation via the loss of contact inhibition, but not the ability for colonies to form from single cells (Fig. 4.11) (Tuveson et al., 2004). Therefore, we investigated whether DUSP5 or DUSP6/MKP-3 loss was able to modulate these phenotypes in colony formation assays. Colony formation through the loss of contact inhibition occurred at a similar frequency in all $KRas^{G12D}$ expressing MEFs regardless of the DUSP5 or DUSP6/MKP-3 genotype (Fig. 4.20A & 4.21A), indicating that the loss of DUSP5 or DUSP6/MKP-3 is not enabling an increased initiation of colony formation. Furthermore, $KRas^{G12D}$ expressing MEFs are refractory to clonogenic growth when seeded at a low cell density (Tuveson et al., 2004), and the additional ablation of neither DUSP5 nor DUSP6/MKP-3 was sufficient to enable this process (Fig. 4.20B & 4.21B). Taken together these results demonstrate that loss of DUSP5 or DUSP6/MKP-3 does not alter the proliferation rate or colony forming ability of $KRas^{G12D}$ expressing MEFs, despite being able to regulate ERK-dependent transcription and p-ERK levels respectively.

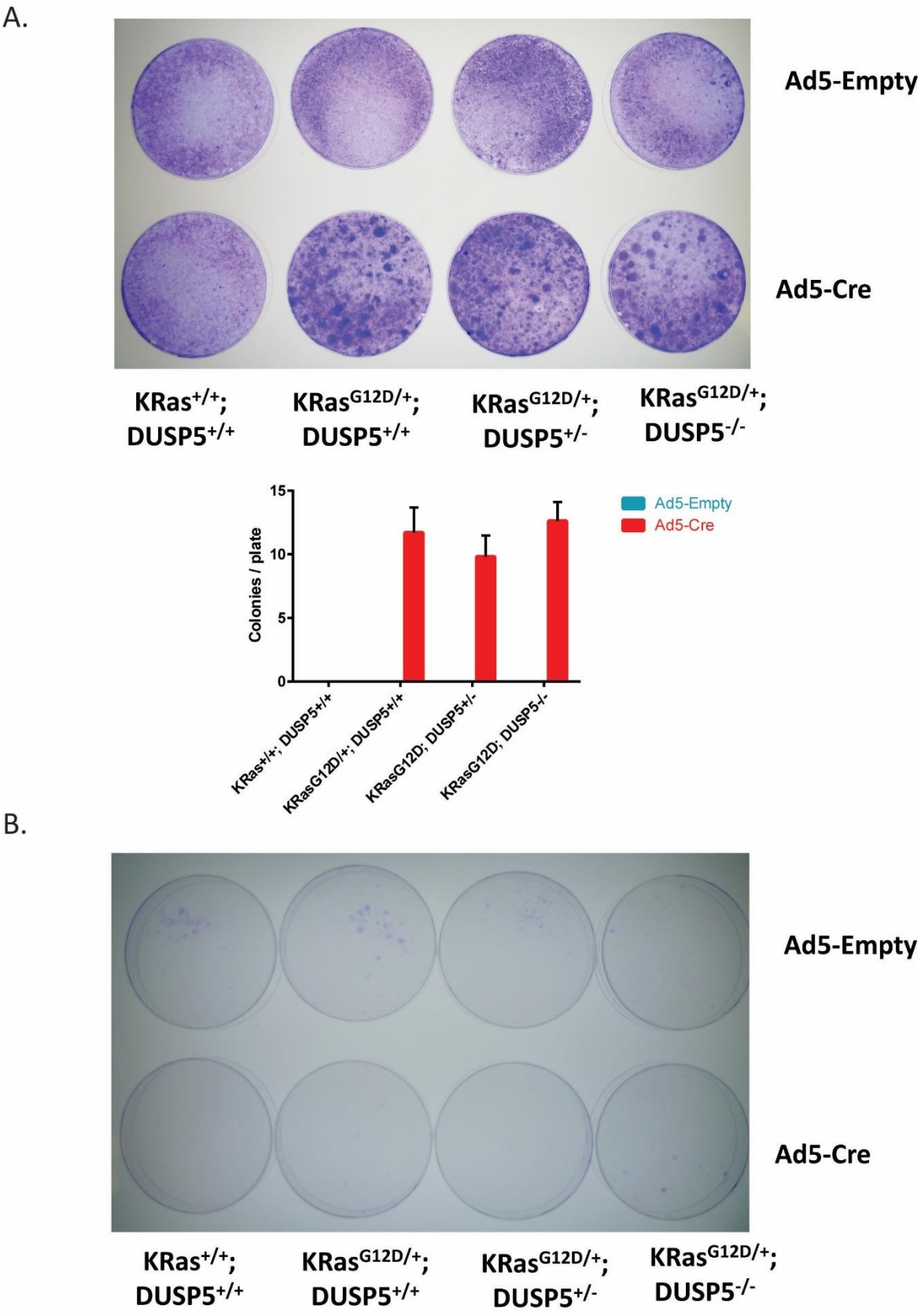

Figure 4.20 DUSP5 loss has no effect on colony formation KRas^{G12D} knock-in MEFs. MEFs of the indicated genotypes were infected with adenoviral-Cre (Ad5-Cre) or empty adenovirus (Ad5-Empty) prior to seeding at high **(A)** or low **(B)** density. MEFs were grown for 2-3 weeks until foci were visible, before fixation and visualisation with crystal violet. A) Representative image shown (Upper panel) and quantification of foci ≥2mm, mean ± SEM, n = 3 (Lower). **B)** No colonies formed from cells seeded at very low density. Representative images shown of experiment performed in triplicate.

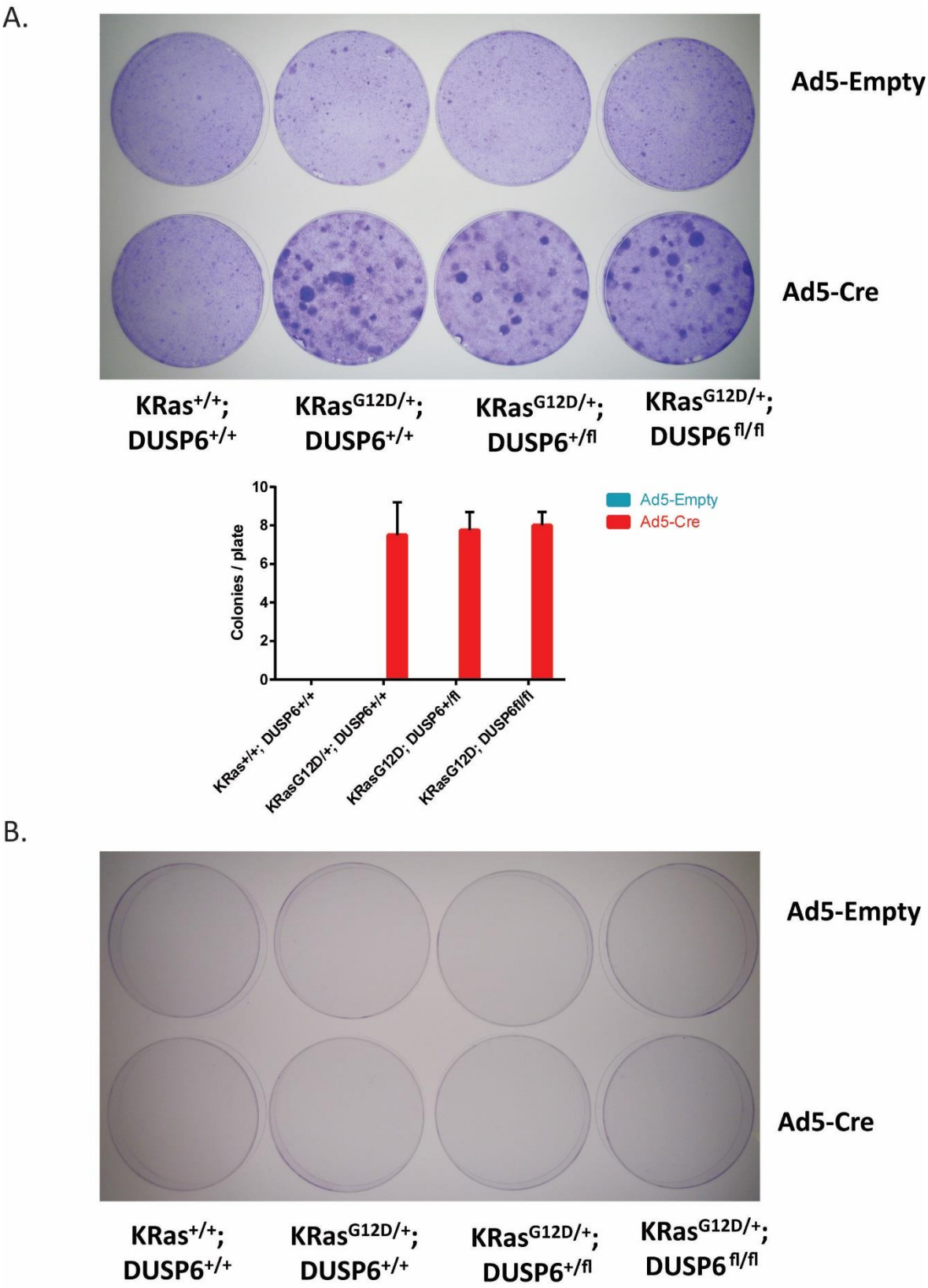

Figure 4.21 DUSP6/MKP-3 loss has no effect on colony formation KRas^{G12D} knock-in MEFs. MEFs of the indicated genotypes were infected with adenoviral-Cre (Ad5-Cre) or empty adenovirus (Ad5-Empty) prior to seeding at high **(A)** or low **(B)** density. MEFs were grown for 2-3 weeks until foci were visible, before fixation and visualisation with crystal violet. A) Representative image shown (Upper panel) and quantification of foci ≥2mm, mean ± SEM, n = 3 (Lower). **B)** No colonies formed from cells seeded at very low density. Representative images shown of experiment performed in triplicate.

4.3 Discussion

The MKPs DUSP5 and DUSP6/MKP-3 are negative feedback regulators of ERK-activity (Kucharska et al., 2009; Smith et al., 2006). Here we demonstrate that both DUSP5 and DUSP6/MKP-3 are upregulated by $KRas^{G12D}$ expression in a dose-dependent manner in MEFs (Fig. 4.8-9), and that this upregulation is dependent on ERK activity (Fig. 4.5-6). The upregulation of DUSP5 and DUSP6/MKP-3 is likely to play a role in constraining ERK activity following $KRas^{G12D}$ expression, as despite the constitutive activation of mutant KRas, *p*-ERK levels are not increased (Fig. 4.8). $KRas^{G12D}$ expression does however induce increased ERK-dependent gene expression (Fig. 4.6 & 4.9), proliferation (Fig. 4.10) and the partial transformation of MEFs (Fig. 4.11A).

DUSP5 ablation does not induce any detectable change in ERK activity or localisation in response to $KRas^{G12D}$ expression in MEFs (Fig. 4.12 & 4.14), making it initially appear that DUSP5 is functionally redundant in the regulation of $KRas^{G12D}$-induced ERK activity. However, DUSP5 loss is able to promote the transcriptional upregulation of multiple ERK-target genes including SerpinB2 and Egr1 (Fig. 4.13B), indicating that DUSP5 loss is likely to be altering nuclear ERK activity to a degree, which is below the sensitivity of our detection methods. In contrast, DUSP6/MKP-3 loss promotes a marginal increase in total *p*-ERK levels (Fig. 4.15), but no increase in ERK-dependent gene expression (Fig. 4.16B) in response to $KRas^{G12D}$ expression. Furthermore, neither the loss of DUSP5 nor DUSP6/MKP-3 is able to modulate $KRas^{G12D}$-driven proliferation or colony formation in MEFs (Fig. 4.17-4.21).

The inability of endogenous expression of mutant Ras to induce elevated levels of *p*-ERK has been reported in multiple studies (Guerra et al., 2003; Haigis et al., 2008; Tuveson et al., 2004; Vartanian et al., 2013), and is replicated by our data (Fig. 4.8). Despite this lack of observable increases in the activation of Ras effector pathways, expression of mutant KRas is able to drive increased proliferation, gene expression and partial transformation, indicating signalling flux through the pathways must be increased (Fig. 4.9-11) (Tuveson et al., 2004; Vartanian et al., 2013). Negative feedback signalling to upstream RTKs has been proposed as one mechanism by which effector pathway activation is constrained following mutant Ras expression (Vartanian et al., 2013). In addition to this, MKP overexpression is observed in many mutant Ras or BRaf-driven human cancers (Kidger

and Keyse, 2016a, 2016b), although in some cases MKP levels are overexpressed in low grade tumours before being lost in high grade, malignant tumours (Furukawa et al., 2003, 2005; Loda et al., 1996; Okudela et al., 2009; Saigusa et al., 2013). This expression pattern supports the hypothesis that MKP expression is induced following oncogenic activation of the Ras-ERK pathway, where is it able to constrain ERK activity and thereby possibly restrict tumour growth. The subsequent loss of MKP expression in certain high-grade tumours could then contribute to their growth and malignancy. In this study we have demonstrated robust upregulation of the MKPs DUSP2, DUSP4/MKP-2, DUSP5 and DUSP6/MKP-3 in a dose-dependent manner following $KRas^{G12D}$ expression in MEFs (Fig. 4.9). This presents strong evidence that MKPs do comprise at least part of the negative feedback system responsible for constraining ERK activity in response to oncogenic activation of the Ras-ERK pathway. This is supported by evidence from multiple microarray studies which have detected increased expression of multiple MKPs in mutant Ras or BRaf-driven cancer cells (Montero-Conde et al., 2013; Pratilas et al., 2009; Vartanian et al., 2013; Yun et al., 2009). Furthermore, DUSP6/MKP-3 has been shown to be upregulated in $KRas^{G13D}$-driven CRC cell lines, compared to isogenic cells in which the mutant allele has been deleted by homologous recombination (Haigis et al., 2008).

Despite the strong upregulation of DUSP5 or DUSP6/MKP-3 following $KRas^{G12D}$ expression we found that ablation of either DUSP5 or DUSP6/MKP-3 alone had limited detectable biochemical effects on ERK signalling in the presence of $KRas^{G12D}$ expression (Fig. 4.12, 4.14 & 4.16). We were unable to detect changes in ERK activity or localisation following DUSP5 loss in the presence of $KRas^{G12D}$ expression using either western blotting of whole cell lysates or high-content microscopy (Fig. 4.12 & 4.14). The latter result was unanticipated as we have previously demonstrated that DUSP5 loss promotes increased nuclear *p*-ERK levels, without significantly altering whole cell p-ERK, in response to TPA stimulation or the ectopic expression of mutant HRas (Fig. 3.3 & 3.10) (Rushworth et al., 2014). Therefore, it would be assumed that DUSP5 loss would promote a similar phenotype following endogenous $KRas^{G12D}$-driven ERK activation, yet this did not seem to be the case. However, in contrast to the lack of detectable changes in either ERK localisation or activity, we did detect transcriptional upregulation of multiple ERK-target genes including SerpinB2 and Egr1 following DUSP5 loss in these cells (Fig. 4.13B). This

replicates the findings in TPA stimulated DUSP5 knockout MEFs, where SerpinB2 and Egr1 were amongst a cohort of 20 genes upregulated following DUSP5 loss (Fig. 3.4).

One possible hypothesis to explain this apparent contradiction is that while acute stimulation promotes robust Ras-ERK pathway activation amplifying the effects of DUSP5 loss on ERK activity and localisation, the constitutive (and lower level) expression of the endogenous oncogene promotes a more prolonged but conservative level of pathway stimulation. In this scenario DUSP5 loss would have more modest effects on ERK activity following endogenous $KRas^{G12D}$ expression, making any changes much harder to detect in our assays. Although some degree of altered ERK activity must be present to be driving the changes in ERK-dependent gene expression observed (Fig. 4.13B). Furthermore, the constitutive pathway activation following $KRas^{G12D}$ expression would give more time to enable the compensatory upregulation of other MKPs (Fig. 4.13A), which could also be minimising detectable changes in ERK activity. Alternatively, it is possible that when present DUSP5 could be preferentially binding and inactivating nuclear *p*-ERK bound to specific transcription factor complexes, therefore it could be selectively regulating the transcription of certain genes. In such a scenario DUSP5 loss could induce increased expression of particular genes without having a significant effect on the total level of nuclear *p*-ERK. The localisation of MAPKs to the promoters of genes undergoing transcriptional activation has been described in multiple studies in both yeast and mammalian cells, as discussed in chapter 3 (Nadal et al., 2011). Therefore, it is possible that MKPs, such as DUSP5, are also able to localise to such sites to regulate the transcription of precise sets of genes.

Conversely, DUSP6/MKP-3 loss in $KRas^{G12D}$ expressing MEFs promotes a marginal increase in whole cell ERK activity, yet is unable to induce any changes in ERK-dependent gene expression (Fig. 4.15 & 4.16B). This inability to alter ERK-dependent gene expression implies that DUSP6/MKP-3 could be solely elevating cytoplasmic *p*-ERK levels, which is in line with its function as a cytoplasmic MKP (Groom et al., 1996; Mourey et al., 1996). Further studies utilising the high content microscopy based approach are required to validate whether DUSP6/MKP-3 loss is able to solely induce changes in cytoplasmic *p*-ERK levels, and to quantify the effects of DUSP6/MKP-3 loss. This result is perhaps surprising given the propensity of cytoplasmic *p*-ERK to be shuttled to the nucleus following its

phosphorylation in the cytoplasm (Lidke et al., 2010). However, we were unable to detect changes in whole cell or cytoplasmic *p*-ERK levels following the stimulation of DUSP6$^{+/+}$ and DUSP6$^{-/-}$ MEFs with either TPA or serum (Jim Caunt, unpublished data). The unexpected divergence of these two models could be due to the use of conditional DUSP6/MKP-3 alleles in combination with KRas^{G12D} expression. Consequently, when utilising the conditional DUSP6/MKP-3 allele the assay was performed in close proximity to the DUSP6/MKP-3 loss, potentially meaning that signalling pathway remodelling following DUSP6/MKP-3 loss was not complete and other negative regulators of ERK were yet to compensate for DUSP6/MKP-3 loss. This theory is supported by observations of lower compensatory upregulation of other MKPs in KRas^{G12D} expressing DUSP6$^{-/-}$ MEFs relative to DUSP5$^{-/-}$ counterparts (Fig. 4.13A & 4.16A). Alternatively, it is possible that DUSP6/MKP-3 loss is unable to induce compensatory upregulation of other MKPs in the presence of KRas^{G12D} expression, which could be the reason why whole cell *p*-ERK levels are increased, yet this would not explain the divergence between the different experimental systems. Increased cytoplasmic *p*-ERK would be expected to alter the regulation of a wide-range of ERK targets within the cytoplasm which control many cellular processes (Yoon and Seger, 2006). Future work could utilise phospho-proteomic approaches to determine which ERK-target proteins show significantly increased phosphorylation upon DUSP6/MKP-3 loss.

Expression of one allele of KRas^{G12D} in MEFs has been shown to induce increased proliferation and partial transformation enabling colony formation via the loss of contact inhibition, but clonogenic growth (Tuveson et al., 2004). Here we have been able to replicate these findings, as well as demonstrate that expression of two KRas^{G12D} alleles promotes further increases in proliferation relative to one allele, but no changes in the colony forming ability (Fig. 4.10-11). This phenotype is in agreement with the current literature as the wild-type Ras allele, when carrying a heterozygous mutation, has been proposed to play a tumour suppressive role in cancer development (Singh et al., 2005). Indeed, wild-type Ras alleles are frequently lost in Ras-driven cancers (Singh et al., 2005), and the ablation of the wild-type Ras allele in combination with mutant Ras promotes increased proliferation *in vitro* (Bentley et al., 2013) and tumourigenesis in certain *in vivo* cancer models (Kong et al., 2016). Consequently, it is not surprising that the replacement

of a wild-type KRas allele with an additional $KRas^{G12D}$ allele promotes increased proliferation in MEFs.

This study also demonstrated that neither DUSP5 nor DUSP6/MKP-3 loss had any effect on $KRas^{G12D}$-driven proliferation and colony formation (Fig. 4.17-4.21). DUSP5 loss in the presence of $KRas^{G12D}$ did appear to demonstrate a slight trend towards increased proliferation rate (Fig. 4.17). However, this was complicated by differing initial proliferation rates of DUSP5 MEF lines prior to Cre-mediated $KRas^{G12D}$ knock-in, therefore these experiments could be repeated utilising MEFs isolated containing the conditional DUSP5 allele which we recently obtained (Fig. 4.19). DUSP6/MKP-3 ablation promoted no change in the proliferation rate of $KRas^{G12D}$ expressing MEFs (Fig. 4.18). This is in contrast to previous reports which have demonstrated increased proliferation following siRNA mediated knockdown of DUSP6/MKP-3 in CRC (Haigis et al., 2008) or NSCLC cell lines (Zhang et al., 2010). The differences between these studies and ours could be due to the different cell context, or the increased mutational burden in human cancer cell lines, compared to our primary MEFs in which solely $KRas^{G12D}$ expression is induced. This could results in a more essential role for DUSP6/MKP-3 in restraining ERK-mediated proliferation in these cancer cell lines.

Neither DUSP5 nor DUSP6/MKP-3 loss induced any changes in $KRas^{G12D}$-driven colony formation or enabled clonogenic growth (Fig. 4.20-21). This is not particularly surprising given that an additional $KRas^{G12D}$ allele was not sufficient to permit clonogenic growth in MEFs (Fig. 4.11). Furthermore, previous studies have shown that either loss of tumour suppressors such as p53, or gain of the oncoprotein E1a are required to enable clonogenic or anchorage-independent growth in $KRas^{G12D}$ expressing MEFs (Tuveson et al., 2004). This indicates that deregulation of additional signalling pathways is likely to be required to permit clonogenic growth of $KRas^{G12D}$ expressing MEFs, making it unlikely that solely further increases in Ras effector pathways such as the ERK pathway will promote this phenotype. Following our work investigating DUSP5 and DUSP6/MKP-3 loss in mouse models of $KRas^{G12D}$-driven pancreatic cancer (Chapter 5), it would be interesting to extend our cellular phenotypic assays in these $KRas^{G12D}$-driven MEFs to investigate potential roles of DUSP5 and DUSP6/MKP-3 loss on their capacity to migrate and invade.

In conclusion, this part of my project has strongly suggested that the MKPs DUSP5 and DUSP6/MKP-3 are components of the negative feedback response to oncogenic $KRas^{G12D}$ activation, which is responsible for maintaining homeostatic levels of *p*-ERK despite constitutive pathway activation. However, loss of DUSP5 or DUSP6/MKP-3 does not modulate $KRas^{G12D}$-driven proliferation or colony formation, despite inducing the transcriptional upregulation of particular ERK target genes or marginal increases in whole cell *p*-ERK levels respectively.

Chapter 5 DUSP5 and DUSP6/MKP-3 suppress the development of KRas^{G12D}-driven pancreatic cancer

5.1 Introduction

In chapter 3 we demonstrated that DUSP5 acts as a tumour suppressor in mutant HRas-driven murine skin carcinogenesis by showing that mice lacking DUSP5 were sensitised to papilloma development following treatment with DMBA/TPA (Fig. 3.1). Mechanistically, this was driven by DUSP5 loss permitting elevated nuclear pERK levels in response to Ras-ERK pathway activation. This induced the upregulation of a subset of ERK-dependent genes including SerpinB2 (Fig. 3.3-4), and the increased expression of SerpinB2 was essential for the increased sensitivity of DUSP5$^{-/-}$ mice to skin carcinogenesis (Fig. 3.14). However, in human skin cancer HRas is not thought to be a predominant driving oncogene (Hodis et al., 2012), therefore we wanted to investigate the role of DUSP5 in a more physiologically relevant murine cancer model.

Consequently, we chose to investigate and compare the effects of either DUSP5 or DUSP6/MKP-3 loss in a mouse model of KRas^{G12D}-driven pancreatic cancer. This model was chosen for a number of reasons. Firstly, both DUSP5 and DUSP6/MKP-3 mRNA's are highly expressed in the pancreas (NCBI RefSeq data: http://www.ncbi.nlm.nih.gov/gene/1847 & http://www.ncbi.nlm.nih.gov/gene/1848). Secondly, activating KRas mutations are the key driver events in human pancreatic ductal adenocarcinoma (PDAC) having been identified in around 90% of tumours (Kleeff et al., 2016), making this a highly clinically relevant disease model. Finally, in chapter 4 we demonstrated that both DUSP5 and DUSP6/MKP-3 are two of the most strongly upregulated MKPs in response to the expression of endogenous KRas^{G12D}, indicating that these phosphatases form part of the negative feedback controls which restrain ERK activity following constitutive pathway activation (Fig. 4.8-9). This suggests that DUSP5 and DUSP6/MKP-3 might be overexpressed in KRas^{G12D}-driven tumours, and that the loss of either MKP could have functional consequences for either tumour initiation or progression. At least in MEFs, neither DUSP5 nor DUSP6/MKP-3 ablation had dramatic biochemical or cellular consequences when coupled with KRas^{G12D} expression (Fig. 4.12-21). DUSP5 loss did not significantly alter ERK activity or localisation, yet did result in

increased ERK-dependent gene expression (Fig. 4.12-14). In contrast, DUSP6/MKP-3 loss caused a slight increase in levels of *p*-ERK but without causing any changes in expression of the ERK-dependent genes we assayed (Fig. 4.15-16). Furthermore, loss of either DUSP5 or DUSP6/MKP-3 did not lead to changes in either $KRas^{G12D}$-driven cell proliferation or cell transformation as assayed by focus formation (Fig. 4.17-21). However, it is possible that the loss of these phosphatases could alter one of the many other cellular phenotypes not investigated here. Alternatively, DUSP5 or DUSP6/MKP-3 loss in the presence of $KRas^{G12D}$ might give rise to more overt phenotypic effects *in vivo* or in different cellular contexts.

Multiple studies have reported increased DUSP6/MKP-3 expression in a range of mutant Ras or BRaf-driven tumours, including pancreatic cancer, NSCLC, thyroid cancer and ALL (Degl'Innocenti et al., 2013; Furukawa et al., 2003, 2005; Lee et al., 2012; Okudela et al., 2009; Shojaee et al., 2015), indicating that DUSP6/MKP-3 expression could be important in these cancers. In pancreatic cancer and NSCLC DUSP6/MKP-3 overexpression has been identified in low-grade neoplastic lesions, whereas DUSP6/MKP-3 expression is frequently lost in high-grade, invasive carcinomas (Furukawa et al., 2003, 2005; Okudela et al., 2009). This suggests that in these cancers, although DUSP6/MKP-3 is initially upregulated as a negative feedback regulator in response to ERK pathway activation, DUSP6/MKP-3 is acting as a tumour suppressor as its loss is selected for during tumour progression. In contrast, in thyroid cancer and ALL, DUSP6/MKP-3 overexpression is maintained and correlates with a worse patient prognosis, suggesting a pro-oncogenic role (Degl'Innocenti et al., 2013; Lee et al., 2012; Shojaee et al., 2015). In ALL an oncogenic role for DUSP6/MKP-3 has been demonstrated experimentally, with $DUSP6^{-/-}$ mice being resistant to $NRas^{G12D}$-induced ALL (Shojaee et al., 2015). Furthermore BCI, a small molecule inhibitor of DUSP6/MKP-3, selectively induced cell death in human pre-B ALL cells expressing hyperactive ERK, demonstrating that DUSP6/MKP-3 could be a putative therapeutic target in this cancer (Shojaee et al., 2015). Overall, this evidence suggests that MKPs, such as DUSP6/MKP-3, are important components of the negative feedback control of ERK activity, which can act as oncogenes or tumour suppressors in a context-dependent manner. However, there is limited experimental evidence definitively proving such roles and investigating the mechanisms by which these occur.

Finally as mentioned above, changes in DUSP6/MKP-3 expression have been identified during pancreatic cancer progression. DUSP6/MKP-3 protein is overexpressed in the PanINs, the pre-neoplastic precursor lesions of PDAC, prior to subsequent downregulation in poorly differentiated, invasive PDAC (Furukawa et al., 2003, 2005). Decreased DUSP6/MKP-3 expression in invasive PDAC was shown to occur due to aberrant hypermethylation of the DUSP6/MKP-3 promoter (Xu et al., 2005), or by LOH of the DUSP6/MKP-3 containing region of chromosome 12q in up to 30% of tumours (Kimura et al., 1996; Yatsuoka et al., 2000). Unlike other tumour suppressors including p53 and CDKN2A which are lost during and contribute to PanIN progression, DUSP6/MKP-3 loss is seemingly only observed in invasive PDAC (Furukawa et al., 2005). This encourages the hypothesis that DUSP6/MKP-3 expression is constraining ERK activity in PanINs, which is preventing progression of PanINs to invasive PDAC (Furukawa, 2009; Furukawa et al., 2006). However, there is currently no experimental evidence demonstrating whether DUSP6/MKP-3 loss can accelerate PDAC development.

In contrast to DUSP6/MKP-3, there are currently no publications linking DUSP5 with a role in pancreatic cancer. However, analysis of transcriptome datasets generated through SAGE (serial analysis of gene expression) on RNA from the 24 pancreatic cancers and multiple PDAC cell lines by Jones et al., (2008) reveals that DUSP5 expression is downregulated in many pancreatic cancer tissues and cell lines relative to the normal pancreatic ductal epithelium. This could suggest that the decrease in DUSP5 expression is selected for during PDAC development. Therefore, this study aimed to utilise $KRas^{G12D}$-driven mouse models of PDAC (Hingorani et al., 2003) to investigate whether loss of DUSP5 or DUSP6/MKP-3 is able to modulate pancreatic tumour initiation and progression. This will determine whether DUSP6/MKP-3 acts as tumour suppressor in this mutant KRas-driven PDAC, as is suggested by current evidence. Furthermore, comparison of any potential phenotypes could determine whether the differential subcellular localisation of MKPs is able to specifically control the spatial activity of ERK, resulting in distinct functional consequences for tumour progression.

5.2 Results

5.2.1 Loss of DUSP5 or DUSP6/MKP-3 does not affect normal pancreatic development

Before investigating any potential roles for DUSP5 and DUSP6/MKP-3 loss in mutant KRas-driven pancreatic carcinogenesis we wanted to determine whether loss of either phosphatase might have consequences for normal pancreatic development. Both DUSP5 (Rushworth et al., 2014) and DUSP6/MKP-3 (Maillet et al., 2008) knockout mice have previously been shown to be viable, fertile, and otherwise overtly normal. However, to investigate any potential consequences of either DUSP5 or DUSP6/MKP-3 loss on pancreatic development in more detail we examined pancreata from wild-type, $DUSP5^{-/-}$ and $DUSP6^{-/-}$ mice isolated at 2, 4 and 6 months of age. All MKP knockout mice and their respective wild-type controls were littermates generated from het x het crosses. Upon histological examination, pancreata of all genotypes displayed normal proportions and disposition of the expected tissue types and structures, including islets of Langerhans (endocrine tissue), acinar cells (exocrine tissue) and pancreatic ducts, when compared to wild type organs (Fig. 5.1). Pancreata from both DUSP5 and DUSP6/MKP-3 knockouts were also examined for the presence of abnormal ducts and neoplastic precursor lesions (PanINs) and none were detected (Fig. 5.1). Finally, the loss of either phosphatase did not cause any significant change in pancreas to body-weight ratios (Data not shown). Therefore, we can conclude that loss of either DUSP5 or DUSP6/MKP-3 alone does not affect normal pancreatic development, at least in terms of tissue morphology, nor does it seem to promote any neoplastic changes in pancreatic tissues.

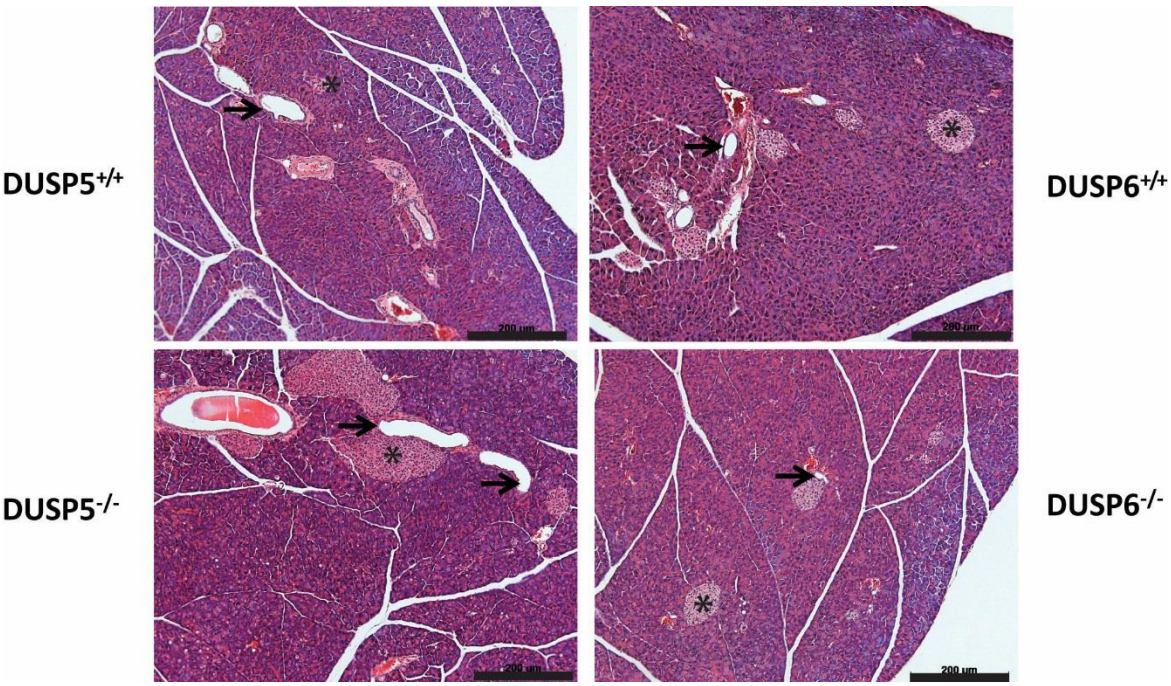

Figure 5.1 Loss of DUSP5 or DUSP6/MKP-3 has no effect on pancreatic development. Representative H&E images of wild-type ($DUSP5^{+/+}$ & $DUSP6^{+/+}$), $DUSP5^{-/-}$ and $DUSP6^{-/-}$ pancreata. Asterisks indicate Islets of Langerhans and arrows indicate pancreatic ducts. Scale, 200µm.

5.2.2 PDX1-Cre driven model of KRas^{G12D}-induced pancreatic cancer

To investigate whether DUSP5 ablation had any effect on the development of KRas^{G12D}-driven PDAC KRas$^{LSL\text{-}G12D/+}$; PDX1-Cre mice (Hingorani et al., 2003) were crossed with DUSP5$^{fl/fl}$ mice. This enabled the generation of mice in which endogenous KRas^{G12D} can be knocked-in through the Cre-mediated excision of the Lox-Stop-Lox (LSL) cassette and DUSP5 can be knocked out. The PDX1-Cre allele was initially utilised to drive pancreatic Cre expression as this is the most frequently used Cre-driver allele in GEMMs of pancreatic cancer (Guerra and Barbacid, 2013; Pérez–Mancera et al., 2012). During mouse development, PDX1 (pancreatic and duodenal homeobox 1, also known as insulin promoter factor 1) a homeodomain containing transcription factor, is expressed in the pre-pancreatic endoderm from E8.5 and is expressed in the progenitors of all major pancreatic cell lineages (acini, islet and ductal cells). In postnatal mice PDX1 expression is retained in acini and islet cells, with the highest expression in β-cells of the islets (Magnuson and Osipovich, 2013).

However, PDX1 expression is not completely restricted to the developing pancreas, with expression also observed in foregut endothelium progenitor cells during early development (Offield et al., 1996), and in cells of the intestine, stomach and skin (Hingorani et al., 2003). When combined with the KRas$^{LSL\text{-}G12D}$ allele the leakiness of PDX1-Cre expression and the resulting recombination in other tissues induces intestinal hyperplasia, occasionally resulting in the formation of intussusceptions (intestinal invaginations resulting in blockage) (Fig. 5.2A), the development of hyperplastic polyps of the duodenum (mucocutaneous papillomas) or intestinal metaplasia of the gastric epithelium (Hingorani et al., 2003). Unfortunately, in our particular study study KRas$^{LSL\text{-}G12D/+}$; PDX1-Cre expressing mice, regardless of their DUSP5 genotype, displayed intestinal intussusceptions with very high penetrance (approx. 60%), typically occurring between 30-150 days of age (Fig. 5.2B-C). This is considerably higher than the ~5% background intussusception rate normally observed when using this model (Owen Sansom, Beatson Institute Glasgow personal communication). We hypothesise that the increased intussusception we see is due to the presence of a persistent pinworm infection within our animal facility. Although pinworm infections are generally considered to be mildly or even non-pathogenic in animals these gastronintestinal parasitic nematodes can

stimulate host humoral immune responses resulting in inflammation. It is therefore likely that this exacerbates $KRas^{G12D}$-induced intestinal hyperplasia, resulting in an increased frequency of intussusceptions in our experimental animals.

The high penetrance of intussusception and resulting lethality prevented us from conducting any meaningful survival analysis to investigate the effect of DUSP5 loss on $KRas^{G12D}$-driven pancreatic tumourigenesis, and also made the generation of age-matched cohorts difficult. To circumvent this and obtain preliminary data from this model, we generated a small age-matched cohort at 42 days, as this was prior to the peak of intussusception occurrence and therefore minimised the loss of mice (Fig. 5.2C). $KRas^{G12D}$-expressing pancreata displayed a marginal increase in pancreatic size and weight relative to control animals (Fig. 5.3A) and the sporadic induction of ADM and low grade PanIN formation (Fig. 5.3B), as described previously (Hingorani et al., 2003). Loss of one or two alleles of DUSP5 in the presence of $KRas^{G12D}$ generated a slight increase in pancreatic weight relative to $KRas^{G12D}$ alone, though this was not statistically significant, perhaps reflecting the small cohort size and magnitude of the phenotype. However, DUSP5 loss in the presence of $KRas^{G12D}$ promoted an increased burden of ADM, and the associated formation of reactive stroma around these lesions (Fig. 5.3B-C). Few clearly defined PanINs were observed in all cohorts and no significant alteration in the progression of pancreatic cancer precursor lesions was observed (Fig. 5.3D). This is not unexpected given the age of this cohort and the relatively slow progression of pancreatic tumourigenesis normally observed in this model (Hingorani et al., 2003).

This limited evidence indicates that DUSP5 loss might promote the initiation of $KRas^{G12D}$-driven PDAC. However, due to the high penetrance of intussusceptions we could not investigate potential effects of DUSP5 loss on PanIN progression, PDAC development and metastasis and how these variables affect survival using the PDX1-Cre driven model. Therefore, we needed to utilise an alternative model to further investigate the effects of DUSP5 loss on $KRas^{G12D}$-driven pancreatic tumourigenesis.

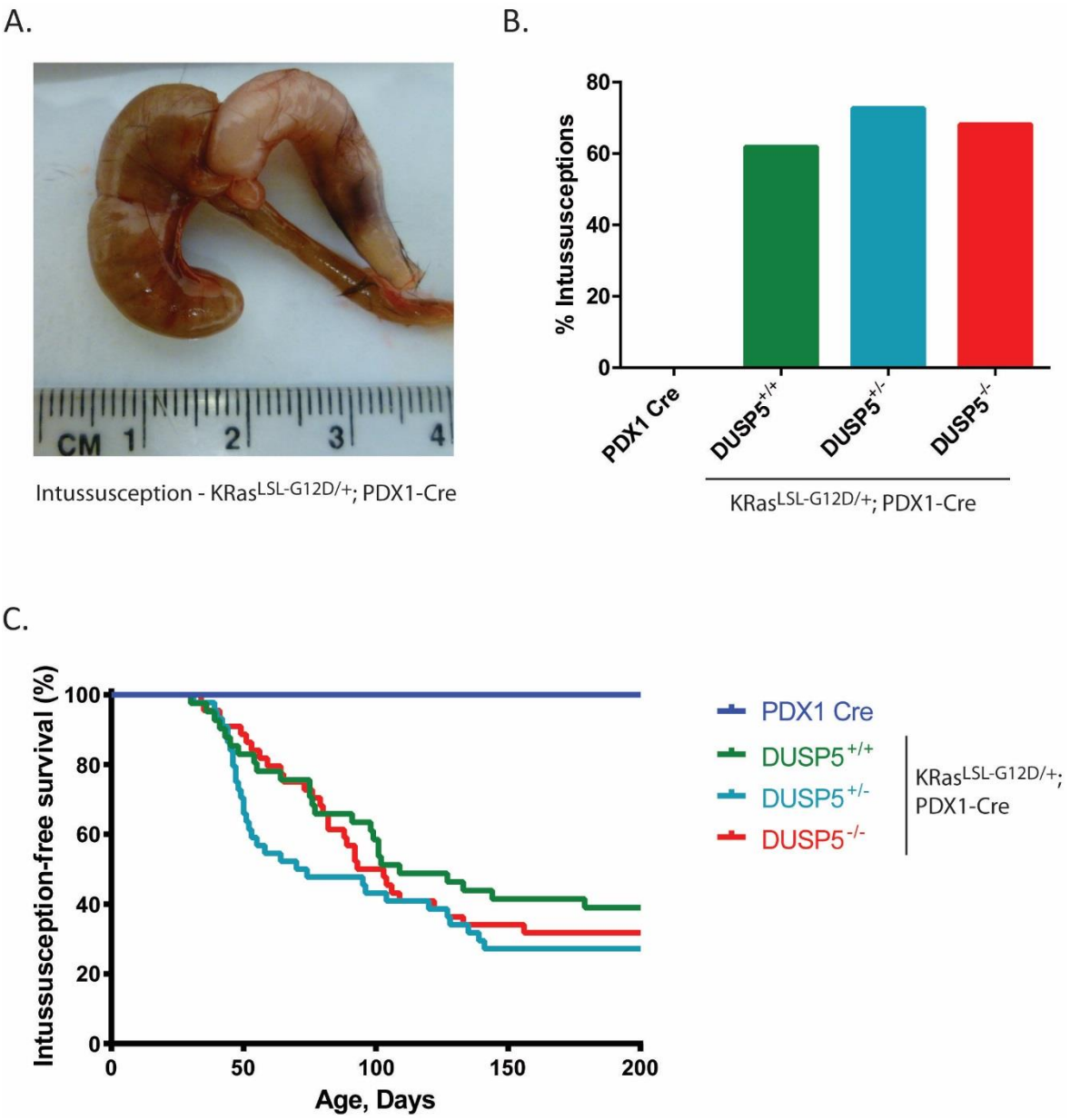

Figure 5.2 KRas$^{LSL-G12D/+}$; PDX1-cre mice displayed high mortality due to intussusceptions. **A)** A representative image of an intussusception removed from a KRas$^{LSL-G12D/+}$; PDX1-cre expressing mouse. **B)** The proportion of mice of the indicated cohorts, which were removed from the study due to intussusceptions. **C)** Kaplan-Meier curves demonstrating the intussusception-free survival of the indicated cohorts. Cohorts consisted of the following genotypes: KRas$^{+/+}$; PDX1-cre; DUSP5$^{+/+}$ (PDX1 Cre, n = 10), KRas$^{LSL-G12D/+}$; PDX1-cre; DUSP5$^{+/+}$ (DUSP5$^{+/+}$, n = 41), KRas$^{LSL-G12D/+}$; PDX1-cre; DUSP5$^{+/fl}$ (DUSP5$^{+/-}$, n = 44) and KRas$^{LSL-G12D/+}$; PDX1-cre; DUSP5$^{fl/fl}$ (DUSP5$^{-/-}$, n = 44).

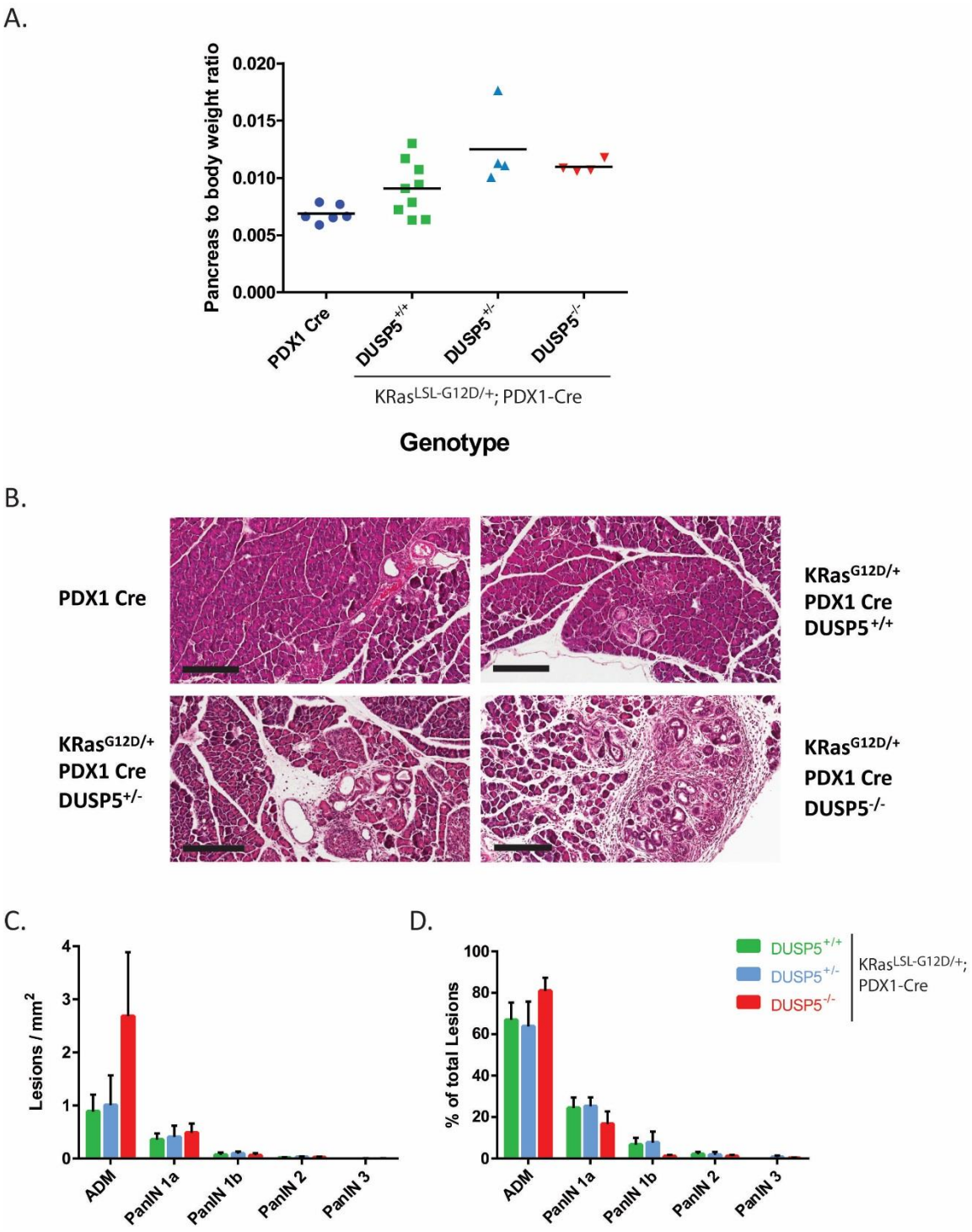

Figure 5.3 DUSP5 loss promotes increased KRas^{G12D}-driven pancreatic cancer initiation. A) Pancreata from 42 day age-matched mice of the indicated cohorts were harvested and their pancreas to body weight ratios calculated. Cohorts consisted of the following genotypes: KRas$^{+/+}$; PDX1-cre; DUSP5$^{+/+}$ (PDX1-Cre, n = 6), KRas$^{LSL-G12D/+}$; PDX1-Cre; DUSP5$^{+/+}$ (DUSP5$^{+/+}$, n = 9), KRas$^{LSL-G12D/+}$; PDX1-Cre; DUSP5$^{+/fl}$ (DUSP5$^{+/-}$, n = 4) and KRas$^{LSL-G12D/+}$; PDX1-Cre; DUSP5$^{fl/fl}$ (DUSP5$^{-/-}$, n = 4). **B)** Representative H&E images of the indicated cohorts. Scale, 200μm. **C-D)** Quantification of the number of pancreatic cancer precursor lesions per mm^2 in the indicated cohorts **(C)**, and these expressed as a percentage of the total number of lesions **(D).** Quantification performed on one representative section per mouse, following serial sectioning of the pancreas. Mean values ± SEM are shown, n = 8, 4, 4.

5.2.3 Ptf1α-Cre driven model of KRas^{G12D}-induced pancreatic cancer

5.2.3.1 Loss of DUSP5 or DUSP6/MKP-3 promotes increased KRas^{G12D}-induced pancreatic cancer initiation

Due to the high penetrance of intestinal intussusceptions in our initial PDX1-Cre driven KRas^{G12D}-induced pancreatic cancer model (Fig. 5.2B-C), we switched the promoter used to drive Cre-recombinase expression to that of the pancreas-specific transcription factor 1α (Ptf1α) gene. In contrast to PDX1, lineage tracing experiments have shown Ptf1α to be a transcription factor expressed solely in the developing pancreas from E9.5, and in postnatal acinar tissue (Hingorani et al., 2003; Kawaguchi et al., 2002). Consequently, Ras-driven pathology and tumours are much less common in other tissues following mutant KRas^{G12D} expression driven by the Ptf1α-Cre allele, and intussusceptions do not occur (Hingorani et al., 2003; Westphalen and Olive, 2012). A further difference between the two Cre-drivers alleles is that while the PDX1-Cre allele results in stochastic Cre expression and recombination across the pancreas, the Ptf1α-Cre allele results in completely uniform expression and recombination throughout all developing pancreatic tissues (Hingorani et al., 2003).

When utilising the Ptf1α-Cre driven model of KRas^{G12D}-induced pancreatic cancer we decided to perform a direct comparison between the potential effects of DUSP5 and DUSP6/MKP-3 loss on pancreatic tumourigenesis. Initially, we validated the Ptf1α-Cre mediated pancreas-specific recombination of the KRas$^{LSL-G12D}$, DUSP5$^{fl/fl}$ and DUSP6$^{fl/fl}$ conditional alleles to be used in this study. DNA was isolated from 100 day old mice containing each allele in combination with Ptf1α-Cre, and genotyping PCRs were performed to identify whether recombination had occurred. Ptf1α-Cre expression was sufficient induce excision of the LSL-cassette in the KRas$^{LSL-G12D}$ allele and of the exons targeted by the DUSP5$^{fl/fl}$ and DUSP6$^{fl/fl}$ alleles (Fig. 5.4A-C). In MEFs, we have previously shown that, Cre-mediated excision of the LSL-cassette in the KRas$^{LSL-G12D}$ allele promotes the expression of mutant KRas^{G12D}, and an associated increase in GTP-bound Ras (Fig. 4.1B). Furthermore, Cre-mediated excision of the targeted exons of the DUSP6$^{fl/fl}$ conditional allele prevented DUSP6/MKP-3 mRNA or protein expression (Fig. 4.15-16). To validate the DUSP5$^{fl/fl}$ allele MEFs were generated, which when subjected to Cre-treatment demonstrated excision of the targeted exons (Fig. 5.5A). However, even

without being subject to Cre-treatment DUSP5$^{fl/fl}$ MEFs demonstrate very low DUSP5 mRNA and protein expression relative to DUSP5$^{+/+}$ MEFs (Fig. 5.5B-C), indicating that this conditional allele is hypomorphic. Despite this, the DUSP5$^{fl/fl}$ allele was utilised for the following *in vivo* models as it was the only conditional allele available at the time and unlike a knockout allele non-pancreatic tissue would retain an albeit reduced level of DUSP5 expression.

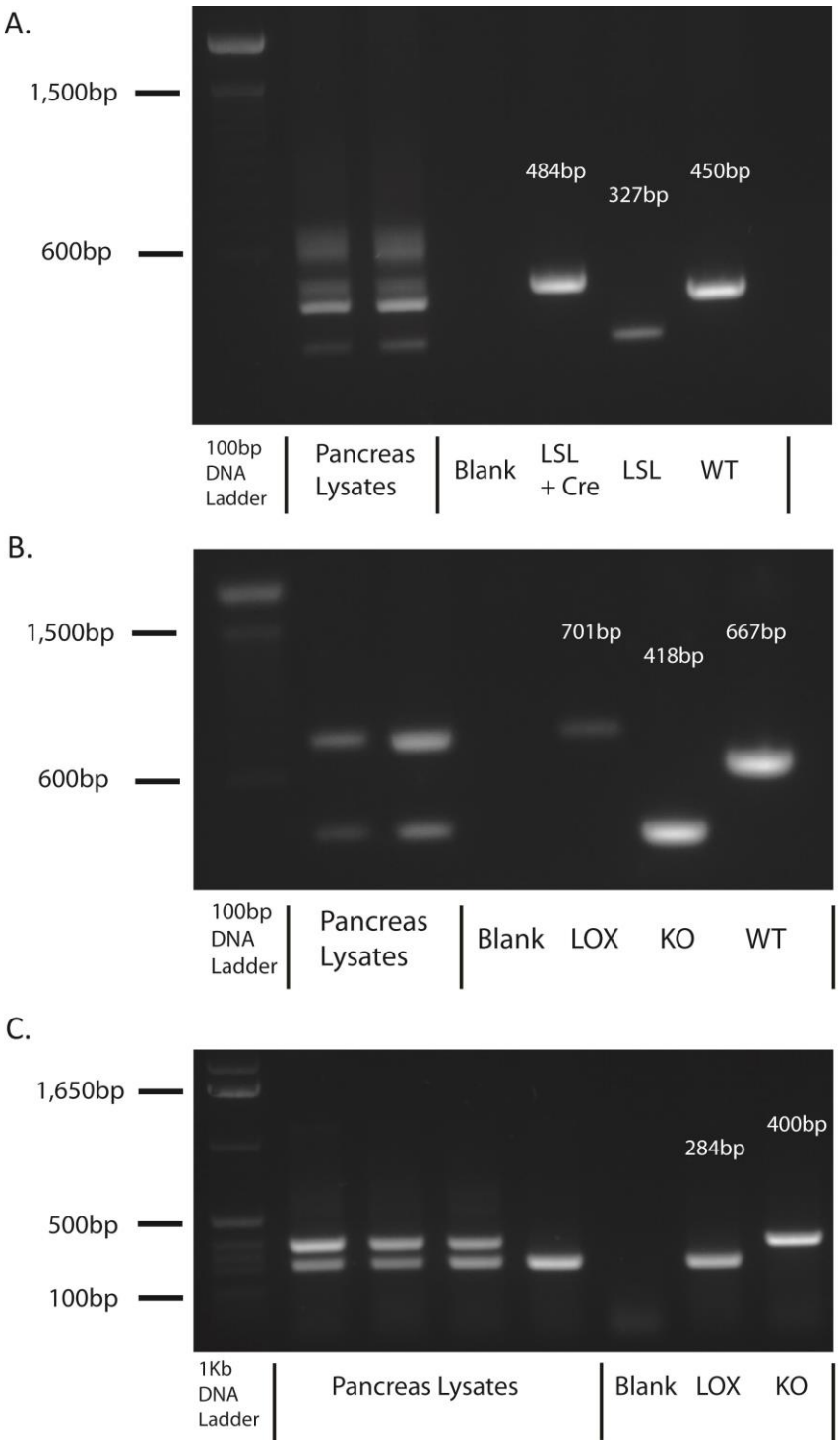

Figure 5.4 Validation of Ptf1a-cre mediated recombination of conditional alleles in the pancreas. A) PCR of genomic DNA from $KRas^{LSL\text{-}G12D/+}$; Ptf1α-cre mice demonstrating the excision of the Lox-STOP-Lox (LSL)-cassette from the $KRas^{LSL\text{-}G12D}$ allele in the presence of Ptf1α-cre in pancreatic lysates. Control lysates from untreated $KRas^{LSL\text{-}G12D/LSL\text{-}G12D}$ (LSL) and $KRas^{+/+}$ (WT) MEFs validate the size of 327bp LSL-cassette and 450bp WT bands. Cre-mediated recombination of the $KRas^{LSL\text{-}G12D}$ allele results in the formation of a 484bp fragment (LSL+Cre). **B)** PCR of pancreatic, genomic DNA from Ptf1α-cre; $DUSP5^{fl/fl}$ mice demonstrating the excision of exon 2 of the DUSP5 allele in the presence of Ptf1α-cre. Control lysates from $DUSP5^{fl/fl}$ (Lox), $DUSP5^{-/-}$ (KO) and $DUSP5^{+/+}$ (WT) mice validate the 701bp, 418bp and 667bp bands respectively. **C)** PCR of pancreatic, genomic DNA from Ptf1α-cre; $DUSP6^{fl/fl}$ mice demonstrating the excision of DUSP6/MKP-3 exons 2 and 3 in the presence of Ptf1α-cre. Control lysates from $DUSP6^{fl/fl}$ (Lox) and $DUSP6^{-/-}$ (KO) mice validate the 284bp and 400bp bands respectively.

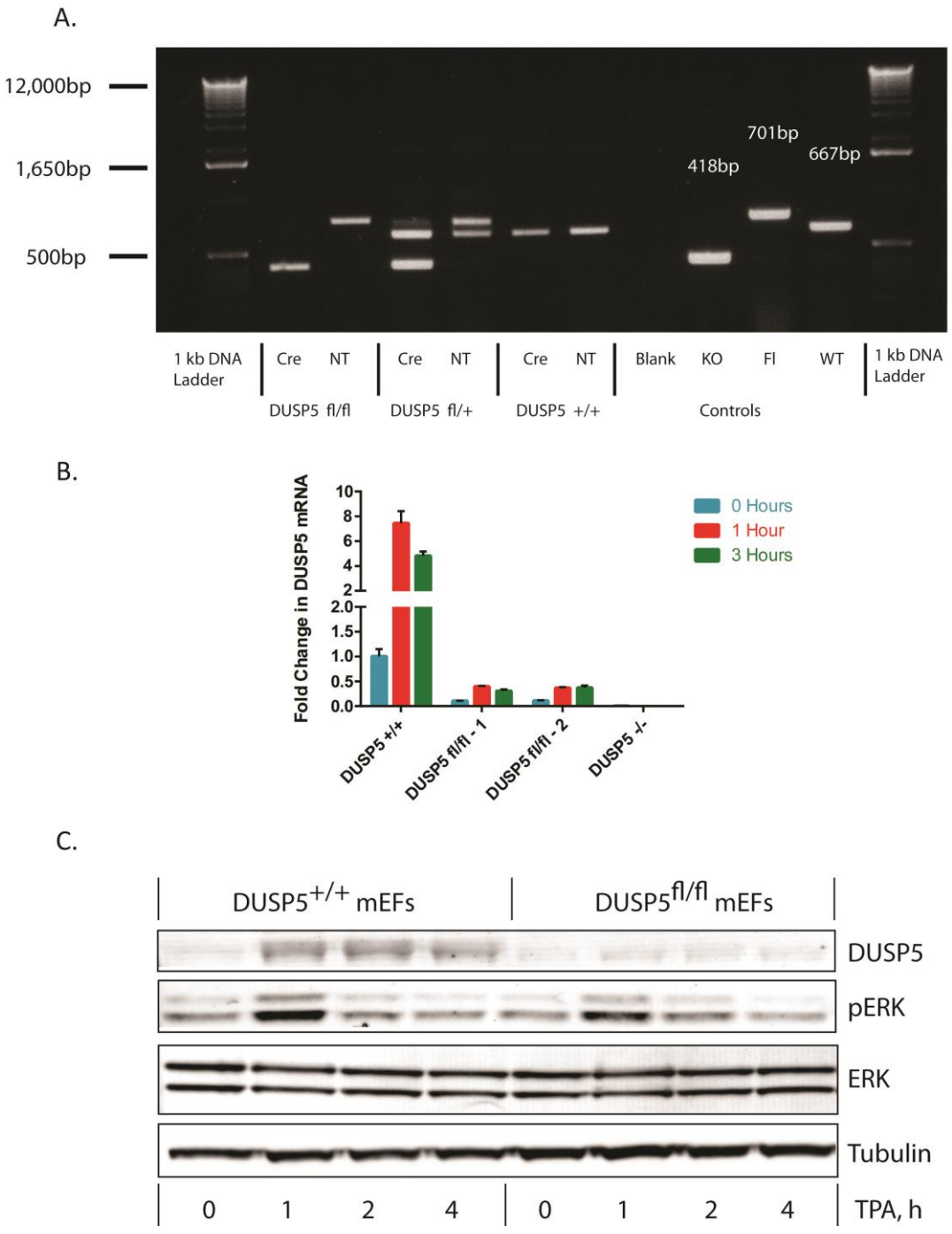

Figure 5.5 The conditional DUSP5 allele is hypomorphic. A) PCR of genomic DNA from DUSP5$^{fl/fl}$, DUSP5$^{fl/+}$ and DUSP5$^{+/+}$ MEFs demonstrating the excision of exon 2 of the DUSP5 floxed allele in the presence of adenoviral-Cre (Cre) but not empty adenovirus (NT). Control lysates from DUSP5$^{-/-}$ (KO), DUSP5$^{fl/fl}$ (Lox) and DUSP5$^{+/+}$ (WT) mice validate the 418bp, 701bp and 667bp bands respectively. **B)** Taqman RT-qPCR assay showing the fold change in DUSP5 mRNA levels of DUSP5$^{+/+}$, DUSP5$^{fl/fl}$ (two cell lines) and DUSP5$^{-/-}$ MEFs following TPA stimulation (100ng/ml) relative to the unstimulated DUSP5$^{+/+}$ MEFs. Representative figure of an experiment performed in duplicate. Mean ± SEM of technical replicates, n =3, shown. **C)** MEFs of the indicated genotype were stimulated with TPA for 0, 1, 2 & 4 hours prior to cell lysis, and immunoblotting using the indicated antibodies. Representative image of experiment performed in duplicate is shown.

To investigate whether loss of either DUSP5 or DUSP6/MKP-3 is able to modulate $KRas^{G12D}$-driven pancreatic cancer initiation and progression, age-matched cohorts of $KRas^{LSL\text{-}G12D/+}$; Ptf1α-Cre (KC) mice which were wild-type, heterozygous or homozygous for either $DUSP5^{fl/fl}$ or $DUSP6^{fl/fl}$ alleles were generated, alongside Ptf1α-Cre controls. Therefore, the experimental cohorts consisted of: $KRas^{+/+}$; Ptf1α-cre; $DUSP^{+/+}$ (Ptf1α-cre), $KRas^{LSL\text{-}G12D/+}$; Ptf1α-cre; $DUSP^{+/+}$ (KC), $KRas^{LSL\text{-}G12D/+}$; Ptf1α-cre; $DUSP5^{+/fl}$ ($KCD5^{+/-}$), $KRas^{LSL\text{-}G12D/+}$; Ptf1α-cre; $DUSP5^{fl/fl}$ ($KCD5^{-/-}$), $KRas^{LSL\text{-}G12D/+}$; Ptf1α-cre; $DUSP6^{+/fl}$ ($KCD6^{+/-}$) and $KRas^{LSL\text{-}G12D/+}$; Ptf1α-cre; $DUSP6^{fl/fl}$ ($KCD6^{-/-}$) mice. Initially, a 56 day (2 month) old cohort was generated. At this age $KCD5^{-/-}$ and $KCD6^{-/-}$ mice demonstrated a significant increase in their pancreas to body weight ratio, compared to KC mice (Fig. 5.6). Furthermore, histological analysis revealed an increased burden of ADM, PanINs and associated reactive stroma following the loss of either DUSP5 or DUSP6/MKP-3 in the presence of $KRas^{G12D}$ when compared to the effects of $KRas^{G12D}$ expression alone (Fig. 5.7). This increased PanIN burden in $KCD5^{-/-}$ and $KCD6^{-/-}$ mice can be clearly observed following Alcian Blue staining (Fig. 5.8A), which stains the mucin secreted by PanINs (Hingorani et al., 2003). Furthermore, the characteristic dense reactive stroma, which forms around developing PanINs can be clearly visualised using immunohistochemical (IHC) detection of αSmooth Muscle Actin (αSMA) (Fig. 5.8B).

Quantification of this phenotype reveals there is a significant decrease in acinar tissue present in $KCD5^{-/-}$ and $KCD6^{-/-}$ pancreata, relative to KC, with heterozygous $KCD5^{+/-}$ and $KCD6^{+/-}$ pancreata displaying an intermediate phenotype (Fig. 5.9A). This acinar atrophy should represent a reliable surrogate measure for the amount of tumour initiation occurring, as pancreatic cancer precursor lesions are thought to arise primarily through acinar dedifferentiation and ADM in $KRas^{G12D}$-driven mouse models of pancreatic cancer when $KRas^{G12D}$-expression is induced in all pancreatic cell lineages (Guerra and Barbacid, 2013; Kopp et al., 2012; Morris et al., 2010). This indicates that following DUSP5 or DUSP6/MKP-3 loss a greater proportion of the pancreas is undergoing $KRas^{G12D}$-driven metaplasia and tumourigenesis. $KCD5^{-/-}$ and $KCD6^{-/-}$ pancreata also display a significant increase in the total number of PanINs per mm^2 of pancreatic tissue when compared to KC pancreata (Fig. 5.9B), although at this young age the vast majority of lesions are either ADM or PanIN1a in all cohorts (Fig. 5.9C). PanINs were scored utilising well established histological criteria (Hingorani et al., 2003; Hruban et al., 2001, 2006a), whereas small

ductal lesions surrounded by reactive stroma which have not fulfilled the required criteria to be confirmed as PanINs were scored as ADM. ADM have been defined as, proliferative lesions appearing as tubular structures, consisting of swollen acinar cells, with a ductal, PanIN-like appearance, often surrounded by a reactive stroma (Hruban et al., 2006b). Therefore, ADM are structures which replace the acinar parenchyma, but contain traits of both acinar and ductal differentiation.

Quantification of the percentage of total lesions which are each histological grade reveals a marginal increase in the number of PanIN1a and PanIN1b lesions following the loss of DUSP6/MKP-3 in the presence of $KRas^{G12D}$ (Fig. 5.9D). This data indicates that DUSP6/MKP-3 loss could be promoting accelerated progression of $KRas^{G12D}$-expressing PanINs, however this could be more conclusively demonstrated in an older age-matched cohort where the pancreata display an increased number of higher grade lesions. A higher percentage of $KCD6^{-/-}$ mice display with higher grade PanIN2s and PanIN3s than KC mice (Fig. 5.9E), which could support the case for accelerated PanIN progression. However, this observation could alternatively be due to $KCD6^{-/-}$ pancreata having an increased number of lesions initiated (Fig. 5.9B-C), therefore increasing the chance that at least one will progress to these higher grades. Taken together these data indicate that loss of either DUSP5 or DUSP6/MKP-3 is able to promote increased, or accelerated, pancreatic cancer initiation in the presence of $KRas^{G12D}$.

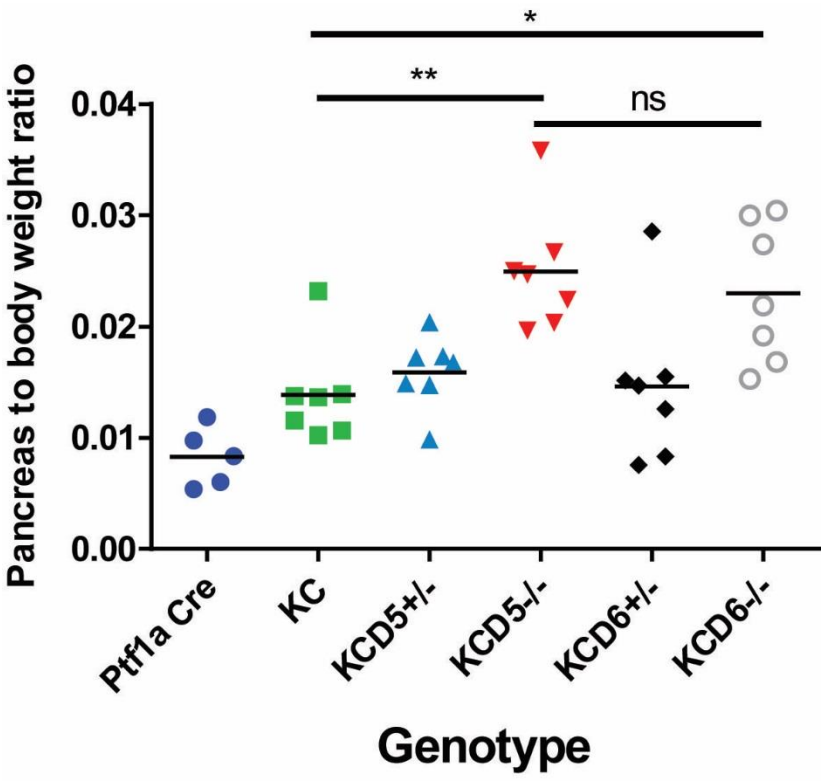

Figure 5.6 Loss of DUSP5 or DUSP6/MKP-3 promotes increased pancreatic weight following the initiation of KRas^{G12D}-driven pancreatic tumourigenesis. Pancreata from 56 day age-matched mice of the indicated cohorts were harvested and their pancreas to body weight ratios calculated. Cohorts consisted of the following genotypes: KRas$^{+/+}$; Ptf1α-cre; DUSP$^{+/+}$ (Ptf1α-cre), KRas$^{LSL\text{-}G12D/+}$; Ptf1α-cre; DUSP$^{+/+}$ (KC), KRas$^{LSL\text{-}G12D/+}$; Ptf1α-cre; DUSP5$^{+/fl}$ (KCD5$^{+/-}$), KRas$^{LSL\text{-}G12D/+}$; Ptf1α-cre; DUSP5$^{fl/fl}$ (KCD5$^{-/-}$), KRas$^{LSL\text{-}G12D/+}$; Ptf1α-cre; DUSP6$^{+/fl}$ (KCD6$^{+/-}$) and KRas$^{LSL\text{-}G12D/+}$; Ptf1α-cre; DUSP6$^{fl/fl}$ (KCD6$^{-/-}$). Mean shown, n = 5, 7, 7, 7, 7, 7. Ns = not significant, *P < 0.05, **P < 0.01, using one-way ANOVA and Bonferroni post hoc test.

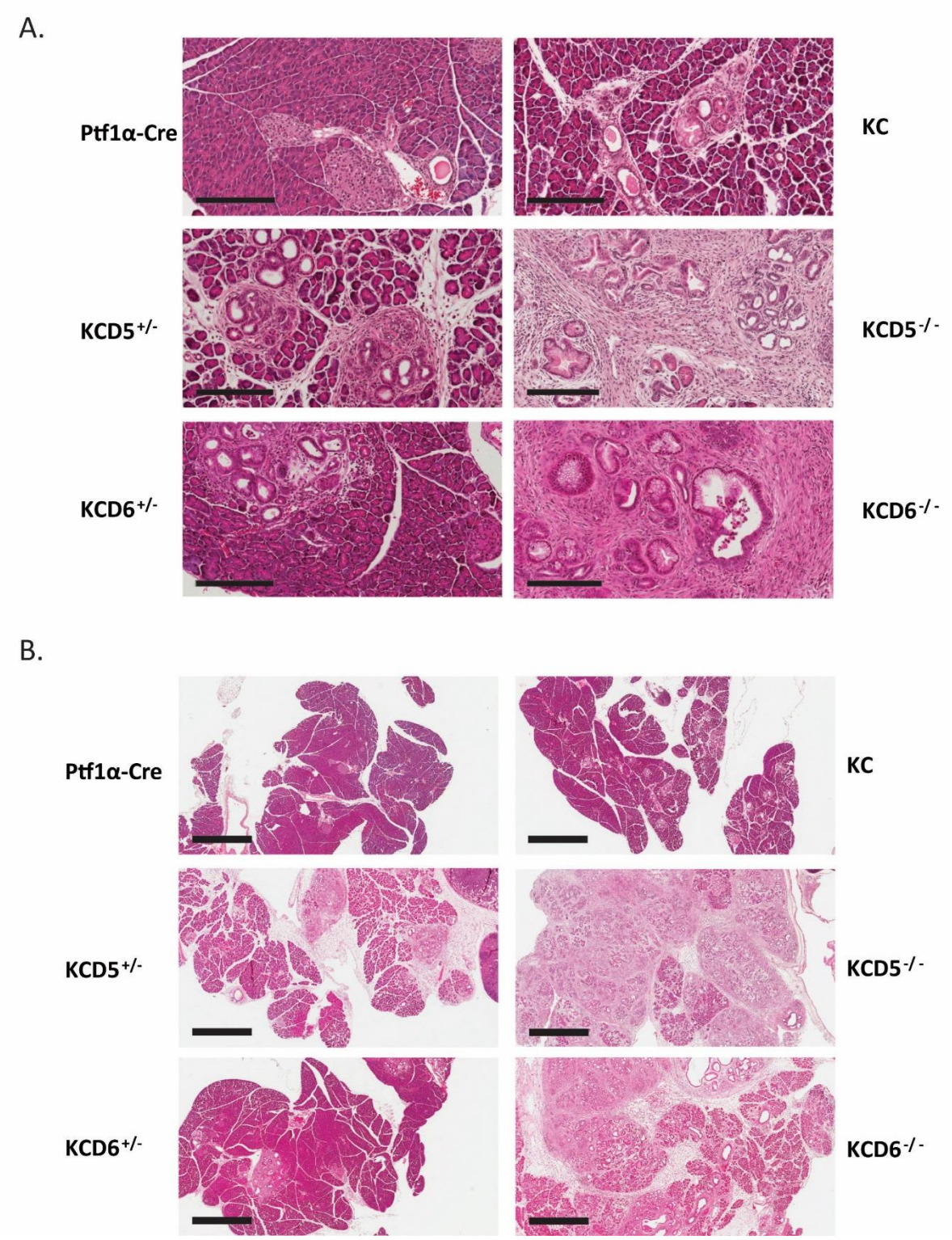

Figure 5.7 Loss of DUSP5 or DUSP6/MKP-3 promotes increased KRas^{G12D}-driven ADM and PanIN initiation. Representative images of H&E stained pancreata from 56 day age-matched mice of the indicated cohorts, with a 200μm **(A)** or 1mm **(B)** scale. Cohorts consisted of the following genotypes: KRas$^{+/+}$; Ptf1α-cre; DUSP$^{+/+}$ (Ptf1α-cre, n = 5), KRas$^{LSL\text{-}G12D/+}$; Ptf1α-cre; DUSP$^{+/+}$ (KC, n = 7), KRas$^{LSL\text{-}G12D/+}$; Ptf1α-cre; DUSP5$^{+/fl}$ (KCD5$^{+/-}$, n = 7), KRas$^{LSL\text{-}G12D/+}$; Ptf1α-cre; DUSP5$^{fl/fl}$ (KCD5$^{-/-}$, n = 7), KRas$^{LSL\text{-}G12D/+}$; Ptf1α-cre; DUSP6$^{+/fl}$ (KCD6$^{+/-}$, n = 7) and KRas$^{LSL\text{-}G12D/+}$; Ptf1α-cre; DUSP6$^{fl/fl}$ (KCD6$^{-/-}$, n = 7).

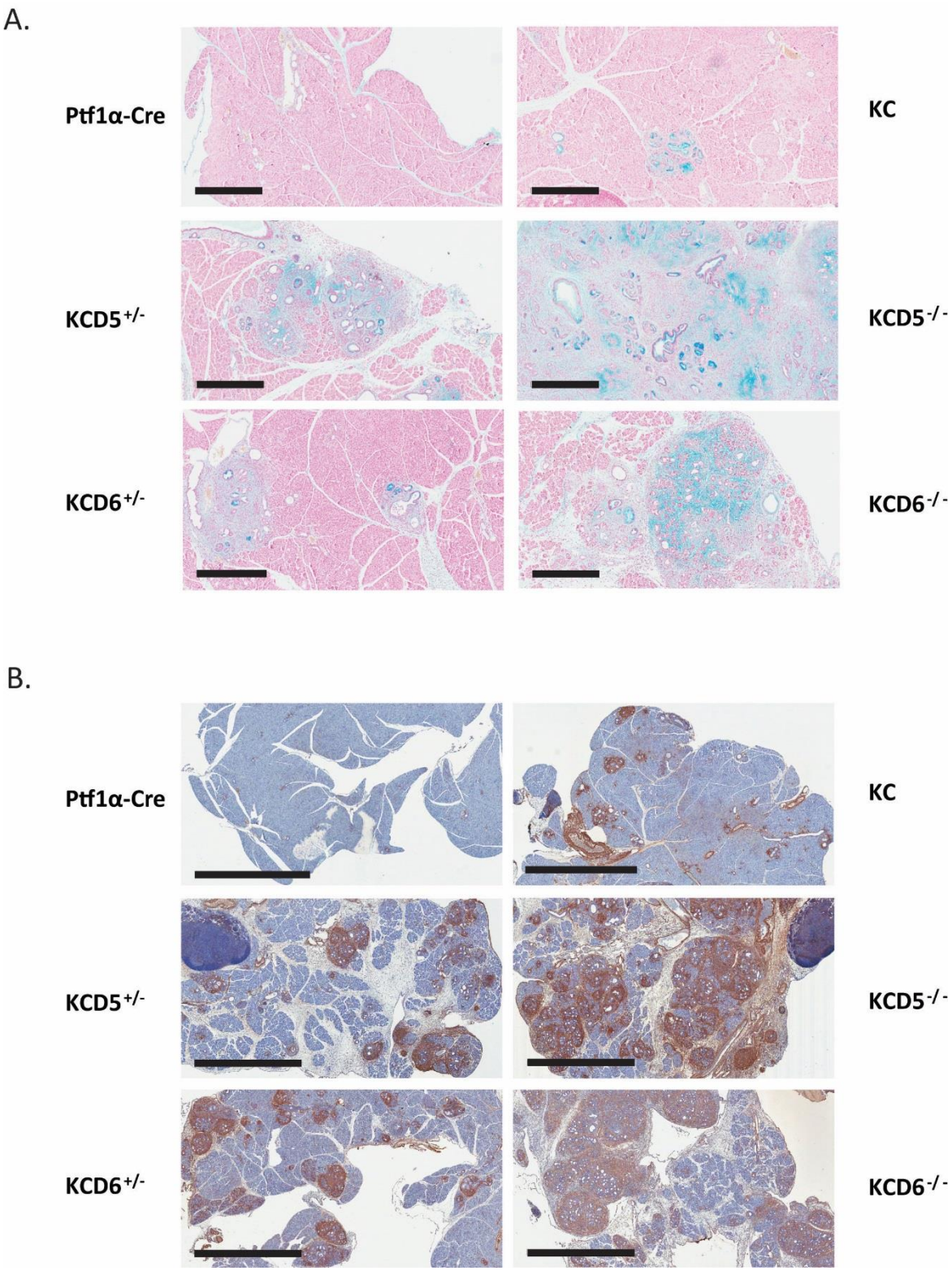

Figure 5.8 DUSP5 or DUSP6/MKP-3 loss promotes increased KRas^{G12D}-driven PanIN initiation and the formation of reactive stroma. Representative images of Alcian Blue/Nuclear Fast Red **(A)** and αSmooth Muscle Actin (αSMA) IHC **(B)** stained pancreata from 56 day age-matched mice of the indicated cohorts. Cohorts consisted of the following genotypes: KRas$^{+/+}$; Ptf1α-cre; DUSP$^{+/+}$ (Ptf1α-cre, n = 5), KRas$^{LSL\text{-}G12D/+}$; Ptf1α-cre; DUSP$^{+/+}$ (KC, n = 7), KRas$^{LSL\text{-}G12D/+}$; Ptf1α-cre; DUSP5$^{+/fl}$ (KCD5$^{+/-}$, n = 7), KRas$^{LSL\text{-}G12D/+}$; Ptf1α-cre; DUSP5$^{fl/fl}$ (KCD5$^{-/-}$, n = 7), KRas$^{LSL\text{-}G12D/+}$; Ptf1α-cre; DUSP6$^{+/fl}$ (KCD6$^{+/-}$, n = 7) and KRas$^{LSL\text{-}G12D/+}$; Ptf1α-cre; DUSP6$^{fl/fl}$ (KCD6$^{-/-}$, n = 7). Scale, 500μm and 2mm respectively.

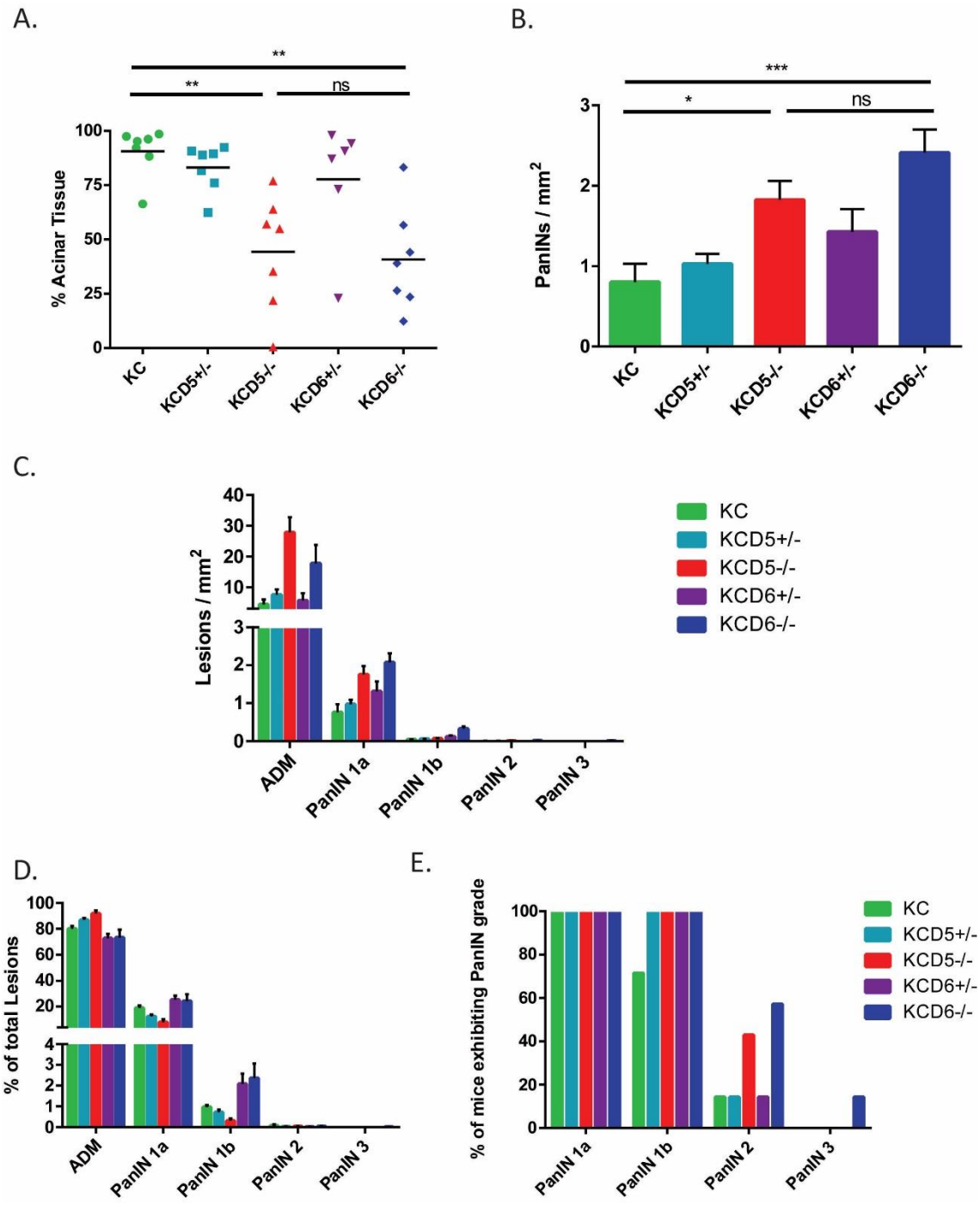

Figure 5.9 Loss of DUSP5 or DUSP6/MKP-3 promotes increased KRas^{G12D}-driven ADM and PanIN initiation. Quantification of the pancreatic precursor lesion development in 56 day age-matched pancreata of the indicated cohorts. Cohorts consisted of the following genotypes: KRas$^{LSL\text{-}G12D/+}$; Ptf1α-cre; DUSP$^{+/+}$ (KC), KRas$^{LSL\text{-}G12D/+}$; Ptf1α-cre; DUSP5$^{+/fl}$ (KCD5$^{+/-}$), KRas$^{LSL\text{-}G12D/+}$; Ptf1α-cre; DUSP5$^{fl/fl}$ (KCD5$^{-/-}$), KRas$^{LSL\text{-}G12D/+}$; Ptf1α-cre; DUSP6$^{+/fl}$ (KCD6$^{+/-}$) and KRas$^{LSL\text{-}G12D/+}$; Ptf1α-cre; DUSP6$^{fl/fl}$ (KCD6$^{-/-}$). **A)** Percentage acinar tissue remaining in the pancreata of each cohort following KRas^{G12D}-driven ADM and PanIN initiation. **B)** Total number of PanINs of all histological grades per mm^2 in the indicated cohorts. **C-D)** Quantification of the number of pancreatic cancer precursor lesions, divided into each histological grade, per mm^2 in the indicated cohorts **(C)**, and these expressed as a percentage of the total number of lesions **(D)**. **E)** Percentage of mice of the indicated cohorts that displayed at least one of each PanIN grade. Quantification performed on one representative section per mouse, following serial sectioning of the pancreas. Mean values ± SEM are shown, n = 7, 7, 7, 6, 7. Ns = not significant, *P < 0.05, **P < 0.01, ***P < 0.001 using one-way ANOVA and Bonferroni post hoc test.

To further investigate the effect of DUSP5 or DUSP6/MKP-3 loss on the progression of $KRas^{G12D}$-driven PanINs through higher histological grades, towards PDAC formation, a second age-matched cohort was generated consisting of 100 day old mice. At 100 days there were no significant differences in the mean pancreas to body weight ratios of the different $KRas^{G12D}$-expressing cohorts (Fig. 5.10). Interestingly, although the mean pancreas to body weight ratios of the $KRas^{G12D}$-expressing DUSP5 or DUSP6/MKP-3 wild-type and heterozygous cohorts increased in relation to their respective 56 day cohorts, the $KCD5^{-/-}$ and $KCD6^{-/-}$ cohorts displayed decreased ratios after 100 days (Fig. 5.6 & 10). Histological analysis demonstrates that both $KCD5^{-/-}$ and $KCD6^{-/-}$ pancreata display increased acinar atrophy and a higher burden of ADM, PanINs and reactive stroma relative to their KC counterparts (Fig. 5.11-12). Quantification of the percentage acinar tissue remaining confirms this observation, as multiple $KCD5^{-/-}$ or $KCD6^{-/-}$ pancreata display an almost complete replacement of acinar tissue with PanINs and associated reactive stroma (Fig. 5.13A). However, some KC pancreata are also nearing complete loss of acinar tissue, indicating that loss of DUSP5 or DUSP6/MKP-3 is potentially accelerating the rate of $KRas^{G12D}$-driven ADM and PanIN initiation, to generate the increased burden of pre-neoplastic lesions observed in the 56 day pancreata.

Interestingly, at this age only $KCD6^{-/-}$ pancreata display a significant increase in the total number of PanINs relative to KC (Fig. 5.13B), whereas in the 56 day cohort both DUSP5 and DUSP6/MKP-3 loss induced a significant increase in PanIN number (Fig. 5.9B). Breakdown of the grades of lesions observed revealed a clear increase in PanIN1a and PanIN1b in $KCD6^{-/-}$ pancreata relative to KC pancreata (Fig. 5.13C). Whereas, $KCD5^{-/-}$ pancreata only display an increase in ADM lesions relative to KC pancreata, with similar numbers of each PanIN grade observed (Fig. 5.13C). These phenotypes are readily visible in the H&E stained pancreata (Fig. 5.11A). $KRas^{G12D}$ expression alone induces scattered ADM and PanIN formation amongst acinar tissue, whereas $KCD6^{-/-}$ pancreata typically display an increased number of tightly packed PanINs covering a larger area of the pancreas. In contrast, although they display a similar loss of acinar tissue to $KCD6^{-/-}$, $KCD5^{-/-}$ pancreata display more diffuse PanIN development with a larger proportion of the tissue covered by ADM lesions and reactive stroma (Fig. 5.11A).

DUSP6/MKP-3 loss also appears to accelerate the progression of pancreatic cancer precursor lesions towards higher, more dysplastic grades. A higher proportion of PanIN1b and PanIN2 are present in KCD6$^{-/-}$, relative to KC, pancreata (Fig. 5.13D) and more KCD6$^{-/-}$ mice present with PanIN2 or PanIN3 than KC mice (Fig. 5.13E). In contrast, DUSP5 loss does not seem to accelerate KRas^{G12D}-driven PanIN progression (Fig. 5.13D), and the observation that more KCD5$^{-/-}$ pancreata present with PanIN2 than KC pancreata could be explained by the increased or accelerated initiation of tumourigenesis occurring following DUSP5 loss (Fig. 5.9A-C).

Overall, the histological analysis of age-matched pancreata demonstrates that loss of either DUSP5 or DUSP6/MKP-3 accelerates or increases the KRas^{G12D}-induced initiation of ADM and PanINs (Fig. 5.9A-C & 5.13A-C). However, only the loss of DUSP6/MKP-3 is also able to promote accelerated progression of pancreatic cancer precursor lesions to higher more dysplastic grades (Fig. 5.13D-E).

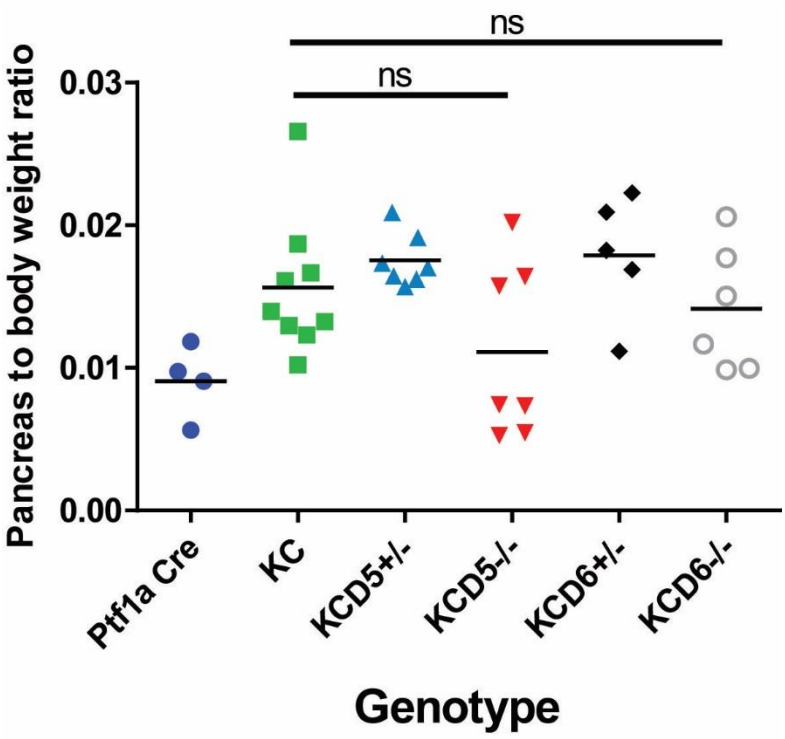

Figure 5.10 Loss of DUSP5 or DUSP6/MKP-3 causes no significant alteration in pancreatic weight in 100d mice, following the initiation of KRas^{G12D}-driven pancreatic tumourigenesis. Pancreata from 100 day age-matched mice of the indicated cohorts were harvested and their pancreas to body weight ratios calculated. Cohorts consisted of the following genotypes: KRas$^{+/+}$; Ptf1α-cre; DUSP$^{+/+}$ (Ptf1α-cre), KRas$^{LSL\text{-}G12D/+}$; Ptf1α-cre; DUSP$^{+/+}$ (KC), KRas$^{LSL\text{-}G12D/+}$; Ptf1α-cre; DUSP5$^{+/fl}$ (KCD5$^{+/-}$), KRas$^{LSL\text{-}G12D/+}$; Ptf1α-cre; DUSP5$^{fl/fl}$ (KCD5$^{-/-}$), KRas$^{LSL\text{-}G12D/+}$; Ptf1α-cre; DUSP6$^{+/fl}$ (KCD6$^{+/-}$) and KRas$^{LSL\text{-}G12D/+}$; Ptf1α-cre; DUSP6$^{fl/fl}$ (KCD6$^{-/-}$). Mean shown, n = 4, 9, 7, 7, 4, 6. Ns = not significant, using one-way ANOVA and Bonferroni post hoc test.

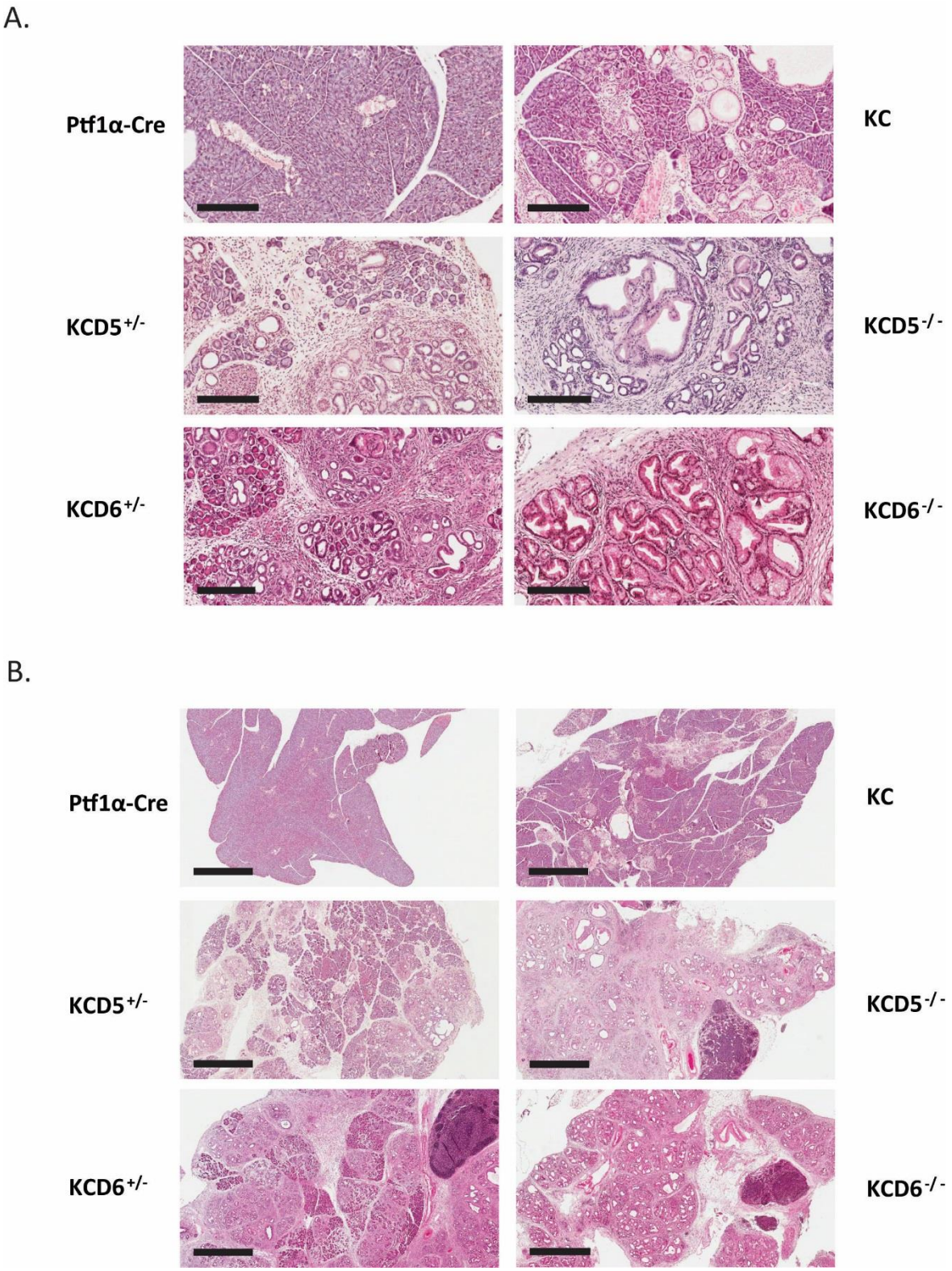

Figure 5.11 Loss of DUSP5 or DUSP6/MKP-3 promotes increased KRas^{G12D}-driven ADM and PanIN initiation, in 100d mice. Representative images of H&E stained pancreata from 100 day age-matched mice of the indicated cohorts, with a 200μm **(A)** or 1mm **(B)** scale. Cohorts consisted of the following genotypes: KRas$^{+/+}$; Ptf1α-cre; DUSP$^{+/+}$ (Ptf1α-cre, n = 4), KRas$^{LSL\text{-}G12D/+}$; Ptf1α-cre; DUSP$^{+/+}$ (KC, n = 9), KRas$^{LSL\text{-}G12D/+}$; Ptf1α-cre; DUSP5$^{+/fl}$ (KCD5$^{+/-}$, n = 7), KRas$^{LSL\text{-}G12D/+}$; Ptf1α-cre; DUSP5$^{fl/fl}$ (KCD5$^{-/-}$, n = 7), KRas$^{LSL\text{-}G12D/+}$; Ptf1α-cre; DUSP6$^{+/fl}$ (KCD6$^{+/-}$, n = 4) and KRas$^{LSL\text{-}G12D/+}$; Ptf1α-cre; DUSP6$^{fl/fl}$ (KCD6$^{-/-}$, n = 6).

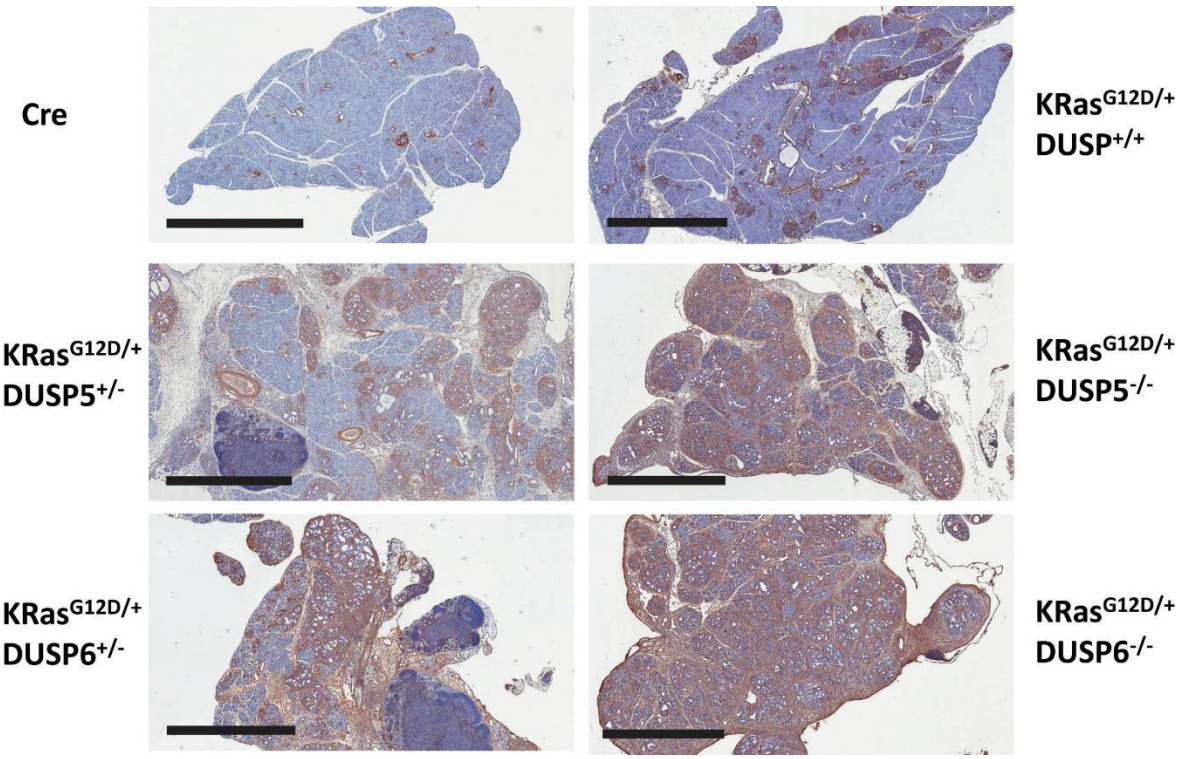

Figure 5.12 DUSP5 or DUSP6/MKP-3 loss promotes increased KRas^{G12D}-driven PanIN initiation and the formation of reactive stroma, in 100d mice. Representative images of αSMA IHC stained pancreata from 100 day age-matched mice of the indicated cohorts. Cohorts consisted of the following genotypes: KRas$^{+/+}$; Ptf1α-cre; DUSP$^{+/+}$ (Ptf1α-cre, n = 4), KRas$^{LSL\text{-}G12D/+}$; Ptf1α-cre; DUSP$^{+/+}$ (KC, n = 9), KRas$^{LSL\text{-}G12D/+}$; Ptf1α-cre; DUSP5$^{+/fl}$ (KCD5$^{+/-}$, n = 7), KRas$^{LSL\text{-}G12D/+}$; Ptf1α-cre; DUSP5$^{fl/fl}$ (KCD5$^{-/-}$, n = 7), KRas$^{LSL\text{-}G12D/+}$; Ptf1α-cre; DUSP6$^{+/fl}$ (KCD6$^{+/-}$, n = 4) and KRas$^{LSL\text{-}G12D/+}$; Ptf1α-cre; DUSP6$^{fl/fl}$ (KCD6$^{-/-}$, n = 6).Scale, 2mm.

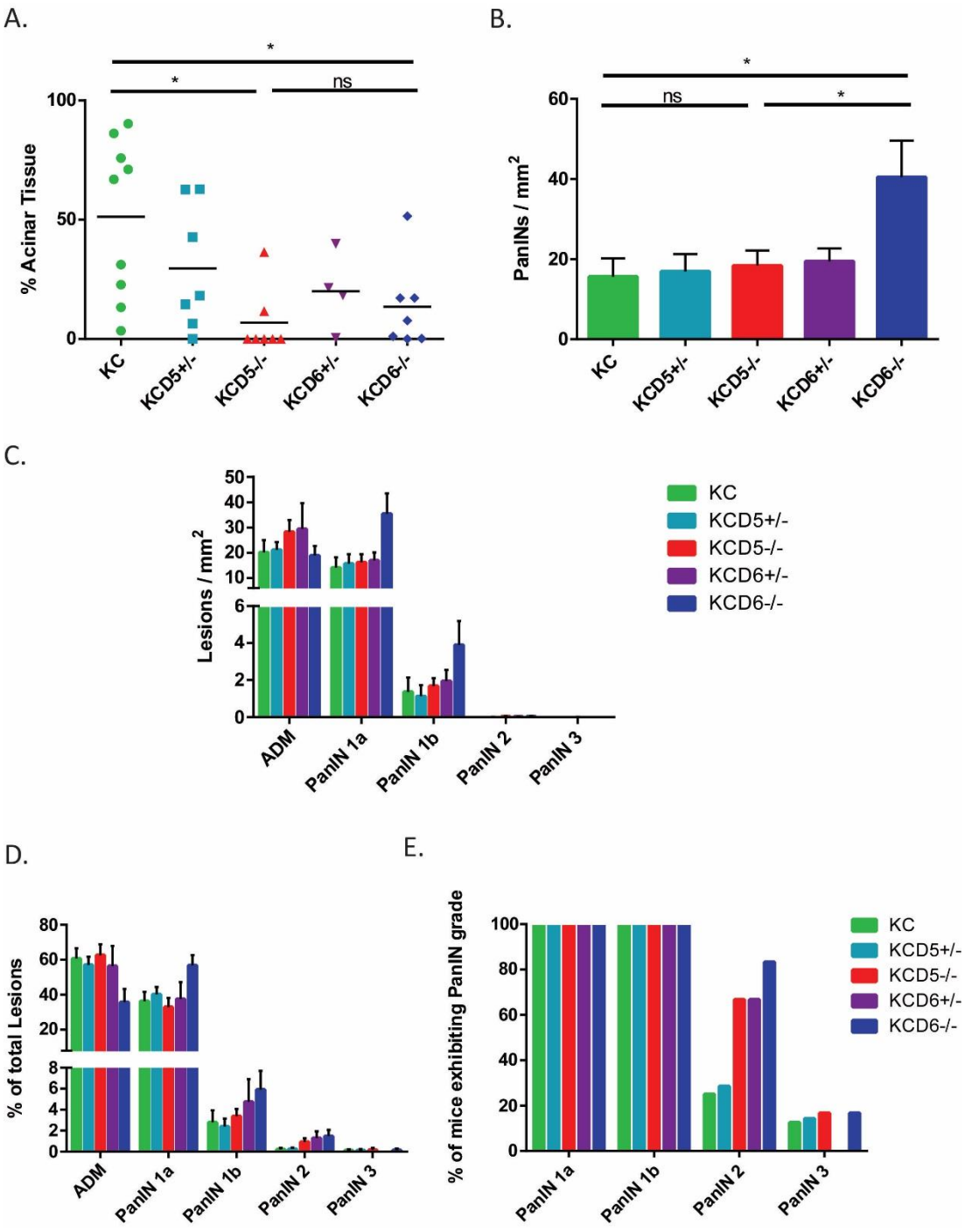

Figure 5.13 Loss of DUSP5 or DUSP6/MKP-3 promotes increased KRas^{G12D}-driven ADM and PanIN initiation, in 100d mice. Quantification of the pancreatic precursor lesion development in 100 day age-matched pancreata of the indicated cohorts. Cohorts consisted of the following genotypes: KRas$^{LSL\text{-}G12D/+}$; Ptf1α-cre; DUSP$^{+/+}$ (KC), KRas$^{LSL\text{-}G12D/+}$; Ptf1α-cre; DUSP5$^{+/fl}$ (KCD5$^{+/-}$), KRas$^{LSL\text{-}G12D/+}$; Ptf1α-cre; DUSP5$^{fl/fl}$ (KCD5$^{-/-}$), KRas$^{LSL\text{-}G12D/+}$; Ptf1α-cre; DUSP6$^{+/fl}$ (KCD6$^{+/-}$) and KRas$^{LSL\text{-}G12D/+}$; Ptf1α-cre; DUSP6$^{fl/fl}$ (KCD6$^{-/-}$). **A)** Percentage acinar tissue remaining in the pancreata of each cohort following KRas^{G12D}-driven ADM and PanIN initiation. **B)** Total number of PanINs of all histological grades per mm^2 in the indicated cohorts. **C-D)** Quantification of the number of pancreatic cancer precursor lesions, divided into each histological grade, per mm^2 in the indicated cohorts **(C)**, and these expressed as a percentage of the total number of lesions **(D). E)** Percentage of mice of the indicated cohorts that displayed at least one of each PanIN grade. Quantification performed on one representative section per mouse, following serial sectioning of the pancreas. Mean values ± SEM are shown, n = 9, 7, 7, 4, 6. Ns = not significant, *P < 0.05 using one-way ANOVA and Bonferroni post hoc test.

5.2.3.2 SerpinB2 does not mediate the increased initiation of ADM and PanINs following DUSP5 loss in KRas^{G12D}-expressing pancreata

We have previously shown that DUSP5 ablation promotes increased DMBA/TPA-induced skin carcinogenesis in a SerpinB2 dependent manner (Fig. 3.14) (Rushworth et al., 2014). Furthermore, endogenous KRas^{G12D} expression (Fig. 4.12-13), as well as TPA or exogenous expression of HRas^{Q61L} (Fig. 3.11), is able to induce the increased expression of SerpinB2 in DUSP5 knockout MEFs, relative to wild-type. Therefore, we investigated whether SerpinB2 overexpression, induced by KRas^{G12D} and DUSP5 loss, might also be involved in the increased initiation of ADM and PanINs observed in KCD5$^{-/-}$ pancreata, relative to KC counterparts.

Before performing such experiments we initially examined whether SerpinB2 is expressed in the pancreas. SerpinB2 expression has not been reported in the murine pancreas in any previously published studies; however microarray and RNA-sequencing datasets show that low levels of SerpinB2 mRNA are present in the human pancreas (http://www.genecards.org/cgi-bin/carddisp.pl?gene=SerpinB2). Furthermore, multiple studies have detected SerpinB2 mRNA and protein in human pancreatic cancer tissue (Takeuchi et al., 1993; Wojtukiewicz et al., 2001; Xue et al., 2008), however in these studies high SerpinB2 expression correlated with improved survival. This might indicate that elevated SerpinB2 expression, induced following DUSP5 loss, is unlikely to promote the development of KRas^{G12D}-driven pancreatic cancer. However, it is possible that SerpinB2 plays opposing roles in the initiation of tumours and their later maintenance, malignant growth and metastasis, in much the same manner in which TGFβ is known to switch between functioning either as a tumour suppressor or an oncogene during cancer development (Massagué, 2008, 2012).

To confirm that SerpinB2 is expressed in the murine pancreas we isolated mRNA from wild-type, DUSP5$^{-/-}$ and SerpinB2$^{-/-}$ mice and compared the expression level of SerpinB2 mRNA in the pancreas with that of the skin, which we already knew to express significant levels of SerpinB2 (Fig. 3.13B). This revealed that SerpinB2 mRNA is expressed in the murine pancreas, although at much lower levels than in the skin (Fig. 5.14A). Furthermore, pancreatic SerpinB2 expression is increased following DUSP5 loss (Fig. 5.14A). Together this evidence suggests it might be formally possible for increased

SerpinB2 expression to promote the increased initiation of $KRas^{G12D}$-driven pancreatic tumourigenesis observed following DUSP5 loss. To investigate this hypothesis, SerpinB2 knockout mice were crossed with the $KRas^{LSL\text{-}G12D/+}$; Ptf1α-Cre (KC) and $KRas^{LSL\text{-}G12D/+}$; Ptf1α-Cre; $DUSP5^{fl/fl}$ ($KCD5^{-/-}$) strains, resulting in the generation of additional $KRas^{LSL\text{-}G12D/+}$; Ptf1α-Cre; $SerpinB2^{-/-}$ ($KCSB2^{-/-}$) and $KRas^{LSL\text{-}G12D/+}$; Ptf1α-Cre; $DUSP5^{fl/fl}$; $SerpinB2^{-/-}$ (KCDKO) strains. Age-matched cohorts of 56 day old mice of all genotypes were generated and the development of $KRas^{G12D}$-driven pancreatic cancer assessed in each cohort. Both the $KCSB2^{-/-}$ and KCDKO cohorts displayed no significant change in their pancreas to body weight ratio relative to their respective SerpinB2 containing cohorts (KC and $KCD5^{-/-}$) (Fig. 5.14B). Histologically $KRas^{G12D}$-expressing, DUSP5 wild-type pancreata appeared very similar in the presence or absence of SerpinB2 (Fig. 5.15). Furthermore, a quantitative analysis of representative stained tissue sections revealed that deletion of SerpinB2 caused no significant changes in the amount of pancreatic tissue undergoing ADM (Fig. 5.16A), the numbers of pancreatic pre-neoplastic lesions (Fig. 5.16B-C) or the rate at which these progress (Fig. 5.16D-E).

SerpinB2 ablation also had no effect on the initiation of ADM and PanINs following $KRas^{G12D}$-driven tumourigenesis in the absence of DUSP5 (Fig. 5.15-16). KCDKO pancreata displayed the expected high levels of acinar atrophy, a high burden of ADM and numbers of PanINs that were directly comparable to those seen in our $KCD5^{-/-}$ pancreata, representing a significant increase over the KC and $KCSB2^{-/-}$ pancreata (Fig. 5.15 & 5.16A-C). Furthermore, the rate of progression of ADM and PanIN lesions was not significantly different between the $KCD5^{-/-}$ and KCDKO pancreata. Overall, these experiments demonstrate that in contrast to our observations in the $HRas^{Q61L}$-driven murine model of skin carcinogenesis (Fig. 3.14; Rushworth et al., 2014), SerpinB2 ablation has no effect on the initiation of $KRas^{G12D}$-driven pancreatic tumourigenesis in either the presence or absence of DUSP5 and is therefore not responsible for mediating the effects of DUSP5 loss in $KRas^{G12D}$-driven pancreatic tumourigenesis.

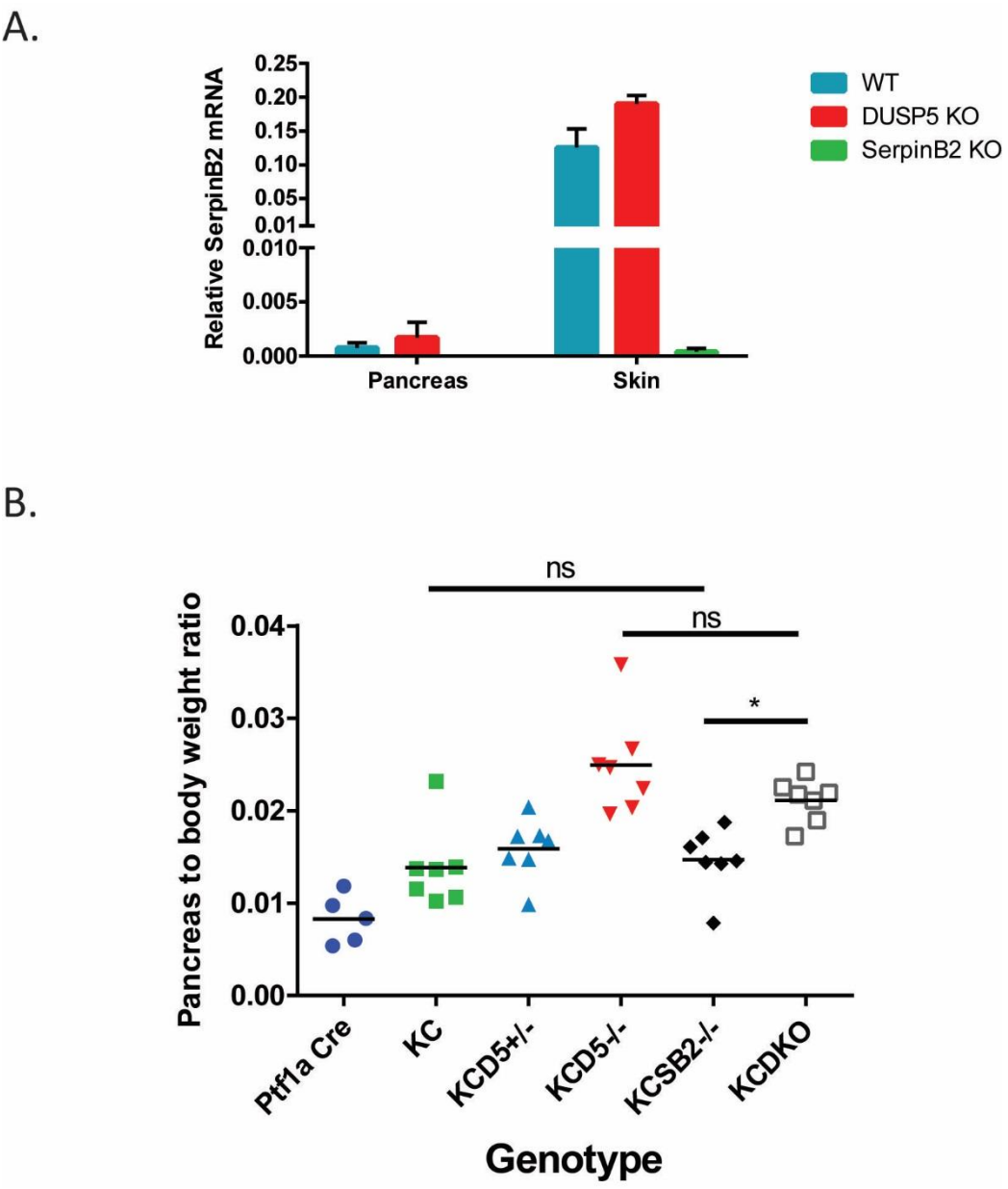

Figure 5.14 SerpinB2 is expressed in the pancreas, yet its ablation has no effect on pancreatic weight following the initiation of KRas^{G12D}-driven pancreatic tumourigenesis. A) Taqman qRT-PCR assay showing mRNA levels of SerpinB2, relative to β-actin, following RNA isolation from the skin and pancreas from mice of the indicated genotypes. Representative figure from age-matched littermate mice. Mean values ± SEM are shown, n=3. **B)** Pancreata from 56 day age-matched mice of the indicated cohorts were harvested and their pancreas to body weight ratios calculated. Cohorts consisted of the following genotypes: KRas$^{+/+}$; Ptf1α-cre; DUSP$^{+/+}$; SerpinB2$^{+/+}$ (Ptf1α-cre), KRas$^{LSL\text{-}G12D/+}$; Ptf1α-cre; DUSP$^{+/+}$; SerpinB2$^{+/+}$ (KC), KRas$^{LSL\text{-}G12D/+}$; Ptf1α-cre; DUSP5$^{+/fl}$; SerpinB2$^{+/+}$ (KCD5$^{+/-}$), KRas$^{LSL\text{-}G12D/+}$; Ptf1α-cre; DUSP5$^{fl/fl}$; SerpinB2$^{+/+}$ (KCD5$^{-/-}$), KRas$^{LSL\text{-}G12D/+}$; Ptf1α-cre; DUSP5$^{+/+}$; SerpinB2$^{-/-}$ (KCSB2$^{-/-}$) and KRas$^{LSL\text{-}G12D/+}$; Ptf1α-cre; DUSP5$^{fl/fl}$; SerpinB2$^{-/-}$ (KCDKO). Mean shown, n = 5, 7, 7, 7, 7, 7. Ns = not significant, *P < 0.05, using one-way ANOVA and Bonferroni post hoc test.

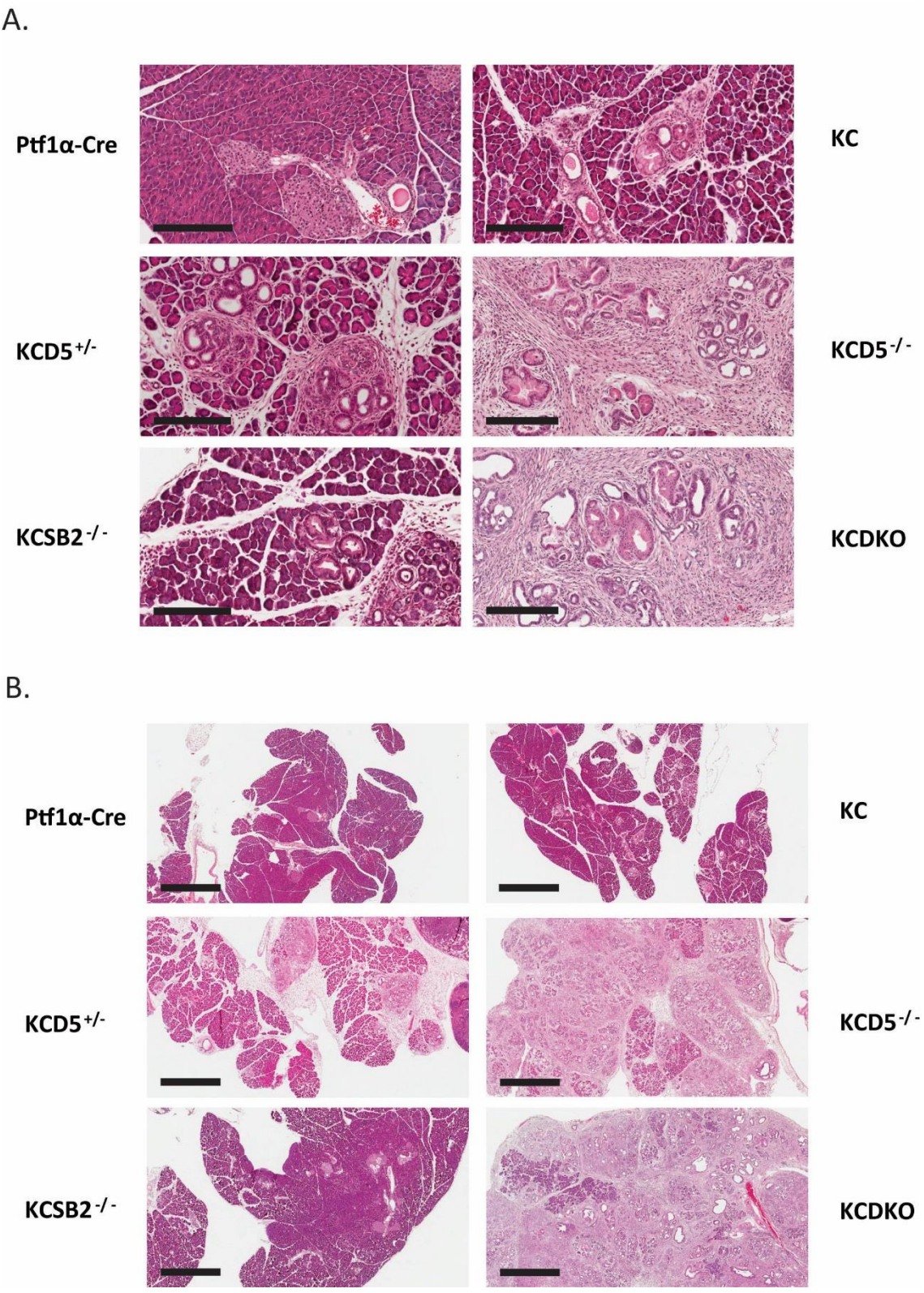

Figure 5.15 Co-ablation of SerpinB2 does not rescue the increased KRas^{G12D}-driven PanIN initiation observed following DUSP5 loss. Representative images of H&E stained pancreata from 56 day age-matched mice of the indicated cohorts, with a 200μm **(A)** or 1mm **(B)** scale. Cohorts consisted of the following genotypes: KRas$^{+/+}$; Ptf1α-cre; DUSP$^{+/+}$; SerpinB2$^{+/+}$ (Ptf1α-cre, n = 5), KRas$^{LSL-G12D/+}$; Ptf1α-cre; DUSP$^{+/+}$; SerpinB2$^{+/+}$ (KC, n = 7), KRas$^{LSL-G12D/+}$; Ptf1α-cre; DUSP5$^{+/fl}$; SerpinB2$^{+/+}$ (KCD5$^{+/-}$, n = 7), KRas$^{LSL-G12D/+}$; Ptf1α-cre; DUSP5$^{fl/fl}$; SerpinB2$^{+/+}$ (KCD5$^{-/-}$, n = 7), KRas$^{LSL-G12D/+}$; Ptf1α-cre; DUSP5$^{+/+}$; SerpinB2$^{-/-}$ (KCSB2$^{-/-}$, n = 7) and KRas$^{LSL-G12D/+}$; Ptf1α-cre; DUSP5$^{fl/fl}$; SerpinB2$^{-/-}$ (KCDKO, n = 7).

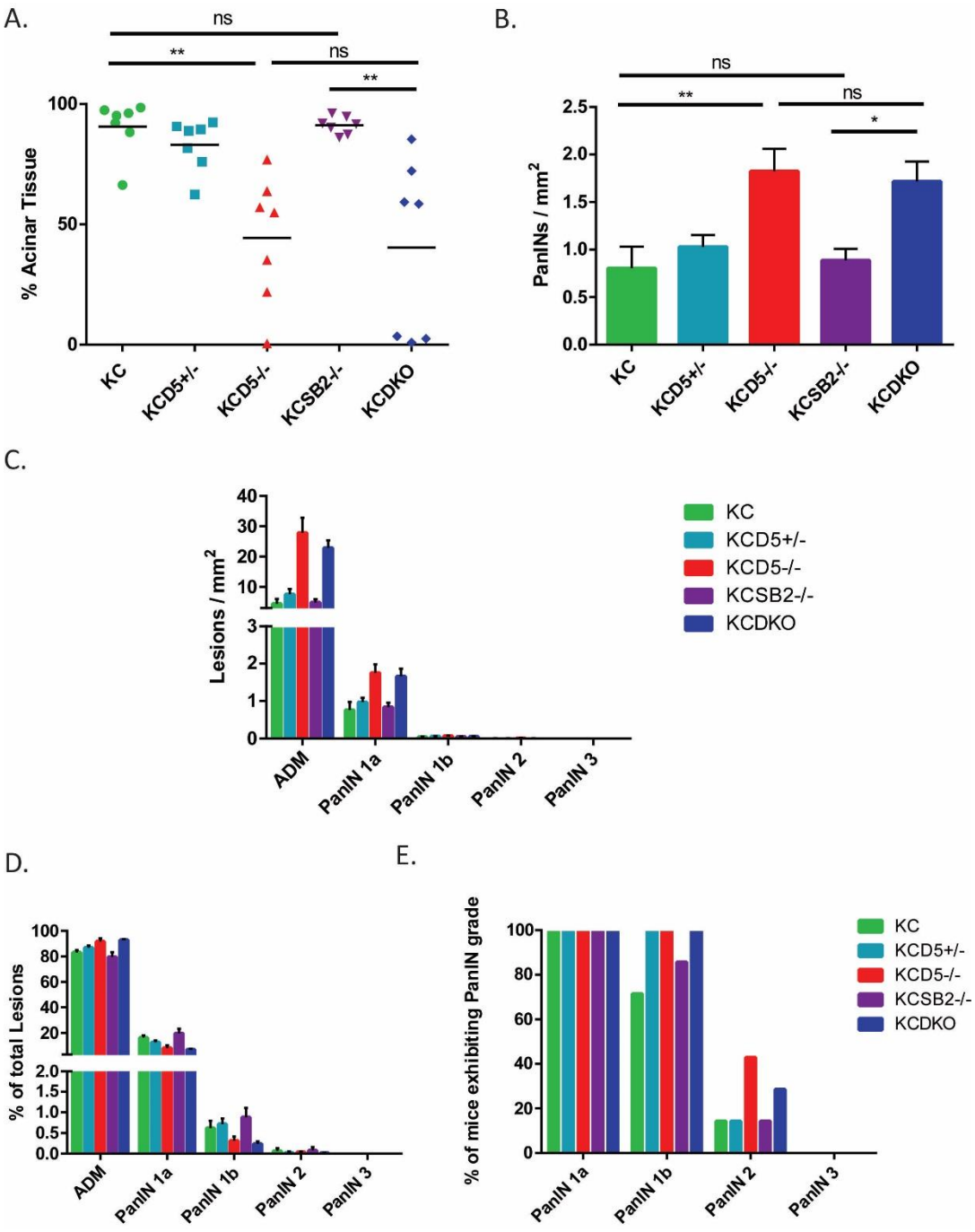

Figure 5.16 Co-ablation of SerpinB2 does not rescue the increased KRas^{G12D}-driven PanIN initiation observed following DUSP5 loss. Quantification of the pancreatic precursor lesion development in 56 day age-matched pancreata of the indicated cohorts Cohorts consisted of the following genotypes: KRas$^{+/+}$; Ptf1α-cre; DUSP$^{+/+}$; SerpinB2$^{+/+}$ (Ptf1α-cre), KRas$^{LSL-G12D/+}$; Ptf1α-cre; DUSP$^{+/+}$; SerpinB2$^{+/+}$ (KC), KRas$^{LSL-G12D/+}$; Ptf1α-cre; DUSP5$^{+/fl}$; SerpinB2$^{+/+}$ (KCD5$^{+/-}$), KRas$^{LSL-G12D/+}$; Ptf1α-cre; DUSP5$^{fl/fl}$; SerpinB2$^{+/+}$ (KCD5$^{-/-}$), KRas$^{LSL-G12D/+}$; Ptf1α-cre; DUSP5$^{+/+}$; SerpinB2$^{-/-}$ (KCSB2$^{-/-}$) and KRas$^{LSL-G12D/+}$; Ptf1α-cre; DUSP5$^{fl/fl}$; SerpinB2$^{-/-}$ (KCDKO). **A)** Percentage acinar tissue remaining in the pancreata of each cohort following KRas^{G12D}-driven ADM and PanIN initiation. **B)** Total number of PanINs of all histological grades per mm^2 in the indicated cohorts. **C-D)** Quantification of the number of pancreatic cancer precursor lesions, divided into each histological grade, per mm^2 in the indicated cohorts **(C)**, and these expressed as a percentage of the total number of lesions **(D)**. **E)** Percentage of mice of the indicated cohorts that displayed at least one of each PanIN grade. Quantification performed on one representative section per mouse, following serial sectioning of the pancreas. Mean values ± SEM are shown, n = 7. Ns = not significant, *P < 0.05, **P < 0.01, using one-way ANOVA and Bonferroni post hoc test.

5.2.3.3 Loss of DUSP5 or DUSP6/MKP-3 promotes increased pancreatic metaplasia, but does not influence either PanIN proliferation or senescence.

So far we have demonstrated that the loss of either DUSP5 or DUSP6/MKP-3 increases $KRas^{G12D}$-induced initiation of ADM and PanINs (Fig. 5.9A-C & 5.13A-C), and the loss of DUSP6/MKP-3 is able to promote accelerated PanIN progression (Fig. 5.13D-E). Therefore, to investigate the mechanism by which the loss of either DUSP5 or DUSP6/MKP-3 is able to promote these phenotypes, aged-matched tissue from each cohort was subjected to immunohistochemical analysis for established markers of KRas effector pathway activation and of cellular phenotypes, such as proliferation or senescence.

Initially, we attempted to determine whether DUSP5 and/or DUSP6/MKP-3 expression is elevated in $KRas^{G12D}$-driven PanINs. We hypothesised that this would be occurring as we have previously demonstrated that endogenous $KRas^{G12D}$ expression in MEFs induces a robust induction of DUSP5 and DUSP6/MKP-3 expression (Fig. 4.3-4 & 4.8-9). Furthermore, DUSP6/MKP-3 has been shown to be overexpressed in PanINs, before its subsequent downregulation in invasive carcinoma, in human pancreatic cancer tissue (Furukawa et al., 2003, 2005). However, unfortunately the most specific DUSP5 and DUSP6/MKP-3 antibodies available (as determined by immunoblotting) produced strong, non-specific background staining in their respective DUSP knockout pancreatic tissues when utilised for IHC (Fig. 5.17A-B). Specific staining in DUSP wild-type tissue could not be observed for either antibody even following extensive titration and use of very low antibody concentrations for IHC. Consequently, in an attempt to identify potential changes in pancreatic DUSP5 and/or DUSP6/MKP-3 expression following $KRas^{G12D}$ expression and PanIN formation, RNA was isolated from 100 day KRas wild-type (Ptf1α-Cre) and $KRas^{G12D}$-expressing (KC) pancreata and analysed via qRT-PCR. Pancreatic $KRas^{G12D}$ expression induced a significant increase in DUSP5 expression and a marginal increase in DUSP6/MKP-3 expression when compared to wild-type (Fig. 5.17C). The high variability of this experiment, and lack of a significant increase in DUSP6/MKP-3 expression, is likely to be due to the imprecise nature of this experiment. RNA was isolated from multiple 100 day $KRas^{G12D}$-expressing pancreata, however there is significant variability in the amount of pancreatic tumourigenesis initiated in these tissues (Fig. 5.17D). Therefore, as pancreatic samples taken for RNA extraction were isolated

from the whole pancreas, without histological examination and microdissection of the regions extracted, some samples could still contain a high proportion of normal acinar tissue and relatively few $KRas^{G12D}$-expressing PanINs, potentially decreasing the levels of DUSP expression we could detect.

DUSP5 and DUSP6/MKP-3 are ERK-specific MKPs (Groom et al., 1996; Mandl et al., 2005; Mourey et al., 1996), therefore it could be hypothesised that their loss could specifically modulate Ras-ERK pathway activity following expression of mutant $KRas^{G12D}$, whereas other Ras effector pathways such as the PI3K-AKT pathway would be unaffected. To test this theory tissue sections from 56 day age-matched pancreata were immunohistochemically stained for both *p*-ERK (Fig. 5.18) and *p*-AKT (Fig. 5.19). IHC staining was quantified utilising the H-score system (Detre et al., 1995). In this system the percentage of cells displaying weak, medium or strong staining are quantified, then a H-score out of 300 generated using the following formula: H-score = (% of cells stained at "weak" intensity x 1) + (% of cells stained at "medium" intensity x 2) + (% of cells stained at "strong" intensity x 3). DUSP5 loss induced a significant increase in nuclear *p*-ERK levels in $KRas^{G12D}$-driven PanINs, yet had no effect on the relative levels of cytoplasmic *p*-ERK or nuclear/cytoplasmic *p*-AKT (Fig. 5.18A & 5.19A). This most likely reflects the role of DUSP5 as a nuclear, ERK-specific MKP (Mandl et al., 2005). In contrast DUSP6/MKP-3 loss caused no significant changes in nuclear or cytoplasmic *p*-ERK or *p*-AKT levels in $KRas^{G12D}$-driven PanINs (Fig. 5.18B & 5.19B). There was a slight trend towards increased cytoplasmic pERK levels following DUSP6/MKP-3 loss, which could be indicative of the loss of a cytoplasmic, ERK-specific MKP (Groom et al., 1996; Mourey et al., 1996). Overall, in $KRas^{G12D}$-expressing PanINs DUSP5 loss induces a clear increase in nuclear *p*-ERK levels and DUSP6/MKP-3 loss a marginal increase in cytoplasmic *p*-ERK, whereas loss of neither MKP affected levels of *p*-AKT. The more limited effect of DUSP6/MKP-3 loss on *p*-ERK levels could reflect an increased capacity for other cytoplasmic negative feedback regulators of ERK to compensate for DUSP6/MKP-3 loss, or the fact the cytoplasmic staining is more diffuse making the quantification of relatively small changes in level more difficult to observe.

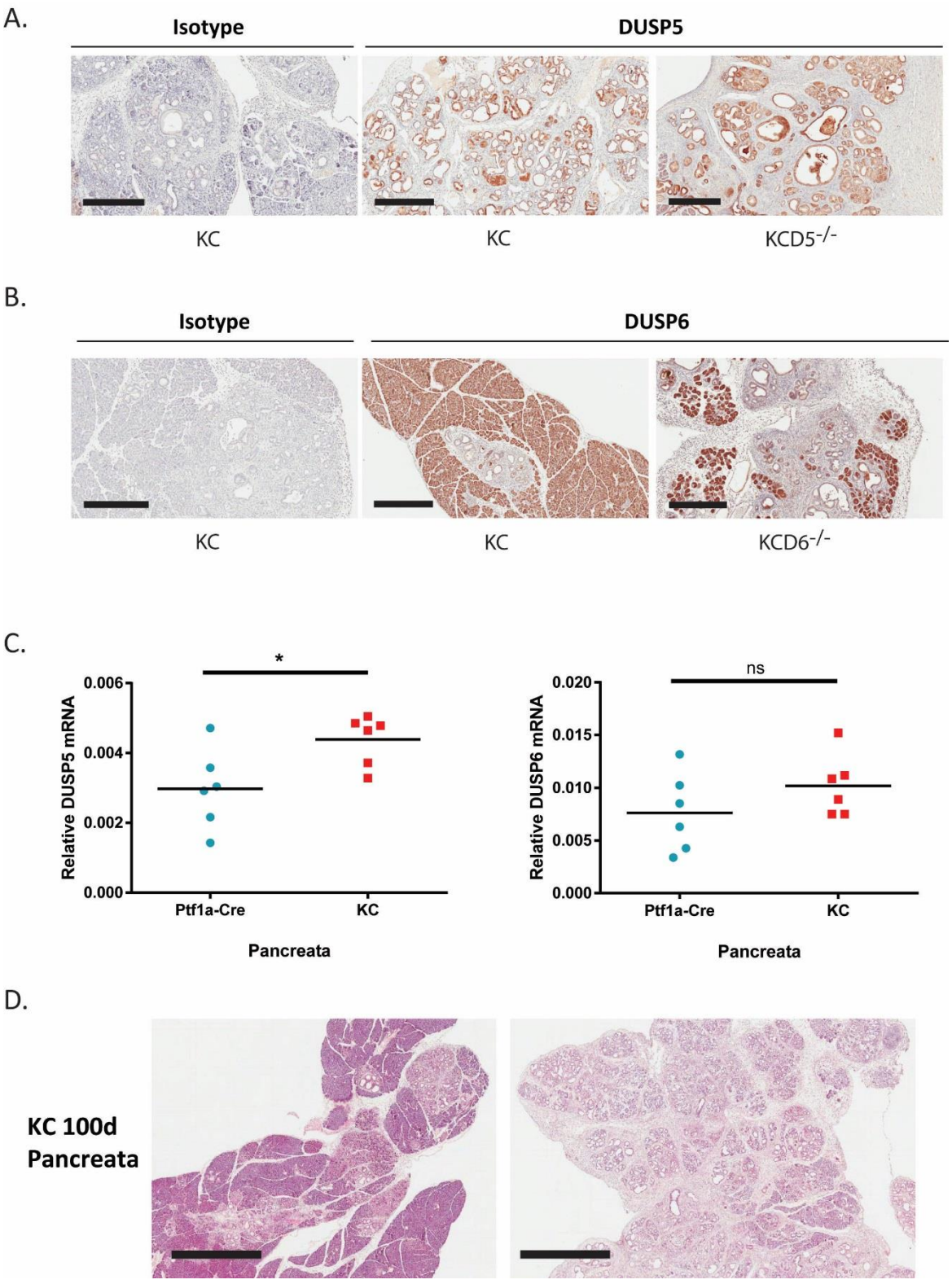

Figure 5.17 Pancreatic KRas^{G12D} expression increases MKP expression. A) Representative images of IHC using a DUSP5 rabbit monoclonal or isotype control antibody on 56 day age-matched pancreata of the indicated cohorts. **B)** Representative images of IHC using a DUSP6/MKP-3 rabbit monoclonal or isotype control antibody on 56 day age-matched pancreata of the indicated cohorts. **C)** Taqman qRT-PCR assays showing mRNA levels of DUSP5 or DUSP6/MKP-3, relative to β-actin, following RNA isolation from 100 day pancreata of the indicated cohorts. Mean shown, n = 6 ns = not significant, *P < 0.05, using an unpaired t-test. **D)** Representative images of H&E stained KRas$^{LSL\text{-}G12D/+}$; Ptf1α-cre 100 day pancreata. Scale, 1mm. Cohorts consisted of the following genotypes: KRas$^{+/+}$; Ptf1α-cre; DUSP$^{+/+}$ (Ptf1α-cre), KRas$^{LSL\text{-}}$

$^{G12D/+}$; Ptf1α-cre; DUSP$^{+/+}$ (KC), KRas$^{LSL-G12D/+}$; Ptf1α-cre; DUSP5$^{fl/fl}$ (KCD5$^{-/-}$) and KRas$^{LSL-G12D/+}$; Ptf1α-cre; DUSP6$^{fl/fl}$ (KCD6$^{-/-}$).

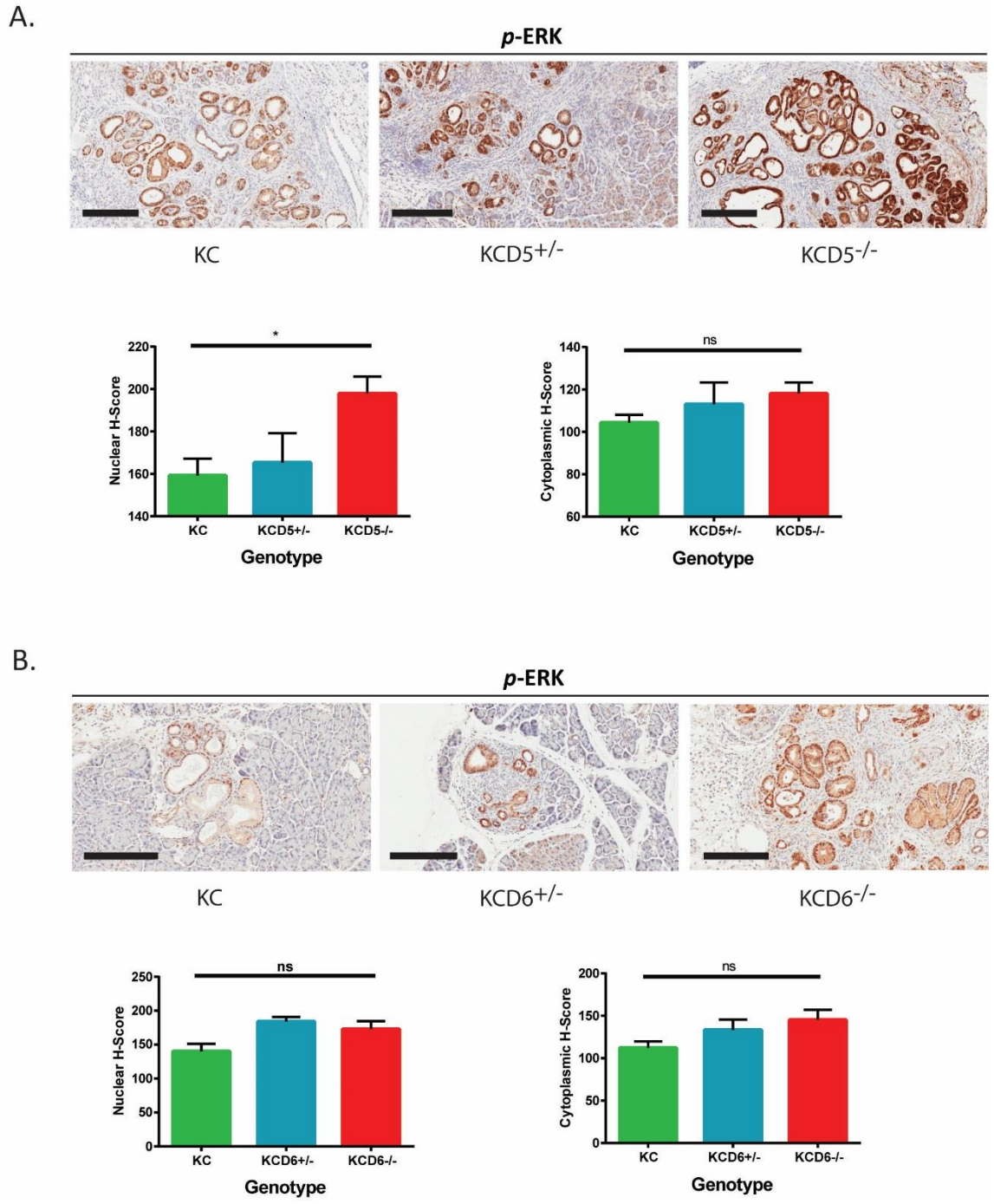

Figure 5.18 DUSP5 loss promotes elevated nuclear p-ERK levels in KRas^{G12D}-driven PanINs. Representative images and H-score quantification of *p*-ERK IHC on 56 day age-matched pancreata of the indicated cohorts. All cohorts contained the KRas$^{LSL-G12D/+}$ and Ptf1α-cre and only varied with respect to their DUSP5 **(A)** or DUSP6/MKP-3 **(B)** genotype: KRas$^{LSL-G12D/+}$; Ptf1α-cre; DUSP$^{+/+}$ (KC), KRas$^{LSL-G12D/+}$; Ptf1α-cre; DUSP5$^{+/fl}$ (KCD5$^{+/-}$), KRas$^{LSL-G12D/+}$; Ptf1α-cre; DUSP5$^{fl/fl}$ (KCD5$^{-/-}$), KRas$^{LSL-G12D/+}$; Ptf1α-cre; DUSP6$^{+/fl}$ (KCD6$^{+/-}$) and KRas$^{LSL-G12D/+}$; Ptf1α-cre; DUSP6$^{fl/fl}$ (KCD6$^{-/-}$). Mean values ± SEM are shown, n = 7. Ns = not significant, *P < 0.05, using one-way ANOVA and Bonferroni post hoc test. Scale, 200μm.

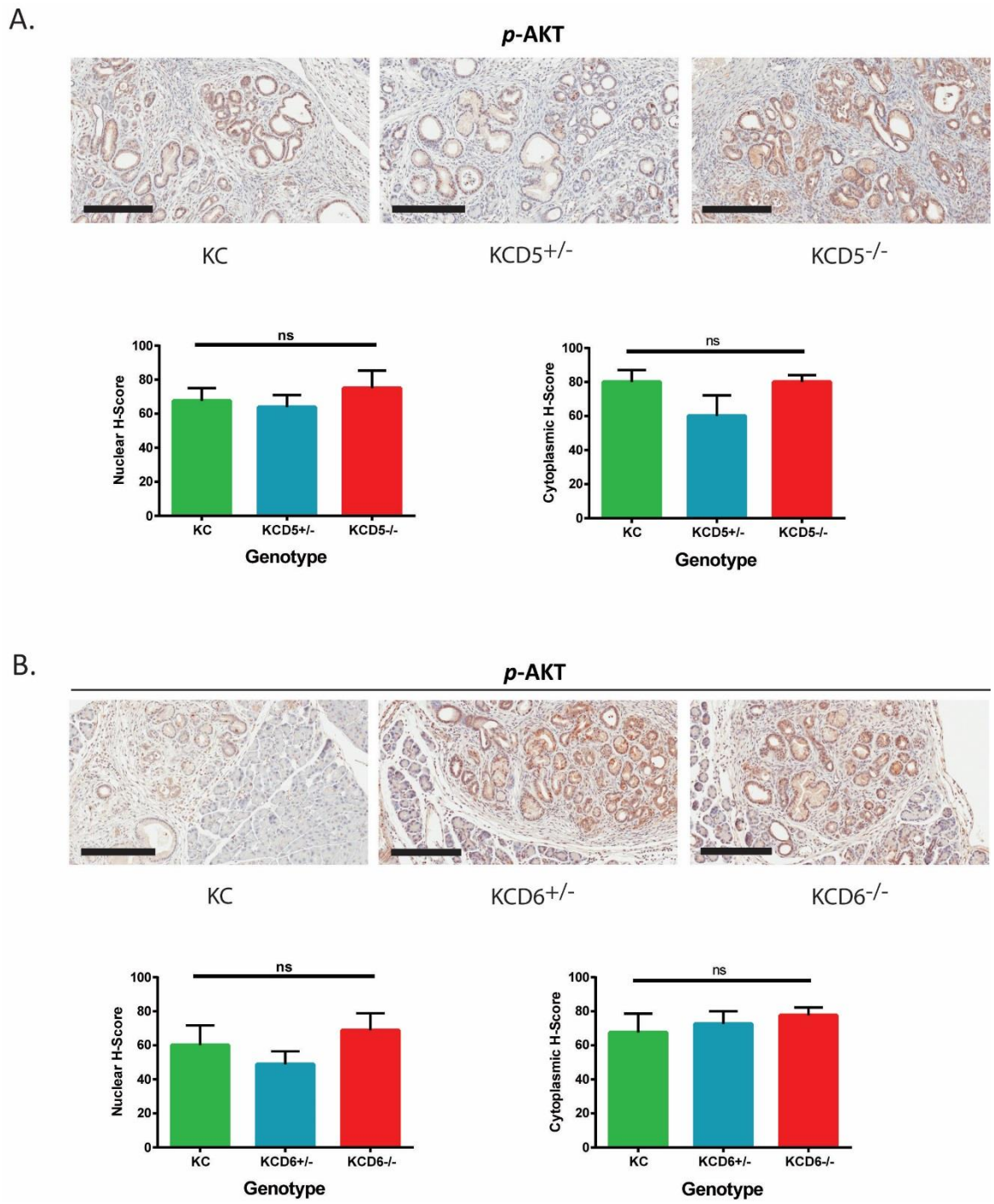

Figure 5.19 DUSP5 or DUSP6/MKP-3 loss has no effect on *p*-AKT level in KRas^{G12D}-driven PanINs. Representative images and H-score quantification of *p*-AKT IHC on 56 day age-matched pancreata of the indicated cohorts. All cohorts contained the KRas$^{LSL\text{-}G12D/+}$ and Ptf1α-cre alleles and only varied with respect to their DUSP5 **(A)** or DUSP6/MKP-3 **(B)** genotype: KRas$^{LSL\text{-}G12D/+}$; Ptf1α-cre; DUSP$^{+/+}$ (KC), KRas$^{LSL\text{-}G12D/+}$; Ptf1α-cre; DUSP5$^{+/fl}$ (KCD5$^{+/-}$), KRas$^{LSL\text{-}G12D/+}$; Ptf1α-cre; DUSP5$^{fl/fl}$ (KCD5$^{-/-}$), KRas$^{LSL\text{-}G12D/+}$; Ptf1α-cre; DUSP6$^{+/fl}$ (KCD6$^{+/-}$) and KRas$^{LSL\text{-}G12D/+}$; Ptf1α-cre; DUSP6$^{fl/fl}$ (KCD6$^{-/-}$). Mean values ± SEM are shown, n = 7. Ns = not significant, *P < 0.05, using one-way ANOVA and Bonferroni post hoc test. Scale, 200μm.

Loss of either DUSP5 or DUSP6/MKP-3 promoted increased $KRas^{G12D}$-driven metaplasia of pancreatic acinar tissue and the formation of ductal precursor lesions of pancreatic cancer (Fig. 5.9A-C & 5.13A-C). To explore this initiation phenotype in more detail we performed IHC for Sox9 on age-matched 56 day pancreata of all cohorts (Fig. 5.20). Sox9 is a transcription factor, which in the pancreas specifies a ductal fate (Belo et al., 2013). Sox9 expression has been identified in acinar cells following $KRas^{G12D}$ expression prior to metaplasia to a duct-like state, as well as in developing ADM or PanIN lesions (Kopp et al., 2012). Furthermore, Sox9 expression is essential for $KRas^{G12D}$-mediated ADM and PanIN induction, with Sox9 knockout pancreata being completely refractory to $KRas^{G12D}$-mediated transformation. Additionally, the ectopic overexpression of Sox9 in the pancreas potentiates $KRas^{G12D}$-mediated ADM and PanIN formation (Kopp et al., 2012).

Sox9 expression was significantly elevated in the acinar tissue of both $KCD5^{-/-}$ and $KCD6^{-/-}$ pancreata, when compared to KC pancreata (Fig. 5.20). This is in addition to these $KCD5^{-/-}$ and $KCD6^{-/-}$ pancreata displaying an increased burden of ADM and PanIN lesions relative to KC pancreata at this age (Fig. 5.9), these lesions also stain positive for Sox9 due to their ductal differentiation, and thus were not included in this analysis. These data demonstrate that effects of DUSP5 or DUSP6/MKP-3 loss are occurring in the $KRas^{G12D}$-expressing acinar tissue prior to ADM or PanIN lesions forming. This indicates that the loss of DUSP5 or DUSP6/MKP-3 is able to potentiate $KRas^{G12D}$-driven acinar metaplasia, which is then responsible for enabling the formation of the elevated burden of ADM and PanIN lesions observed. However, we have not yet determined whether DUSP5 or DUSP6/MKP-3 loss are directly responsible for this increased acinar Sox9 expression and that this is the mechanism by which their loss is actually able to promote the increased initiation of $KRas^{G12D}$-driven pancreatic cancer. Alternatively, Sox9 expression could be induced as a consequence of ADM, which could in theory be promoted through a quite distinct mechanism upon the loss of DUSP5 or DUSP6/MKP-3.

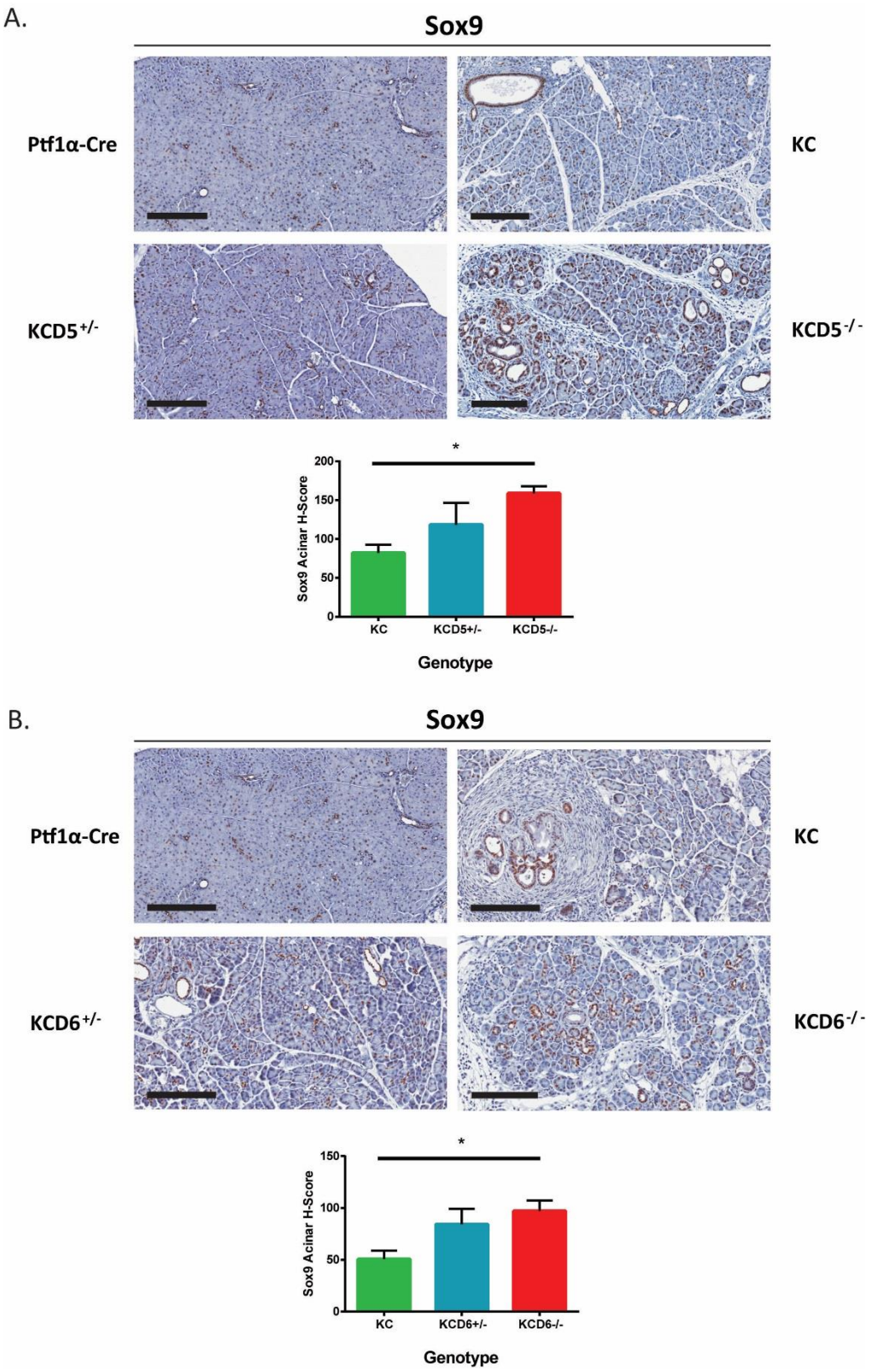

Figure 5.20 Loss of DUSP5 or DUSP6/MKP-3 promotes increased Sox9 expression in the pancreatic acinar tissue following KRas^{G12D}-driven pancreatic tumourigenesis. Representative images and H-score quantification of Sox9 IHC on 56 day age-matched pancreata of the indicated cohorts. All cohorts contained the KRas$^{LSL\text{-}G12D/+}$ and Ptf1α-cre alleles and only varied with respect to their DUSP5 **(A)** or DUSP6/MKP-3 (**B**) genotype: KRas$^{LSL\text{-}G12D/+}$; Ptf1α-cre; DUSP$^{+/+}$ (KC), KRas$^{LSL\text{-}G12D/+}$; Ptf1α-cre; DUSP5$^{+/fl}$ (KCD5$^{+/-}$), KRas$^{LSL\text{-}G12D/+}$; Ptf1α-cre; DUSP5$^{fl/fl}$ (KCD5$^{-/-}$), KRas$^{LSL\text{-}G12D/+}$; Ptf1α-cre; DUSP6$^{+/fl}$ (KCD6$^{+/-}$) and KRas$^{LSL\text{-}G12D/+}$; Ptf1α-cre; DUSP6$^{fl/fl}$ (KCD6$^{-/-}$). Mean values ± SEM are shown, n = 7. Ns = not significant, *P < 0.05, using one-way ANOVA and Bonferroni post hoc test. Scale, 200μm.

DUSP6/MKP-3 loss promoted accelerated $KRas^{G12D}$-driven PanIN progression, whereas loss of DUSP5 did not (Fig. 5.13D-E). To investigate potential cellular mechanisms mediating these phenotypes we performed immunohistochemical analysis for markers of proliferation (Ki67), senescence (p53 & p21) and apoptosis (cleaved Caspase 3) on age-matched pancreatic tissue. Ki67 is a marker of cell proliferation which is expressed during G_1, S, G_2 and mitotic phases of the cell cycle and is only absent during either quiescence or in the G_0 phase (Lopez et al., 1991; Scholzen and Gerdes, 2000). Quantification of the average number of Ki67-positive cells per PanIN revealed that loss of neither DUSP5 nor DUSP6/MKP-3 alters the proliferation rate of $KRas^{G12D}$-driven PanINs in either 56 day (Fig. 5.21A) or 100 day (Fig. 5.21B) pancreata.

It has been established previously established that PanINs express many components of the senescence response including, p53, p21, p16INK4A and p19, and that either the loss or mutation of the genes encoding these tumour suppressors can result in accelerated PanIN progression and the development of invasive, metastatic PDAC (Aguirre et al., 2003; Bardeesy et al., 2006; Guerra et al., 2007; Hingorani et al., 2005; Morton et al., 2010). This suggests that the senescence system is activated in response to oncogenic activation of KRas, and this OIS response is constraining PanIN progression and tumour development. Consistent with these previous studies, we identified p53 (Fig. 5.22) and p21 (Fig. 5.23) expression in multiple cells across the majority of PanINs. However, H-score quantification of the extent and intensity of p53 and p21 staining did not reveal any significant changes in the expression of these senescence markers following either DUSP5 or DUSP6/MKP-3 loss in $KRas^{G12D}$-expressing pancreata (Fig. 5.22-23).

Finally, the induction of apoptosis in PanINs was assessed utilising cleaved-Caspase3 expression as a marker. Cleaved-Caspase3 expression was very low across all genotypes, being very rarely observed in PanIN cells (Fig. 5.24). Only cells which had been released into the lumen of PanINs stained positively for cleaved-Caspase3, these cells are probably undergoing anoikis (von Figura et al., 2014), and therefore act as an internal control. This low level of apoptosis in $KRas^{G12D}$-driven PanINs is consistent with previous studies (Rosenfeldt et al., 2013), and indicates that the lack of accelerated PanIN progression following DUSP5 loss, relative to DUSP6/MKP-3 loss, is not due to increased levels of apoptosis in DUSP5 knockout pancreata. Overall, we have been unable to identify any

changes in the proliferation rate or activation of the senescence and apoptotic programmes in $KRas^{G12D}$-driven PanINs following the loss of DUSP5 or DUSP6/MKP-3. Therefore, so far we have been unable to dissect out any significant elements of the mechanism(s) by which loss of DUSP6/MKP-3, but not DUSP5, promotes accelerated PanIN progression. However, there are many other cellular mechanisms that have been shown to promote pancreatic cancer development by which this could be occurring, such as autophagy (Rosenfeldt et al., 2013), oxidative stress (Chio et al., 2016; DeNicola et al., 2011) or the potentiation of an inflammatory response (Pylayeva-Gupta et al., 2012), that have not been investigated in this study to date.

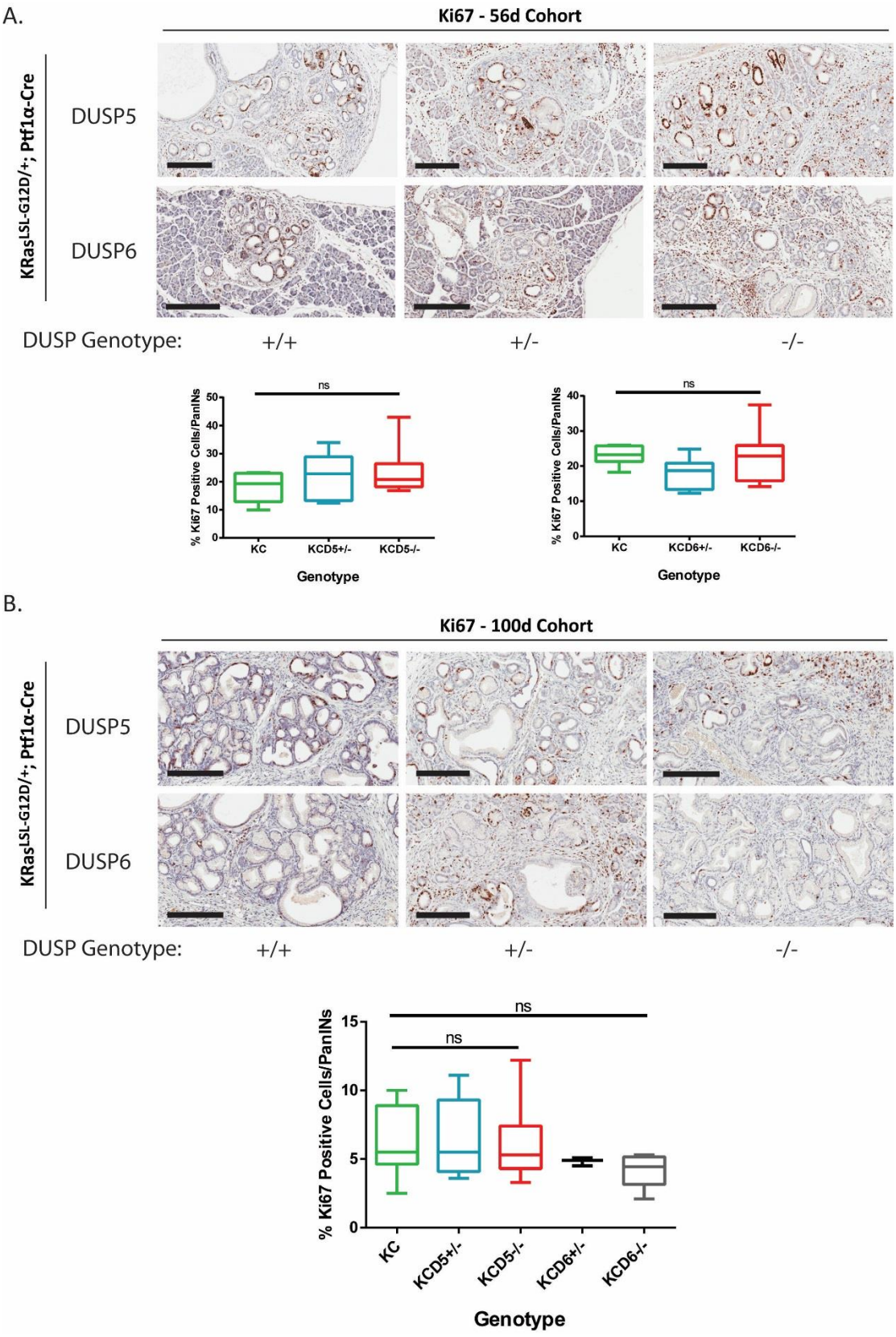

Figure 5.21 Loss of DUSP5 or DUSP6/MKP-3 has no effect on Ki67 expression in KRas^{G12D}-driven PanINs. Representative images and quantification of Ki67 IHC on age-matched 56 day **(A)** or 100 day **(B)** pancreata of the indicated cohorts: KRas$^{LSL\text{-}G12D/+}$; Ptf1α-cre; DUSP$^{+/+}$ (KC), KRas$^{LSL\text{-}G12D/+}$; Ptf1α-cre; DUSP5$^{+/fl}$ (KCD5$^{+/-}$), KRas$^{LSL\text{-}G12D/+}$; Ptf1α-cre; DUSP5$^{fl/fl}$ (KCD5$^{-/-}$), KRas$^{LSL\text{-}G12D/+}$; Ptf1α-cre; DUSP6$^{+/fl}$ (KCD6$^{+/-}$) and KRas$^{LSL\text{-}G12D/+}$; Ptf1α-cre; DUSP6$^{fl/fl}$ (KCD6$^{-/-}$). Staining was quantified as % Ki67 positive cells per PanIN, with up to 25 PanINs scored per section. Median ± IQR shown, n = 7 **(A)**, n = 9, 7, 7, 4, 6 **(B)**. Ns = not significant, using a Kruskal-Wallis test and Dunn's post hoc test. Scale, 200μm.

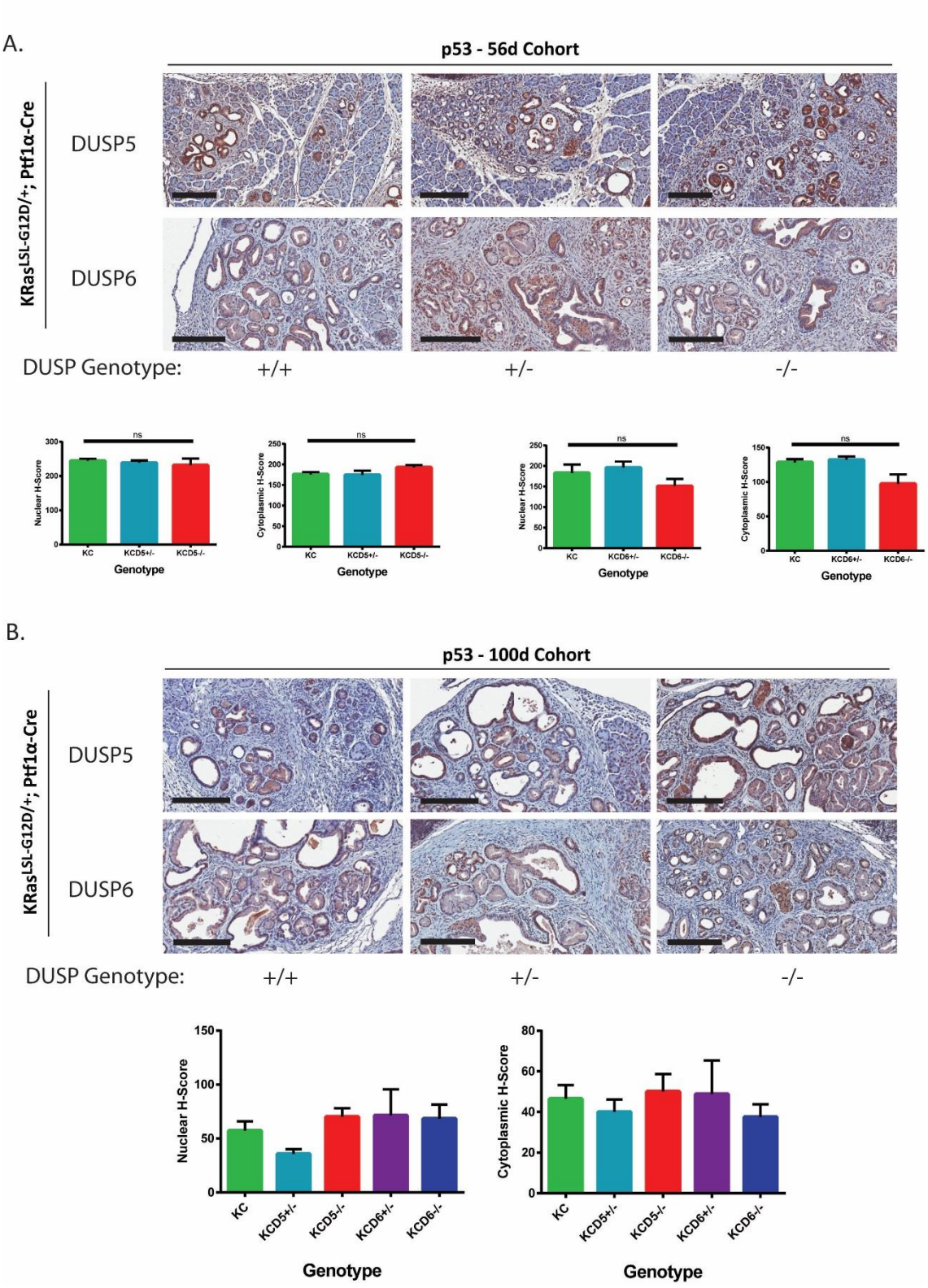

Figure 5.22 DUSP5 or DUSP6/MKP-3 loss has no effect on p53 expression in KRas^{G12D}-driven PanINs. Representative images and H-score quantification of p53 IHC on age-matched 56 day **(A)** or 100 day **(B)** pancreata of the indicated cohorts: KRas$^{LSL\text{-}G12D/+}$; Ptf1α-cre; DUSP$^{+/+}$ (KC), KRas$^{LSL\text{-}G12D/+}$; Ptf1α-cre; DUSP5$^{+/fl}$ (KCD5$^{+/-}$), KRas$^{LSL\text{-}G12D/+}$; Ptf1α-cre; DUSP5$^{fl/fl}$ (KCD5$^{-/-}$), KRas$^{LSL\text{-}G12D/+}$; Ptf1α-cre; DUSP6$^{+/fl}$ (KCD6$^{+/-}$) and KRas$^{LSL\text{-}G12D/+}$; Ptf1α-cre; DUSP6$^{fl/fl}$ (KCD6$^{-/-}$). Mean values ± SEM are shown, n = 7 **(A)**, n = 9, 7, 7, 4, 6 **(B)**. Ns = not significant, using one-way ANOVA and Bonferroni post hoc test. Scale, 200μm.

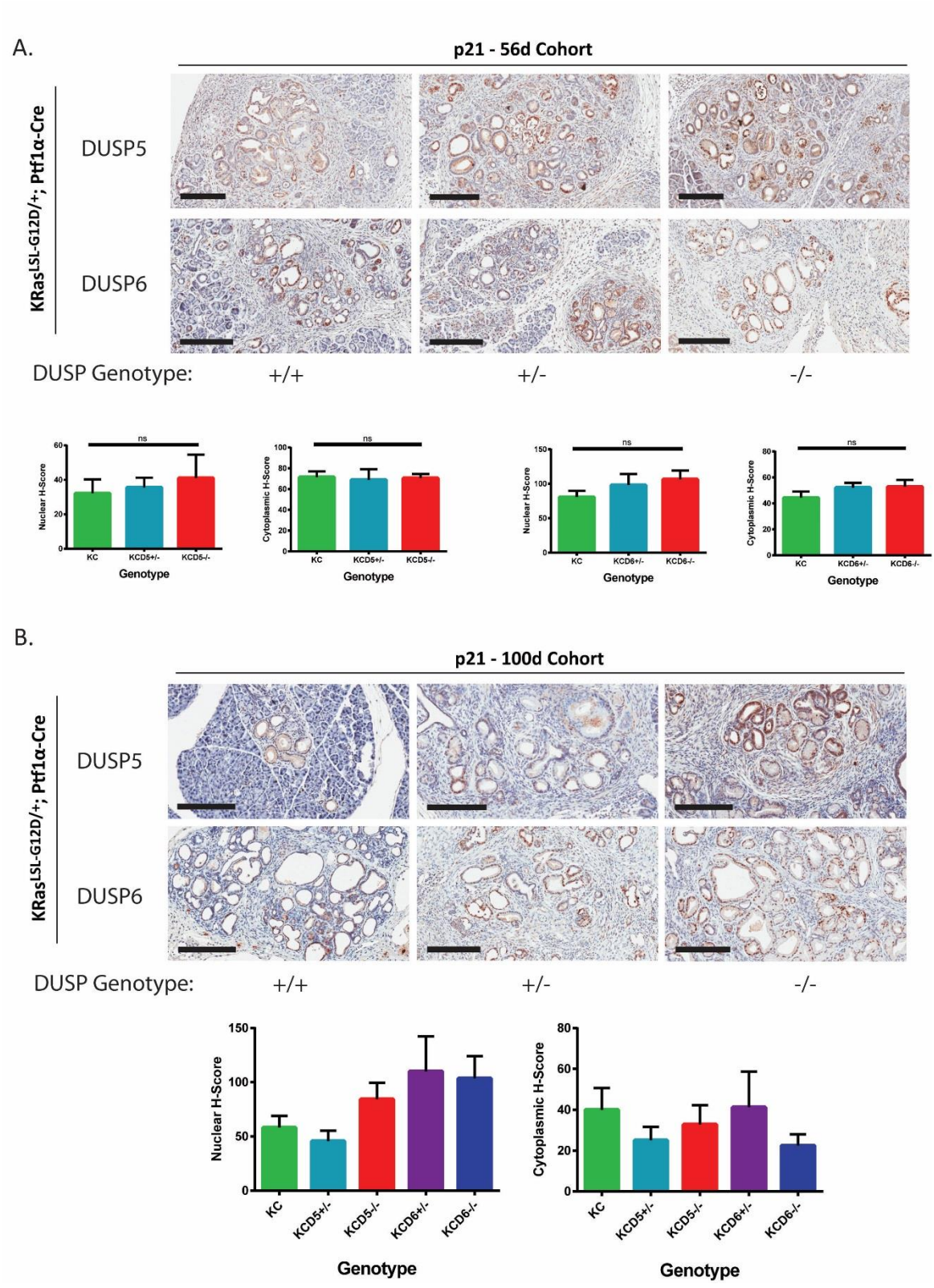

Figure 5.23 DUSP5 or DUSP6/MKP-3 loss has no effect on p21 expression in KRas^{G12D}-driven PanINs. Representative images and H-score quantification of p21 IHC on age-matched 56 day **(A)** or 100 day **(B)** pancreata of the indicated cohorts: KRas$^{LSL\text{-}G12D/+}$; Ptf1α-cre; DUSP$^{+/+}$ (KC), KRas$^{LSL\text{-}G12D/+}$; Ptf1α-cre; DUSP5$^{+/fl}$ (KCD5$^{+/-}$), KRas$^{LSL\text{-}G12D/+}$; Ptf1α-cre; DUSP5$^{fl/fl}$ (KCD5$^{-/-}$), KRas$^{LSL\text{-}G12D/+}$; Ptf1α-cre; DUSP6$^{+/fl}$ (KCD6$^{+/-}$) and KRas$^{LSL\text{-}G12D/+}$; Ptf1α-cre; DUSP6$^{fl/fl}$ (KCD6$^{-/-}$). Mean values ± SEM are shown, n = 7 **(A)**, n = 9, 7, 7, 4, 6 **(B)**. Ns = not significant, using one-way ANOVA and Bonferroni post hoc test. Scale, 200μm.

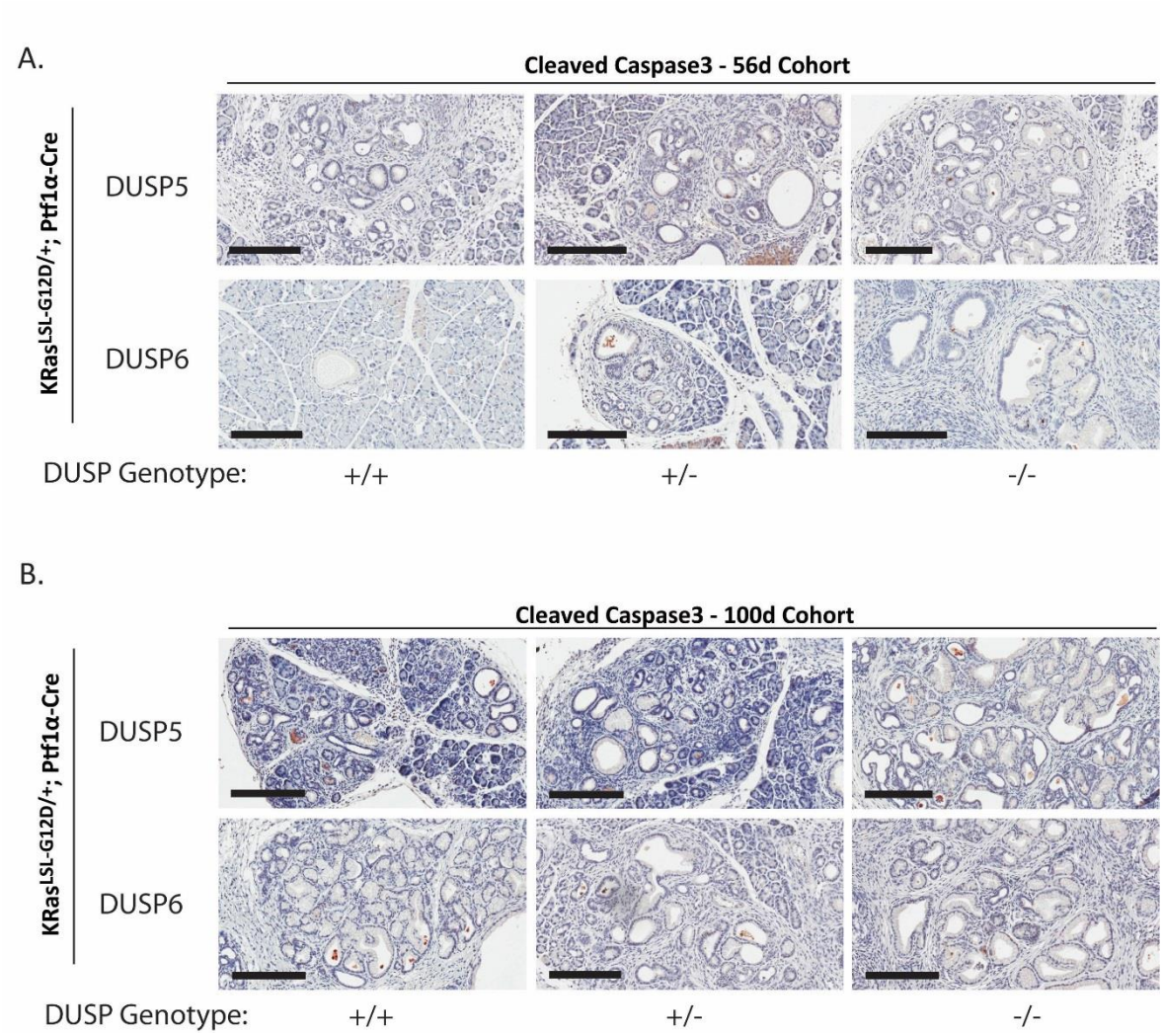

Figure 5.24 Loss of DUSP5 or DUSP6/MKP-3 does not promote cleaved-Caspase3 expression in KRas^{G12D}-driven PanINs. Representative images of cleaved-caspase3 IHC on age-matched 56 day **(A)** or 100 day **(B)** pancreata of the indicated cohorts: KRas$^{LSL\text{-}G12D/+}$; Ptf1α-cre; DUSP$^{+/+}$ (KC), KRas$^{LSL\text{-}G12D/+}$; Ptf1α-cre; DUSP5$^{+/fl}$ (KCD5$^{+/-}$), KRas$^{LSL\text{-}G12D/+}$; Ptf1α-cre; DUSP5$^{fl/fl}$ (KCD5$^{-/-}$), KRas$^{LSL\text{-}G12D/+}$; Ptf1α-cre; DUSP6$^{+/fl}$ (KCD6$^{+/-}$) and KRas$^{LSL\text{-}G12D/+}$; Ptf1α-cre; DUSP6$^{fl/fl}$ (KCD6$^{-/-}$). n = 7 **(A)**, n = 9, 7, 7, 4, 6 **(B)**.

5.2.3.4 DUSP5 or DUSP6/MKP-3 loss promotes accelerated mortality following KRas^{G12D}-driven pancreatic tumourigenesis

The loss of either DUSP5 or DUSP6/MKP-3 increases KRas^{G12D}-induced ADM and the initiation of PanIN lesions (Fig. 5.9A-C & 5.13A-C), whereas only the loss of DUSP6/MKP-3 is able to promote accelerated PanIN progression (Fig. 5.13D-E). Therefore, we hypothesised that the loss of either MKP could have different effects on the rate of PDAC development and associated mortality. To address this hypothesis we performed a survival study, whereby cohorts of KRas$^{LSL\text{-}G12D/+}$; Ptf1α-Cre mice which were wild-type, heterozygous or homozygous for either DUSP5$^{fl/fl}$ or DUSP6$^{fl/fl}$ alleles were generated. These mice were monitored for signs of pancreatic cancer development and removed from the study once they became moribund or visibly unwell, generated visible ascites, lost over 20% of their maximal body-weight or reached a maximum age of 18 months.

Consistent with previously published studies, KRas$^{LSL\text{-}G12D/+}$; Ptf1α-Cre (KC) mice had a median survival of 467 days (Fig. 5.25A), with the vast majority of mice succumbing following the gradual development of invasive PDAC (Fig. 5.25B) (Eser et al., 2013; Hingorani et al., 2003). Cohorts, heterozygous for the expression of either DUSP5 or DUSP6/MKP-3, in the presence of KRas^{G12D}, predominantly replicated this phenotype, with median survivals of 465 and 479 days respectively (Fig. 5.25A-B). In contrast, KRas$^{LSL\text{-}G12D/+}$; Ptf1α-Cre; DUSP6$^{-/-}$ (KCD6$^{-/-}$) mice displayed a significant decrease in overall survival when compared with KC mice, with a median survival of only 148 days (Fig. 5.25A). The majority of KCD6$^{-/-}$ mice presented with PDAC when they showed any cardinal signs of having succumbed to illness (Fig. 5.25B), however a small number of mice which were removed from the study due to sustained weight loss (-20% of body weight) at a relatively young age did not present with PDAC (Fig. 5.26A). The median onset of PDAC in KCD6$^{-/-}$ mice was 237 days, relative to 501 days in KC mice, which represents a significant decrease in PDAC-free survival (Fig. 5.25B).

KRas$^{LSL\text{-}G12D/+}$; Ptf1α-Cre; DUSP5$^{-/-}$ (KCD5$^{-/-}$) mice also displayed a significant decrease in total survival compared to KC mice, with the majority of mice succumbing before 150 days of age and displaying a median survival of 107.5 days (Fig. 5.25A). However, in contrast to KC mice, the majority of KCD5$^{-/-}$ mice did not present with PDAC upon histological examination (Fig. 5.25B & 5.26A). Of the six KCD5$^{-/-}$ mice, which developed

PDAC, two did so at a significantly younger age than any KC mice, but the remaining four did not (Fig. 5.25B). Overall, the median survival of the KCD5$^{-/-}$ mice, which presented with PDAC was 333.5 days. However, due to the low sample size and lack of any prominent phenotype, it is not possible to conclusively determine whether DUSP5 loss is promoting the accelerated development of KRas^{G12D}-driven PDAC and resulting in an increased mortality.

The KCD5$^{-/-}$ mice which did not display PDAC succumbed following terminal weight loss at a young age, in a similar manner to a much smaller fraction of the KCD6$^{-/-}$ mice. However, the penetrance of this phenotype was significantly higher in KCD5$^{-/-}$ mice with around 80% succumbing before the development of PDAC (Fig. 5.26A). These KCD5$^{-/-}$ "weight-loss" pancreata characteristically displayed a decreased pancreatic size relative to KC pancreata, or even younger KCD5$^{-/-}$ pancreata (Fig. 26B), as well as a complete loss of acinar tissue and the majority of their islets of Langerhans (Fig. 5.26C). To determine whether this failure to generate PDAC and loss of pancreatic size is due to increased apoptosis of developing PanINs, cleaved-Caspase3 expression was assessed in KCD5$^{-/-}$ "weight-loss" pancreata. However, these pancreata expressed very low levels of cleaved-Caspase3, and their PanINs were still proliferative, as demonstrated by Ki67 expression (Fig. 26D). Therefore, we hypothesise that due to the increased initiation of ADM and PanINs induced following DUSP5 loss in KRas^{G12D}-expressing pancreata (Fig. 5.7-9 & 5.11-13), a high proportion of KCD5$^{-/-}$ mice do not contain sufficient functional acinar and islet tissue to sustain normal homeostasis (Fig. 5.26C). Consequently, this loss of pancreatic function could result in the terminal weight loss observed in these mice due to a failure to produce digestive enzymes and therefore obtain necessary nutrition, as well as difficulties in controlling blood glucose levels.

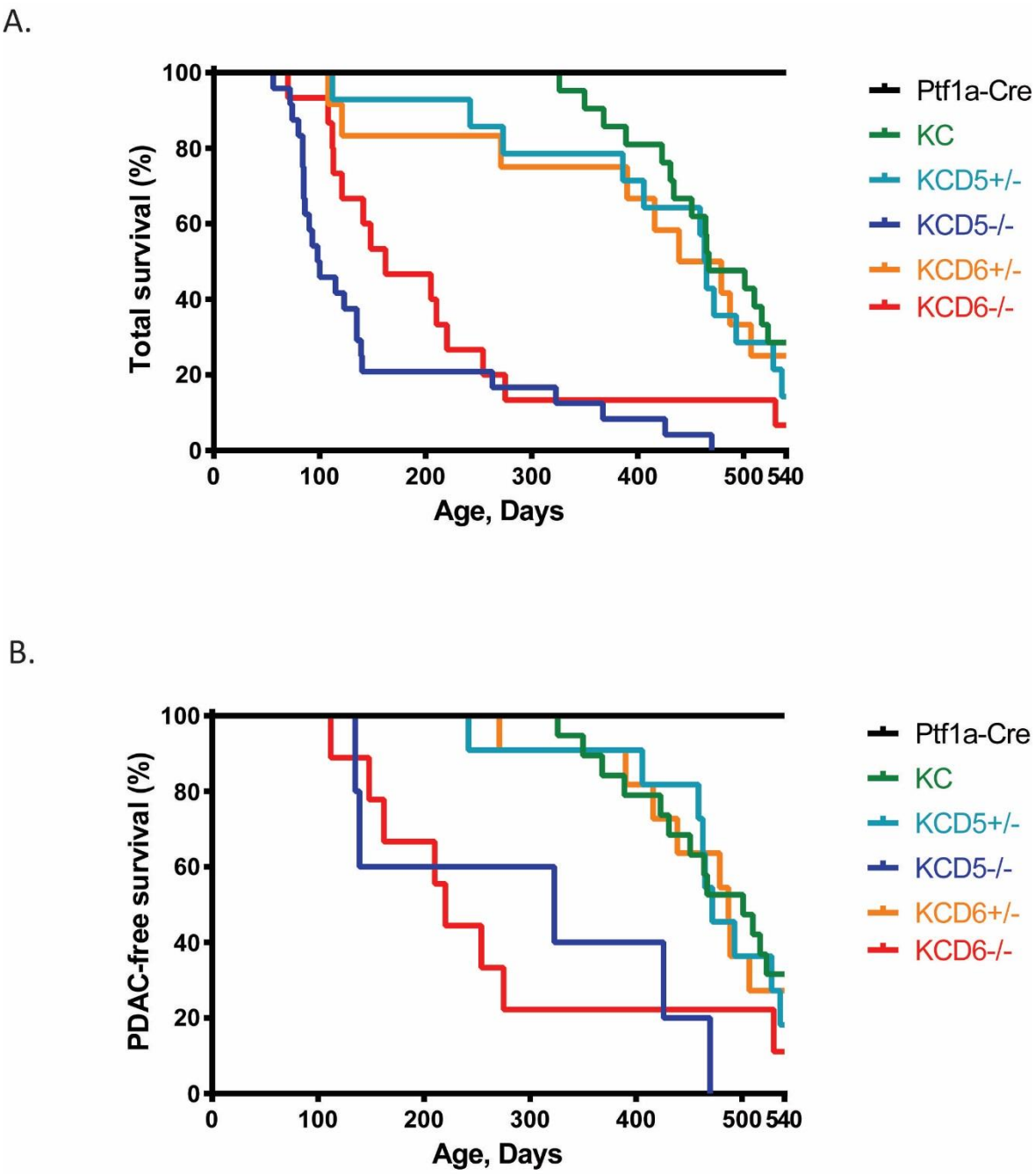

Figure 5.25 Loss of DUSP5 or DUSP6/MKP-3 promotes accelerated KRas^{G12D}-driven pancreatic tumourigenesis associated mortality. Kaplan-Meier curves showing the Total survival **(A)** and PDAC-free survival **(B)** of the indicated cohorts. Cohorts consisted of the following genotypes: KRas$^{+/+}$; Ptf1α-cre; DUSP$^{+/+}$ (Ptf1α-cre), KRas$^{LSL\text{-}G12D/+}$; Ptf1α-cre; DUSP$^{+/+}$ (KC), KRas$^{LSL\text{-}G12D/+}$; Ptf1α-cre; DUSP5$^{+/fl}$ (KCD5$^{+/-}$), KRas$^{LSL\text{-}G12D/+}$; Ptf1α-cre; DUSP5$^{fl/fl}$ (KCD5$^{-/-}$), KRas$^{LSL\text{-}G12D/+}$; Ptf1α-cre; DUSP6$^{+/fl}$ (KCD6$^{+/-}$) and KRas$^{LSL\text{-}G12D/+}$; Ptf1α-cre; DUSP6$^{fl/fl}$ (KCD6$^{-/-}$). **A)** Total survival, n = 12, 21, 14, 24, 12, 15 respectively. Log-rank test: KC v KCD5$^{-/-}$ p<0.0001, KC v KCD6$^{-/-}$ p<0.0001. **B)** PDAC-free survival, n = 12, 19, 11, 5, 11, 9 respectively. Log-rank test: KC v KCD5$^{-/-}$ p = 0.0033, KC v KCD6$^{-/-}$ p = 0.0140.

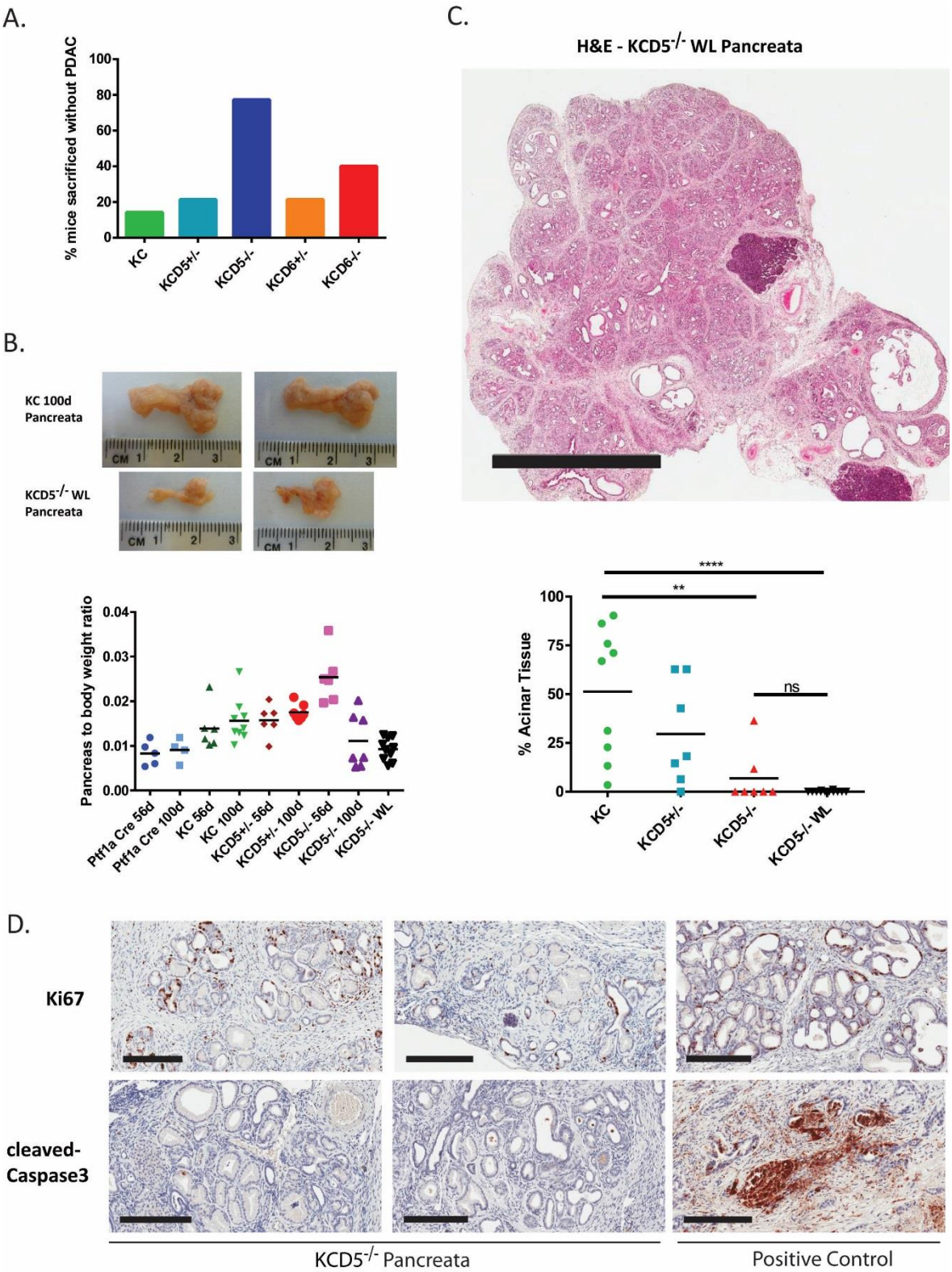

Figure 5.26 DUSP5 loss, in the presence of KRas^{G12D}, promotes complete loss of pancreatic acinar tissue and its replacement with pancreatic cancer precursor lesions. A) The percentage of mice of the indicated cohorts sacrificed due to ill health, which upon dissection did not present with PDAC. Cohorts consisted of the following genotypes: KRas$^{LSL\text{-}G12D/+}$; Ptf1α-cre; DUSP$^{+/+}$ (KC, n = 21), KRas$^{LSL\text{-}G12D/+}$; Ptf1α-cre; DUSP5$^{+/fl}$ (KCD5$^{+/-}$, n = 14), KRas$^{LSL\text{-}G12D/+}$; Ptf1α-cre; DUSP5$^{fl/fl}$ (KCD5$^{-/-}$, n =24), KRas$^{LSL\text{-}G12D/+}$; Ptf1α-cre; DUSP6$^{+/fl}$ (KCD6$^{+/-}$, n = 12) and KRas$^{LSL\text{-}G12D/+}$; Ptf1α-cre; DUSP6$^{fl/fl}$ (KCD6$^{-/-}$, n =15). **B)** Representative images demonstrating the reduction in size of KCD5$^{-/-}$ pancreata, relative to KC (Upper panel), and associated quantification of the pancreas to body weight ratio of the indicated cohorts (Lower panel). The KCD5$^{-/-}$ WL cohort

represents all the DUSP5$^{-/-}$ mice which were in the survival study, but which had to be removed following terminal weight-loss, but did not display with PDAC. KO WL cohort median age, 94 days. Mean shown, n = 5, 4, 7, 9, 7, 7, 7, 7, 10. **C)** A representative image of an H&E stained KCD5$^{-/-}$ WL cohort pancreata (Upper panel - Scale, 2mm) and quantification of the percentage acinar tissue remaining in the pancreata of the indicated 100d age-matched cohorts alongside the KCD5$^{-/-}$ WL cohort (Lower panel). Mean shown, n = 9, 7, 7, 10. Ns = not significant, **P < 0.01, ****P < 0.0001, using one-way ANOVA and Bonferroni post hoc test. **D)** Representative images of Ki67 or cleaved-caspase3 IHC of KCD5$^{-/-}$ WL cohort pancreata compared to positive control tissue. Scale, 200μm.

Histological analysis of PDAC tumours revealed a significant increase in the proportion of poorly-differentiated tumours in KCD6$^{-/-}$ mice relative all other genotypes (Fig. 5.27A-B). Approximately 80% of KCD6$^{-/-}$ tumours displayed a poorly differentiated morphology, whereas the majority of KC tumours were well-differentiated (Fig. 5.27B). This indicates that DUSP6/MKP-3 loss is highly likely to promote the poorly differentiated phenotype. However, DUSP6/MKP-3 loss, in the presence of KRas^{G12D}, is not always sufficient to induce a poorly-differentiated phenotype (Fig. 5.27B), indicating that the spontaneous acquisition of additional mutations during tumourigenesis is likely to be required to generate this outcome. Poorly differentiated PDAC has been associated with a worse prognosis and increased proliferative capacity in human patients (Cleary et al., 2004; Hruban and Fukushima, 2007). These traits are apparent in our model with KCD6$^{-/-}$ mice, which predominantly displayed poorly-differentiated tumours (Fig. 5.27B), also demonstrating accelerated PDAC formation and associated mortality (Fig. 5.25B). In addition, poorly-differentiated tumours of all genotypes display increased proliferation relative to well-differentiated tumours (Fig. 5.27A & C).

The KRas^{G12D}-driven mouse models of pancreatic cancer display metastasis following a long latency, or more rapidly following the mutation of additional tumour suppressors including p53 or CDKN2A (Aguirre et al., 2003; Hingorani et al., 2003, 2005). Therefore, to determine whether loss of DUSP5 or DUSP6/MKP-3 promote increased metastatic potential of KRas^{G12D}-expressing PDAC, liver metastases were identified via gross appearance or histological examination and were confirmed to be of pancreatic origin through PDX1 expression as determined by IHC (Fig. 5.27D). In contrast to liver metastasis, lung metastasis was observed very infrequently, with only two mice out of the whole study presenting with lung metastasis. KCD6$^{-/-}$ mice displayed a significant increase in the frequency of liver metastasis relative to KC mice, with KCD6$^{+/-}$ mice demonstrating an intermediate phenotype (Fig. 5.27D). KCD5$^{-/-}$ mice displayed a marginal increase in liver metastasis, relative to KC mice, but this is unlikely to be significant due to the low number of KCD5$^{-/-}$ mice, which developed PDAC (Fig. 5.25B & 5.27D). Therefore, loss of DUSP6/MKP-3, but not DUSP5, promotes an increased propensity for KRas^{G12D}-driven pancreatic tumours to metastasise.

In summary, here we show that pancreas-specific DUSP6/MKP-3 loss, in the presence of $KRas^{G12D}$, can promote accelerated PDAC development and mortality (Fig. 5.25B). $KCD6^{-/-}$ PDAC is characterised by a high frequency of highly proliferative, poorly-differentiated tumours (Fig. 5.27A-C), which display an elevated metastatic potential relative to KC tumours (Fig. 5.27D). In contrast, although $KCD5^{-/-}$ mice displayed decreased total survival relative to KC mice, this was primarily not due to PDAC development (Fig. 5.25). Instead, $KCD5^{-/-}$ mice developed a more extensive pancreatic atrophy and ADM with a very high burden of pre-neoplastic lesions, this most likely results in a loss of normal pancreatic function and consequently significant weight-loss (Fig. 5.26). $KCD5^{-/-}$ mice did not display an increased proportion of poorly-differentiated tumours or any evidence of increased metastatic potential relative to KC tumours (Fig. 5.27).

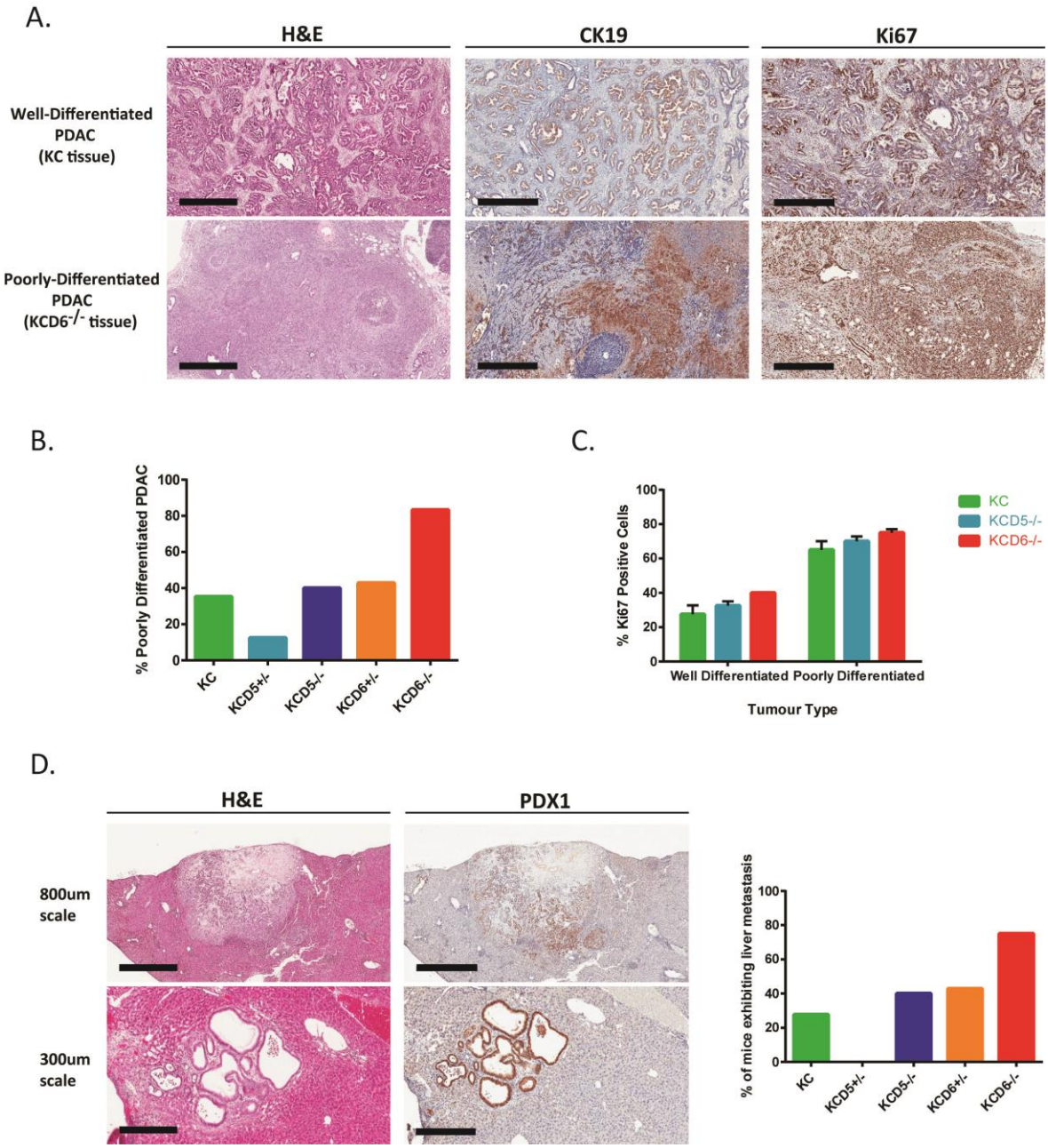

Figure 5.27 DUSP6/MKP-3 loss, in the presence of KRas^{G12D}, promotes the development of poorly-differentiated, highly proliferative and frequently metastatic PDAC. A) Representative images of H&E staining and Cytokeratin-19 (CK19) or Ki67 IHC of either well-differentiated or poorly-differentiated PDAC tissue, taken from tumours arising from KRas$^{LSL\text{-}G12D/+}$ and Ptf1α-cre (KC) expressing mice which were either DUSP6$^{+/+}$ (KC) or DUSP6$^{fl/fl}$ (KCD6$^{-/-}$) respectively. Scale, 500μm. **B)** Quantification of the percentage of mice which displayed poorly-differentiated PDAC of the indicated cohorts. Cohorts consisted of the following genotypes: KRas$^{LSL\text{-}G12D/+}$; Ptf1α-cre; DUSP$^{+/+}$ (KC, n = 18), KRas$^{LSL\text{-}G12D/+}$; Ptf1α-cre; DUSP5$^{+/fl}$ (KCD5$^{+/-}$, n = 9), KRas$^{LSL\text{-}G12D/+}$; Ptf1α-cre; DUSP5$^{fl/fl}$ (KCD5$^{-/-}$, n =5), KRas$^{LSL\text{-}G12D/+}$; Ptf1α-cre; DUSP6$^{+/fl}$ (KCD6$^{+/-}$, n = 7) and KRas$^{LSL\text{-}G12D/+}$; Ptf1α-cre; DUSP6$^{fl/fl}$ (KCD6$^{-/-}$, n =9). **C)** Quantification of the percentage Ki67-positive tumour cells in either well- or poorly-differentiated tumours of the indicated cohorts. Mean values ± SEM are shown, n = 6 tumours per cohort. **D)** Representative images of H&E staining and PDX1 IHC of liver metastases presented by KRas$^{LSL\text{-}G12D/+}$ and Ptf1α-cre (KC) expressing mice (Left panel). Quantification of the percentage of mice presenting with PDAC which also displayed associated liver metastasis of the indicated cohorts, n = 18, 9, 5, 7, 8 respectively (Right panel).

5.3 Discussion

DUSP5 and DUSP6/MKP-3 are ERK-specific MKPs, which are induced by ERK activity as negative feedback regulators (Ekerot et al., 2008; Groom et al., 1996; Kucharska et al., 2009; Mandl et al., 2005; Mourey et al., 1996), therefore these proteins have the potential to modulate ERK activity following oncogenic activation of the Ras-ERK pathway. Furthermore, DUSP5 and DUSP6/MKP-3 display differential localisation, with DUSP5 localised to the nucleus (Mandl et al., 2005) and DUSP6/MKP-3 to the cytoplasm (Groom et al., 1996; Mourey et al., 1996), therefore it is possible that loss of these MKPs could induce distinct changes in the spatial activity of ERK and consequently distinct phenotypes in cancers driven by oncogenic activation of the Ras-ERK pathway. Here we show that DUSP5 or DUSP6/MKP-3 ablation display differing abilities to modulate the oncogenic potential of mutant $KRas^{G12D}$ in mouse models of pancreatic cancer.

Utilising the $KRas^{LSL\text{-}G12D/+}$; Ptf1α-Cre (KC) model of pancreatic cancer (Hingorani et al., 2003) we show that the loss of DUSP6/MKP-3 promotes the increased initiation of $KRas^{G12D}$-driven ADM and PanIN lesions as well as the accelerated progression of PanINs towards higher more dysplastic grades (Fig. 5.7-9 & 5.11-13). Furthermore, $KCD6^{-/-}$ mice displayed accelerated mortality, compared to KC mice, due to the rapid formation of PDAC and a high frequency of liver metastasis (Fig. 5.25 & 5.27C). PDAC tumours arising from $KCD6^{-/-}$ mice are also characterised by a higher proportion of highly proliferative, poorly differentiated tumours than their KC counterparts (Fig. 5.27A-B).

The loss of DUSP5 also promotes the increased initiation of $KRas^{G12D}$-driven ADM and PanINs (Fig. 5.7-9 & 5.11-13). However, in contrast to the loss of DUSP6/MKP-3, DUSP5 loss does not promote the accelerated progression of PanINs (Fig. 5.7-9 & 5.11-13), or a high frequency of poorly differentiated tumours or liver metastasis (Fig. 5.27). Furthermore, although some $KCD5^{-/-}$ mice developed PDAC at a significantly younger age than KC mice, we were unable to conclusively determine whether DUSP5 loss promotes accelerated PDAC development due to the low number of mice surviving until PDAC formation (Fig. 5.25). This was because $KCD5^{-/-}$ mice displayed accelerated mortality following to terminal weight-loss, but with the absence of PDAC formation (Fig. 5.25 & 5.26A). Such mice displayed an extremely high burden of ADM and PanIN lesions, resulting in the complete loss of pancreatic acinar and islet tissue (Fig. 5.26C). Therefore,

we hypothesise that these mice became extremely ill due to a lack of normal pancreatic function induced by their high burden of benign neoplastic lesions. Some KCD6$^{-/-}$ mice also displayed this phenotype, however it occurred with a much lower penetrance than in KCD5$^{-/-}$ mice (Fig. 5.25 & 5.26A), perhaps reflecting a stronger promotion of tumour initiation following DUSP5 loss relative to DUSP6/MKP-3 loss in KRasG^{12D}-expressing pancreata.

These data demonstrating that the loss of DUSP6/MKP-3 promotes the accelerated initiation and development of invasive, metastatic PDAC in KRas^{G12D}-driven mouse models of pancreatic cancer indicate that DUSP6/MKP-3 acts as a tumour suppressor in pancreatic cancer development (Fig. 5.7-13, 5.25 & 5.27). This conclusion is consistent with previous studies in human pancreatic tumour samples which have demonstrated that DUSP6/MKP-3 expression is selectively downregulated in invasive carcinomas, but not the PanIN precursors, via either aberrant hypermethylation or genomic LOH (Furukawa et al., 2003, 2005; Kimura et al., 1996; Xu et al., 2005). Therefore, these studies proposed that DUSP6/MKP-3 is tumour suppressor in pancreatic cancer as the downregulation of its expression is selected for during pancreatic tumourigenesis, implying that the loss of this protein confers a selective advantage to the tumour (Furukawa et al., 2003, 2005, 2006). Additionally, it was hypothesised that DUSP6/MKP-3 loss might be a key determinant to enable the progression from PanIN to invasive carcinoma, as DUSP6/MKP-3 loss correlated with this aspect of tumour progression (Furukawa et al., 2003, 2005, 2006). Furthermore, these studies identified that in human PDAC tissue samples DUSP6/MKP-3 loss correlated with tumours displaying a poorly-differentiated morphology (Furukawa et al., 2003, 2005; Xu et al., 2005). This is in agreement with our data, which demonstrates that DUSP6/MKP-3 loss in combination with KRas^{G12D} expression promotes a significant increase in the proportion of poorly-differentiated tumours relative to KRas^{G12D} expression alone (Fig. 5.27A-B).

It would be interesting to determine whether the KC tumours which displayed a poorly-differentiated morphology had autonomously lost DUSP6/MKP-3 expression. If this was the case this would provide strong evidence that loss of DUSP6/MKP-3 expression is an important factor in the development of poorly-differentiated PDAC. However, unfortunately in our hands the most specific DUSP6/MKP-3 antibody available did not

specifically stain murine DUSP6/MKP-3 wild-type pancreatic tissue when used for IHC (Fig. 5.17B). This technical issue also prevented the investigation into whether $KRas^{G12D}$-expressing PanINs display upregulated DUSP6/MKP-3 expression as previously demonstrated in human pancreatic cancer tissue (Furukawa et al., 2005) and indicated by our studies in $KRas^{G12D}$-expressing MEFs (Fig. 4.3-4 & 4.8-9). In a similar manner to DUSP6/MKP-3, the activation of $KRas^{G12D}$ expression induced DUSP5 expression in MEFs. However, we encountered a similar problem attempting to utilise a DUSP5 antibody in IHC (Fig. 5.17A), so could not effectively investigate whether DUSP5 induction occurred in $KRas^{G12D}$-driven PanINs. Analysis of DUSP5 and DUSP6/MKP-3 mRNA expression from $KRas^{G12D}$ expressing pancreata did demonstrate marginal increases in DUSP5 and DUSP6/MKP-3 expression (Fig. 5.17C). However, as mentioned previously this approach was very imprecise as it was not possible to determine what proportion of the tissue utilised for mRNA isolation had undergone pancreatic tumourigenesis. To resolve these problems and to investigate DUSP5 and DUSP6/MKP-3 expression in PanINs and tumour samples, we have formed a collaboration to have DUSP5 and DUSP6/MKP-3 mRNA expression levels investigated in pancreatic tissue utilising an *in situ* hybridisation based approach (RNAscope - Advanced Cell Diagnostics).

DUSP5 ablation promoted the increased or accelerated initiation of ADM and PanIN lesions in $KRas^{G12D}$-expressing pancreata (Fig. 5.7-9 & 5.11-13). This result mirrors the phenotype observed following DMBA/TPA-induced skin carcinogenesis, where the loss of DUSP5 induced an increased burden of skin papillomas, which are benign neoplasia's like PanINs, relative to wild-type mice (Fig. 3.1) (Rushworth et al., 2014). However in contrast to skin carcinogenesis (Fig. 3.14), the increase in ADM and PanIN initiation observed following DUSP5 ablation is not mediated by increased SerpinB2 expression as this phenotype cannot be rescued by SerpinB2 ablation (Fig. 5.14-16). This is potentially due to the significantly lower level of SerpinB2 expression in the pancreas relative to the skin (Fig. 5.14A), meaning that although its expression is increased following the loss of DUSP5, SerpinB2 might not be expressed at a high enough level to have a significant role in modulating tumourigenesis. Alternatively, as different tissues are known to be predisposed to the development of cancer following the mutation of characteristic driver genes and processes (Greenman et al., 2007), SerpinB2 might not have a role in the processes which are deregulated during the development of pancreatic cancer.

The majority of KCD5$^{-/-}$ mice became ill prior to the development of PDAC (Fig. 5.25). We hypothesise this to be due to the extreme extent of pancreatic transformation and the high burden of ADM and PanIN lesions formed in KCD5$^{-/-}$ pancreata, resulting in a loss of pancreatic function and severe weight-loss due to malnutrition (Fig. 5.26). However, this phenotype prevented us from drawing reliable conclusions as to whether the loss of DUSP5 accelerates the development of PDAC tumours following KRas^{G12D}-driven tumourigenesis or whether DUSP5 loss affects the tumour morphology or metastatic frequency, as observed following DUSP6/MKP-3 loss (Fig. 5.27). We hypothesise that DUSP5 loss would be likely to cause accelerated PDAC development in this KC model, as by increasing the initiation of ADM and PanINs DUSP5 loss would create a larger pool of precursor lesions, therefore increasing the probability that one of these lesions will acquire the additional mutational burden to develop into an invasive tumour. The occurrence of PDAC in two KCD5$^{-/-}$ mice at a significantly younger age than any KC mice is potential evidence supporting this hypothesis (Fig. 5.25B). However, alternatively DUSP5 loss could be promoting the initiation of KRas^{G12D}-driven pancreatic tumourigenesis, but subsequently delaying progression to invasive tumours. This could occur through the induction of cellular senescence, which has been shown to be a consequence of hyperactive ERK signalling *in vitro* and *in vivo* (Cisowski et al., 2015; Deschênes-Simard et al., 2013; Meloche and Pouysségur, 2007). In support of this theory KCD5$^{-/-}$ pancreata display elevated nuclear *p*-ERK expression (Fig. 5.18A), and although these pancreata did not display increased expression of senescence markers (Fig. 5.22A & 5.23A), only markers from the p53 pathway were investigated. Therefore, the increased induction of senescence in KCD5$^{-/-}$ pancreata via another mechanism cannot be discounted.

To investigate whether the loss of DUSP5 accelerates the development of KRas^{G12D}-driven pancreatic tumours we plan to have the KRas$^{LSL\text{-}G12D/+}$; PDX1-Cre driven model repeated in a sterile animal facility. This should prevent the excessive penetrance of intussusceptions we observed with this model (Fig. 5.2). Furthermore, the PDX1-Cre allele has been shown to promote stochastic Cre expression across the pancreas, whereas the Ptf1α-Cre allele induces uniform expression throughout the pancreas (Hingorani et al., 2003). Therefore, use of the PDX1-Cre allele should ensure that KRas$^{LSL\text{-}G12D/+}$; PDX1-Cre; DUSP5$^{fl/fl}$ mice do not demonstrate the total loss of acinar tissue apparent in the Ptf1α-Cre driven KCD5$^{-/-}$

mice and therefore ensure that the majority of PDX1-Cre driven animals progress to develop PDAC.

Recently, we have obtained and validated a new DUSP5$^{fl/fl}$ allele which is a true conditional allele (Fig. 4.19A), demonstrating wild-type levels of DUSP5 protein prior to Cre-mediated excision. Therefore, the second PDX1-Cre driven cohort will utilise this allele and a second Ptf1α-Cre driven 56 day age-matched cohort will be generated. This additional cohort containing the true conditional allele will be used to validate that the initiation phenotype observed following loss of DUSP5 (Fig. 5.7-5.9) is due to the cell autonomous effects of DUSP5 ablation in the pancreas, rather than the effects of effectively a whole body DUSP5 knockout. It is essential to validate whether the effects of DUSP5 loss on KRas^{G12D}-driven pancreatic tumourigenesis are cell autonomous because pancreatic cancer development is well established to be strongly regulated by the inflammatory response (Guerra et al., 2007, 2011; Lee and Bar-Sagi, 2010; Pylayeva-Gupta et al., 2012). The importance of the inflammatory response in pancreatic cancer development is highlighted by the fact that the induction of KRas^{G12D} expression alone is not sufficient to induce pancreatic cancer development in adult mice, however KRas^{G12D} expression coupled with caerulein-induced chronic pancreatitis results in widespread PanIN formation and the development of PDAC (Guerra et al., 2007). Furthermore, in humans chronic pancreatitis, often induced by excessive alcohol consumption, is a major risk factor of pancreatic cancer, increasing the risk by more than tenfold (Kleeff et al., 2016).

The genetic deletion of multiple MKPs has been shown to generate immune phenotypes (Jeffrey et al., 2007), with DUSP5 ablation resulting in prolonged eosinophil survival and increased effector function following helminth infection (Holmes et al., 2015). An earlier study utilising transgenic mice overexpressing DUSP5 demonstrated autoimmune symptoms, an inhibition of T-cell development and decreased T-cell proliferation (Kovanen et al., 2008). However, subsequent studies in DUSP5 knockout mice do not show any DUSP5-dependent effects on T-cell, B-cell, monocyte or natural killer cell development, or cytokine or chemokine synthesis in LPS-treated macrophages (Holmes et al., 2015; Rushworth et al., 2014). Furthermore, in the DMBA/TPA-induced model of skin carcinogenesis DUSP5 loss did not alter the infiltration of immune effector cells into skin

papillomas (Rushworth et al., 2014). These data indicate it is unlikely that the effects of DUSP5 loss on $KRas^{G12D}$-driven pancreatic tumourigenesis could be driven by the potential effects of DUSP5 loss on the development or function of immune cells. However, this question should be conclusively addressed by the generation of $KCD5^{-/-}$ mice expressing the truly conditional $DUSP5^{fl/fl}$ allele.

Cell autonomous effects of DUSP5 or DUSP6/MKP-3 loss in the pancreas could influence heterocellular signalling between $KRas^{G12D}$-expressing tumour cells and either stromal cells or infiltrating immune cells (Tape et al., 2016). Such effects could modulate the inflammatory response following $KRas^{G12D}$ expression in the pancreas and thereby mediate the phenotypes observed following the loss of either DUSP5 or DUSP6/MKP-3. Therefore, to investigate whether the inflammatory response is altered in $KRas^{G12D}$-driven pancreatic tumourigenesis following the loss of either DUSP5 or DUSP6/MKP-3 expression, tissue sections from the age-matched cohorts generated have been sent to a collaborator for IHC staining for a panel of immune cell markers.

As well as investigating whether inflammatory responses play a role in the phenotypes driven by loss of either DUSP5 or DUSP6/MKP-3 in $KRas^{G12D}$-expressing pancreata, a range of further mechanistic studies are required to further characterise the development of these phenotypes. Such studies could involve, treating the $KCD5^{-/-}$ and $KCD6^{-/-}$ cohorts with a MEK inhibitor to enable confirmation that the effects of DUSP5 or DUSP6/MKP-3 loss occur through the ERK pathway, as predicted by their known biochemical features (Ekerot et al., 2008; Groom et al., 1996; Kucharska et al., 2009; Mandl et al., 2005; Mourey et al., 1996). If the effects of DUSP5 or DUSP6/MKP-3 loss occur in an ERK-dependent manner MEK inhibitor treatment would be expected to reverse the sensitisation of $KCD5^{-/-}$ and $KCD6^{-/-}$ mice to $KRas^{G12D}$-driven pancreatic tumourigenesis. Multiple studies have proposed non-MAPK substrates for MKPs (Caunt and Keyse, 2013), including a potential role for DUSP6/MKP-3 in dephosphorylating the transcription factor forkhead box O1 (FOXO1) (Wu et al., 2010). These non-MAPK substrates and mechanisms of action for MKPs are fairly controversial, however it is still essential to validate that the phenotypic effects of DUSP5 or DUSP6/MKP-3 loss occur in an ERK-dependent manner.

To investigate the mechanism enabling the increased initiation of $KRas^{G12D}$-driven pancreatic tumourigenesis following DUSP5 or DUSP6/MKP-3 ablation acinar explant

experiments could be performed. Such experiments involve the 3D-culture of pancreatic acinar tissue followed by the induction of ADM via TGFα or EGF treatment of wild-type acinar tissue or through the culture of $KRas^{G12D}$-expressing acinar tissue (Chen et al., 2015; Shi et al., 2013). Alternatively, acinar tissue can be cultured containing the $KRAS^{LSL-G12D/+}$ allele and any conditional genes of interest, then ADM can be induced through infection with adenoviral or lentiviral Cre systems (Liou et al., 2015). Such systems enable the quantification of duct formation via ADM *in vitro*, enabling examination of the effect of loss of a gene of interest, such as DUSP5 or DUSP6/MKP-3, on the propensity for ADM to occur. Furthermore, as *in vitro* systems, they allow simple manipulation via siRNA (Liou et al., 2015) or inhibitor treatment (Shi et al., 2013), making them an effective system to investigate the biochemical mechanism by which alteration of a gene of interest can induce changes in the propensity for ADM to occur. One potential avenue, which is worthy of further investigation using such an approach would be the potential upregulation of Sox9 following DUSP5 loss. Sox9 upregulation was detected following $KRas^{G12D}$ expression and DUSP5 ablation in MEFs (Fig. 4.13), and Sox9 is a transcription factor which induces a ductal fate in the pancreas which has been shown to be essential for $KRas^{G12D}$-mediated ADM and PanIN induction (Kopp et al., 2012).

PDAC tumour cell lines were generated and tumour mRNA isolated from mice that developed PDAC as part of the survival study during this project. These should form useful resources to investigate the mechanism by which the loss of DUSP6/MKP-3 promotes accelerated mortality due to PDAC (Fig. 5.25) and an increased metastatic propensity (Fig. 5.27C) following $KRas^{G12D}$-driven pancreatic tumourigenesis. KC and $KCD6^{-/-}$ tumour cell lines could be characterised and the migratory or invasive capacity of these cell lines investigated *in vitro*. If any phenotypes are observed these cell lines could then be utilised to elucidate the molecular mechanisms driving such processes. As we have yet to identify any ERK-target proteins which are specifically regulated upon the loss of DUSP6, proteomic and phospho-proteomic approaches might enable us to determine the proteins which are most strongly differentially regulated in this scenario. Furthermore, RNAseq or microarray analyses could be performed utilising the tumour mRNA or mRNA isolated from our pancreatic cancer cell lines to identify any significant differences in the activation of specific signalling networks or cellular processes across the KC, $KCD5^{-/-}$ and $KCD6^{-/-}$ cohorts. This might identify key processes, which are altered following the loss of

DUSP5 or DUSP6/MKP-3, thereby providing a starting point for more detailed mechanistic studies.

These mechanistic studies could be further advanced through the generation of 3D organoid cultures of pancreatic tissue. Such approaches utilise culture conditions optimised to promote cells dissociated from primary tissue to self-organize into structures which mimic the 3D architecture of the organ from which they were derived (Baker et al., 2016). Organoid cultures have similar advantages over murine models to 2D cell culture approaches in that they allow simpler manipulation of the experimental system, and an increased experimental throughput. However, 2D cell culture approaches do not faithfully represent in vivo tumour biology. A striking demonstration of this being the fact that pancreatic cancer cell lines display a significant difference in gene expression in comparison to their parental primary PDAC following their isolation and culture *in vitro* (Gadaleta et al., 2011; Stein et al., 2004). In contrast, organoid cultures recapitulate many more features of the tumour environment including, a 3D organisation, continual cell-cell contact and interactions with stromal cells and the ECM (Baker et al., 2016).

In summary, here we have shown that the loss of DUSP6/MKP-3 promotes the increased initiation and accelerated progression of $KRas^{G12D}$-driven PanINs, resulting in the accelerated development PDAC, which displayed an increased propensity to metastasise. In contrast, although the loss of DUSP5 also promoted the increased initiation of $KRas^{G12D}$-driven ADM and PanINs, it did not induce accelerated PanIN progression and had no influence on the frequency of metastasis. Furthermore, the rate of PDAC development could not be reliably assessed following loss of DUSP5 in the presence of $KRas^{G12D}$ expression because such mice carried an excessive burden of PanINs, resulting in the majority of these mice becoming ill prior to the development of PDAC. These phenotypic differences could be due to the differential subcellular localisation of DUSP5 and DUSP6/MKP-3, enabling their loss to modulate the activity of ERK in unique ways. However, much of the mechanistic detail underpinning how loss of DUSP5 or DUSP6/MKP-3 promotes changes in $KRas^{G12D}$-driven pancreatic tumourigenesis is still poorly understood and is the basis of ongoing work.

Chapter 6 Concluding Remarks

The work presented in this thesis comprises some of the first evidence from *in vivo* genetic knockout studies that DUSP5 plays a functional role in cancer development. Following up our studies in the mouse model of DMBA/TPA-driven skin carcinogenesis we have analysed changes in nuclear ERK activation and gene expression, which give mechanistic insight into the increased tumour sensitivity of mice lacking DUSP5 in the latter model. The potential role of DUSP5 as a tumour suppressor is also reinforced by our studies of $KRas^{G12D}$-driven pancreatic cancer where DUSP5 acts as a tumour suppressor to restrain the initiation of benign pre-neoplastic lesions. In MEFs following acute Ras-ERK pathway stimulation DUSP5 performs a non-redundant role in the regulation of nuclear ERK activity and ERK-dependent gene expression. Therefore, despite the ability of ERK to shuttle rapidly between the cytoplasm and the nucleus, MKPs can mediate the precise control of ERK activity in specific subcellular compartments.

In MEFs expressing endogenous levels of mutant $KRas^{G12D}$ many ERK-targeting MKPs including both DUSP5 and DUSP6/MKP-3 are upregulated, indicating that these proteins are involved in the negative feedback response which constrains ERK activity following constitutive pathway activation. Furthermore, in a mouse model of mutant KRas-driven pancreatic cancer we demonstrate that DUSP6/MKP-3 functions as a potent tumour suppressor, restraining the initiation, malignant progression and metastatic potential of these tumours. However, in contrast to the tumour suppressive role observed in $KRas^{G12D}$-driven pancreatic cancer, the only other *in vivo* genetic model investigating the role of DUSP6/MKP-3 in cancer demonstrated that DUSP6/MKP-3 expression was essential for oncogenic transformation in $NRas^{G12D}$-driven models for pre-B acute lymphoblastic leukemia (ALL) (Shojaee et al., 2015). Together these contrasting reports demonstrate that MKPs may exhibit differential roles in cancer development, indicating that the ways in which MKPs influence cancer-related endpoints are likely to be context-dependent and influenced by factors including the tissue type and/or nature of the driving oncogene/s involved in the initiation and progression of particular cancer types.

Together this work demonstrates that MKPs play an important role in modulating the oncogenic potential of ERK signalling in mutant Ras-driven cancers of different tissues, suggesting that these enzymes might have a wider role across tumours displaying Ras-ERK

pathway activation. Further studies are required to extend these findings into models of additional cancer types, driven by a variety of oncogenes and to elucidate the mechanisms by which the loss of individual MKPs are able to promote such distinct phenotypic consequences for cancer progression.

References

Abel, E.L., Angel, J.M., Kiguchi, K., and DiGiovanni, J. (2009). Multi-stage chemical carcinogenesis in mouse skin: Fundamentals and applications. Nat. Protoc. *4*, 1350–1362.

Adachi, M., Fukuda, M., and Nishida, E. (1999). Two co-existing mechanisms for nuclear import of MAP kinase: passive diffusion of a monomer and active transport of a dimer. EMBO J. *18*, 5347–5358.

Adachi, M., Fukuda, M., and Nishida, E. (2000). Nuclear Export of Map Kinase (ERK) Involves a Map Kinase Kinase (Mek-Dependent) Active Transport Mechanism. J. Cell Biol. *148*, 849–856.

Adams, R.H., Porras, A., Alonso, G., Jones, M., Vintersten, K., Panelli, S., Valladares, A., Perez, L., Klein, R., and Nebreda, A.R. (2000). Essential Role of p38α MAP Kinase in Placental but Not Embryonic Cardiovascular Development. Mol. Cell *6*, 109–116.

Aguirre, A.J., Bardeesy, N., Sinha, M., Lopez, L., Tuveson, D.A., Horner, J., Redston, M.S., and DePinho, R.A. (2003). Activated Kras and Ink4a/Arf deficiency cooperate to produce metastatic pancreatic ductal adenocarcinoma. Genes Dev. *17*, 3112–3126.

Alagesan, B., Contino, G., Guimaraes, A.R., Corcoran, R.B., Desphande, V., Wojtkiewicz, G.R., Hezel, A.F., Wong, K.-K., Loda, M., Weissleder, R., et al. (2014). Combined MEK and PI3K inhibition in a mouse model of pancreatic cancer. Clin. Cancer Res. clincanres.1591.2014.

Alonso, A., Sasin, J., Bottini, N., Friedberg, I., Friedberg, I., Osterman, A., Godzik, A., Hunter, T., Dixon, J., and Mustelin, T. (2004). Protein Tyrosine Phosphatases in the Human Genome. Cell *117*, 699–711.

Apte, M.V., Wilson, J.S., Lugea, A., and Pandol, S.J. (2013). A Starring Role for Stellate Cells in the Pancreatic Cancer Microenvironment. Gastroenterology *144*, 1210–1219.

Ardito, C.M., Grüner, B.M., Takeuchi, K.K., Lubeseder-Martellato, C., Teichmann, N., Mazur, P.K., DelGiorno, K.E., Carpenter, E.S., Halbrook, C.J., Hall, J.C., et al. (2012). EGF Receptor Is Required for KRAS-Induced Pancreatic Tumorigenesis. Cancer Cell *22*, 304–317.

Baer, R., Cintas, C., Dufresne, M., Cassant-Sourdy, S., Schönhuber, N., Planque, L., Lulka, H., Couderc, B., Bousquet, C., Garmy-Susini, B., et al. (2014). Pancreatic cell plasticity and cancer initiation induced by oncogenic Kras is completely dependent on wild-type PI 3-kinase p110α. Genes Dev. *28*, 2621–2635.

Bailey, J.M., Hendley, A.M., Lafaro, K.J., Pruski, M.A., Jones, N.C., Alsina, J., Younes, M., Maitra, A., McAllister, F., Iacobuzio-Donahue, C.A., et al. (2015). p53 mutations cooperate with oncogenic Kras to promote adenocarcinoma from pancreatic ductal cells. Oncogene *doi: 10.1038/onc.2015.441. [Epub ahead of print]*.

Bailey, P., Chang, D.K., Nones, K., Johns, A.L., Patch, A.-M., Gingras, M.-C., Miller, D.K., Christ, A.N., Bruxner, T.J.C., Quinn, M.C., et al. (2016). Genomic analyses identify molecular subtypes of pancreatic cancer. Nature *advance online publication*.

Baker, L.A., Tiriac, H., Clevers, H., and Tuveson, D.A. (2016). Modeling pancreatic cancer with organoids. Trends Cancer *2*, 176–190.

Balmanno, K., and Cook, S.J. (2009). Tumour cell survival signalling by the ERK1/2 pathway. Cell Death Differ. *16*, 368–377.

Bardeesy, N., Aguirre, A.J., Chu, G.C., Cheng, K., Lopez, L.V., Hezel, A.F., Feng, B., Brennan, C., Weissleder, R., Mahmood, U., et al. (2006a). Both p16Ink4a and the p19Arf-p53 pathway constrain progression of pancreatic adenocarcinoma in the mouse. Proc. Natl. Acad. Sci. *103*, 5947–5952.

Bardeesy, N., Cheng, K., Berger, J.H., Chu, G.C., Pahler, J., Olson, P., Hezel, A.F., Horner, J., Lauwers, G.Y., Hanahan, D., et al. (2006b). Smad4 is dispensable for normal pancreas development yet critical in progression and tumor biology of pancreas cancer. Genes Dev. *20*, 3130–3146.

Barford, D. (1996). Molecular mechanisms of theprotein serine/threonine phosphatases. Trends Biochem. Sci. *21*, 407–412.

Bayne, L.J., Beatty, G.L., Jhala, N., Clark, C.E., Rhim, A.D., Stanger, B.Z., and Vonderheide, R.H. (2012). Tumor-Derived Granulocyte-Macrophage Colony-Stimulating Factor Regulates Myeloid Inflammation and T Cell Immunity in Pancreatic Cancer. Cancer Cell *21*, 822–835.

Belo, J., Krishnamurthy, M., Oakie, A., and Wang, R. (2013). The role of SOX9 transcription factor in pancreatic and duodenal development. Stem Cells Dev. *22*, 2935–2943.

Bentley, C., Jurinka, S.S., Kljavin, N.M., Vartanian, S., Ramani, S.R., Gonzalez, L.C., Yu, K., Modrusan, Z., Du, P., Bourgon, R., et al. (2013). A requirement for wild-type Ras isoforms in mutant KRas-driven signalling and transformation. Biochem. J. *452*, 313–320.

Bermudez, O., Marchetti, S., Pagès, G., and Gimond, C. (2008). Post-translational regulation of the ERK phosphatase DUSP6/MKP3 by the mTOR pathway. Oncogene *27*, 3685–3691.

Bermudez, O., Pagès, G., and Gimond, C. (2010). The dual-specificity MAP kinase phosphatases: critical roles in development and cancer. Am. J. Physiol. - Cell Physiol. *299*, C189–C202.

Biankin, A.V., Waddell, N., Kassahn, K.S., Gingras, M.-C., Muthuswamy, L.B., Johns, A.L., Miller, D.K., Wilson, P.J., Patch, A.-M., Wu, J., et al. (2012). Pancreatic cancer genomes reveal aberrations in axon guidance pathway genes. Nature *491*, 399–405.

Blasco, R.B., Francoz, S., Santamaría, D., Cañamero, M., Dubus, P., Charron, J., Baccarini, M., and Barbacid, M. (2011). c-Raf, but Not B-Raf, Is Essential for Development of K-Ras Oncogene-Driven Non-Small Cell Lung Carcinoma. Cancer Cell *19*, 652–663.

Bloethner, S., Chen, B., Hemminki, K., Müller-Berghaus, J., Ugurel, S., Schadendorf, D., and Kumar, R. (2005). Effect of common B-RAF and N-RAS mutations on global gene expression in melanoma cell lines. Carcinogenesis *26*, 1224–1232.

Bollag, G., Hirth, P., Tsai, J., Zhang, J., Ibrahim, P.N., Cho, H., Spevak, W., Zhang, C., Zhang, Y., Habets, G., et al. (2010). Clinical efficacy of a RAF inhibitor needs broad target blockade in BRAF-mutant melanoma. Nature *467*, 596–599.

Borràs, E., Jurado, I., Hernan, I., Gamundi, M.J., Dias, M., Martí, I., Mañé, B., Arcusa, À., Agúndez, J.A., Blanca, M., et al. (2011). Clinical pharmacogenomic testing of KRAS, BRAF and EGFRmutations by high resolution melting analysis and ultra-deep pyrosequencing. BMC Cancer *11*, 1–10.

Bosetti, C., Rosato, V., Li, D., Silverman, D., Petersen, G.M., Bracci, P.M., Neale, R.E., Muscat, J., Anderson, K., Gallinger, S., et al. (2014). Diabetes, antidiabetic medications, and pancreatic cancer risk: an analysis from the International Pancreatic Cancer Case-Control Consortium. Ann. Oncol. Off. J. Eur. Soc. Med. Oncol. ESMO *25*, 2065–2072.

Boulding, T., Wu, F., McCuaig, R., Dunn, J., Sutton, C.R., Hardy, K., Tu, W., Bullman, A., Yip, D., Dahlstrom, J.E., et al. (2016). Differential Roles for DUSP Family Members in Epithelial-to-Mesenchymal Transition and Cancer Stem Cell Regulation in Breast Cancer. PLoS ONE *11*, e0148065.

Boulton, T.G., Yancopoulos, G.D., Gregory, J.S., Slaughter, C., Moomaw, C., Hsu, J., and Cobb, M.H. (1990). An insulin-stimulated protein kinase similar to yeast kinases involved in cell cycle control. Science *249*, 64–67.

Boulton, T.G., Nye, S.H., Robbins, D.J., Ip, N.Y., Radzlejewska, E., Morgenbesser, S.D., DePinho, R.A., Panayotatos, N., Cobb, M.H., and Yancopoulos, G.D. (1991). ERKs: A family of protein-serine/threonine kinases that are activated and tyrosine phosphorylated in response to insulin and NGF. Cell *65*, 663–675.

Bournet, B., Buscail, C., Muscari, F., Cordelier, P., and Buscail, L. (2016). Targeting KRAS for diagnosis, prognosis, and treatment of pancreatic cancer: Hopes and realities. Eur. J. Cancer *54*, 75–83.

Brembeck, F.H., Schreiber, F.S., Deramaudt, T.B., Craig, L., Rhoades, B., Swain, G., Grippo, P., Stoffers, D.A., Silberg, D.G., and Rustgi, A.K. (2003). The Mutant K-ras Oncogene Causes Pancreatic Periductal Lymphocytic Infiltration and Gastric Mucous Neck Cell Hyperplasia in Transgenic Mice. Cancer Res. *63*, 2005–2009.

Brondello, J.-M., Brunet, A., Pouysségur, J., and McKenzie, F.R. (1997). The Dual Specificity Mitogen-activated Protein Kinase Phosphatase-1 and −2 Are Induced by the p42/p44MAPK Cascade. J. Biol. Chem. *272*, 1368–1376.

Brondello, J.-M., Pouysségur, J., and McKenzie, F.R. (1999). Reduced MAP Kinase Phosphatase-1 Degradation After p42/p44MAPK-Dependent Phosphorylation. Science *286*, 2514–2517.

Brynczka, C., Labhart, P., and Merrick, B.A. (2007). NGF-mediated transcriptional targets of p53 in PC12 neuronal differentiation. BMC Genomics *8*, 139.

Buck, M.J., and Lieb, J.D. (2004). ChIP-chip: considerations for the design, analysis, and application of genome-wide chromatin immunoprecipitation experiments. Genomics *83*, 349–360.

Buffet, C., Catelli, M.-G., Hecale-Perlemoine, K., Bricaire, L., Garcia, C., Gallet-Dierick, A., Rodriguez, S., Cormier, F., and Groussin, L. (2015). Dual Specificity Phosphatase 5, a Specific Negative Regulator of ERK Signaling, Is Induced by Serum Response Factor and Elk-1 Transcription Factor. PLoS ONE *10*, e0145484.

Bulavin, D.V., Demidov, O.N., Saito, S. 'ichi, Kauraniemi, P., Phillips, C., Amundson, S.A., Ambrosino, C., Sauter, G., Nebreda, A.R., Anderson, C.W., et al. (2002). Amplification of PPM1D in human tumors abrogates p53 tumor-suppressor activity. Nat. Genet. *31*, 210–215.

Bulavin, D.V., Phillips, C., Nannenga, B., Timofeev, O., Donehower, L.A., Anderson, C.W., Appella, E., and Fornace, A.J. (2004). Inactivation of the Wip1 phosphatase inhibits mammary tumorigenesis through p38 MAPK–mediated activation of the p16Ink4a-p19Arf pathway. Nat. Genet. *36*, 343–350.

Cagnol, S., and Rivard, N. (2012). Oncogenic KRAS and BRAF activation of the MEK/ERK signaling pathway promotes expression of dual-specificity phosphatase 4 (DUSP4/MKP2) resulting in nuclear ERK1/2 inhibition. Oncogene *32*, 564–576.

Cai, C., Chen, J.-Y., Han, Z.-D., He, H.-C., Chen, J.-H., Chen, Y.-R., Yang, S.-B., Wu, Y.-D., Zeng, Y.-R., Zou, J., et al. (2015). Down-regulation of dual-specificity phosphatase 5 predicts poor prognosis of patients with prostate cancer. Int. J. Clin. Exp. Med. *8*, 4186–4194.

Caldas, C., Hahn, S.A., Costa, L.T. da, Redston, M.S., Schutte, M., Seymour, A.B., Weinstein, C.L., Hruban, R.H., Yeo, C.J., and Kern, S.E. (1994). Frequent somatic mutations and homozygous deletions of the p16 (MTS1) gene in pancreatic adenocarcinoma. Nat. Genet. *8*, 27–32.

Caldwell, M.E., DeNicola, G.M., Martins, C.P., Jacobetz, M.A., Maitra, A., Hruban, R.H., and Tuveson, D.A. (2012). Cellular features of senescence during the evolution of human and murine ductal pancreatic cancer. Oncogene *31*, 1599–1608.

Calhoun, E.S., Jones, J.B., Ashfaq, R., Adsay, V., Baker, S.J., Valentine, V., Hempen, P.M., Hilgers, W., Yeo, C.J., Hruban, R.H., et al. (2003). BRAF and FBXW7 (CDC4, FBW7, AGO, SEL10) mutations in distinct subsets of pancreatic cancer: potential therapeutic targets. Am. J. Pathol. *163*, 1255–1260.

Camps, M., Nichols, A., Gillieron, C., Antonsson, B., Muda, M., Chabert, C., Boschert, U., and Arkinstall, S. (1998). Catalytic Activation of the Phosphatase MKP-3 by ERK2 Mitogen-Activated Protein Kinase. Science *280*, 1262–1265.

Cao, X.M., Koski, R.A., Gashler, A., McKiernan, M., Morris, C.F., Gaffney, R., Hay, R.V., and Sukhatme, V.P. (1990). Identification and characterization of the Egr-1 gene product, a DNA-binding zinc finger protein induced by differentiation and growth signals. Mol. Cell. Biol. *10*, 1931–1939.

Cargnello, M., and Roux, P.P. (2011). Activation and Function of the MAPKs and Their Substrates, the MAPK-Activated Protein Kinases. Microbiol. Mol. Biol. Rev. *75*, 50–83.

Casar, B., Pinto, A., and Crespo, P. (2008). Essential Role of ERK Dimers in the Activation of Cytoplasmic but Not Nuclear Substrates by ERK-Scaffold Complexes. Mol. Cell *31*, 708–721.

Catalanotti, F., Reyes, G., Jesenberger, V., Galabova-Kovacs, G., de Matos Simoes, R., Carugo, O., and Baccarini, M. (2009). A Mek1–Mek2 heterodimer determines the strength and duration of the Erk signal. Nat. Struct. Mol. Biol. *16*, 294–303.

Caunt, C.J., and Keyse, S.M. (2013). Dual-specificity MAP kinase phosphatases (MKPs). FEBS J. *280*, 489–504.

Caunt, C.J., Sale, M.J., Smith, P.D., and Cook, S.J. (2015). MEK1 and MEK2 inhibitors and cancer therapy: the long and winding road. Nat. Rev. Cancer *15*, 577–592.

Cerezo-Guisado, M.I., Reino, P. del, Remy, G., Kuma, Y., Arthur, J.S.C., Gallego-Ortega, D., and Cuenda, A. (2011). Evidence of p38γ and p38δ involvement in cell transformation processes. Carcinogenesis *32*, 1093–1099.

Čermák, V., Kosla, J., Plachý, J., Trejbalová, K., Hejnar, J., and Dvořák, M. (2010). The transcription factor EGR1 regulates metastatic potential of v-src transformed sarcoma cells. Cell. Mol. Life Sci. *67*, 3557–3568.

Chadha, K.S., Khoury, T., Yu, J., Black, J.D., Gibbs, J.F., Kuvshinoff, B.W., Tan, D., Brattain, M.G., and Javle, M.M. (2006). Activated Akt and Erk expression and survival after surgery in pancreatic carcinoma. Ann. Surg. Oncol. *13*, 933–939.

Chakravarti, D., Pelling, J.C., Cavalieri, E.L., and Rogan, E.G. (1995). Relating aromatic hydrocarbon-induced DNA adducts and c-H-ras mutations in mouse skin papillomas: the role of apurinic sites. Proc. Natl. Acad. Sci. *92*, 10422–10426.

Chang, L., and Karin, M. (2001). Mammalian MAP kinase signalling cascades. Nature *410*, 37–40.

Chen, N., Nomura, M., She, Q.-B., Ma, W.-Y., Bode, A.M., Wang, L., Flavell, R.A., and Dong, Z. (2001). Suppression of Skin Tumorigenesis in c-Jun NH2-Terminal Kinase-2-Deficient Mice. Cancer Res. *61*, 3908–3912.

Chen, N.-M., Singh, G., Koenig, A., Liou, G.-Y., Storz, P., Zhang, J.-S., Regul, L., Nagarajan, S., Kühnemuth, B., Johnsen, S.A., et al. (2015). NFATc1 Links EGFR Signaling to Induction of Sox9 Transcription and Acinar–Ductal Transdifferentiation in the Pancreas. Gastroenterology *148*, 1024–1034.e9.

Chio, I.I.C., Jafarnejad, S.M., Ponz-Sarvise, M., Park, Y., Rivera, K., Palm, W., Wilson, J., Sangar, V., Hao, Y., Öhlund, D., et al. (2016). NRF2 Promotes Tumor Maintenance by Modulating mRNA Translation in Pancreatic Cancer. Cell *doi: 10.1016/j.cell.2016.06.056. [Epub ahead of print]*.

Chitale, D., Gong, Y., Taylor, B.S., Broderick, S., Brennan, C., Somwar, R., Golas, B., Wang, L., Motoi, N., Szoke, J., et al. (2009). An integrated genomic analysis of lung cancer reveals loss of DUSP4 in EGFR-mutant tumors. Oncogene *28*, 2773–2783.

Chow, C.-W., and Davis, R.J. (2006). Proteins Kinases: Chromatin-Associated Enzymes? Cell *127*, 887–890.

Christy, B., and Nathans, D. (1989). DNA binding site of the growth factor-inducible protein Zif268. Proc. Natl. Acad. Sci. U. S. A. *86*, 8737–8741.

Chu, Y., Solski, P.A., Khosravi-Far, R., Der, C.J., and Kelly, K. (1996). The Mitogen-activated Protein Kinase Phosphatases PAC1, MKP-1, and MKP-2 Have Unique Substrate Specificities and Reduced Activity in Vivo toward the ERK2 sevenmaker Mutation. J. Biol. Chem. *271*, 6497–6501.

Chuang, S.-Y., Yang, C.-H., Chou, C.-C., Chiang, Y.-P., Chuang, T.-H., and Hsu, L.-C. (2013). TLR-induced PAI-2 expression suppresses IL-1β processing via increasing autophagy and NLRP3 degradation. Proc. Natl. Acad. Sci. U. S. A. *110*, 16079–16084.

Chuderland, D., Konson, A., and Seger, R. (2008). Identification and Characterization of a General Nuclear Translocation Signal in Signaling Proteins. Mol. Cell *31*, 850–861.

Cisowski, J., Sayin, V.I., Liu, M., Karlsson, C., and Bergo, M.O. (2015). Oncogene-induced senescence underlies the mutual exclusive nature of oncogenic KRAS and BRAF. Oncogene *35*, 1328–1333.

Clark, A., Dean, J., Tudor, C., and Saklatvala, J. (2009). Post-transcriptional gene regulation by MAP kinases via AU-rich elements. Front. Biosci. Landmark Ed. *14*, 847–871.

Clark, G.J., Westwick, J.K., and Der, C.J. (1997). p120 GAP Modulates Ras Activation of Jun Kinases and Transformation. J. Biol. Chem. *272*, 1677–1681.

Cleary, S.P., Gryfe, R., Guindi, M., Greig, P., Smith, L., Mackenzie, R., Strasberg, S., Hanna, S., Taylor, B., Langer, B., et al. (2004). Prognostic factors in resected pancreatic adenocarcinoma: Analysis of actual 5-year survivors1. J. Am. Coll. Surg. *198*, 722–731.

Cobb, M.H., and Goldsmith, E.J. (2000). Dimerization in MAP-kinase signaling. Trends Biochem. Sci. *25*, 7–9.

Cohen, P.T.W. (2004). Overview of protein serine/threonine phosphatases. In Protein Phosphatases, J. n Ariño, and D.R. Alexander, eds. (Springer Berlin Heidelberg), pp. 1–20.

Collins, M.A., Bednar, F., Zhang, Y., Brisset, J.-C., Galbán, S., Galbán, C.J., Rakshit, S., Flannagan, K.S., Adsay, N.V., and Pasca di Magliano, M. (2012). Oncogenic Kras is required for both the initiation and maintenance of pancreatic cancer in mice. J. Clin. Invest. *122*, 639–653.

Collisson, E.A., Sadanandam, A., Olson, P., Gibb, W.J., Truitt, M., Gu, S., Cooc, J., Weinkle, J., Kim, G.E., Jakkula, L., et al. (2011). Subtypes of pancreatic ductal adenocarcinoma and their differing responses to therapy. Nat. Med. *17*, 500–503.

Collisson, E.A., Trejo, C.L., Silva, J.M., Gu, S., Korkola, J.E., Heiser, L.M., Charles, R.-P., Rabinovich, B.A., Hann, B., Dankort, D., et al. (2012). A Central Role for RAF→MEK→ERK Signaling in the Genesis of Pancreatic Ductal Adenocarcinoma. Cancer Discov. *2*, 685–693.

Comes, F., Matrone, A., Lastella, P., Nico, B., Susca, F.C., Bagnulo, R., Ingravallo, G., Modica, S., Sasso, G.L., Moschetta, A., et al. (2007). A novel cell type-specific role of p38α

in the control of autophagy and cell death in colorectal cancer cells. Cell Death Differ. *14*, 693–702.

Corcoran, R.B., Contino, G., Deshpande, V., Tzatsos, A., Conrad, C., Benes, C.H., Levy, D.E., Settleman, J., Engelman, J.A., and Bardeesy, N. (2011). STAT3 Plays a Critical Role in KRAS-Induced Pancreatic Tumorigenesis. Cancer Res. *71*, 5020–5029.

Coulombe, P., and Meloche, S. (2007). Atypical mitogen-activated protein kinases: Structure, regulation and functions. Biochim. Biophys. Acta BBA - Mol. Cell Res. *1773*, 1376–1387.

Countaway, J.L., Nairn, A.C., and Davis, R.J. (1992). Mechanism of desensitization of the epidermal growth factor receptor protein-tyrosine kinase. J. Biol. Chem. *267*, 1129–1140.

Cowley, S., Paterson, H., Kemp, P., and Marshall, C.J. (1994). Activation of MAP kinase kinase is necessary and sufficient for PC12 differentiation and for transformation of NIH 3T3 cells. Cell *77*, 841–852.

Croonquist, P.A., Linden, M.A., Zhao, F., and Ness, B.G.V. (2003). Gene profiling of a myeloma cell line reveals similarities and unique signatures among IL-6 response, N-ras-activating mutations, and coculture with bone marrow stromal cells. Blood *102*, 2581–2592.

Croucher, D.R., Saunders, D.N., Lobov, S., and Ranson, M. (2008). Revisiting the biological roles of PAI2 (SERPINB2) in cancer. Nat. Rev. Cancer *8*, 535–545.

Cuadrado, A., and Nebreda, A.R. (2010). Mechanisms and functions of p38 MAPK signalling. Biochem. J. *429*, 403–417.

Cui, Y., Parra, I., Zhang, M., Hilsenbeck, S.G., Tsimelzon, A., Furukawa, T., Horii, A., Zhang, Z.-Y., Nicholson, R.I., and Fuqua, S.A.W. (2006). Elevated Expression of Mitogen-Activated Protein Kinase Phosphatase 3 in Breast Tumors: A Mechanism of Tamoxifen Resistance. Cancer Res. *66*, 5950–5959.

Davies, C.C., Harvey, E., McMahon, R.F.T., Finegan, K.G., Connor, F., Davis, R.J., Tuveson, D.A., and Tournier, C. (2014). Impaired JNK Signaling Cooperates with KrasG12D Expression to Accelerate Pancreatic Ductal Adenocarcinoma. Cancer Res. *74*, 3344–3356.

Davies, H., Hunter, C., Smith, R., Stephens, P., Greenman, C., Bignell, G., Teague, J., Butler, A., Edkins, S., Stevens, C., et al. (2005). Somatic Mutations of the Protein Kinase Gene Family in Human Lung Cancer. Cancer Res. *65*, 7591–7595.

De La O, J.-P., Emerson, L.L., Goodman, J.L., Froebe, S.C., Illum, B.E., Curtis, A.B., and Murtaugh, L.C. (2008). Notch and Kras reprogram pancreatic acinar cells to ductal intraepithelial neoplasia. Proc. Natl. Acad. Sci. *105*, 18907–18912.

Degl'Innocenti, D., Romeo, P., Tarantino, E., Sensi, M., Cassinelli, G., Catalano, V., Lanzi, C., Perrone, F., Pilotti, S., Seregni, E., et al. (2013). DUSP6/MKP3 is overexpressed in papillary and poorly differentiated thyroid carcinoma and contributes to neoplastic properties of thyroid cancer cells. Endocr. Relat. Cancer *20*, 23–37.

DeNicola, G.M., Karreth, F.A., Humpton, T.J., Gopinathan, A., Wei, C., Frese, K., Mangal, D., Yu, K.H., Yeo, C.J., Calhoun, E.S., et al. (2011). Oncogene-induced Nrf2 transcription promotes ROS detoxification and tumorigenesis. Nature *475*, 106–109.

Dérijard, B., Raingeaud, J., Barrett, T., Wu, I.H., Han, J., Ulevitch, R.J., and Davis, R.J. (1995). Independent human MAP-kinase signal transduction pathways defined by MEK and MKK isoforms. Science *267*, 682–685.

Deschênes-Simard, X., Gaumont-Leclerc, M.-F., Bourdeau, V., Lessard, F., Moiseeva, O., Forest, V., Igelmann, S., Mallette, F.A., Saba-El-Leil, M.K., Meloche, S., et al. (2013). Tumor suppressor activity of the ERK/MAPK pathway by promoting selective protein degradation. Genes Dev. *27*, 900–915.

Deschênes-Simard, X., Kottakis, F., Meloche, S., and Ferbeyre, G. (2014). ERKs in Cancer: Friends or Foes? Cancer Res. *74*, 412–419.

Detre, S., Jotti, G.S., and Dowsett, M. (1995). A “quickscore” method for immunohistochemical semiquantitation: validation for oestrogen receptor in breast carcinomas. J. Clin. Pathol. *48*, 876–878.

Dhanasekaran, D.N., and Reddy, E.P. (2008). JNK signaling in apoptosis. Oncogene *27*, 6245–6251.

Dhillon, A.S., Hagan, S., Rath, O., and Kolch, W. (2007). MAP kinase signalling pathways in cancer. Oncogene *26*, 3279–3290.

Díaz-García, C.V., Agudo-López, A., Pérez, C., Prieto-García, E., Iglesias, L., Ponce, S., Garzotto, A.R., Rodríguez-Peralto, J.L., Cortés-Funes, H., López-Martín, J.A., et al. (2014). Prognostic value of dual-specificity phosphatase 6 expression in non-small cell lung cancer. Tumor Biol. *36*, 1199–1206.

Dickinson, R.J., and Keyse, S.M. (2006). Diverse physiological functions for dual-specificity MAP kinase phosphatases. J. Cell Sci. *119*, 4607–4615.

Dickinson, R.J., Eblaghie, M.C., Keyse, S.M., and Morriss-Kay, G.M. (2002). Expression of the ERK-specific MAP kinase phosphatase PYST1/MKP3 in mouse embryos during morphogenesis and early organogenesis. Mech. Dev. *113*, 193–196.

Dickinson, R.J., Delavaine, L., Cejudo-Marín, R., Stewart, G., Staples, C.J., Didmon, M.P., Trinidad, A.G., Alonso, A., Pulido, R., and Keyse, S.M. (2011). Phosphorylation of the Kinase Interaction Motif in Mitogen-activated Protein (MAP) Kinase Phosphatase-4 Mediates Cross-talk between Protein Kinase A and MAP Kinase Signaling Pathways. J. Biol. Chem. *286*, 38018–38026.

Dolado, I., Swat, A., Ajenjo, N., De Vita, G., Cuadrado, A., and Nebreda, A.R. (2007). p38α MAP Kinase as a Sensor of Reactive Oxygen Species in Tumorigenesis. Cancer Cell *11*, 191–205.

Dougherty, K.M., Pearson, J.M., Yang, A.Y., Westrick, R.J., Baker, M.S., and Ginsburg, D. (1999). The plasminogen activator inhibitor-2 gene is not required for normal murine development or survival. Proc. Natl. Acad. Sci. U. S. A. *96*, 686–691.

Dougherty, M.K., Müller, J., Ritt, D.A., Zhou, M., Zhou, X.Z., Copeland, T.D., Conrads, T.P., Veenstra, T.D., Lu, K.P., and Morrison, D.K. (2005). Regulation of Raf-1 by Direct Feedback Phosphorylation. Mol. Cell *17*, 215–224.

Douville, E., and Downward, J. (1997). EGF induced SOS phosphorylation in PC12 cells involves P90 RSK-2. Oncogene *15*, 373–383.

Downward, J. (2003). Targeting RAS signalling pathways in cancer therapy. Nat. Rev. Cancer *3*, 11–22.

Ebisuya, M., Kondoh, K., and Nishida, E. (2005). The duration, magnitude and compartmentalization of ERK MAP kinase activity: mechanisms for providing signaling specificity. J. Cell Sci. *118*, 2997–3002.

Eblaghie, M.C., Lunn, J.S., Dickinson, R.J., Münsterberg, A.E., Sanz-Ezquerro, J.-J., Farrell, E.R., Mathers, J., Keyse, S.M., Storey, K., and Tickle, C. (2003). Negative Feedback Regulation of FGF Signaling Levels by Pyst1/MKP3 in Chick Embryos. Curr. Biol. *13*, 1009–1018.

Eblen, S.T., Slack-Davis, J.K., Tarcsafalvi, A., Parsons, J.T., Weber, M.J., and Catling, A.D. (2004). Mitogen-Activated Protein Kinase Feedback Phosphorylation Regulates MEK1 Complex Formation and Activation during Cellular Adhesion. Mol. Cell. Biol. *24*, 2308–2317.

Ekerot, M., Stavridis, M.P., Delavaine, L., Mitchell, M.P., Staples, C., Owens, D.M., Keenan, I.D., Dickinson, R.J., Storey, K.G., and Keyse, S.M. (2008). Negative-feedback regulation of FGF signalling by DUSP6/MKP-3 is driven by ERK1/2 and mediated by Ets factor binding to a conserved site within the DUSP6/MKP-3 gene promoter. Biochem. J. *412*, 287–298.

English, J., Pearson, G., Wilsbacher, J., Swantek, J., Karandikar, M., Xu, S., and Cobb, M.H. (1999). New Insights into the Control of MAP Kinase Pathways. Exp. Cell Res. *253*, 255–270.

Eser, S., Reiff, N., Messer, M., Seidler, B., Gottschalk, K., Dobler, M., Hieber, M., Arbeiter, A., Klein, S., Kong, B., et al. (2013). Selective Requirement of PI3K/PDK1 Signaling for Kras Oncogene-Driven Pancreatic Cell Plasticity and Cancer. Cancer Cell *23*, 406–420.

Fan, F., Geurts, A.M., Pabbidi, M.R., Smith, S.V., Harder, D.R., Jacob, H., and Roman, R.J. (2014). Zinc-Finger Nuclease Knockout of Dual-Specificity Protein Phosphatase-5 Enhances the Myogenic Response and Autoregulation of Cerebral Blood Flow in FHH.1BN Rats. PLoS ONE *9*, e112878.

Feng, B., He, Q., and Xu, H. (2014a). FOXO1-dependent up-regulation of MAP kinase phosphatase 3 (MKP-3) mediates glucocorticoid-induced hepatic lipid accumulation in mice. Mol. Cell. Endocrinol. *393*, 46–55.

Feng, B., Jiao, P., Helou, Y., Li, Y., He, Q., Walters, M.S., Salomon, A., and Xu, H. (2014b). MAP Kinase Phosphatase 3 (MKP-3) Deficient Mice Are Resistant to Diet Induced-Obesity. Diabetes *63*, 2924–2934.

Ferguson, B.S., Harrison, B.C., Jeong, M.Y., Reid, B.G., Wempe, M.F., Wagner, F.F., Holson, E.B., and McKinsey, T.A. (2013). Signal-dependent repression of DUSP5 by class I HDACs

controls nuclear ERK activity and cardiomyocyte hypertrophy. Proc. Natl. Acad. Sci. *110*, 9806–9811.

Ferlay, J., Soerjomataram, I., Dikshit, R., Eser, S., Mathers, C., Rebelo, M., Parkin, D.M., Forman, D., and Bray, F. (2015). Cancer incidence and mortality worldwide: Sources, methods and major patterns in GLOBOCAN 2012. Int. J. Cancer *136*, E359–E386.

Fey, D., Croucher, D.R., and Kholodenko, B.N. (2012). Crosstalk and signaling switches in mitogen-activated protein kinase cascades. Front. Syst. Biol. *3*, 355.

von Figura, G., Fukuda, A., Roy, N., Liku, M.E., Morris Iv, J.P., Kim, G.E., Russ, H.A., Firpo, M.A., Mulvihill, S.J., Dawson, D.W., et al. (2014). The chromatin regulator Brg1 suppresses formation of intraductal papillary mucinous neoplasm and pancreatic ductal adenocarcinoma. Nat. Cell Biol. *16*, 255–267.

Fish, R.J., and Kruithof, E.K.O. (2006). Evidence for serpinB2-independent protection from TNF-alpha-induced apoptosis. Exp. Cell Res. *312*, 350–361.

Formstecher, E., Ramos, J.W., Fauquet, M., Calderwood, D.A., Hsieh, J.-C., Canton, B., Nguyen, X.-T., Barnier, J.-V., Camonis, J., Ginsberg, M.H., et al. (2001). PEA-15 Mediates Cytoplasmic Sequestration of ERK MAP Kinase. Dev. Cell *1*, 239–250.

Frémin, C., Saba-El-Leil, M.K., Lévesque, K., Ang, S.-L., and Meloche, S. (2015). Functional Redundancy of ERK1 and ERK2 MAP Kinases during Development. Cell Rep. *12*, 913–921.

Friedlander, S.Y.G., Chu, G.C., Snyder, E.L., Girnius, N., Dibelius, G., Crowley, D., Vasile, E., DePinho, R.A., and Jacks, T. (2009). Context-Dependent Transformation of Adult Pancreatic Cells by Oncogenic K-Ras. Cancer Cell *16*, 379–389.

Furukawa, T. (2009). Molecular Pathology of Pancreatic Cancer: Implications for Molecular Targeting Therapy. Clin. Gastroenterol. Hepatol. *7*, S35–S39.

Furukawa, T., Yatsuoka, T., Youssef, E.M., Abe, T., Yokoyama, T., Fukushige, S., Soeda, E., Hoshi, M., Hayashi, Y., Sunamura, M., et al. (1998). Genomic analysis of DUSP6, a dual specificity MAP kinase phosphatase, in pancreatic cancer. Cytogenet. Cell Genet. *82*, 156–159.

Furukawa, T., Sunamura, M., Motoi, F., Matsuno, S., and Horii, A. (2003). Potential Tumor Suppressive Pathway Involving DUSP6/MKP-3 in Pancreatic Cancer. Am. J. Pathol. *162*, 1807–1815.

Furukawa, T., Fujisaki, R., Yoshida, Y., Kanai, N., Sunamura, M., Abe, T., Takeda, K., Matsuno, S., and Horii, A. (2005). Distinct progression pathways involving the dysfunction of DUSP6/MKP-3 in pancreatic intraepithelial neoplasia and intraductal papillary-mucinous neoplasms of the pancreas. Mod. Pathol. *18*, 1034–1042.

Furukawa, T., Sunamura, M., and Horii, A. (2006). Molecular mechanisms of pancreatic carcinogenesis. Cancer Sci. *97*, 1–7.

Gadaleta, E., Cutts, R.J., Kelly, G.P., Crnogorac-Jurcevic, T., Kocher, H.M., Lemoine, N.R., and Chelala, C. (2011). A global insight into a cancer transcriptional space using pancreatic data: importance, findings and flaws. Nucleic Acids Res. *39*, 7900–7907.

Gaestel, M. (2013). What goes up must come down: molecular basis of MAPKAP kinase 2/3-dependent regulation of the inflammatory response and its inhibition. Biol. Chem. *394*, 1301–1315.

Gillen, S., Schuster, T., Büschenfelde, C.M. zum, Friess, H., and Kleeff, J. (2010). Preoperative/Neoadjuvant Therapy in Pancreatic Cancer: A Systematic Review and Meta-analysis of Response and Resection Percentages. PLOS Med *7*, e1000267.

Gopinathan, A., Morton, J.P., Jodrell, D.I., and Sansom, O.J. (2015). GEMMs as preclinical models for testing pancreatic cancer therapies. Dis. Model. Mech. *8*, 1185–1200.

Goydos, J.S., Mann, B., Kim, H.J., Gabriel, E.M., Alsina, J., Germino, F.J., Shih, W., and Gorski, D.H. (2005). Detection of B-RAF and N-RAS mutations in human melanoma. J. Am. Coll. Surg. *200*, 362–370.

Greene, L.A., and Kaplan, D.R. (1995). Early events in neurotrophin signalling via Trk and p75 receptors. Curr. Opin. Neurobiol. *5*, 579–587.

Greenman, C., Stephens, P., Smith, R., Dalgliesh, G.L., Hunter, C., Bignell, G., Davies, H., Teague, J., Butler, A., Stevens, C., et al. (2007). Patterns of somatic mutation in human cancer genomes. Nature *446*, 153–158.

Grippo, P.J., Nowlin, P.S., Demeure, M.J., Longnecker, D.S., and Sandgren, E.P. (2003). Preinvasive pancreatic neoplasia of ductal phenotype induced by acinar cell targeting of mutant Kras in transgenic mice. Cancer Res. *63*, 2016–2019.

Groom, L.A., Sneddon, A.A., Alessi, D.R., Dowd, S., and Keyse, S.M. (1996). Differential regulation of the MAP, SAP and RK/p38 kinases by Pyst1, a novel cytosolic dual-specificity phosphatase. EMBO J. *15*, 3621–3632.

Guerra, C., and Barbacid, M. (2013). Genetically engineered mouse models of pancreatic adenocarcinoma. Mol. Oncol. *7*, 232–247.

Guerra, C., Mijimolle, N., Dhawahir, A., Dubus, P., Barradas, M., Serrano, M., Campuzano, V., and Barbacid, M. (2003). Tumor induction by an endogenous K-ras oncogene is highly dependent on cellular context. Cancer Cell *4*, 111–120.

Guerra, C., Schuhmacher, A.J., Cañamero, M., Grippo, P.J., Verdaguer, L., Pérez-Gallego, L., Dubus, P., Sandgren, E.P., and Barbacid, M. (2007). Chronic Pancreatitis Is Essential for Induction of Pancreatic Ductal Adenocarcinoma by K-Ras Oncogenes in Adult Mice. Cancer Cell *11*, 291–302.

Guerra, C., Collado, M., Navas, C., Schuhmacher, A.J., Hernández-Porras, I., Cañamero, M., Rodriguez-Justo, M., Serrano, M., and Barbacid, M. (2011). Pancreatitis-Induced Inflammation Contributes to Pancreatic Cancer by Inhibiting Oncogene-Induced Senescence. Cancer Cell *19*, 728–739.

Gupta, S., Barrett, T., Whitmarsh, A.J., Cavanagh, J., Sluss, H.K., Dérijard, B., and Davis, R.J. (1996). Selective interaction of JNK protein kinase isoforms with transcription factors. EMBO J. *15*, 2760–2770.

Habbe, N., Shi, G., Meguid, R.A., Fendrich, V., Esni, F., Chen, H., Feldmann, G., Stoffers, D.A., Konieczny, S.F., Leach, S.D., et al. (2008). Spontaneous induction of murine pancreatic intraepithelial neoplasia (mPanIN) by acinar cell targeting of oncogenic Kras in adult mice. Proc. Natl. Acad. Sci. *105*, 18913–18918.

Haigis, K.M., Kendall, K.R., Wang, Y., Cheung, A., Haigis, M.C., Glickman, J.N., Niwa-Kawakita, M., Sweet-Cordero, A., Sebolt-Leopold, J., Shannon, K.M., et al. (2008). Differential effects of oncogenic K-Ras and N-Ras on proliferation, differentiation and tumor progression in the colon. Nat. Genet. *40*, 600–608.

Han, J., Lee, J.D., Bibbs, L., and Ulevitch, R.J. (1994). A MAP kinase targeted by endotoxin and hyperosmolarity in mammalian cells. Science *265*, 808–811.

Han, J., Lee, J.-D., Jiang, Y., Li, Z., Feng, L., and Ulevitch, R.J. (1996). Characterization of the Structure and Function of a Novel MAP Kinase Kinase (MKK6). J. Biol. Chem. *271*, 2886–2891.

Hanafusa, H., Torii, S., Yasunaga, T., and Nishida, E. (2002). Sprouty1 and Sprouty2 provide a control mechanism for the Ras/MAPK signalling pathway. Nat. Cell Biol. *4*, 850–858.

Hanahan, D., and Weinberg, R.A. (2000). The Hallmarks of Cancer. Cell *100*, 57–70.

Hanahan, D., and Weinberg, R.A. (2011). Hallmarks of Cancer: The Next Generation. Cell *144*, 646–674.

Hanks, S.K., Quinn, A.M., and Hunter, T. (1988). The protein kinase family: conserved features and deduced phylogeny of the catalytic domains. Science *241*, 42–52.

Hayes, T.K., Neel, N.F., Hu, C., Gautam, P., Chenard, M., Long, B., Aziz, M., Kassner, M., Bryant, K.L., Pierobon, M., et al. (2016). Long-term ERK Inhibition in KRAS-Mutant Pancreatic Cancer Is Associated with MYC Degradation and Senescence-like Growth Suppression. Cancer Cell *29*, 75–89.

He, G., Zhang, L., Li, Q., and Yang, L. (2014). miR-92a/DUSP10/JNK signalling axis promotes human pancreatic cancer cells proliferation. Biomed. Pharmacother. *68*, 25–30.

Herreros-Villanueva, M. (2012). Mouse models of pancreatic cancer. World J. Gastroenterol. *18*, 1286.

Hezel, A.F., Kimmelman, A.C., Stanger, B.Z., Bardeesy, N., and DePinho, R.A. (2006). Genetics and biology of pancreatic ductal adenocarcinoma. Genes Dev. *20*, 1218–1249.

Hibi, M., Lin, A., Smeal, T., Minden, A., and Karin, M. (1993). Identification of an oncoprotein- and UV-responsive protein kinase that binds and potentiates the c-Jun activation domain. Genes Dev. *7*, 2135–2148.

Hijiya, N., Tsukamoto, Y., Nakada, C., Tung, N.L., Kai, T., Matsuura, K., Shibata, K., Inomata, M., Uchida, T., Tokunaga, A., et al. (2016). Genomic loss of DUSP4 contributes to the progression of intraepithelial neoplasm of pancreas to invasive carcinoma. Cancer Res. *76*, 2612-25.

Hill, R., Calvopina, J.H., Kim, C., Wang, Y., Dawson, D.W., Donahue, T.R., Dry, S., and Wu, H. (2010). PTEN loss accelerates KrasG12D-induced pancreatic cancer development. Cancer Res. *70*, 7114–7124.

Hingorani, S.R., Petricoin III, E.F., Maitra, A., Rajapakse, V., King, C., Jacobetz, M.A., Ross, S., Conrads, T.P., Veenstra, T.D., Hitt, B.A., et al. (2003). Preinvasive and invasive ductal pancreatic cancer and its early detection in the mouse. Cancer Cell *4*, 437–450.

Hingorani, S.R., Wang, L., Multani, A.S., Combs, C., Deramaudt, T.B., Hruban, R.H., Rustgi, A.K., Chang, S., and Tuveson, D.A. (2005). Trp53R172H and KrasG12D cooperate to promote chromosomal instability and widely metastatic pancreatic ductal adenocarcinoma in mice. Cancer Cell *7*, 469–483.

Hodis, E., Watson, I.R., Kryukov, G.V., Arold, S.T., Imielinski, M., Theurillat, J.-P., Nickerson, E., Auclair, D., Li, L., Place, C., et al. (2012). A Landscape of Driver Mutations in Melanoma. Cell *150*, 251–263.

Holmes, D.A., Yeh, J.-H., Yan, D., Xu, M., and Chan, A.C. (2015). Dusp5 negatively regulates IL-33-mediated eosinophil survival and function. EMBO J. *34*, 218–235.

Holzenberger, M., Lenzner, C., Leneuve, P., Zaoui, R., Hamard, G., Vaulont, S., and Bouc, Y.L. (2000). Cre-mediated germline mosaicism: a method allowing rapid generation of several alleles of a target gene. Nucleic Acids Res. *28*, e92–e92.

Hruban, R.H., and Fukushima, N. (2007). Pancreatic adenocarcinoma: update on the surgical pathology of carcinomas of ductal origin and PanINs. Mod. Pathol. *20*, S61–S70.

Hruban, R.H., Goggins, M., Parsons, J., and Kern, S.E. (2000). Progression Model for Pancreatic Cancer. Clin. Cancer Res. *6*, 2969–2972.

Hruban, R.H., Adsay, N.V., Albores-Saavedra, J., Compton, C., Garrett, E.S., Goodman, S.N., Kern, S.E., Klimstra, D.S., Klöppel, G., Longnecker, D.S., et al. (2001). Pancreatic intraepithelial neoplasia: a new nomenclature and classification system for pancreatic duct lesions. Am. J. Surg. Pathol. *25*, 579–586.

Hruban, R.H., Rustgi, A.K., Brentnall, T.A., Tempero, M.A., Wright, C.V., and Tuveson, D.A. (2006a). Pancreatic Cancer in Mice and Man: The Penn Workshop 2004. Cancer Res. *66*, 14–17.

Hruban, R.H., Adsay, N.V., Albores-Saavedra, J., Anver, M.R., Biankin, A.V., Boivin, G.P., Furth, E.E., Furukawa, T., Klein, A., Klimstra, D.S., et al. (2006b). Pathology of Genetically Engineered Mouse Models of Pancreatic Exocrine Cancer: Consensus Report and Recommendations. Cancer Res. *66*, 95–106.

Hrustanovic, G., Olivas, V., Pazarentzos, E., Tulpule, A., Asthana, S., Blakely, C.M., Okimoto, R.A., Lin, L., Neel, D.S., Sabnis, A., et al. (2015). RAS-MAPK dependence underlies a rational polytherapy strategy in EML4-ALK-positive lung cancer. Nat. Med. *21*, 1038–1047.

Hui, L., Bakiri, L., Mairhorfer, A., Schweifer, N., Haslinger, C., Kenner, L., Komnenovic, V., Scheuch, H., Beug, H., and Wagner, E.F. (2007). p38α suppresses normal and cancer cell proliferation by antagonizing the JNK–c-Jun pathway. Nat. Genet. *39*, 741–749.

Hui, L., Zatloukal, K., Scheuch, H., Stepniak, E., and Wagner, E.F. (2008). Proliferation of human HCC cells and chemically induced mouse liver cancers requires JNK1-dependent p21 downregulation. J. Clin. Invest. *118*, 3943–3953.

Ischenko, I., Petrenko, O., and Hayman, M.J. (2015). A MEK/PI3K/HDAC inhibitor combination therapy for KRAS mutant pancreatic cancer cells. Oncotarget *6*, 15814–15827.

Ishibashi, T., Bottaro, D.P., Michieli, P., Kelley, C.A., and Aaronson, S.A. (1994). A novel dual specificity phosphatase induced by serum stimulation and heat shock. J. Biol. Chem. *269*, 29897–29902.

Ishibe, S., Joly, D., Liu, Z.-X., and Cantley, L.G. (2004). Paxillin Serves as an ERK-Regulated Scaffold for Coordinating FAK and Rac Activation in Epithelial Morphogenesis. Mol. Cell *16*, 257–267.

Izeradjene, K., Combs, C., Best, M., Gopinathan, A., Wagner, A., Grady, W.M., Deng, C.-X., Hruban, R.H., Adsay, N.V., Tuveson, D.A., et al. (2007). KrasG12D and Smad4/Dpc4 Haploinsufficiency Cooperate to Induce Mucinous Cystic Neoplasms and Invasive Adenocarcinoma of the Pancreas. Cancer Cell *11*, 229–243.

Jackson, E.L., Willis, N., Mercer, K., Bronson, R.T., Crowley, D., Montoya, R., Jacks, T., and Tuveson, D.A. (2001). Analysis of lung tumor initiation and progression using conditional expression of oncogenic K-ras. Genes Dev. *15*, 3243–3248.

Jackson, E.L., Olive, K.P., Tuveson, D.A., Bronson, R., Crowley, D., Brown, M., and Jacks, T. (2005). The Differential Effects of Mutant p53 Alleles on Advanced Murine Lung Cancer. Cancer Res. *65*, 10280–10288.

Jaster, R. (2004). Molecular regulation of pancreatic stellate cell function. Mol. Cancer *3*, 26.

Javle, M.M., Shroff, R.T., Xiong, H., Varadhachary, G.A., Fogelman, D., Reddy, S.A., Davis, D., Zhang, Y., Wolff, R.A., and Abbruzzese, J.L. (2010). Inhibition of the mammalian target of rapamycin (mTOR) in advanced pancreatic cancer: results of two phase II studies. BMC Cancer *10*, 368.

Jeffrey, K.L., Camps, M., Rommel, C., and Mackay, C.R. (2007). Targeting dual-specificity phosphatases: manipulating MAP kinase signalling and immune responses. Nat. Rev. Drug Discov. *6*, 391–403.

Jemal, A., Siegel, R., Xu, J., and Ward, E. (2010). Cancer statistics, 2010. CA. Cancer J. Clin. *60*, 277–300.

Jeong, D.G., Yoon, T.-S., Kim, J.H., Shim, M.Y., Jung, S.-K., Son, J.H., Ryu, S.E., and Kim, S.J. (2006). Crystal structure of the catalytic domain of human MAP kinase phosphatase 5: structural insight into constitutively active phosphatase. J. Mol. Biol. *360*, 946–955.

Jeong, D.G., Cho, Y.H., Yoon, T.-S., Kim, J.H., Ryu, S.E., and Kim, S.J. (2007). Crystal structure of the catalytic domain of human DUSP5, a dual specificity MAP kinase protein phosphatase. Proteins Struct. Funct. Bioinforma. *66*, 253–258.

Jiao, P., Feng, B., and Xu, H. (2012). Mapping MKP-3/FOXO1 Interaction and Evaluating the Effect on Gluconeogenesis. PLOS ONE *7*, e41168.

Johnson, L.N., and O'Reilly, M. (1996). Control by phosphorylation. Curr. Opin. Struct. Biol. *6*, 762–769.

Johnson, L., Greenbaum, D., Cichowski, K., Mercer, K., Murphy, E., Schmitt, E., Bronson, R.T., Umanoff, H., Edelmann, W., Kucherlapati, R., et al. (1997). K-ras is an essential gene in the mouse with partial functional overlap with N-ras. Genes Dev. *11*, 2468–2481.

Johnson, L., Mercer, K., Greenbaum, D., Bronson, R.T., Crowley, D., Tuveson, D.A., and Jacks, T. (2001). Somatic activation of the K-ras oncogene causes early onset lung cancer in mice. Nature *410*, 1111–1116.

Jones, S., Zhang, X., Parsons, D.W., Lin, J.C.-H., Leary, R.J., Angenendt, P., Mankoo, P., Carter, H., Kamiyama, H., Jimeno, A., et al. (2008). Core Signaling Pathways in Human Pancreatic Cancers Revealed by Global Genomic Analyses. Science *321*, 1801–1806.

Joseph, E.W., Pratilas, C.A., Poulikakos, P.I., Tadi, M., Wang, W., Taylor, B.S., Halilovic, E., Persaud, Y., Xing, F., Viale, A., et al. (2010). The RAF inhibitor PLX4032 inhibits ERK signaling and tumor cell proliferation in a V600E BRAF-selective manner. Proc. Natl. Acad. Sci. *107*, 14903–14908.

Junttila, M.R., Devasthali, V., Cheng, J.H., Castillo, J., Metcalfe, C., Clermont, A.C., Otter, D.D., Chan, E., Bou-Reslan, H., Cao, T., et al. (2014). Modeling targeted inhibition of MEK and PI3 kinase in human pancreatic cancer. Mol. Cancer Ther. *14*, 41–47.

Jurek, A., Amagasaki, K., Gembarska, A., Heldin, C.-H., and Lennartsson, J. (2009). Negative and Positive Regulation of MAPK Phosphatase 3 Controls Platelet-derived Growth Factor-induced Erk Activation. J. Biol. Chem. *284*, 4626–4634.

Kanda, M., Matthaei, H., Wu, J., Hong, S., Yu, J., Borges, M., Hruban, R.H., Maitra, A., Kinzler, K., Vogelstein, B., et al. (2012). Presence of Somatic Mutations in Most Early-Stage Pancreatic Intraepithelial Neoplasia. Gastroenterology *142*, 730–733.e9.

Kapoor, A., Yao, W., Ying, H., Hua, S., Liewen, A., Wang, Q., Zhong, Y., Wu, C.-J., Sadanandam, A., Hu, B., et al. (2014). Yap1 Activation Enables Bypass of Oncogenic Kras Addiction in Pancreatic Cancer. Cell *158*, 185–197.

Karachaliou, N., Mayo, C., Costa, C., Magrí, I., Gimenez-Capitan, A., Molina-Vila, M.A., and Rosell, R. (2013). KRAS Mutations in Lung Cancer. Clin. Lung Cancer *14*, 205–214.

Karlsson, M., Mathers, J., Dickinson, R.J., Mandl, M., and Keyse, S.M. (2004). Both Nuclear-Cytoplasmic Shuttling of the Dual Specificity Phosphatase MKP-3 and Its Ability to Anchor MAP Kinase in the Cytoplasm Are Mediated by a Conserved Nuclear Export Signal. J. Biol. Chem. *279*, 41882–41891.

Karnoub, A.E., and Weinberg, R.A. (2008). Ras oncogenes: split personalities. Nat. Rev. Mol. Cell Biol. *9*, 517–531.

Kawaguchi, Y., Cooper, B., Gannon, M., Ray, M., MacDonald, R.J., and Wright, C.V.E. (2002). The role of the transcriptional regulator Ptf1a in converting intestinal to pancreatic progenitors. Nat. Genet. *32*, 128–134.

Kawakami, Y., Rodríguez-León, J., Koth, C.M., Büscher, D., Itoh, T., Raya, Á., Ng, J.K., Esteban, C.R., Takahashi, S., Henrique, D., et al. (2003). MKP3 mediates the cellular response to FGF8 signalling in the vertebrate limb. Nat. Cell Biol. *5*, 513–519.

Kennedy, A.L., Morton, J.P., Manoharan, I., Nelson, D.M., Jamieson, N.B., Pawlikowski, J.S., McBryan, T., Doyle, B., McKay, C., Oien, K.A., et al. (2011). Activation of the PIK3CA/AKT Pathway Suppresses Senescence Induced by an Activated RAS Oncogene to Promote Tumorigenesis. Mol. Cell *42*, 36–49.

Kennedy, N.J., Sluss, H.K., Jones, S.N., Bar-Sagi, D., Flavell, R.A., and Davis, R.J. (2003). Suppression of Ras-stimulated transformation by the JNK signal transduction pathway. Genes Dev. *17*, 629–637.

Keyse, S. (2008). Dual-specificity MAP kinase phosphatases (MKPs) and cancer. Cancer Metastasis Rev. *27*, 253–261.

Keyse, S.M. (2000). Protein phosphatases and the regulation of mitogen-activated protein kinase signalling. Curr. Opin. Cell Biol. *12*, 186–192.

Khokhlatchev, A.V., Canagarajah, B., Wilsbacher, J., Robinson, M., Atkinson, M., Goldsmith, E., and Cobb, M.H. (1998). Phosphorylation of the MAP Kinase ERK2 Promotes Its Homodimerization and Nuclear Translocation. Cell *93*, 605–615.

Kholodenko, B.N., Hancock, J.F., and Kolch, W. (2010). Signalling ballet in space and time. Nat. Rev. Mol. Cell Biol. *11*, 414–426.

Kidger, A.M., and Keyse, S.M. (2016a). Dual-Specificity Map Kinase (MAPK) Phosphatases (MKPs) and Their Involvement in Cancer. In Protein Tyrosine Phosphatases in Cancer, Benjamin G. Neel and Nicholas Tonks, Eds, (Springer), p. In press.

Kidger, A.M., and Keyse, S.M. (2016b). The regulation of oncogenic Ras/ERK signalling by dual-specificity mitogen activated protein kinase phosphatases (MKPs). Semin. Cell Dev. Biol. *50*, 125–132.

Kim, Y.H., Choi, Y.W., Han, J.H., Lee, J., Soh, E.Y., Park, S.H., Kim, J.-H., and Park, T.J. (2014). TSH Signaling Overcomes B-RafV600E–Induced Senescence in Papillary Thyroid Carcinogenesis through Regulation of DUSP6. Neoplasia *16*, 1107–1120.

Kimura, M., Abe, T., Sunamura, M., Matsuno, S., and Horii, A. (1996). Detailed deletion mapping on chromosome arm 12q in human pancreatic adenocarcinoma: identification of a I-cM region of common allelic loss. Genes. Chromosomes Cancer *17*, 88–93.

Kimura, M., Furukawa, T., Abe, T., Yatsuoka, T., Youssef, E.M., Yokoyama, T., Ouyang, H., Ohnishi, Y., Sunamura, M., Kobari, M., et al. (1998). Identification of two common regions of allelic loss in chromosome arm 12q in human pancreatic cancer. Cancer Res. *58*, 2456–2460.

Kinno, T., Tsuta, K., Shiraishi, K., Mizukami, T., Suzuki, M., Yoshida, A., Suzuki, K., Asamura, H., Furuta, K., Kohno, T., et al. (2014). Clinicopathological features of nonsmall cell lung carcinomas with BRAF mutations. Ann. Oncol. *25*, 138–142.

Kleeff, J., Korc, M., Apte, M., Vecchia, C.L., Johnson, C.D., Biankin, A.V., Neale, R.E., Tempero, M., Tuveson, D.A., Hruban, R.H., et al. (2016). Pancreatic cancer. Nat. Rev. Dis. Primer *2*, 16022.

Klemke, R.L., Cai, S., Giannini, A.L., Gallagher, P.J., Lanerolle, P. de, and Cheresh, D.A. (1997). Regulation of Cell Motility by Mitogen-activated Protein Kinase. J. Cell Biol. *137*, 481–492.

Kojima, K., Vickers, S.M., Adsay, N.V., Jhala, N.C., Kim, H.-G., Schoeb, T.R., Grizzle, W.E., and Klug, C.A. (2007). Inactivation of Smad4 Accelerates KrasG12D-Mediated Pancreatic Neoplasia. Cancer Res. *67*, 8121–8130.

Kolch, W. (2005). Coordinating ERK/MAPK signalling through scaffolds and inhibitors. Nat. Rev. Mol. Cell Biol. *6*, 827–837.

Kong, G., Chang, Y.-I., Damnernsawad, A., You, X., Du, J., Ranheim, E.A., Lee, W., Ryu, M.-J., Zhou, Y., Xing, Y., et al. (2016). Loss of wild-type Kras promotes activation of all Ras isoforms in oncogenic Kras-induced leukemogenesis. Leukemia *30*, 1542–1551.

Kopp, J.L., von Figura, G., Mayes, E., Liu, F.-F., Dubois, C.L., Morris IV, J.P., Pan, F.C., Akiyama, H., Wright, C.V.E., Jensen, K., et al. (2012). Identification of Sox9-Dependent Acinar-to-Ductal Reprogramming as the Principal Mechanism for Initiation of Pancreatic Ductal Adenocarcinoma. Cancer Cell *22*, 737–750.

Korotchenko, V.N., Saydmohammed, M., Vollmer, L.L., Bakan, A., Sheetz, K., Debiec, K.T., Greene, K.A., Agliori, C.S., Bahar, I., Day, B.W., et al. (2014). In vivo structure-activity relationship studies support allosteric targeting of a dual specificity phosphatase. Chembiochem Eur. J. Chem. Biol. *15*, 1436–1445.

Kotlyarov, A., Neininger, A., Schubert, C., Eckert, R., Birchmeier, C., Volk, H.-D., and Gaestel, M. (1999). MAPKAP kinase 2 is essential for LPS-induced TNF-α biosynthesis. Nat. Cell Biol. *1*, 94–97.

Kovanen, P.E., Rosenwald, A., Fu, J., Hurt, E.M., Lam, L.T., Giltnane, J.M., Wright, G., Staudt, L.M., and Leonard, W.J. (2003). Analysis of gamma c-family cytokine target genes. Identification of dual-specificity phosphatase 5 (DUSP5) as a regulator of mitogen-activated protein kinase activity in interleukin-2 signaling. J. Biol. Chem. *278*, 5205–5213.

Kovanen, P.E., Bernard, J., Al-Shami, A., Liu, C., Bollenbacher-Reilley, J., Young, L., Pise-Masison, C., Spolski, R., and Leonard, W.J. (2008). T-cell Development and Function Are Modulated by Dual Specificity Phosphatase DUSP5. J. Biol. Chem. *283*, 17362–17369.

Kreeger, P.K., Mandhana, R., Alford, S.K., Haigis, K.M., and Lauffenburger, D.A. (2009). RAS Mutations Affect Tumor Necrosis Factor–Induced Apoptosis in Colon Carcinoma Cells via ERK-Modulatory Negative and Positive Feedback Circuits Along with Non-ERK Pathway Effects. Cancer Res. *69*, 8191–8199.

von Kriegsheim, A., Baiocchi, D., Birtwistle, M., Sumpton, D., Bienvenut, W., Morrice, N., Yamada, K., Lamond, A., Kalna, G., Orton, R., et al. (2009). Cell fate decisions are specified by the dynamic ERK interactome. Nat. Cell Biol. *11*, 1458–1464.

Krones-Herzig, A., Mittal, S., Yule, K., Liang, H., English, C., Urcis, R., Soni, T., Adamson, E.D., and Mercola, D. (2005). Early Growth Response 1 Acts as a Tumor Suppressor In vivo and In vitro via Regulation of p53. Cancer Res. *65*, 5133–5143.

Kuan, C.-Y., Yang, D.D., Roy, D.R.S., Davis, R.J., Rakic, P., and Flavell, R.A. (1999). The Jnk1 and Jnk2 Protein Kinases Are Required for Regional Specific Apoptosis during Early Brain Development. Neuron *22*, 667–676.

Kubosaki, A., Tomaru, Y., Tagami, M., Arner, E., Miura, H., Suzuki, T., Suzuki, M., Suzuki, H., and Hayashizaki, Y. (2009). Genome-wide investigation of in vivo EGR-1 binding sites in monocytic differentiation. Genome Biol. *10*, R41.

Kucharska, A., Rushworth, L.K., Staples, C., Morrice, N.A., and Keyse, S.M. (2009). Regulation of the inducible nuclear dual-specificity phosphatase DUSP5 by ERK MAPK. Cell. Signal. *21*, 1794–1805.

Kumar, S., Boehm, J., and Lee, J.C. (2003). p38 MAP kinases: key signalling molecules as therapeutic targets for inflammatory diseases. Nat. Rev. Drug Discov. *2*, 717–726.

Kwak, S.P., and Dixon, J.E. (1995). Multiple Dual Specificity Protein Tyrosine Phosphatases Are Expressed and Regulated Differentially in Liver Cell Lines. J. Biol. Chem. *270*, 1156–1160.

Kyriakis, J.M., and Avruch, J. (1990). pp54 microtubule-associated protein 2 kinase. A novel serine/threonine protein kinase regulated by phosphorylation and stimulated by poly-L-lysine. J. Biol. Chem. *265*, 17355–17363.

Kyriakis, J.M., and Avruch, J. (2012). Mammalian MAPK Signal Transduction Pathways Activated by Stress and Inflammation: A 10-Year Update. Physiol. Rev. *92*, 689–737.

Labbé, D.P., Hardy, S., and Tremblay, M.L. (2012). Protein Tyrosine Phosphatases in Cancer: Friends and Foes! In Progress in Molecular Biology and Translational Science, S. Shenolikar, ed. (Academic Press), pp. 253–306.

Landt, S.G., Marinov, G.K., Kundaje, A., Kheradpour, P., Pauli, F., Batzoglou, S., Bernstein, B.E., Bickel, P., Brown, J.B., Cayting, P., et al. (2012). ChIP-seq guidelines and practices of the ENCODE and modENCODE consortia. Genome Res. *22*, 1813–1831.

Lawrence, M.C., McGlynn, K., Shao, C., Duan, L., Naziruddin, B., Levy, M.F., and Cobb, M.H. (2008). Chromatin-bound mitogen-activated protein kinases transmit dynamic signals in transcription complexes in β-cells. Proc. Natl. Acad. Sci. *105*, 13315–13320.

Lee, K.E., and Bar-Sagi, D. (2010). Oncogenic KRas Suppresses Inflammation-Associated Senescence of Pancreatic Ductal Cells. Cancer Cell *18*, 448–458.

Lee, J.C., Laydon, J.T., McDonnell, P.C., Gallagher, T.F., Kumar, S., Green, D., McNulty, D., Blumenthal, M.J., Keys, J.R., Land Vatter, S.W., et al. (1994). A protein kinase involved in the regulation of inflammatory cytokine biosynthesis. Nature *372*, 739–746.

Lee, J.U., Huang, S., Lee, M.H., Lee, S.E., Ryu, M.J., Kim, S.J., Kim, Y.K., Kim, S.Y., Joung, K.H., Kim, J.M., et al. (2012). Dual specificity phosphatase 6 as a predictor of invasiveness in papillary thyroid cancer. Eur. J. Endocrinol. *167*, 93–101.

Lee, S.L., Tourtellotte, L.C., Wesselschmidt, R.L., and Milbrandt, J. (1995). Growth and differentiation proceeds normally in cells deficient in the immediate early gene NGFI-A. J. Biol. Chem. *270*, 9971–9977.

Lefloch, R., Pouysségur, J., and Lenormand, P. (2008). Single and Combined Silencing of ERK1 and ERK2 Reveals Their Positive Contribution to Growth Signaling Depending on Their Expression Levels. Mol. Cell. Biol. *28*, 511–527.

Lemmon, M.A., Freed, D.M., Schlessinger, J., and Kiyatkin, A. (2016). The Dark Side of Cell Signaling: Positive Roles for Negative Regulators. Cell *164*, 1172–1184.

Li, C., Scott, D.A., Hatch, E., Tian, X., and Mansour, S.L. (2007). Dusp6 (Mkp3) is a negative feedback regulator of FGF-stimulated ERK signaling during mouse development. Development *134*, 167–176.

Li, W., Song, L., Ritchie, A.-M., and Melton, D.W. (2012). Increased levels of DUSP6 phosphatase stimulate tumourigenesis in a molecularly distinct melanoma subtype. Pigment Cell Melanoma Res. *25*, 188–199.

Liao, Q., Guo, J., Kleeff, J., Zimmermann, A., Büchler, M.W., Korc, M., and Friess, H. (2003). Down-regulation of the dual-specificity phosphatase MKP-1 suppresses tumorigenicity of pancreatic cancer cells. Gastroenterology *124*, 1830–1845.

Lidke, D.S., Huang, F., Post, J.N., Rieger, B., Wilsbacher, J., Thomas, J.L., Pouysségur, J., Jovin, T.M., and Lenormand, P. (2010). ERK Nuclear Translocation Is Dimerization-independent but Controlled by the Rate of Phosphorylation. J. Biol. Chem. *285*, 3092–3102.

Lin, Y.-W., and Yang, J.-L. (2006). Cooperation of ERK and SCFSkp2 for MKP-1 Destruction Provides a Positive Feedback Regulation of Proliferating Signaling. J. Biol. Chem. *281*, 915–926.

Lin, S.-C., Chien, C.-W., Lee, J.-C., Yeh, Y.-C., Hsu, K.-F., Lai, Y.-Y., Lin, S.-C., and Tsai, S.-J. (2011). Suppression of dual-specificity phosphatase–2 by hypoxia increases chemoresistance and malignancy in human cancer cells. J. Clin. Invest. *121*, 1905–1916.

Lin, Y.-W., Chuang, S.-M., and Yang, J.-L. (2003). ERK1/2 Achieves Sustained Activation by Stimulating MAPK Phosphatase-1 Degradation via the Ubiquitin-Proteasome Pathway. J. Biol. Chem. *278*, 21534–21541.

Lindberg, R.A., Quinn, A.M., and Hunter, T. (1992). Dual-specificity protein kinases: will any hydroxyl do? Trends Biochem. Sci. *17*, 114–119.

Liou, G.-Y., Döppler, H., Braun, U.B., Panayiotou, R., Scotti Buzhardt, M., Radisky, D.C., Crawford, H.C., Fields, A.P., Murray, N.R., Wang, Q.J., et al. (2015). Protein kinase D1 drives pancreatic acinar cell reprogramming and progression to intraepithelial neoplasia. Nat. Commun. *20*, 6200.

Lito, P., Pratilas, C.A., Joseph, E.W., Tadi, M., Halilovic, E., Zubrowski, M., Huang, A., Wong, W.L., Callahan, M.K., Merghoub, T., et al. (2012). Relief of Profound Feedback Inhibition of Mitogenic Signaling by RAF Inhibitors Attenuates Their Activity in BRAFV600E Melanomas. Cancer Cell *22*, 668–682.

Little, A.S., Balmanno, K., Sale, M.J., Newman, S., Dry, J.R., Hampson, M., Edwards, P.A.W., Smith, P.D., and Cook, S.J. (2011). Amplification of the Driving Oncogene, KRAS or BRAF, Underpins Acquired Resistance to MEK1/2 Inhibitors in Colorectal Cancer Cells. Sci. Signal. *4*, ra17.

Liu, Y.-X., Wang, J., Guo, J., Wu, J., Lieberman, H.B., and Yin, Y. (2008). DUSP1 Is Controlled by p53 during the Cellular Response to Oxidative Stress. Mol. Cancer Res. *6*, 624–633.

Loda, M., Capodieci, P., Mishra, R., Yao, H., Corless, C., Grigioni, W., Wang, Y., Magi-Galluzzi, C., and Stork, P.J. (1996). Expression of mitogen-activated protein kinase phosphatase-1 in the early phases of human epithelial carcinogenesis. Am. J. Pathol. *149*, 1553–1564.

Loonstra, A., Vooijs, M., Beverloo, H.B., Allak, B.A., Drunen, E. van, Kanaar, R., Berns, A., and Jonkers, J. (2001). Growth inhibition and DNA damage induced by Cre recombinase in mammalian cells. Proc. Natl. Acad. Sci. *98*, 9209–9214.

Lopez, F., Belloc, F., Lacombe, F., Dumain, P., Reiffers, J., Bernard, P., and Boisseau, M.R. (1991). Modalities of synthesis of Ki67 antigen during the stimulation of lymphocytes. Cytometry *12*, 42–49.

Lu, X., Nguyen, T.-A., Moon, S.-H., Darlington, Y., Sommer, M., and Donehower, L.A. (2008). The type 2C phosphatase Wip1: An oncogenic regulator of tumor suppressor and DNA damage response pathways. Cancer Metastasis Rev. *27*, 123–135.

Lucci, M.A., Orlandi, R., Triulzi, T., Tagliabue, E., Balsari, A., and Villa-Moruzzi, E. (2010). Expression profile of tyrosine phosphatases in HER2 breast cancer cells and tumors. Cell. Oncol. Off. J. Int. Soc. Cell. Oncol. *32*, 361–372.

Ma, J., Yu, X., Guo, L., and Lu, S.H. (2013). DUSP6, a tumor suppressor, is involved in differentiation and apoptosis in esophageal squamous cell carcinoma. Oncol. Lett. *6*, 1624–1630.

Magi-Galluzzi, C., Mishra, R., Fiorentino, M., Montironi, R., Yao, H., Capodieci, P., Wishnow, K., Kaplan, I., Stork, P.J., and Loda, M. (1997). Mitogen-activated protein kinase phosphatase 1 is overexpressed in prostate cancers and is inversely related to apoptosis. Lab. Investig. J. Tech. Methods Pathol. *76*, 37–51.

Magnuson, M.A., and Osipovich, A.B. (2013). Pancreas-Specific Cre Driver Lines and Considerations for Their Prudent Use. Cell Metab. *18*, 9–20.

Maillet, M., Purcell, N.H., Sargent, M.A., York, A.J., Bueno, O.F., and Molkentin, J.D. (2008). DUSP6 (MKP3) Null Mice Show Enhanced ERK1/2 Phosphorylation at Baseline and Increased Myocyte Proliferation in the Heart Affecting Disease Susceptibility. J. Biol. Chem. *283*, 31246–31255.

Maitra, A., Adsay, N.V., Argani, P., Iacobuzio-Donahue, C., De Marzo, A., Cameron, J.L., Yeo, C.J., and Hruban, R.H. (2003). Multicomponent analysis of the pancreatic adenocarcinoma progression model using a pancreatic intraepithelial neoplasia tissue microarray. Mod. Pathol. Off. J. U. S. Can. Acad. Pathol. Inc *16*, 902–912.

Major, L., Schroder, W.A., Gardner, J., Fish, R.J., and Suhrbier, A. (2011). Human papilloma virus transformed CaSki cells constitutively express high levels of functional SerpinB2. Exp. Cell Res. *317*, 338–347.

Mandl, M., Slack, D.N., and Keyse, S.M. (2005). Specific Inactivation and Nuclear Anchoring of Extracellular Signal-Regulated Kinase 2 by the Inducible Dual-Specificity Protein Phosphatase DUSP5. Mol. Cell. Biol. *25*, 1830–1845.

Mann, K.M., Ward, J.M., Yew, C.C.K., Kovochich, A., Dawson, D.W., Black, M.A., Brett, B.T., Sheetz, T.E., Dupuy, A.J., Chang, D.K., et al. (2012). Sleeping Beauty mutagenesis reveals cooperating mutations and pathways in pancreatic adenocarcinoma. Proc. Natl. Acad. Sci. *109*, 5934–5941.

Manning, G., Whyte, D.B., Martinez, R., Hunter, T., and Sudarsanam, S. (2002). The Protein Kinase Complement of the Human Genome. Science *298*, 1912–1934.

Marchetti, S., Gimond, C., Chambard, J.-C., Touboul, T., Roux, D., Pouysségur, J., and Pagès, G. (2005). Extracellular Signal-Regulated Kinases Phosphorylate Mitogen-Activated Protein Kinase Phosphatase 3/DUSP6 at Serines 159 and 197, Two Sites Critical for Its Proteasomal Degradation. Mol. Cell. Biol. *25*, 854–864.

Marshall, C.. (1995). Specificity of receptor tyrosine kinase signaling: Transient versus sustained extracellular signal-regulated kinase activation. Cell *80*, 179–185.

Marshall, C.J. (1994). MAP kinase kinase kinase, MAP kinase kinase and MAP kinase. Curr. Opin. Genet. Dev. *4*, 82–89.

Martell, K.J., Kwak, S., Hakes, D.J., Dixon, J.E., and Trent, J.M. (1994). Chromosomal Localization of Four Human VH1-like Protein-Tyrosine Phosphatases. Genomics *22*, 462–464.

Mason, J.M., Morrison, D.J., Albert Basson, M., and Licht, J.D. (2006). Sprouty proteins: multifaceted negative-feedback regulators of receptor tyrosine kinase signaling. Trends Cell Biol. *16*, 45–54.

Massagué, J. (2008). TGFβ in Cancer. Cell *134*, 215–230.

Massagué, J. (2012). TGFβ signalling in context. Nat. Rev. Mol. Cell Biol. *13*, 616–630.

McKay, M.M., and Morrison, D.K. (2007). Integrating signals from RTKs to ERK/MAPK. Oncogene *26*, 3113–3121.

Meier, R., Rouse, J., Cuenda, A., Nebreda, A.R., and Cohen, P. (1996). Cellular Stresses and Cytokines Activate Multiple Mitogen-Activated-Protein Kinase Kinase Homologues in PC12 and KB Cells. Eur. J. Biochem. *236*, 796–805.

Meloche, S., and Pouysségur, J. (2007). The ERK1/2 mitogen-activated protein kinase pathway as a master regulator of the G1- to S-phase transition. Oncogene *26*, 3227–3239.

Messina, S., Frati, L., Leonetti, C., Zuchegna, C., Di Zazzo, E., Calogero, A., and Porcellini, A. (2011). Dual-specificity phosphatase DUSP6 has tumor-promoting properties in human glioblastomas. Oncogene *30*, 3813–3820.

Moffitt, R.A., Marayati, R., Flate, E.L., Volmar, K.E., Loeza, S.G.H., Hoadley, K.A., Rashid, N.U., Williams, L.A., Eaton, S.C., Chung, A.H., et al. (2015). Virtual microdissection identifies distinct tumor- and stroma-specific subtypes of pancreatic ductal adenocarcinoma. Nat. Genet. *47*, 1168–1178.

Mohit, A.A., Martin, J.H., and Miller, C.A. (1995). p493F12 kinase: a novel MAP kinase expressed in a subset of neurons in the human nervous system. Neuron *14*, 67–78.

Molina, G., Vogt, A., Bakan, A., Dai, W., de Oliveira, P.Q., Znosko, W., Smithgall, T.E., Bahar, I., Lazo, J.S., Day, B.W., et al. (2009). Zebrafish chemical screening reveals an inhibitor of Dusp6 that expands cardiac cell lineages. Nat. Chem. Biol. *5*, 680–687.

Molton, S.A., Weston, C., Balmanno, K., Newson, C., Todd, D.E., Garner, A.P., and Cook, S.J. (2005). The conditional kinase ΔMEKK1:ER* selectively activates the JNK pathway and protects against serum withdrawal-induced cell death. Cell. Signal. *17*, 1412–1422.

Montero-Conde, C., Ruiz-Llorente, S., Dominguez, J.M., Knauf, J.A., Viale, A., Sherman, E.J., Ryder, M., Ghossein, R.A., Rosen, N., and Fagin, J.A. (2013). Relief of Feedback Inhibition of HER3 Transcription by RAF and MEK Inhibitors Attenuates Their Antitumor Effects in BRAF-Mutant Thyroid Carcinomas. Cancer Discov. *3*, 520–533.

Moodie, S.A., Paris, M.J., Kolch, W., and Wolfman, A. (1994). Association of MEK1 with p21ras.GMPPNP is dependent on B-Raf. Mol. Cell. Biol. *14*, 7153–7162.

Moon, S.-J., Lim, M.-A., Park, J.-S., Byun, J.-K., Kim, S.-M., Park, M.-K., Kim, E.-K., Moon, Y.-M., Min, J.-K., Ahn, S.-M., et al. (2014). Dual-specificity phosphatase 5 attenuates autoimmune arthritis via reciprocal regulation of Th17/Treg balance and inhibition of osteoclastogenesis. Arthritis Rheumatol. *66*, 3083–3095.

Morris, J.P., Wang, S.C., and Hebrok, M. (2010a). KRAS, Hedgehog, Wnt and the twisted developmental biology of pancreatic ductal adenocarcinoma. Nat. Rev. Cancer *10*, 683–695.

Morris, J.P., Cano, D.A., Sekine, S., Wang, S.C., and Hebrok, M. (2010b). Beta-catenin blocks Kras-dependent reprogramming of acini into pancreatic cancer precursor lesions in mice. J. Clin. Invest. *120*, 508–520.

Morris IV, J.P., and Hebrok, M. (2009). It's a Free for All—Insulin-Positive Cells Join the Group of Potential Progenitors for Pancreatic Ductal Adenocarcinoma. Cancer Cell *16*, 359–361.

Morrison, D.K., Kaplan, D.R., Rapp, U., and Roberts, T.M. (1988). Signal transduction from membrane to cytoplasm: growth factors and membrane-bound oncogene products increase Raf-1 phosphorylation and associated protein kinase activity. Proc. Natl. Acad. Sci. U. S. A. *85*, 8855–8859.

Morton, J.P., Timpson, P., Karim, S.A., Ridgway, R.A., Athineos, D., Doyle, B., Jamieson, N.B., Oien, K.A., Lowy, A.M., Brunton, V.G., et al. (2010). Mutant p53 drives metastasis

and overcomes growth arrest/senescence in pancreatic cancer. Proc. Natl. Acad. Sci. *107*, 246–251.

Mourey, R.J., Vega, Q.C., Campbell, J.S., Wenderoth, M.P., Hauschka, S.D., Krebs, E.G., and Dixon, J.E. (1996). A Novel Cytoplasmic Dual Specificity Protein Tyrosine Phosphatase Implicated in Muscle and Neuronal Differentiation. J. Biol. Chem. *271*, 3795–3802.

Muda, M., Theodosiou, A., Rodrigues, N., Boschert, U., Camps, M., Gillieron, C., Davies, K., Ashworth, A., and Arkinstall, S. (1996). The Dual Specificity Phosphatases M3/6 and MKP-3 Are Highly Selective for Inactivation of Distinct Mitogen-activated Protein Kinases. J. Biol. Chem. *271*, 27205–27208.

Mudgett, J.S., Ding, J., Guh-Siesel, L., Chartrain, N.A., Yang, L., Gopal, S., and Shen, M.M. (2000). Essential role for p38α mitogen-activated protein kinase in placental angiogenesis. Proc. Natl. Acad. Sci. *97*, 10454–10459.

Mustelin, T. (2007). A Brief Introduction to the Protein Phosphatase Families. In Protein Phosphatase Protocols, G. Moorhead, ed. (Springer New York), pp. 9–22.

Nadal, E. de, and Posas, F. (2010). Multilayered control of gene expression by stress-activated protein kinases. EMBO J. *29*, 4–13.

Nadal, E., Ammerer, G., and Posas, F. (2011). Controlling gene expression in response to stress. Nat. Rev. Genet. *12*, 833–845.

Nakamura, Y. (2004). Isolation of p53-target genes and their functional analysis. Cancer Sci. *95*, 7–11.

Navas, C., Hernández-Porras, I., Schuhmacher, A.J., Sibilia, M., Guerra, C., and Barbacid, M. (2012). EGF Receptor Signaling Is Essential for K-Ras Oncogene-Driven Pancreatic Ductal Adenocarcinoma. Cancer Cell *22*, 318–330.

Nelson, J.D., LeBoeuf, R.C., and Bomsztyk, K. (2011). Direct Recruitment of Insulin Receptor and ERK Signaling Cascade to Insulin-Inducible Gene Loci. Diabetes *60*, 127–137.

Nichols, A., Camps, M., Gillieron, C., Chabert, C., Brunet, A., Wilsbacher, J., Cobb, M., Pouyssegur, J., Shaw, J.P., and Arkinstall, S. (2000). Substrate Recognition Domains within Extracellular Signal-regulated Kinase Mediate Binding and Catalytic Activation of Mitogen-activated Protein Kinase Phosphatase-3. J. Biol. Chem. *275*, 24613–24621.

Nunes-Xavier, C.E., Tárrega, C., Cejudo-Marín, R., Frijhoff, J., Sandin, Å., Östman, A., and Pulido, R. (2010). Differential Up-regulation of MAP Kinase Phosphatases MKP3/DUSP6 and DUSP5 by Ets2 and c-Jun Converge in the Control of the Growth Arrest Versus Proliferation Response of MCF-7 Breast Cancer Cells to Phorbol Ester. J. Biol. Chem. *285*, 26417–26430.

Offield, M.F., Jetton, T.L., Labosky, P.A., Ray, M., Stein, R.W., Magnuson, M.A., Hogan, B.L., and Wright, C.V. (1996). PDX-1 is required for pancreatic outgrowth and differentiation of the rostral duodenum. Development *122*, 983–995.

Okudela, K., Yazawa, T., Woo, T., Sakaeda, M., Ishii, J., Mitsui, H., Shimoyamada, H., Sato, H., Tajiri, M., Ogawa, N., et al. (2009). Down-Regulation of DUSP6 Expression in Lung Cancer: Its Mechanism and Potential Role in Carcinogenesis. Am. J. Pathol. *175*, 867–881.

Owens, D.M., and Keyse, S.M. (2007). Differential regulation of MAP kinase signalling by dual-specificity protein phosphatases. Oncogene *26*, 3203–3213.

Packer, L.M., East, P., Reis-Filho, J.S., and Marais, R. (2009). Identification of direct transcriptional targets of V600EBRAF/MEK signalling in melanoma. Pigment Cell Melanoma Res. *22*, 785–798.

Pagès, G., Guérin, S., Grall, D., Bonino, F., Smith, A., Anjuere, F., Auberger, P., and Pouysségur, J. (1999). Defective Thymocyte Maturation in p44 MAP Kinase (Erk 1) Knockout Mice. Science *286*, 1374–1377.

Park, Y.J., Lee, J.M., Shin, S.Y., and Kim, Y.H. (2014). Constitutively active Ras negatively regulates Erk MAP kinase through induction of MAP kinase phosphatase 3 (MKP3) in NIH3T3 cells. BMB Rep. *47*, 685–690.

Patterson, K.I., Brummer, T., O'Brien, P.M., and Daly, R.J. (2009). Dual-specificity phosphatases: critical regulators with diverse cellular targets. Biochem. J. *418*, 475–489.

Payne, S.N., Maher, M.E., Tran, N.H., Van De Hey, D.R., Foley, T.M., Yueh, A.E., Leystra, A.A., Pasch, C.A., Jeffrey, J.J., Clipson, L., et al. (2015). PIK3CA mutations can initiate pancreatic tumorigenesis and are targetable with PI3K inhibitors. Oncogenesis *4*, e169.

Pearson, G., Robinson, F., Gibson, T.B., Xu, B., Karandikar, M., Berman, K., and Cobb, M.H. (2001). Mitogen-Activated Protein (MAP) Kinase Pathways: Regulation and Physiological Functions. Endocr. Rev. *22*, 153–183.

Pérez–Mancera, P.A., Guerra, C., Barbacid, M., and Tuveson, D.A. (2012). What We Have Learned About Pancreatic Cancer From Mouse Models. Gastroenterology *142*, 1079–1092.

Pérez-Mancera, P.A., Rust, A.G., van der Weyden, L., Kristiansen, G., Li, A., Sarver, A.L., Silverstein, K.A.T., Grützmann, R., Aust, D., Rümmele, P., et al. (2012). The deubiquitinase USP9X suppresses pancreatic ductal adenocarcinoma. Nature *486*, 266–270.

Phuchareon, J., McCormick, F., Eisele, D.W., and Tetsu, O. (2015). EGFR inhibition evokes innate drug resistance in lung cancer cells by preventing Akt activity and thus inactivating Ets-1 function. Proc. Natl. Acad. Sci. 201510733.

Pokholok, D.K., Zeitlinger, J., Hannett, N.M., Reynolds, D.B., and Young, R.A. (2006). Activated Signal Transduction Kinases Frequently Occupy Target Genes. Science *313*, 533–536.

Poulikakos, P.I., and Rosen, N. (2011). Mutant BRAF Melanomas—Dependence and Resistance. Cancer Cell *19*, 11–15.

Pratilas, C.A., Taylor, B.S., Ye, Q., Viale, A., Sander, C., Solit, D.B., and Rosen, N. (2009). V600EBRAF is associated with disabled feedback inhibition of RAF–MEK signaling and elevated transcriptional output of the pathway. Proc. Natl. Acad. Sci. *106*, 4519–4524.

Prior, I.A., Lewis, P.D., and Mattos, C. (2012). A Comprehensive Survey of Ras Mutations in Cancer. Cancer Res. *72*, 2457–2467.

Pulverer, B.J., Kyriakis, J.M., Avruch, J., Nikolakaki, E., and Woodgett, J.R. (1991). Phosphorylation of c-jun mediated by MAP kinases. Nature *353*, 670–674.

Pylayeva-Gupta, Y., Grabocka, E., and Bar-Sagi, D. (2011). RAS oncogenes: weaving a tumorigenic web. Nat. Rev. Cancer *11*, 761–774.

Pylayeva-Gupta, Y., Lee, K.E., Hajdu, C.H., Miller, G., and Bar-Sagi, D. (2012). Oncogenic Kras-Induced GM-CSF Production Promotes the Development of Pancreatic Neoplasia. Cancer Cell *21*, 836–847.

Rahib, L., Smith, B.D., Aizenberg, R., Rosenzweig, A.B., Fleshman, J.M., and Matrisian, L.M. (2014). Projecting Cancer Incidence and Deaths to 2030: The Unexpected Burden of Thyroid, Liver, and Pancreas Cancers in the United States. Cancer Res. *74*, 2913–2921.

Raitano, A.B., Halpern, J.R., Hambuch, T.M., and Sawyers, C.L. (1995). The Bcr-Abl leukemia oncogene activates Jun kinase and requires Jun for transformation. Proc. Natl. Acad. Sci. U. S. A. *92*, 11746–11750.

Rajalingam, K., Schreck, R., Rapp, U.R., and Albert, Š. (2007). Ras oncogenes and their downstream targets. Biochim. Biophys. Acta BBA - Mol. Cell Res. *1773*, 1177–1195.

Raman, M., Chen, W., and Cobb, M.H. (2007). Differential regulation and properties of MAPKs. Oncogene *26*, 3100–3112.

Ramesh, S., Qi, X.-J., Wildey, G.M., Robinson, J., Molkentin, J., Letterio, J., and Howe, P.H. (2008). TGFβ-mediated BIM expression and apoptosis are regulated through SMAD3-dependent expression of the MAPK phosphatase MKP2. EMBO Rep. *9*, 990–997.

Ramos, J.W. (2008). The regulation of extracellular signal-regulated kinase (ERK) in mammalian cells. Int. J. Biochem. Cell Biol. *40*, 2707–2719.

Rauch, J., Volinsky, N., Romano, D., and Kolch, W. (2011). The secret life of kinases: functions beyond catalysis. Cell Commun. Signal. *9*, 23.

Ray, L.B., and Sturgill, T.W. (1988). Insulin-stimulated microtubule-associated protein kinase is phosphorylated on tyrosine and threonine in vivo. Proc. Natl. Acad. Sci. U. S. A. *85*, 3753–3757.

Reino, P. del, Alsina-Beauchamp, D., Escós, A., Cerezo-Guisado, M.I., Risco, A., Aparicio, N., Zur, R., Fernandez-Estévez, M., Collantes, E., Montans, J., et al. (2014). Pro-Oncogenic Role of Alternative p38 Mitogen-Activated Protein Kinases p38γ and p38δ, Linking Inflammation and Cancer in Colitis-Associated Colon Cancer. Cancer Res. *74*, 6150–6160.

Reuter, C.W.M., Catling, A.D., Jelinek, T., and Weber, M.J. (1995). Biochemical analysis of MEK activation in NIH3T3 fibroblasts. Identification of B-Raf and other activators. J. Biol. Chem. *270*, 7644–7655.

Richards, D.A., Kuefler, P.R., Becerra, C., Wilfong, L.S., Gersh, R.H., Boehm, K.A., Zhan, F., Asmar, L., Myrand, S.P., Hozak, R.R., et al. (2011). Gemcitabine plus enzastaurin or single-

agent gemcitabine in locally advanced or metastatic pancreatic cancer: results of a phase II, randomized, noncomparative study. Invest. New Drugs *29*, 144–153.

Rincón, M., and Davis, R.J. (2009). Regulation of the immune response by stress-activated protein kinases. Immunol. Rev. *228*, 212–224.

Roberts, P.J., and Der, C.J. (2007). Targeting the Raf-MEK-ERK mitogen-activated protein kinase cascade for the treatment of cancer. Oncogene *26*, 3291–3310.

Rodrigues, G.A., Park, M., and Schlessinger, J. (1997). Activation of the JNK pathway is essential for transformation by the Met oncogene. EMBO J. *16*, 2634–2645.

Rosenfeldt, M.T., O'Prey, J., Morton, J.P., Nixon, C., MacKay, G., Mrowinska, A., Au, A., Rai, T.S., Zheng, L., Ridgway, R., et al. (2013). p53 status determines the role of autophagy in pancreatic tumour development. Nature *504*, 296–300.

Rouse, J., Cohen, P., Trigon, S., Morange, M., Alonso-Llamazares, A., Zamanillo, D., Hunt, T., and Nebreda, A.R. (1994). A novel kinase cascade triggered by stress and heat shock that stimulates MAPKAP kinase-2 and phosphorylation of the small heat shock proteins. Cell *78*, 1027–1037.

Rousseau, S., Dolado, I., Beardmore, V., Shpiro, N., Marquez, R., Nebreda, A.R., Arthur, J.S.C., Case, L.M., Tessier-Lavigne, M., Gaestel, M., et al. (2006). CXCL12 and C5a trigger cell migration via a PAK1/2-p38α MAPK-MAPKAP-K2-HSP27 pathway. Cell. Signal. *18*, 1897–1905.

Rovira, M., Scott, S.-G., Liss, A.S., Jensen, J., Thayer, S.P., and Leach, S.D. (2010). Isolation and characterization of centroacinar/terminal ductal progenitor cells in adult mouse pancreas. Proc. Natl. Acad. Sci. U. S. A. *107*, 75–80.

Roy, N., and Hebrok, M. (2015). Regulation of Cellular Identity in Cancer. Dev. Cell *35*, 674–684.

Rubinfeld, H., Hanoch, T., and Seger, R. (1999). Identification of a cytoplasmic-retention sequence in ERK2. J. Biol. Chem. *274*, 30349–30352.

Rushworth, L.K., Kidger, A.M., Delavaine, L., Stewart, G., Schelven, S. van, Davidson, J., Bryant, C.J., Caddye, E., East, P., Caunt, C.J., et al. (2014). Dual-specificity phosphatase 5 regulates nuclear ERK activity and suppresses skin cancer by inhibiting mutant Harvey-Ras (HRasQ61L)-driven SerpinB2 expression. Proc. Natl. Acad. Sci. *111*, 18267–18272.

Russo, A., Franchina, T., Ricciardi, G.R.R., Picone, A., Ferraro, G., Zanghì, M., Toscano, G., Giordano, A., Adamo, V., Russo, A., et al. (2015). A decade of EGFR inhibition in EGFR-mutated non small cell lung cancer (NSCLC): Old successes and future perspectives. Oncotarget *6*, 26814–26825.

Rustgi, A.K. (2014). Familial pancreatic cancer: genetic advances. Genes Dev. *28*, 1–7.

Ryan, D.P., Hong, T.S., and Bardeesy, N. (2014). Pancreatic Adenocarcinoma. N. Engl. J. Med. *371*, 1039–1049.

Sabapathy, K., Hochedlinger, K., Nam, S.Y., Bauer, A., Karin, M., and Wagner, E.F. (2004). Distinct Roles for JNK1 and JNK2 in Regulating JNK Activity and c-Jun-Dependent Cell Proliferation. Mol. Cell *15*, 713–725.

Sage, J., Mulligan, G.J., Attardi, L.D., Miller, A., Chen, S., Williams, B., Theodorou, E., and Jacks, T. (2000). Targeted disruption of the three Rb-related genes leads to loss of G1 control and immortalization. Genes Dev. *14*, 3037–3050.

Saigusa, S., Inoue, Y., Tanaka, K., Toiyama, Y., Okugawa, Y., Shimura, T., Hiro, J., Uchida, K., Mohri, Y., and Kusunoki, M. (2013). Decreased expression of DUSP4 is associated with liver and lung metastases in colorectal cancer. Med. Oncol. *30*, 1–7.

Sakurai, T., Maeda, S., Chang, L., and Karin, M. (2006). Loss of hepatic NF-κB activity enhances chemical hepatocarcinogenesis through sustained c-Jun N-terminal kinase 1 activation. Proc. Natl. Acad. Sci. *103*, 10544–10551.

Schieven, G. (2009). The p38alpha Kinase Plays a Central Role In Inflammation. Curr. Top. Med. Chem. *9*, 1038–1048.

Schindler, E.M., Hindes, A., Gribben, E.L., Burns, C.J., Yin, Y., Lin, M.-H., Owen, R.J., Longmore, G.D., Kissling, G.E., Arthur, J.S.C., et al. (2009). p38δ Mitogen-Activated Protein Kinase Is Essential for Skin Tumor Development in Mice. Cancer Res. *69*, 4648–4655.

Scholzen, T., and Gerdes, J. (2000). The Ki-67 protein: from the known and the unknown. J. Cell. Physiol. *182*, 311–322.

Schroder, W.A., Major, L.D., Le, T.T., Gardner, J., Sweet, M.J., Janciauskiene, S., and Suhrbier, A. (2014). Tumor cell-expressed SerpinB2 is present on microparticles and inhibits metastasis. Cancer Med. *3*, 500–513.

Sebolt-Leopold, J.S., Dudley, D.T., Herrera, R., Becelaere, K.V., Wiland, A., Gowan, R.C., Tecle, H., Barrett, S.D., Bridges, A., Przybranowski, S., et al. (1999). Blockade of the MAP kinase pathway suppresses growth of colon tumors in vivo. Nat. Med. *5*, 810–816.

Sensi, M., Nicolini, G., Petti, C., Bersani, I., Lozupone, F., Molla, A., Vegetti, C., Nonaka, D., Mortarini, R., Parmiani, G., et al. (2006). Mutually exclusive NRASQ61R and BRAFV600E mutations at the single-cell level in the same human melanoma. Oncogene *25*, 3357–3364.

Serrano, M., Hannon, G.J., and Beach, D. (1993). A new regulatory motif in cell-cycle control causing specific inhibition of cyclin D/CDK4. Nature *366*, 704–707.

Serrano, M., Lin, A.W., McCurrach, M.E., Beach, D., and Lowe, S.W. (1997). Oncogenic ras Provokes Premature Cell Senescence Associated with Accumulation of p53 and p16INK4a. Cell *88*, 593–602.

Shao, D.D., Xue, W., Krall, E.B., Bhutkar, A., Piccioni, F., Wang, X., Schinzel, A.C., Sood, S., Rosenbluh, J., Kim, J.W., et al. (2014). KRAS and YAP1 Converge to Regulate EMT and Tumor Survival. Cell *158*, 171–184.

Shapiro, P.S., Whalen, A.M., Tolwinski, N.S., Wilsbacher, J., Froelich-Ammon, S.J., Garcia, M., Osheroff, N., and Ahn, N.G. (1999). Extracellular signal-regulated kinase activates

topoisomerase IIalpha through a mechanism independent of phosphorylation. Mol. Cell. Biol. *19*, 3551–3560.

Shaul, Y.D., and Seger, R. (2007). The MEK/ERK cascade: From signaling specificity to diverse functions. Biochim. Biophys. Acta BBA - Mol. Cell Res. *1773*, 1213–1226.

She, Q.-B., Chen, N., Bode, A.M., Flavell, R.A., and Dong, Z. (2002). Deficiency of c-Jun-NH2-terminal Kinase-1 in Mice Enhances Skin Tumor Development by 12-O-Tetradecanoylphorbol-13-Acetate. Cancer Res. *62*, 1343–1348.

Shi, C., and Hruban, R.H. (2012). Intraductal papillary mucinous neoplasm. Hum. Pathol. *43*, 1–16.

Shi, G., DiRenzo, D., Qu, C., Barney, D., Miley, D., and Konieczny, S.F. (2013). Maintenance of acinar cell organization is critical to preventing Kras-induced acinar-ductal metaplasia. Oncogene *32*, 1950–1958.

Shin, S.-H., Park, S.-Y., and Kang, G.H. (2013). Down-Regulation of Dual-Specificity Phosphatase 5 in Gastric Cancer by Promoter CpG Island Hypermethylation and Its Potential Role in Carcinogenesis. Am. J. Pathol. *184*, 1275–1285.

Shin, S.-Y., Rath, O., Choo, S.-M., Fee, F., McFerran, B., Kolch, W., and Cho, K.-H. (2009). Positive- and negative-feedback regulations coordinate the dynamic behavior of the Ras-Raf-MEK-ERK signal transduction pathway. J. Cell Sci. *122*, 425–435.

Shojaee, S., Caeser, R., Buchner, M., Park, E., Swaminathan, S., Hurtz, C., Geng, H., Chan, L.N., Klemm, L., Hofmann, W.-K., et al. (2015). Erk Negative Feedback Control Enables Pre-B Cell Transformation and Represents a Therapeutic Target in Acute Lymphoblastic Leukemia. Cancer Cell *28*, 114–128.

Sieben, N.L.G., Oosting, J., Flanagan, A.M., Prat, J., Roemen, G.M.J.M., Kolkman-Uljee, S.M., Eijk, R. van, Cornelisse, C.J., Fleuren, G.J., and Engeland, M. van (2005). Differential Gene Expression in Ovarian Tumors Reveals Dusp 4 and Serpina 5 As Key Regulators for Benign Behavior of Serous Borderline Tumors. J. Clin. Oncol. *23*, 7257–7264.

Siegel, R.L., Miller, K.D., and Jemal, A. (2015). Cancer statistics, 2015. CA. Cancer J. Clin. *65*, 5–29.

Singh, A., Sowjanya, A.P., and Ramakrishna, G. (2005). The wild-type Ras: road ahead. FASEB J. *19*, 161–169.

Skrzypski, M., Dziadziuszko, R., Jassem, E., Szymanowska-Narloch, A., Gulida, G., Rzepko, R., Biernat, W., Taron, M., Jelitto-Górska, M., Marjański, T., et al. (2013). Main Histologic Types of Non–small-cell Lung Cancer Differ in Expression of Prognosis-related Genes. Clin. Lung Cancer *14*, 666–673.

Slack, D.N., Seternes, O.-M., Gabrielsen, M., and Keyse, S.M. (2001). Distinct Binding Determinants for ERK2/p38α and JNK MAP Kinases Mediate Catalytic Activation and Substrate Selectivity of MAP Kinase Phosphatase-1 ,. J. Biol. Chem. *276*, 16491–16500.

Smith, T.G., Karlsson, M., Lunn, J.S., Eblaghie, M.C., Keenan, I.D., Farrell, E.R., Tickle, C., Storey, K.G., and Keyse, S.M. (2006). Negative feedback predominates over cross-

regulation to control ERK MAPK activity in response to FGF signalling in embryos. FEBS Lett. *580*, 4242–4245.

Solit, D.B., Garraway, L.A., Pratilas, C.A., Sawai, A., Getz, G., Basso, A., Ye, Q., Lobo, J.M., She, Y., Osman, I., et al. (2006). BRAF mutation predicts sensitivity to MEK inhibition. Nature *439*, 358–362.

Son, J., Lyssiotis, C.A., Ying, H., Wang, X., Hua, S., Ligorio, M., Perera, R.M., Ferrone, C.R., Mullarky, E., Shyh-Chang, N., et al. (2013). Glutamine supports pancreatic cancer growth through a KRAS-regulated metabolic pathway. Nature *496*, 101–105.

Song, H., Wu, C., Wei, C., Li, D., Hua, K., Song, J., Xu, H., Chen, L., and Fang, L. (2015). Silencing of DUSP6 gene by RNAi-mediation inhibits proliferation and growth in MDA-MB-231 breast cancer cells: an in vitro study. Int. J. Clin. Exp. Med. *8*, 10481–10490.

Stanger, B.Z., Stiles, B., Lauwers, G.Y., Bardeesy, N., Mendoza, M., Wang, Y., Greenwood, A., Cheng, K., McLaughlin, M., Brown, D., et al. (2005). Pten constrains centroacinar cell expansion and malignant transformation in the pancreas. Cancer Cell *8*, 185–195.

Staples, C.J., Owens, D.M., Maier, J.V., Cato, A.C.B., and Keyse, S.M. (2010). Cross-talk between the p38α and JNK MAPK Pathways Mediated by MAP Kinase Phosphatase-1 Determines Cellular Sensitivity to UV Radiation. J. Biol. Chem. *285*, 25928–25940.

Stein, W.D., Litman, T., Fojo, T., and Bates, S.E. (2004). A Serial Analysis of Gene Expression (SAGE) Database Analysis of Chemosensitivity. Cancer Res. *64*, 2805–2816.

Stewart, A.E., Dowd, S., Keyse, S.M., and McDonald, N.Q. (1999). Crystal structure of the MAPK phosphatase Pyst1 catalytic domain and implications for regulated activation. Nat. Struct. Mol. Biol. *6*, 174–181.

Stringer, B., Udofa, E.A., and Antalis, T.M. (2012). Regulation of the Human Plasminogen Activator Inhibitor Type 2 Gene COOPERATION OF AN UPSTREAM SILENCER AND TRANSACTIVATOR. J. Biol. Chem. *287*, 10579–10589.

Suda, K., Tomizawa, K., and Mitsudomi, T. (2010). Biological and clinical significance of KRAS mutations in lung cancer: an oncogenic driver that contrasts with EGFR mutation. Cancer Metastasis Rev. *29*, 49–60.

Takeuchi, Y., Nakao, A., Harada, A., Nonami, T., Fukatsu, T., and Takagi, H. (1993). Expression of plasminogen activators and their inhibitors in human pancreatic carcinoma: immunohistochemical study. Am. J. Gastroenterol. *88*, 1928–1933.

Tanoue, T., Moriguchi, T., and Nishida, E. (1999). Molecular Cloning and Characterization of a Novel Dual Specificity Phosphatase, MKP-5. J. Biol. Chem. *274*, 19949–19956.

Tao, H., Yang, J.-J., Hu, W., Shi, K.-H., Deng, Z.-Y., and Li, J. (2015). MeCP2 regulation of cardiac fibroblast proliferation and fibrosis by down-regulation of DUSP5. Int. J. Biol. Macromol. *82*, 68–75.

Tape, C.J., Ling, S., Dimitriadi, M., McMahon, K.M., Worboys, J.D., Leong, H.S., Norrie, I.C., Miller, C.J., Poulogiannis, G., Lauffenburger, D.A., et al. (2016). Oncogenic KRAS Regulates Tumor Cell Signaling via Stromal Reciprocation. Cell *165*, 910–920.

Tarcic, G., Avraham, R., Pines, G., Amit, I., Shay, T., Lu, Y., Zwang, Y., Katz, M., Ben-Chetrit, N., Jacob-Hirsch, J., et al. (2012). EGR1 and the ERK-ERF axis drive mammary cell migration in response to EGF. FASEB J. *26*, 1582–1592.

Thayer, S.P., Magliano, M.P. di, Heiser, P.W., Nielsen, C.M., Roberts, D.J., Lauwers, G.Y., Qi, Y.P., Gysin, S., Castillo, C.F., Yajnik, V., et al. (2003). Hedgehog is an early and late mediator of pancreatic cancer tumorigenesis. Nature *425*, 851–856.

Theodosiou, A., and Ashworth, A. (2002). MAP kinase phosphatases. Genome Biol. *3*, Reviews 3009.

Thornton, T.M., and Rincon, M. (2008). Non-Classical P38 Map Kinase Functions: Cell Cycle Checkpoints and Survival. Int. J. Biol. Sci. *5*, 44–52.

Togel, L., Arango, D., Chueh, A.C., Sieber, O.M., and Mariadason, J.M. (2012). 654 Epigenetic Silencing of the Negative Feedback Regulator of Mitogen-activated Protein Kinase (MAPK) Signalling, DUSP5, in Colorectal Cancer. Eur. J. Cancer *48*, *Supplement 5*, S155.

Tonks, N.K. (2006). Protein tyrosine phosphatases: from genes, to function, to disease. Nat. Rev. Mol. Cell Biol. *7*, 833–846.

Tonnetti, L., Netzel-Arnett, S., Darnell, G.A., Hayes, T., Buzza, M.S., Anglin, I.E., Suhrbier, A., and Antalis, T.M. (2008). SerpinB2 Protection of Retinoblastoma Protein from Calpain Enhances Tumor Cell Survival. Cancer Res. *68*, 5648–5657.

Tournier, C., Whitmarsh, A.J., Cavanagh, J., Barrett, T., and Davis, R.J. (1997). Mitogen-activated protein kinase kinase 7 is an activator of the c-Jun NH2-terminal kinase. Proc. Natl. Acad. Sci. *94*, 7337–7342.

Tournier, C., Hess, P., Yang, D.D., Xu, J., Turner, T.K., Nimnual, A., Bar-Sagi, D., Jones, S.N., Flavell, R.A., and Davis, R.J. (2000). Requirement of JNK for Stress- Induced Activation of the Cytochrome c-Mediated Death Pathway. Science *288*, 870–874.

Traverse, S., Gomez, N., Paterson, H., Marshall, C., and Cohen, P. (1992). Sustained activation of the mitogen-activated protein (MAP) kinase cascade may be required for differentiation of PC12 cells. Comparison of the effects of nerve growth factor and epidermal growth factor. Biochem. J. *288*, 351–355.

Traverse, S., Seedorf, K., Paterson, H., Marshall, C.J., Cohen, P., and Ullrich, A. (1994). EGF triggers neuronal differentiation of PC12 cells that overexpress the EGF receptor. Curr. Biol. *4*, 694–701.

Tsang, M., Maegawa, S., Kiang, A., Habas, R., Weinberg, E., and Dawid, I.B. (2004). A role for MKP3 in axial patterning of the zebrafish embryo. Development *131*, 2769–2779.

Tuveson, D.A., Shaw, A.T., Willis, N.A., Silver, D.P., Jackson, E.L., Chang, S., Mercer, K.L., Grochow, R., Hock, H., Crowley, D., et al. (2004). Endogenous oncogenic K-rasG12D stimulates proliferation and widespread neoplastic and developmental defects. Cancer Cell *5*, 375–387.

Tuveson, D.A., Zhu, L., Gopinathan, A., Willis, N.A., Kachatrian, L., Grochow, R., Pin, C.L., Mitin, N.Y., Taparowsky, E.J., Gimotty, P.A., et al. (2006). Mist1-KrasG12D Knock-In Mice Develop Mixed Differentiation Metastatic Exocrine Pancreatic Carcinoma and Hepatocellular Carcinoma. Cancer Res. *66*, 242–247.

Udofa, E.A., Stringer, B.W., Gade, P., Mahony, D., Buzza, M.S., Kalvakolanu, D.V., and Antalis, T.M. (2013). The Transcription Factor C/EBP-β Mediates Constitutive and LPS-Inducible Transcription of Murine SerpinB2. PLoS ONE *8*, e57855.

Ueda, K., Arakawa, H., and Nakamura, Y. (2003). Dual-specificity phosphatase 5 (DUSP5) as a direct transcriptional target of tumor suppressor p53. Oncogene *22*, 5586–5591.

Unni, A.M., Lockwood, W.W., Zejnullahu, K., Lee-Lin, S.-Q., and Varmus, H. (2015). Evidence that synthetic lethality underlies the mutual exclusivity of oncogenic KRAS and EGFR mutations in lung adenocarcinoma. eLife *4*, e06907.

Valiente, M., Obenauf, A.C., Jin, X., Chen, Q., Zhang, X.H.-F., Lee, D.J., Chaft, J.E., Kris, M.G., Huse, J.T., Brogi, E., et al. (2014). Serpins Promote Cancer Cell Survival and Vascular Co-Option in Brain Metastasis. Cell *156*, 1002–1016.

Vantaggiato, C., Formentini, I., Bondanza, A., Bonini, C., Naldini, L., and Brambilla, R. (2006). ERK1 and ERK2 mitogen-activated protein kinases affect Ras-dependent cell signaling differentially. J. Biol. *5*, 14.

Vartanian, S., Bentley, C., Brauer, M.J., Li, L., Shirasawa, S., Sasazuki, T., Kim, J.-S., Haverty, P., Stawiski, E., Modrusan, Z., et al. (2013). Identification of Mutant K-Ras-dependent Phenotypes Using a Panel of Isogenic Cell Lines. J. Biol. Chem. *288*, 2403–2413.

Ventura, J.J., Tenbaum, S., Perdiguero, E., Huth, M., Guerra, C., Barbacid, M., Pasparakis, M., and Nebreda, A.R. (2007). p38α MAP kinase is essential in lung stem and progenitor cell proliferation and differentiation. Nat. Genet. *39*, 750–758.

Wada, T., and Penninger, J.M. (2004). Mitogen-activated protein kinases in apoptosis regulation. Oncogene *23*, 2838–2849.

Waddell, N., Pajic, M., Patch, A.-M., Chang, D.K., Kassahn, K.S., Bailey, P., Johns, A.L., Miller, D., Nones, K., Quek, K., et al. (2015). Whole genomes redefine the mutational landscape of pancreatic cancer. Nature *518*, 495–501.

Wagner, E.F., and Nebreda, Á.R. (2009). Signal integration by JNK and p38 MAPK pathways in cancer development. Nat. Rev. Cancer *9*, 537–549.

Wan, P.T.C., Garnett, M.J., Roe, S.M., Lee, S., Niculescu-Duvaz, D., Good, V.M., Project, C.G., Jones, C.M., Marshall, C.J., Springer, C.J., et al. (2004). Mechanism of Activation of the RAF-ERK Signaling Pathway by Oncogenic Mutations of B-RAF. Cell *116*, 855–867.

Wang, H., Cheng, Z., and Malbon, C.C. (2003). Overexpression of mitogen-activated protein kinase phosphatases MKP1, MKP2 in human breast cancer. Cancer Lett. *191*, 229–237.

Wang, Z., Reinach, P.S., Zhang, F., Vellonen, K.-S., Urtti, A., Turner, H., and Wolosin, J.M. (2010). DUSP5 and DUSP6 modulate corneal epithelial cell proliferation. Mol. Vis. *16*, 1696–1704.

Wasif, N., Ko, C.Y., Farrell, J., Wainberg, Z., Hines, O.J., Reber, H., and Tomlinson, J.S. (2010). Impact of Tumor Grade on Prognosis in Pancreatic Cancer: Should We Include Grade in AJCC Staging? Ann. Surg. Oncol. *17*, 2312–2320.

Werlen, G., Hausmann, B., Naeher, D., and Palmer, E. (2003). Signaling Life and Death in the Thymus: Timing Is Everything. Science *299*, 1859–1863.

Weston, C.R., and Davis, R.J. (2007). The JNK signal transduction pathway. Curr. Opin. Cell Biol. *19*, 142–149.

Westphalen, C.B., and Olive, K.P. (2012). Genetically Engineered Mouse Models of Pancreatic Cancer. Cancer J. Sudbury Mass *18*, 502–510.

White, M.A., Nicolette, C., Minden, A., Polverino, A., Aelst, L.V., Karin, M., and Wigler, M.H. (1995). Multiple ras functions can contribute to mammalian cell transformation. Cell *80*, 533–541.

Wickramasekera, N.T., Gebremedhin, D., Carver, K.A., Vakeel, P., Ramchandran, R., Schuett, A., and Harder, D.R. (2013). Role of dual-specificity protein phosphatase-5 in modulating the myogenic response in rat cerebral arteries. J. Appl. Physiol. *114*, 252–261.

Witkiewicz, A.K., McMillan, E.A., Balaji, U., Baek, G., Lin, W.-C., Mansour, J., Mollaee, M., Wagner, K.-U., Koduru, P., Yopp, A., et al. (2015). Whole-exome sequencing of pancreatic cancer defines genetic diversity and therapeutic targets. Nat. Commun. *6*, 6744.

Wojtukiewicz, M.Z., Rucinska, M., Zacharski, L.R., Kozlowski, L., Zimnoch, L., Piotrowski, Z., Kudryk, B.J., and Kisiel, W. (2001). Localization of blood coagulation factors in situ in pancreatic carcinoma. Thromb. Haemost. *86*, 1416–1420.

Wong, V.C.L., Chen, H., Ko, J.M.Y., Chan, K.W., Chan, Y.P., Law, S., Chua, D., Kwong, D.L.-W., Lung, H.L., Srivastava, G., et al. (2012). Tumor suppressor dual-specificity phosphatase 6 (DUSP6) impairs cell invasion and epithelial-mesenchymal transition (EMT)-associated phenotype. Int. J. Cancer *130*, 83–95.

Wortzel, I., and Seger, R. (2011). The ERK Cascade Distinct Functions within Various Subcellular Organelles. Genes Cancer *2*, 195–209.

Wu, C.-Y.C., Carpenter, E.S., Takeuchi, K.K., Halbrook, C.J., Peverley, L.V., Bien, H., Hall, J.C., DelGiorno, K.E., Pal, D., Song, Y., et al. (2014). PI3K Regulation of RAC1 Is Required for Kras-Induced Pancreatic Tumorigenesis in Mice. Gastroenterology *147*, 1405–1416.

Wu, Z., Jiao, P., Huang, X., Feng, B., Feng, Y., Yang, S., Hwang, P., Du, J., Nie, Y., Xiao, G., et al. (2010). MAPK phosphatase-3 promotes hepatic gluconeogenesis through dephosphorylation of forkhead box O1 in mice. J. Clin. Invest. *120*, 3901–3911.

Xu, H., Yang, Q., Shen, M., Huang, X., Dembski, M., Gimeno, R., Tartaglia, L.A., Kapeller, R., and Wu, Z. (2005a). Dual Specificity MAPK Phosphatase 3 Activates PEPCK Gene

Transcription and Increases Gluconeogenesis in Rat Hepatoma Cells. J. Biol. Chem. *280*, 36013–36018.

Xu, S., Furukawa, T., Kanai, N., Sunamura, M., and Horii, A. (2005b). Abrogation of DUSP6 by hypermethylation in human pancreatic cancer. J. Hum. Genet. *50*, 159–167.

Xue, A., Scarlett, C.J., Jackson, C.J., Allen, B.J., and Smith, R.C. (2008). Prognostic significance of growth factors and the urokinase-type plasminogen activator system in pancreatic ductal adenocarcinoma. Pancreas *36*, 160–167.

Yao, Y., Li, W., Wu, J., Germann, U.A., Su, M.S.S., Kuida, K., and Boucher, D.M. (2003). Extracellular signal-regulated kinase 2 is necessary for mesoderm differentiation. Proc. Natl. Acad. Sci. *100*, 12759–12764.

Yatsuoka, T., Sunamura, M., Furukawa, T., Fukushige, S., Yokoyama, T., Inoue, H., Shibuya, K., Takeda, K., Matsuno, S., and Horii, A. (2000). Association of poor prognosis with loss of 12q, 17p, and 18q, and concordant loss of 6q/17p and 12q/18q in human pancreatic ductal adenocarcinoma. Am. J. Gastroenterol. *95*, 2080–2085.

Yin, N., Qi, X., Tsai, S., Lu, Y., Basir, Z., Oshima, K., Thomas, J.P., Myers, C.R., Stoner, G., and Chen, G. (2016). p38γ MAPK is required for inflammation-associated colon tumorigenesis. Oncogene *35*, 1039–1048.

Ying, H., Elpek, K.G., Vinjamoori, A., Zimmerman, S.M., Chu, G.C., Yan, H., Fletcher-Sananikone, E., Zhang, H., Liu, Y., Wang, W., et al. (2011). PTEN Is a Major Tumor Suppressor in Pancreatic Ductal Adenocarcinoma and Regulates an NF-κB–Cytokine Network. Cancer Discov. *1*, 158–169.

Ying, H., Kimmelman, A.C., Lyssiotis, C.A., Hua, S., Chu, G.C., Fletcher-Sananikone, E., Locasale, J.W., Son, J., Zhang, H., Coloff, J.L., et al. (2012). Oncogenic Kras Maintains Pancreatic Tumors through Regulation of Anabolic Glucose Metabolism. Cell *149*, 656–670.

Ying, H., Dey, P., Yao, W., Kimmelman, A.C., Draetta, G.F., Maitra, A., and DePinho, R.A. (2016). Genetics and biology of pancreatic ductal adenocarcinoma. Genes Dev. *30*, 355–385.

Yip-Schneider, M.T., Lin, A., and Marshall, M.S. (2001). Pancreatic Tumor Cells with Mutant K-ras Suppress ERK Activity by MEK-Dependent Induction of MAP Kinase Phosphatase-2. Biochem. Biophys. Res. Commun. *280*, 992–997.

Yoon, S., and Seger, R. (2006). The extracellular signal-regulated kinase: Multiple substrates regulate diverse cellular functions. Growth Factors *24*, 21–44.

Yun, J., Rago, C., Cheong, I., Pagliarini, R., Angenendt, P., Rajagopalan, H., Schmidt, K., Willson, J.K.V., Markowitz, S., Zhou, S., et al. (2009). Glucose Deprivation Contributes to the Development of KRAS Pathway Mutations in Tumor Cells. Science *325*, 1555–1559.

Yuvaniyama, J., Denu, J.M., Dixon, J.E., and Saper, M.A. (1996). Crystal structure of the dual specificity protein phosphatase VHR. Science *272*, 1328–1331.

Zehorai, E., Yao, Z., Plotnikov, A., and Seger, R. (2010). The subcellular localization of MEK and ERK—A novel nuclear translocation signal (NTS) paves a way to the nucleus. Mol. Cell. Endocrinol. *314*, 213–220.

Zeller, E., Mock, K., Horn, M., Colnot, S., Schwarz, M., and Braeuning, A. (2012). Dual-specificity phosphatases are targets of the Wnt/β-catenin pathway and candidate mediators of β-catenin/Ras signaling interactions. Biol. Chem. *393*, 1183–1191.

Zhang, H., Chen, X., Wang, J., Guang, W., Han, W., Zhang, H., Tan, X., and Gu, Y. (2014). EGR1 decreases the malignancy of human non-small cell lung carcinoma by regulating KRT18 expression. Sci. Rep. *4*, 5416.

Zhang, H.-M., Li, L., Papadopoulou, N., Hodgson, G., Evans, E., Galbraith, M., Dear, M., Vougier, S., Saxton, J., and Shaw, P.E. (2008). Mitogen-induced recruitment of ERK and MSK to SRE promoter complexes by ternary complex factor Elk-1. Nucleic Acids Res. *36*, 2594–2607.

Zhang, Z., Kobayashi, S., Borczuk, A.C., Leidner, R.S., LaFramboise, T., Levine, A.D., and Halmos, B. (2010). Dual specificity phosphatase 6 (DUSP6) is an ETS-regulated negative feedback mediator of oncogenic ERK signaling in lung cancer cells. Carcinogenesis *31*, 577–586.

Zheng, C.F., and Guan, K.L. (1994). Activation of MEK family kinases requires phosphorylation of two conserved Ser/Thr residues. EMBO J. *13*, 1123–1131.

Zhou, H.-M., Bolon, I., Nichols, A., Wohlwend, A., and Vassalli, J.-D. (2001). Overexpression of Plasminogen Activator Inhibitor Type 2 in Basal Keratinocytes Enhances Papilloma Formation in Transgenic Mice. Cancer Res. *61*, 970–976.

Zur, R., Garcia-Ibanez, L., Nunez-Buiza, A., Aparicio, N., Liappas, G., Escós, A., Risco, A., Page, A., Saiz-Ladera, C., Alsina-Beauchamp, D., et al. (2015). Combined deletion of p38γ and p38δ reduces skin inflammation and protects from carcinogenesis. Oncotarget *6*, 12920–12935.